TIAGO HENRIQUE ZANINELLI

EXPLORANDO A TERAPÊUTICA DA RESOLUÇÃO DO PROCESSO INFLAMATÓRIO NA ARTRITE GOTOSA: EFEITO ANALGÉSICO DA RESOLVINA D1, UM MEDIADOR LIPÍDICO PRÓ-RESOLUÇÃO, E DO TPPU, UM INIBIDOR DE EPÓXIDO-HIDROLASE SOLÚVEL EM CAMUNDONGOS

Londrina
2022

TIAGO HENRIQUE ZANINELLI

EXPLORANDO A TERAPÊUTICA DA RESOLUÇÃO DO PROCESSO INFLAMATÓRIO NA ARTRITE GOTOSA: EFEITO ANALGÉSICO DA RESOLVINA D1, UM MEDIADOR LIPÍDICO PRÓ-RESOLUÇÃO, E DO TPPU, UM INIBIDOR DE EPÓXIDO-HIDROLASE SOLÚVEL EM CAMUNDONGOS

Tese de doutorado apresentada ao programa de pós-graduação em Patologia Experimental da Universidade Estadual de Londrina, como requisito parcial à obtenção do título de Doutor em Patologia Experimental.

Orientador: Prof. Dr. Waldiceu Aparecido Verri Junior

Londrina
2022

Ficha de identificação da obra elaborada pelo autor, através do Programa de Geração Automática do Sistema de Bibliotecas da UEL

Z31e Zaninelli, Tiago Henrique.

Explorando a terapêutica da resolução do processo inflamatório na artrite gotosa : efeito analgésico da resolvina D1, um mediador lipídico pró-resolução, e do TPPU, um inibidor de epóxido-hidrolase solúvel em camundongos / Tiago Henrique Zaninelli. - Londrina, 2022.
314 f. : il.

Orientador: Waldiceu Aparecido Verri Jr..
Tese (Doutorado em Patologia Experimental) - Universidade Estadual de Londrina, Centro de Ciências Biológicas, Programa de Pós-Graduação em Patologia Experimental, 2022.
Inclui bibliografia.

1. artrite gotosa (gota) - Tese. 2. interação neuroimune - Tese. 3. CGRP - Tese. 4. mediadores lipídicos pró-resolução - Tese. I. Verri Jr., Waldiceu Aparecido. II. Universidade Estadual de Londrina. Centro de Ciências Biológicas. Programa de Pós-Graduação em Patologia Experimental. III. Título.

CDU 616

TIAGO HENRIQUE ZANINELLI

EXPLORANDO A TERAPÊUTICA DA RESOLUÇÃO DO PROCESSO INFLAMATÓRIO NA ARTRITE GOTOSA: EFEITO ANALGÉSICO DA RESOLVINA D1, UM MEDIADOR LIPÍDICO PRÓ-RESOLUÇÃO, E DO TPPU, UM INIBIDOR DE EPÓXIDO-HIDROLASE SOLÚVEL EM CAMUNDONGOS

Tese de doutorado apresentada ao programa de pós-graduação em Patologia Experimental da Universidade Estadual de Londrina, como requisito parcial à obtenção do título de Doutor em Patologia Experimental.

COMISSÃO EXAMINADORA

_____
Prof. Dr. Waldiceu Aparecido Verri Jr.
Universidade Estadual de Londrina - UEL

_____
Dra. Camila Rodrigues Ferraz
University of Maryland School of Medicine

_____
Prof. Dr. Felipe Almeida de Pinho Ribeiro
Washington University School of Medicine in St. Louis

_____
Dra. Marília Fernandes Manchope
University of Würzburg

_____
Dr. Victor Fattori
Boston Children's Hospital - Harvard Medical School

Londrina, 28 de novembro de 2022.

Dedico este trabalho aos meus afilhados, Breno, Maitê e Pedro Antônio, e meu bebê em idade gestacional. Que minhas contribuições à ciência possam auxiliá-los no futuro.

AGRADECIMENTOS

Através do meu olhar cristão, sempre consegui enxergar a mão de Deus em cada processo biológico. Agradeço à Ele pela conclusão de mais uma etapa em minha formação acadêmica. E por ter me guiado com fé e esperança no caminho da ciência. Que minhas contribuições à pesquisa básica acrescentem, em algum nível, à vida do próximo.

À minha esposa e futura mãe dos meus descendentes, Luna M. M. Ganassin, pelo seu incondicional e constante suporte durante toda minha formação acadêmica. Grande parte desta tese dedico ao seu companheirismo e compreensão. Com seus gestos resilientes e maduros aprendi a ver o mundo sob outra perspectiva, contribuindo muito no desenvolvimento das minhas atividades profissionais e pessoais. Além do meu agradecimento, deixo aqui registrado minha admiração.

À Bombom, sem dúvidas, a mais fiel escudeira. Pelas inúmeras interrupções durante a escrita desta tese para uma demonstração canina de carinho. Agradeço também a cumplicidade em todos os momentos.

Aos meus pais, Odécio e Vera Zaninelli, pelo perene incentivo na buscar de meus objetivos. Vocês são uma inspiração de força e coragem para mim. Agradeço pelos exemplos de humildade, simplicidade e educação. Obrigado por valorizarem a formação acadêmica e o desejo em proporcionar uma vida mais tranquila financeiramente daquela que vocês tiveram.

Ao meu irmão, Mateus H. Zaninelli, por toda a parceria e ávida prontidão. As consultorias de engenheiro civil para projetos de fomento, e as contribuições na rotina laboratorial. Por ele e minha e minha cunhada Milena Kondratowski Estabile serem meus olhos e braços próximos aos meus pais.

À minha sogra Ivone, por cada xícara de café carinhosamente servida durante reuniões e trabalhos na modalidade home office. Aos meus cunhados e cunhadas por todo apoio e compreensão. Em especial, a minha cunhadinha Ana Vitória que se fez presente em toda graduação e pós-graduação, e por suas ajudas em experimentos durante as férias. Espero ter incentivando-a cientificamente. Não poderia deixar de agradecer a toda família Zaninelli, Oliveira, Matiazzo e Ganassin pelo suporte.

Ao meu amigo, mentor e companheiro, Victor Fattori. Você foi uma peça fundamental no meu crescimento científico. Obrigado por sempre me desafiar mentalmente e acreditar no meu potencial.

Ao meu amigo, futuro patrão e profissional inspirador, Felipe Almeida de Pinho Ribeiro. Obrigado por todo o companheirismo em meu período de doutorado sanduiche em Boston e pelas oportunidades de aprendizado.

As minhas parceiras de experimento, Telma Saraiva dos Santos, Mariana Marques Bertozzi, Camila Rodrigues Ferraz e Marilia F. Manchope que contribuíram de forma ímpar para a conclusão dessa tese. E ao Sergio Marques Borghi pela parceria no desenvolvimento de inúmeros estudos.

A todos os membros do Laboratório de Dor, Inflamação, Neuropatia e Câncer (LADINC) pela resiliência e persistência no desenvolvimento científico do Brasil. E por todo o suporte direto ou indireto no desenvolvimento das atividades laboratoriais.

Aos amigos de Boston, Natasha Ludwig, Érica Alexandre, Suellen Mello, Fabíola Boaventura, Gabriel Horta e Hussain Bukhari. Obrigado por serem nossa família fora do Brasil e nos apoiarem nessa experiência incrível.

Ao Prof. Dr. Waldiceu Aparecido Verri Júnior, deixo meu agradecimento e mais profunda admiração. Obrigado pela orientação, incentivo, oportunidades e mentoria nesses últimos 7 anos.

Aos membros da banca Dra. Camila Rodrigues Ferraz, Prof. Dr. Felipe Almeida de Pinho Ribeiro, Dra. Marília Fernandes Manchope, e Dr. Victor Fattori pela disposição, paciência e contribuição para a construção dessa tese.

Ao Prof. Dr. Michael S. Rogers do Boston Children's Hospital, Harvard Medical School pelo acolhimento e ensinamentos durante meu Período de Doutorado Sanduíche no Exterior (PDSE). Foi uma honra participar do ambiente científico inspirador do *Vascular Biology Program* e desenvolver parte de minhas pesquisas nessas reputadas instituições.

Aos servidores da universidade Estadual de Londrina, em especial à Maria Rosana de Paula pelo carinho e suporte técnico.

À Coordenadoria de Coordenação de Aperfeiçoamento de Pessoal de Nível Superior (CAPES) pela oportunidade da graduação e doutorado sanduíche no exterior.

A todos aqueles que porventura não foram mencionados, mas, de alguma forma contribuíram para a realização deste trabalho.

Epígrafe

"A ciência é mais que um corpo de conhecimento, é uma forma de pensar, uma forma cética de interrogar o universo, com pleno conhecimento da falibilidade humana."

Carl Sagan, Entrevista de lançamento do livro O Mundo Assombrado pelos Demônios, 1996

ZANINELLI, Tiago Henrique. **EXPLORANDO A TERAPÊUTICA DA RESOLUÇÃO DO PROCESSO INFLAMATÓRIO NA ARTRITE GOTOSA: EFEITO ANALGÉSICO DA RESOLVINA D1, UM MEDIADOR LIPÍDICO PRÓ-RESOLUÇÃO, E DO TPPU, UM INIBIDOR DE EPÓXIDO-HIDROLASE SOLÚVEL EM CAMUNDONGOS**. 2022. 314 páginas. Tese de doutorado (Patologia Experimental) – Universidade Estadual de Londrina, Londrina, 2022.

RESUMO

A resolução da inflamação é um processo ativo e altamente regulado por mediadores lipídicos pró-resolução (SPMs). SPMs são lipídeos derivados dos ácidos graxos ômega-3 ou ômega-6, os quais são divididos em quatro principais famílias “lipoxinas, resolvinas, maresinas e protectinas”. Na presente tese, inicialmente buscamos estabelecer uma relação dos níveis de SPMs e as características clínicas de doenças reumáticas. Por meio de um artigo de revisão discutimos a relação entre os níveis endógenos de SPMs e os sinais e sintomas de doenças reumáticas intermitentes, como a artrite reumatoide e gotosa. Baixos níveis de SPMs estão relacionados com uma percepção elevada da dor, por exemplo. Ademais elencamos os estudos pré-clínicos demonstrando os efeitos farmacológicos dos SPMs, e a importância dos SPMs para o monitoramento da eficácia de drogas modificadoras de doenças (DMARDs) que são potentes aliadas no tratamento e controle da progressão de doenças reumáticas. Por fim, vislumbramos quatro possíveis abordagens terapêuticas utilizando SPMs para o tratamento de artrites. Nos demais trabalhos investigamos os efeitos da Resolvina D1 (RvD1) e do inibidor de epóxido-hidrolase solúvel (sEH), TPPU, em um modelo de artrite gotosa induzido por cristais de urato monossódico (MSU, estímulo intra-articular no joelho) em camundongos Swiss. A gota afeta aproximadamente 10% da população mundial e é caracterizada por ataques agudos intercalados por fases assintomáticas. Dor articular excruciante, recrutamento de leucócitos e edema são os principais sintomas, e os mais desafiadores no tratamento. As terapias disponíveis para o tratamento da gota comummente oferecem efeitos colaterais severos, alto custo, e eficácia analgésica limitada em muitos pacientes. Portando além de contribuir na investigação dos efeitos e mecanismos de ação de novos fármacos para modulação dos sinais e sintomas, baseados na literatura atualizamos os mecanismos patofisiológicos da artrite gotosa, assim como as novas perspectivas para o tratamento dessa doença em uma segunda revisão. Em nosso segundo artigo pautamos a discussão na lacuna existente entre uma vasta quantidade de dados pré-clínicos e a medicina translacional, além de revisamos os efeitos benéficos de produtos naturais, drogas com múltiplos alvos e os SPMs como perspectivas futuras no controle da doença. Os dois artigos de revisão reiteram que o papel dos SPMs para doenças reumáticas e a necessidade no desenvolvimento de novas terapias. Portanto para o terceiro artigo, os camundongos foram tratados com RvD1 em dois protocolos experimentais, utilizando duas vias de administração (intraperitoneal [i.p.] e intratecal [i.t.]). A dose e o tempo de pré-tratamento foram selecionados baseado nos dados de redução da hiperalgesia mecânica (versão

eletrônica dos filamentos do von Frey) e edema articular (paquímetro). O efeito analgésico da dose de 3 ng (72 horas antes do estímulo) foram confirmados pela distribuição do peso das patas traseiras do animal (ensaio com o *Static weight bearing*), um método não reflexivo de análise de dor. Dessa forma, a dose de 3 ng e pré-tratamento de 72 horas foram selecionados para os próximos experimentos. Tratamentos com RvD1 local (i.t.) ou sistêmico (i.p.) reduziram o recrutamento de leucócitos (contagem no lavado articular) e os níveis de IL-1β no tecido articular por ELISA. Em cultura de macrófagos derivados da medula óssea, o tratamento *in vitro* com RvD1 reduziu a fosforilação e translocação do fator de transcrição NF-κB para o núcleo, diminuiu a expressão da molécula adaptadora ASC e a maturação da citocina pró-inflamatória IL-1β avaliados por imunofluorescência e ELISA, respectivamente. Estes resultados demonstram que a RvD1 bloqueia a ativação de macrófagos, que são células chave na fisiopatologia da doença. Além disso, nós demonstramos que o tratamento i.t. com RvD1 reduz a expressão de mRNA para canais iônicos (Trpv1 e Nav1.8) e neuropeptídios (substância P e Cgrp) no gânglio da raiz dorsal (DRG) através do RT-qPCR. RvD1 também reduz a ativação de neurônios peptidergicos (CGRP+) no DRG, e bloqueia a liberação de CGRP *in vitro* (determinado por EIA, em cultura de neurônios do DRG) e *in vivo* (por imunofluorescência). Por fim, nós também demonstramos que o CGRP aumenta a fagocitose de cristais de MSU por macrófagos, e consequente aumenta os níveis de IL-1β maturada, fenômenos que são reduzidos com o tratamento com RvD1. Portanto, neste estudo, além de demonstrar o importante efeito farmacológico da RvD1, nós também revelamos um mecanismo neuroimune nunca estudado na artrite gotosa. Em conclusão, nossos achados sugerem que RvD1 é um forte candidato para o controle da dor e inflamação na artrite gotosa, e que a comunicação entre nociceptor e células imunes são também alvo para abordagens terapêuticas. Para o quarto artigo nos propusemos a investigar os efeitos farmacológicos do inibidor de epóxido-hidrolase solúvel (sEH), TPPU, no mesmo modelo experimental. Durante o metabolismo do ácido araquidônico, via citocromo P450, são originados os ácidos epoxieicosatrienoicos (EETs) que exercem atividade protetiva e são moléculas precursoras na geração de SPMs, como a lipoxina A4, por exemplo. Embora esses mediadores apresentem atividades biológicas protetivas eles são rapidamente metabolizados em compostos não ativos através da ação de epóxi hidrolases solúveis (sEH). Portando, utilizando o tratamento com TPPU, é possível avaliar indiretamente os efeitos endógenos dos EETs na dor induzida por cristais de MSU. Neste estudo demonstramos que o tratamento com TPPU reduz a hiperalgesia mecânica (versão eletrônica dos filamentos do von Frey) e térmica (placa quente e Hargreaves), edema (paquímetro), e restabelece as mudanças na distribuição de peso nos membros traseiros (ensaio com o *Static weight bearing*), indicando que o TPPU reduz a dor e inflamação na artrite gotosa. Em conclusão, neste trabalho demonstramos o papel analgésico de duas moléculas explorando a resolução do processo inflamatório. Além disso, desvendamos um eixo de comunicação neuroimune na artrite gotosa, contribuindo na compreensão de novos mecanismos fisiopatológicos e novos alvos terapêuticos.

Palavras-chave: RvD1, interação neuroimune, CGRP, TPPU, IL-1β, specialized pro-resoling mediators (SPMs), ácido epóxi-eicosatrienóico (EETs).

ZANINELLI, Tiago Henrique. **EXPLORING THE THERAPEUTIC OF RESOLUTION OF THE INFLAMMATORY PROCESS IN GUTY ARTHRITIS: ANALGESTIC EFFECT OF RESOLVIN D1, A SPECIALIZED PRO-RESOLVING MEDIATOR, AND OF TPPU, A SOLUBLE EPOXIDE HYDROLASE INHIBITOR IN MICE**. 2022. 314pages. Doctoral thesis (Experimental Pathology) – Londrina State University, Londrina, 2022

ABSTRACT

Inflammation resolution is an active and highly regulated process orchastrated by specialized pro-resolving mediators (SPMs). SPMs are lipid mediators derived from omega-3 or omega-6 fatty acids, which are divided into four major families: lipoxins, resolvins, maresins, and protectins. In the present thesis, at first, we seek to establish the relationship between the levels of SPMs and the clinical chrarachteristics of rheumatic diseases. Through a review article, we discussed the relationship between endogenous levels of SPMs and the signs and symptoms of intermittent rheumatic diseases, such as rheumatoid and gouty arthritis. Low levels of SPMs are related to a increased perception of pain, for example. Another objective of this review was to list pre-clinical studies demonstrating the pharmacological effects of SPMs, in addition to addressing the importance of those mediators for monitoring the effectiveness of disease-modifying drugs (DMARDs) that are potent allies in the treatment and control of the progression of rheumatic disease. For this review article, we envision four possible therapeutic approaches using SPMs for the treatment of arthritis. For our next studies we focus to investigate the effects of Resolvin D1 (RvD1) and the soluble epoxide hydrolase (sEH) inhibitor, TPPU, in a model of monosodium urate crystals (MSU)-induced gouty arthritis (intra-articular stimulus in the knee) in swiss mice. Gout affects approximately 10% of the world's population and is characterized by acute attacks (gout flares) interspersed with asymptomatic phases. Excruciating joint pain and swelling are the main symptoms, and the most challenging to treat. The therapies available for the treatment of gout commonly offer severe side effects, high cost, and limited analgesic efficacy for many patients. Therefore, in addition to contributing to the investigation of effects and mechanisms of action of new, based on the literature, we update the pathophysiological mechanisms of gouty arthritis, as well as discussed future perspectives for the treatment of this disease in a second review. In our second study, we focus the discussion on the existing gap between a vast amount of preclinical data and translational medicine, in addition to reviewing the beneficial effects of natural products, multi-targeted drugs and SPMs in disease control. This two review articles reiterate the role of SPMs for rheumatic diseases and the need in the development of new therapies. So for the third article, mice were treated with RvD1 in two experimental protocols, using two routes of administration (intraperitoneal [i.p.] and intrathecal [i.t.]). The pretreatment dose and time were selected based on data on mechanical hyperalgesia (electronic version of von Frey filaments) and joint edema (caliper rule). The analgesic effect of the 3 ng dose (72 hours before MSU stimulus) was confirmed by changes in rear member weight distribution (determined by Static weight bearing assay), a non-reflective method of pain analysis.Therefore, the dose of 3 ng and the pretreatment of 72 hours were selected for the next experiments. Treatments with local (i.t.) or systemic (i.p.) RvD1 reduced leukocyte recruitment (joint lavage count) and IL-1β levels in joint tissue by ELISA. In cultured bone marrow-derived macrophages, *in vitro* treatment with RvD1 reduced the phosphorylation and translocation of the

transcription factor NF-κB to the nucleus, decreased the expression of the ASC adapter molecule and the maturation of the pro-inflammatory cytokine IL-1β assessed by immunofluorescence and ELISA, respectively. These results demonstrate that RvD1 blocks the activation of macrophages, which are key cells in the pathophysiology of the disease. Furthermore, we demonstrate that the i.t. treatement with RvD1 reduces mRNA expression for ion channels (Trpv1 and Nav1.8) and neuropeptides (substance P and Cgrp) in the dorsal root ganglion (DRG) analysed by. RvD1 also reduces the activation of peptidergic neurons (CGRP+) in the DRG, and blocks the release of CGRP *in vitro* (determined by EIA, in DRG neuron culture) and *in vivo* (by immunofluorescence). Finally, we also demonstrated that CGRP increases the phagocytosis of MSU crystals by macrophages, and consequently increases the levels of matured IL-1β, phenomena that are reduced by RvD1. Therefore, in this study, in addition to demonstrating the important pharmacological effect of RvD1, we also unveiled an hitherto unknown neuroimmune mechanism in gouty arthritis. In conclusion, our findings suggest that RvD1 is a strong candidate for the control of pain and inflammation in gouty arthritis, and that communication between nociceptor and immune cells are also targeted with this therapeutic approache. For the third article we aimed to investigate the pharmacological effects of the soluble epoxide hydrolase inhibitor (sEHi), TPPU, in the same experimental model. During the metabolism of arachidonic acid, via cytochrome P450, epoxyeicosatrienoic acids (EETs) are originated, which exert protective effects and are precursor molecules in the generation of SPMs, such as lipoxin A4, for example. Although these mediators have protective biological activities, they are rapidly metabolized into non-active compounds through the action of soluble epoxy hydrolases (sEH). Therefore, using TPPU treatment, it is possible to indirectly assess the endogenous effects of EETs in MSU-induced pain i. In this study we demonstrate that TPPU treatment reduces mechanical (electronic version of von Frey filaments) and thermal (hot plate and Hargreaves) hyperalgesia, edema (caliper), and restores changes in rear member weight distribution (Static weight bearing assay), indicating that TPPU reduces pain and inflammation in gouty arthritis. In conclusion, in this work we demonstrate the analgesic role of two molecules exploring the therapeutics of the resolution of the inflammatory process. In addition, we also unravel a neuroimmune communication axis in gouty arthritis, contributing to the understanding of new pathophysiological mechanisms of the disease and establishing new therapeutic targets.

Keywords: RvD1, neuroimmune interaction, CGRP, TPPU, IL-1β, specialized pro-resoling mediators (SPMs), epoxy-eicosatrienoic acid (EETs).

LISTA DE ILUSTRAÇÕES

LISTA DE ABREVIATURAS E SIGLAS

AIES	Anti-inflamatório esteroidal
AINES	Anti-inflamatório não esteroidal
AKT	Proteína kinase B
ALX/FPR2	Receptor de peptídeo formilado 2
ASC	Proteína adaptadora de CARD
ATP	Adenosina trifosfato
BMDM	Macrófagos derivados da medula óssea
CFA	Adjuvante completo de Freund
CGRP	Peptídeo relacionado ao gene da calcitonina
CXCL1	Ligante CXC 1
CXCL2	Ligante CXC 2
CXCR2	Receptor de quimiocina CXC 2
DAMP	Padrão molecular associado ao dano
DHA	Ácido docosahexaenoico
EPA	Ácido eicosapentaenoico
ERO	Espécie reativa de oxigênio
FFA	Ácido graxo livre de cadeia longa
fMLP	Peptídeo formilado
FoxO3a	Proteína Forkhead box O3
GM-CSF	Fator estimulador de colônias de granulócitos e macrófagos
GPR32	Receptor associado a proteína G 32
ICAM-1	Molécula de adesão intercelular-1
IκBα	Inibidor de NF-κB alpha
IL	Interleucina
INF-γ	Interferon-gamma
LPS	Lipopolissacarídeo
LTB_4	Leucotrieno B_4
SPM	Mediador lipídico pró-resolução
mRNA	RNA mensageiro
MSU	Urato monossódico
Nav1.8	Canal iônico voltagem dependente de sódio
Nek7	Kinase 7 relacionada a NIMA

NET	Armadilhas extracelulares de neutrófilos
NF-κB	Fator nuclear κappa B
NLR	Receptor semelhante a NOD
NLRP3	NLR família pyrin domínio contendo 3
PAMP	Padrões moleculares associados a patógenos
PGE_2	Prostaglandina E_2
PI3K	Fosfatidilinositol Kinase-3
PKA	Proteína kinase A
PKC	Proteína kinase C
PPAR-γ	Receptor ativado por proliferador de peroxisoma-gamma
PRR	Receptores de reconhecimento de padrão
RLR	Receptor semelhante a Rig
RvD1	Resolvina D1
TLR	Receptor semelhante a Toll
TNF-α	Fator de necrose tumoral-alpha
TRPA1	Receptor de Potencial Transitório Subfamília A, membro 1
TRPV1	Receptor de Potencial Transitório Subfamília V, membro 1
TRPV3	Receptor de Potencial Transitório Subfamília V, membro 3
TRPV4	Receptor de Potencial Transitório Subfamília V, membro 4

SUMÁRIO

1 INTRODUÇÃO

O processo inflamatório está presente ativamente em nosso cotidiano, desde um simples corte com papel, uma espinha, em resposta a um alérgeno, ou no processo fisiopatológico de inúmeras doenças. Mediadores lipídicos, quimiocinas, citocinas, e células imunes orquestram o processo culminando no aparecimento de seus sinais e sintomas. Embora primeiramente descrito por Aulus Cornelius Celsus no primeiro século d.C. os sinais cardinais da inflamação – calor, vermelhidão, edema, e dor – tiveram seus primeiros registros entre 2700 e 1500 a.C (ROCHA E SILVA, 1994). Muito estudiosos contribuíram para o entendimento causal do processo , os benefícios para proteção do hospedeiro (MADERNA; GODSON, 2009), mecanismos compensatórios e fatores reguladores para a limitação da resposta (LAWRENCE; WILLOUGHBY; GILROY, 2002; BUCKLEY; GILROY; SERHAN, 2014). No entendimento contemporâneo, a inflamação é dividida em fases – iniciação, fase vascular, fase celular, e resolução do processo inflamatório – as quais propiciam, em condições fisiológicas, a restauração da homeostase tecidual. Dentre os fatores regulatórios estão os mediadores lipídicos pro-resolução (*Specialized pro-resolving mediators*, SPMs) e a descrição do papel dessas moléculas na resolução do processo inflamatório (LEVY et al., 2001).

O processo de resolução da inflamação que outrora era compreendido como um efeito da redução dos mediadores pró-inflamatórios (MLPI) no tecido, atualmente é descrito como um processo ativo e altamente regulado pelos SPMs (LEVY et al., 2001; BUCKLEY; GILROY; SERHAN, 2014; CHIANG; SERHA, 2020). A compreensão do papel anti-inflamatório e analgésico desses mediadores (FATTORI et al., 2020), possibilitou a exploração terapêutica do processo de resolução e o uso dos SPMs no tratamento de sinais e sintomas de doenças inflamatórias e neuropatias. Nesse sentido, o primeiro trabalho dessa tese (item 3.1) publicado no periódico *Frontiers in Physiology* (ZANINELLI; FATTORI; VERRI, 2021), teve como objetivo revisar a relação entre os níveis de SPMs e os sinais e sintomas de doenças reumáticas. Além disso, demonstramos os efeitos com tratamento exógeno com SPMs em modelos animais de artrite, ou o papel isolado *in vitro* no contexto das doenças reumáticas. Nesse trabalho também exploramos como explorar o processo de resolução da inflamação para o desenvolvimento de novas terapias. Este

trabalho contribuiu diretamente para o desenvolvimento dos demais artigos científicos apresentados nessa tese (itens 3.2 e 3.3), nos quais avaliamos o processo de resolução da inflamação em um modelo experimental de artrite gotosa em camundongos.

A artrite gotosa (AG) ou gota, é caracterizada pela inflamação das articulações pela deposição de cristais de urato monossódico (MSU). A etiologia da doença tem como principais componentes hábitos alimentares ricos em carne vermelha e cerveja, e o desequilíbrio no metabolismo do ácido úrico (SO; MARTINON, 2017). Esses fatores levam a um quadro de hiperuricemia que culmina na precipitação de cristais de MSU no tecido articular e periarticular. Células residentes – sinoviócitos – reconhecem e fagocitam os cristais de MSU, iniciando um intenso processo inflamatório dependente da ativação do inflamassoma NLRP3 e a maturação de IL-1β (MARTINON et al., 2006). Os sinais clínicos da AG são caracterizados por edema e vermelhidão da articulação e dor excruciante (MARTINON et al., 2006). As terapias atuais para AG não são totalmente eficazes em reduzir a dor além de apresentar inúmeros efeitos colaterais, e alto custo no caso de imunobiológicos (SO; MARTINON, 2017). Desta forma existe uma lacuna terapêutica no controle da dor articular associada à AG. Fazendo-se necessário uma constante busca por novas terapias que sejam eficazes em reduzir este principal sintoma, a dor.

Tendo em vista a relação do processo de resolução da inflamação e sua importância para os sinais e sintomas de doenças reumáticas, a presente tese teve como objetivo geral investigarmos os efeitos e mecanismos de ação do SPM Resolvina D1 (RvD1), e do inibidor de epóxido-hidrolase solúvel (sEHi), N-[1-(1-oxopropyl)-4-piperidinyl]-N'-[4-(trifluoromethoxy)phenyl)-urea (TPPU) na artrite gotosa em camundongos. Especificamente, os objetivos foram investigar 1) os efeitos analgésicos e anti-inflamatórios incluindo a produção da interleucina (IL)-1β para ambas as moléculas, 2) avaliar os efeitos da RvD1 na ativação de macrófagos e neurônios $CGRP^+$ e $TRPV1^+$, e 3) elucidar o papel do neuropeptídeo CGRP na fagocitose e maturação da IL-1β em macrófagos *in vitro*. Nosso esforços originaram dois trabalhos, um já publicado no periódico *British Journal of Pharmacology* (ZANINELLI et al., 2022) e outro trabalho ainda em andamento, ambos descritos nos itens 3.2 e 3.3 desta tese, respectivamente.

2 REVISÃO DA LITERATURA

2.1 INFLAMAÇÃO

Atualmente a inflamação é caracterizada como uma resposta apropriada para a defesa do hospedeiro e a manutenção da homeostase tecidual (MADERNA; GODSON, 2009). Este processo essencial e conservado evolutivamente está presente em nosso cotidiano e na fisiopatologia de inúmeras doenças infecciosas e não-infeciosas. Historicamente, os primeiros relatos de sinais e sintomas da inflamação datam de 2700 e 1500 a.C. nas civilizações egípcias. Formalmente, os sinais cardinais da inflamação foram documentos pelo romano Aulus Cornelius Celsus apenas no primeiro século d.C. (ROCHA E SILVA, 1994). Celsus postulou que a inflamação é acompanhada dos sinais cardinais vermelhidão (*rubor),* calor, edema (*tumor*), e dor (*dolor*). por sinais cardinais que foram primeiramente documentados por Aulus Cornelius Celsus no primeiro século d.C. Posteriormente, no século XVIII, John Hunter, inspirado nas definições de Celsus, postulou que “a inflamação não é uma doença, mas uma resposta inespecífica que tem um efeito salutar ao hospedeiro” (HUNTER, 2007). No século XIX, a perda de função (*fuction laesa*) foi postulada como o quinto sinal cardinal por Rudolf Virchow (SCHMIDT; WEBER, 2006). De fato, a exacerbação do processo inflamatório pode levar a destruição de tecidos, fibrose e a eventual perda de função do órgão afetado (MADERNA; GODSON, 2009). Importantemente, todos os fatos históricos e estudiosos contribuíram para a atual definição de inflamação e suas consequências.

Felizmente, em contrapartida a exacerbação, mecanismos compensatórios e fatores reguladores também foram selecionados evolutivamente, garantindo através da produção de citocinas anti-inflamatórias e moléculas resolutivas a limitação da resposta (LAWRENCE; WILLOUGHBY; GILROY, 2002; SERHAN; CHIANG; DALLI, 2015). As fases do processo inflamatório são divididas em iniciação, fase vascular, fase celular e resolução. Desta forma em um contexto não patológico, a resolução do processo inflamatório é uma fase ativa e altamente regulada que culmina na restauração da homeostase tecidual. Os mediadores responsáveis e o entendimento contemporâneo deste processo serão abordados em detalhes nos próximos tópicos.

Em linhas gerais, a inflamação se inicia através do reconhecimento de padrões através do reconhecimento de padrões moleculares associados a patógenos (PAMPs) ou padrões moleculares associados ao dano (DAMPs) aos receptores de reconhecimento do padrão (PRRs), como por exemplo os receptores semelhantes a Toll (TLRs), a Nod (NLR) e a Rig (RLR), presentes em células imune inatas residentes, principalmente macrófagos e mastócitos (MEDZHITOV, 2008; TAKEUCHI; AKIRA, 2010). Esta interação desencadeia uma sequência de sinais intracelulares que culminam na ativação e translocação do Fator Nuclear Kappa B (NF-κB) para o núcleo (IWASAKI; MEDZHITOV, 2010; TAKEUCHI; AKIRA, 2010). Em consequência, ocorre a expressão de citocinas pro-inflamatórias (interleucina-1β [IL-1β], fator de necrose tumore-α [TNF-α]), citocina anti-inflamatória (interleucina-10 [IL-10]), quimiocinas (Ligante de quimiocina CXC 1 [CXCL1] e ligante de quimiocina CXC 2 [CXCL2]), mediadores lipídios pró-inflamatórios (prostaglandina E_2 [PGE_2] e leucotrieno B_4 [LTB_4]) e endotelina-1 que amplificam o processo inflamatório (CUNHA; FERREIRA, 1986; FERREIRA; ROMITELLI; DE NUCCI, 1989; RIBEIRO et al., 1997; VERRI et al., 2006; GUERRERO et al., 2008).

Os eventos vasculares da inflamação consistem no aumento do fluxo sanguíneo seguido pelo aumento do extravasamento de líquidos e permeabilidade endotelial. Esses eventos são mediados por aminas vasoativas como histamina e serotonina. Estes eventos acarretam modificações hemodinâmicas e a ativação endotelial, que contribuem para guiar precisamente os neutrófilos para o foco inflamatório. Os mecanismos envolvidos na migração e ativação de neutrófilos foram intensamente estudados na última década. Este processo depende da característica do estímulo (PAMP ou DAMP) e segue uma cascata temporal, espacial e hierárquica de mediadores (MCDONALD et al., 2012; SREERAMKUMAR et al., 2014). Por exemplo, em um modelo de inflamação estéril, os neutrófilos são guiados pelos sinusóides hepaticos pela interação da integrina Mac-1 expressa em neutrófilos com a ICAM-1 do endotélio (MCDONALD et al., 2012). Por outro lado, a adesão e o recrutamento de neutrófilos por um estímulo não estéril, neste caso *Escherichia coli*, é dependente de CD44 e não Mac-1 (MCDONALD et al., 2012). Posteriormente a diapedese, a atração e direcionamento dos neutrófilos para o foco inflamatório respeita um gradiente espacial de moléculas quimioatraentes, como por exemplo peptídeos formilados (fMLP), proteínas do sistema complemento (C5a), e

moléculas adjacentes provenientes do endotélio vascular ativado como como interleucina-18 (IL-8) e leucotrieno B_4 (LTB_4) (CAMPBELL; FOXMAN; BUTCHER, 1997; FOXMAN; CAMPBELL; BUTCHER, 1997). O microambiente inflamatório estimula a expressão do FoxO3a, o qual aumenta a longevidade dos neutrófilos através da supressão do promotor de FasL (ligante de Fas) no neutrófilo, além de promover a ativação do fator nuclear kappa B (NF-κB), expressão de citocinas pro-inflamatórias e de espécies reativas de oxigênio (JONSSON; ALLEN; PENG, 2005; WRIGHT et al., 2010).

Nas últimas décadas muitos estudos desmistificaram o paradigma dos mecanismos da resolução do processo inflamatório. Antes disso, esse processo era considerado passivo e dependente da abundância de mediadores pró-inflamatórios nos tecidos. A partir da compreensão contemporânea, a resolução da inflamação é um processo ativo, cronológico, e orquestrados por SPMs (SERHAN, 2014; CHIANG; SERHA, 2020). No foco inflamatório, a presença de neutrófilos apoptóticos e níveis elevados de PGE_2 induzem a troca de classe (*class switch*) da produção de MLPI para síntese de SPMs (LEVY et al., 2001). Importantemente, a síntese dos SPMs, em grande parte é realizada por enzimas que também catalisam a formação de MLPI. O aumento dos níveis de SPMs no foco inflamatório induz a ativação de macrófagos não flogísticos e a eferocitose de corpos apoptóticos de neutrófilos a fim de restabelecer a homeostase tecidual (SERHAN, 2014). O papel endógeno e os efeitos farmacológicos dos SPMs serão revisados mais profundamente em um próximo tópico. Ademais, o item 3.1 desta tese apresenta um artigo de revisão acerca do tema.

2.2 DOR INFLAMATÓRIA E INTERAÇÃO NEUROIMUNE

De acordo com a Associação Internacional para o Estudo da Dor (IASP) a dor é definida como *"uma experiência sensorial e emocional desagradável associada ou semelhante àquela associada a dano tecidual real ou potencial".* Embora desagradável, o processo de percepção doloroso, ou nocicepção, é extremamente conservado evolutivamente em várias espécies. Possuir a capacidade de sentir dor confere ao organismo a capacidade de autopreservação. Desta forma, sentir dor é essencial para a identificação de situações que possam causar danos, ou controlar aqueles já existentes, garantindo assim a autopreservação do indivíduo. No entanto, sensações nociceptivas agudas (dor patológica) e, principalmente as prolongadas (dor crônica) reduzem significativamente a qualidade de vida. Nesse sentido, existe uma forte correlação entre a persistência de dor como um fator de risco para pensamentos depressivos e comportamentos suicidas (CALATI et al., 2015). Portanto, é imprescindível determinar os mecanismos fisiológicos da transmissão da dor e compreender o papel não-sensorial dos neurônios nociceptores na fisiopatologia de doenças. Esses avanços possibilitam o desenvolvimento de novas terapias e a busca de novos alvos para o controle da dor patológica.

A icônica ilustração do menino próximo a fogueira de René Descartes no livro "*Treatise of Man*" (1964) demonstrou o entendimento da fisiologia da dor no mundo moderno. Neste, Descartes propunha que o fogo induz a ativação de fibras em regiões periféricas para posterior transmissão para o cérebro. O reconhecimento dessa informação leva por vez à retirada do membro do fogo. Na concepção de Descartes, a dor era uma consequência da ativação linear periférica para o cérebro (MOAYEDI; DAVIS, 2013). Embora incompleta, esta concepção não estava errada. Acontece que a percepção da dor, além de envolver mecanismos fisiológicos complexos, depende das experiências e perfil emocional de cada indivíduo. Portanto, o limiar nociceptivo pode variar de acordo experiências emocionais passadas, estado de humor e atenção (BUSHNELL; ČEKO; LOW, 2013) e expectativas em relação à intensidade do estímulo (WIECH et al., 2014).

Contudo, as definições mais recentes da fisiologia da dor consistem na sensibilização

periférica de nociceptores, sensibilização espinal, plasticidade neural e mudança de fenótipo de células do sistema imune (MOGIL; YU; BASBAUM, 2000; WOOLF; SALTER, 2000; SCHOLZ; WOOLF, 2002; REICHLING; LEVINE, 2009). Este processo envolve a transdução, condução, transmissão e percepção dos estímulos nóxicos. A partir da sensibilização periférica por um estímulo nociceptivo desencadeia um mecanismo ascendente que consiste na despolarização de nociceptores de primeira ordem e a condução do impulso nervoso até o corno da raiz dorsal da medula espinal, ou até o núcleo trigeminal. Nesta região, por meio de neurotransmissores excitatórios, ocorre a transmissão da informação para nociceptores de segunda ordem. Por fim, a percepção e o fornecimento da informação referente ao estímulo inicial, através de sinapses no córtex somatosensorial, sobre a localização e intensidade do estímulo. Outras projeções nervosas contribuem para o componente emocional do processo doloroso, que fazem sinapse na região da amígdala (BASBAUM et al., 2009; BRAZ et al., 2014).

Existe uma grande gama de estímulos nocivos que podem ativar nociceptores. Na dor inflamatória, por exemplo, neurônios periféricos são ativados por moléculas pro-inflamatórias. Dentre elas podemos destacar citocinas (IL-1β, TNF-α), quimiocinas, mediadores lipídicos pro-inflamatórios (LTB_4, PGE_2), adenosina trifosfato (ATP), e proteínas do sistema complemento (MOGIL; YU; BASBAUM, 2000; WOOLF; SALTER, 2000; SCHOLZ; WOOLF, 2002; VERRI et al., 2006; GUERRERO et al., 2008; BRAZ et al., 2014).

Importantemente, a presença de neutrófilos no local da inflamação é um denominador comum para na dor inflamatória (CUNHA et al., 2008). Perante um estimulo nocivo, a ativação de neutrófilos leva a produção de uma cascata de citocinas pró-inflamatórias que inclui a IL-1β, TNF-α e IL-33 (VERRI et al., 2006), seguindo essa cascata de citocinas pro-inflamatórias a liberação de PGE_2 e aminas simpáticas. Atuando em receptores específicos, esses mediadores inflamatórios como a PGE_2, histamina e citocinas são os principais responsáveis pela redução do limiar de ativação neuronal e pela produção de sensibilização periférica (PINHO-RIBEIRO; VERRI; CHIU, 2017). Esta cascata de citocinas é iniciada pela liberação da alarmina IL-33 (ZARPELON et al., 2013) estimulando a produção sequencial de TNF-α→IL-6→IL-1β→ PGE_2, por vez, TNF-α→CXCL1→IL-1β→ aminas vasoativas (CUNHA et al., 2005; VERRI et al., 2006). Estas

moléculas, ao se ligarem aos respectivos receptores ativam proteínas kinases (PKA e PKC), que por vez, fosforilam canais iônicos (TRPV1, TRPA1 e Nav1.8). A entrada de íons de Na^+ e Ca^{2+} reduzem o potencial de ativação dos neurônios, levando a sensibilização e ativação (despolarização - *firing*) (SCHOLZ; WOOLF, 2002; BRAZ et al., 2014) Scholz e Woolf, 2002; Braz et al., 2014).

Embora os nociceptores tenham como principal papel a percepção e transmissão da informação dolorosa, o entendimento contemporâneo mostrou que suas funções extrapolam seu papel primário. De fato, os nociceptores expressam receptores de reconhecimento de padrão (PRRs – TLR 2, 3, 4 e 7; e NLR) e são capazes de ser ativados na presença de DAMPs ou PAMPs (LIU et al., 2010; QI et al., 2011). Neurônios TRPV1+ do DRG também expressão receptores FcγRI e FcγRIIb, os quais a partir do reconhecimento de imunocomplexo de colágeno tipo 2, são responsáveis por aumentar a excitabilidade neuronal e liberação do neuropetídeo (*p. ex.*, CGRP) para produzir dor (BERSELLINI FARINOTTI et al., 2019). Proteínas do sistema complemento, como o C5a, também participam na ativação direta de neurônios durante a inflamação (TING et al., 2008). Neste trabalho também foi demonstrado que a dor induzida pelo C5a não é dependente da produção de citocinas, mas sim da presença de neutrófilos no local da inflamação (TING et al., 2008). Recentemente, também foi descrito que o quimioterápico paclitaxel induz dor neuropática periférica através da sinalização via C5aR1 em neurônios, demonstrando um importante alvo para o tratamento desse sintoma (BRANDOLINI et al., 2022). Moléculas provenientes de células mortas como ATP e fMLP, também induzem a ativação direta de neurônios.

Além dos mediadores supracitados, os nociceptores também reconhecem produtos derivados de patógenos (CHIU et al., 2013; BLAKE et al., 2018; PINHO-RIBEIRO et al., 2018; LAI et al., 2019). Por exemplo componentes bacterianos como a estreptolisina S (PINHO-RIBEIRO et al., 2018), a α-hemolisina (CHIU et al., 2013), e componentes fúngicos como a β-glucana (MARUYAMA et al., 2017) ativam neurônios nociceptores, induzindo a dor e a liberação de neuropeptídeos. Dentre os neuropeptídeos vale citar o CGRP, substância P (SP), e peptídeo vasoativo intestinal (VIP). Essas moléculas atuam diretamente em células da imunidade inata, regulando a resposta do hospedeiro à um patógeno. Por exemplo, a estreptolisina S liberada durante a infeção por *Streptococcus*

pyogenes na pele de camundongos, diretamente ativa os neurônios nociceptores e induzem a liberação de CGRP (PINHO-RIBEIRO et al., 2018). Por vez, CGRP sinaliza através do receptor RAMP1 em neutrófilos, reduzindo a atividade bactericida e piorando a infecção. Ademais, a utilização de antagonistas do receptor RAMP1, aplicação de toxina botulínica, ou a depleção de neurônios $TRPV1^+$ - uso de animais nocautes condicionais para neurônios $TRPV1^+$ - reduzem ou eliminam a infecção (PINHO-RIBEIRO et al., 2018). Por outro lado, em um modelo de infeção intestinal por *Salmonella enterica serovar Typhimurium*, o bloqueio dos nociceptores piora a infecção, demonstrando um efeito opositor ao observado anteriormente (LAI et al., 2020). Além disso, outro estudo demonstrou que a ativação de nociceptores $TRPV1^+$ é suficiente para iniciar uma resposta imune antecipatória na ausência de outros estímulos inflamatórios (COHEN et al., 2019). Portanto, o componente neuroimune de neurônios nociceptores tem um importante papel modulatório na resposta imune. Tendo em vista que os níveis de CGRP estão elevados no líquido sinovial de pacientes com artrite gotosa (HERNANZ et al., 1993), e levando em consideração as interações neuroimunes, no trabalho publicado na *British Journal of Pharmacology* (item 3.2), nos investigamos o efeito do neuropeptídeo CGRP na fagocitose de cristais de MSU e na produção da citocina IL-1β em macrófagos derivados da medula óssea (BMDM) *in vitro*. Neste estudo foi observado que o CGRP aumenta a fagocitose de cristais e consequentemente os níveis de IL-1b liberados no sobrenadante (ZANINELLI et al., 2022). Portanto, estabelecendo pela primeira vez, um potencial eixo neuroimune na progressão de sinais e sintomas da gota artrite, a qual terá sua fisiopatologia descrita a seguir.

2.3 ARTRITE GOTOSA

A artrite gotosa (AG) é uma doença inflamatória intermitente que afeta cerca de 10% da população, sendo mais homens que mulheres (KUO et al., 2015). Essa doença é considerada uma das condições agudas mais dolorosas que os seres humanos podem experimentar (MARTINON et al., 2006). Historicamente, as primeiras descrições foram realizadas por civilizações egípcias e datam do ano 2640 a.C, onde essa condição foi nomeada *podagra* (NUKI; SIMKIN, 2006). Um século mais tarde, Hipócrates descreveu a podagra como a “artrite dos ricos” ou “doença de reis”, pelo fato de o aparecimento dos sintomas estarem relacionados com os hábitos alimentares fartos da época (NUKI; SIMKIN, 2006). No século III d.C., Galeno descreveu o tophus, no entanto, sem saber que se tratava do acúmulo de ácido úrico e cristais de urato monossódio. No século XIII d.C., o monge dominicano Randolphus de Bocking nomeou a doença gota, do latim gutta. Seus motivos foram baseados na concepção medieval, de que um organismo em equilíbrio possuía quatro humores, através do desequilíbrio, um dos humores se deslocava para as articulações, gerando os sintomas da doença (Nuki e Simkin, 2006). A definição do agente etiológico da doença, como sendo os cristais de urato monossódico (MSU) ocorreu apenas na década de 1960. Em um ato audacioso, Faires e MacCarty, injetaram 20mg de MSU em suas próprias articulações. Conforme esperado, após algumas horas ambos desenvolveram os sintomas (FAIRES; MCCARTY, 1962; RAGAB; ELSHAHALY; BARDIN, 2017).

Atualmente a AG é classificada como uma doença inflamatória prototípica, que se desenvolve pela ativação do sistema imune inato (SO; MARTINON, 2017). O agente causador são os cristais de MSU, precipitados nas articulações e tecidos periarticulares (DALBETH; HASKARD, 2005). A precipitação se dá pelo desequilíbrio no metabolismo do ácido úrico, o que gera o acúmulo dessa substancia no sangue, uma condição chamada de hiperuricemia (níveis de urato plasmáticos > 7 mg/L). Clinicamente, a doença é caracterizada por episódios agudos de inflamação articular intercalado por períodos não-inflamatórios de durações variáveis (SO; MARTINON, 2017). Embora seja uma doença autolimitante, com resolução em até 10 dias, múltiplos episódios da fase aguda (*ataques*) podem gerar sérios danos articulares, incluindo degradação de cartilagens e ossos (SCHLESINGER; THIELE, 2010).

A fisiopatologia da gota tem como principais componentes o inflamassoma NLRP3 e sua participação na maturação da citocina pro-inflamatória IL-1β (MARTINON et al., 2006; AMARAL et al., 2012). A montagem e ativação do inflamassoma NLRP3 consiste em dois sinais ou estímulos independentes. O primeiro sinal, sinal 1, controla a expressão de todos os componentes necessários para montagem e ativação do inflamassoma (NLRP3, ASC e por-CASPASE-1) e o produto a substrato da CASPASE-1 ativada, pro-IL-1β (MARTINON et al., 2006). A expressão de todos estes componentes são dependentes do fator NF-κB e as suas vias de sinalização. Fisiologicamente a origem do sinal 1 não é bem estabelecida, mas é associada à ativação de receptores TLR (LIU-BRYAN et al., 2005). Dentre os possíveis candidatos se destacam: ácidos graxos livres de cadeia longa (FFAs) (JOOSTEN et al., 2010), fator estimulante de colônias de granulócitos-macrófagos (GM-CSF) (AN et al., 2014), as proteínas endógenas ligantes de TLR, S100A8 e S100A9 (HOLZINGER et al., 2014), e proteína C5a do complemento (AN et al., 2014; KHAMENEH et al., 2017). Além desses ligantes, a própria IL-1β participa na ativação, estabelecendo um “loop” de auto amplificação (SO; MARTINON, 2017). A **figura 1** ilustra a fisiopatologia da artrite gotosa.

O sinal 2, consiste na ativação do inflamassoma NLRP3. Este sinal mais específico propicia a clivagem da pró-CASPASE-1 em CASPASE-1 que, uma vez ativa, cliva a pró-IL-1β em IL-1β madura (Martinon et al., 2006). Os mecanismos pelos quais a ativação do NLRP3 ocorre também não são inteiramente compreendidos. No entanto, sugere-se que a ativação do NLRP3 ocorre pela perturbação do equilíbrio iônico celular provocadas pelos cristais de MSU (PÉTRILLI et al., 2007; YARON et al., 2015), consequente liberação de EROs provenientes das mitocôndrias, o que evoca a ativação da kinase Nek7. Nestas condições, Nek7 se liga diretamente ao NLRP3 ativando-o (HE et al., 2016; SCHMID-BURGK et al., 2016; SHI et al., 2016). Interessantemente, a ativação do inflamasoma por cristais de MSU também é associada ao rompimento do fagolisossomo e a liberação de seu conteúdo no espaço citosólico (MARTINON et al., 2006; DUEWELL et al., 2010). Catepsina B e L induzem a ativação do NLRP3 (DUEWELL et al., 2010) **(Figura 1).**

O reconhecimento e fagocitose de cristais de MSU por macrófagos residentes (sinoviócitos) induzem a liberação de citocinas. No caso da AG, a IL-1β é uma

citocina chave na fisiopatologia da doença e responsável por desencadear a resposta inflamatória em diversos tipos celulares (DINARELLO, 2009). O recrutamento de neutrófilos é um marcador das doenças reumáticas (FATTORI; AMARAL; VERRI JR., 2016) e de fato são o tipo celular predominante no liquido sinovial de pacientes durante os ataques inflamatórios da gota (MITROULIS; KAMBAS; RITIS, 2013). Essas células contribuem para a produção de IL-1β e LTB4 no foco inflamatório (AMARAL et al., 2012), o reconhecimento dos cristais de MSU por neutrófilos induz a degranulação (POPA-NITA et al., 2007) e a formação de armadilhas extracelulares (NETs - Neutrophils Extracellular Traps), processo denominado NETose (MITROULIS et al., 2011). Em conjunto, esses fatores contribuem para a amplificação da resposta inflamatória, aumentando a ativação do NF-κB e produção de citocinas pró-inflamatórias.

Figura 1 – Fisiopatologia da artrite gotosa.

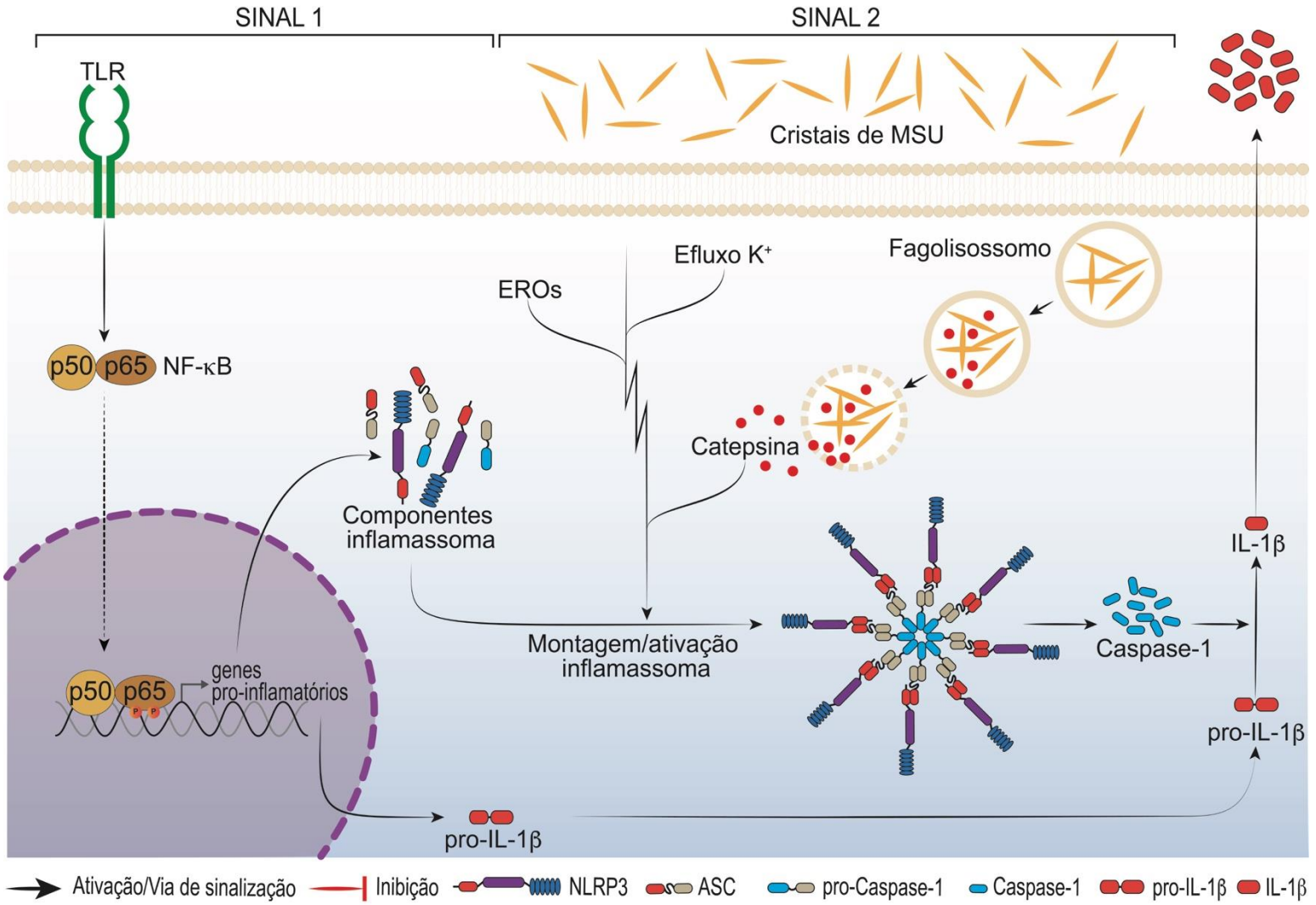

Fonte: adaptado de Zaninelli 2018.

O principal sintoma da gota é a dor. Durante os ataques de AG as dores excruciantes estão associadas a mecanismos de dor inflamatória, nos quais as citocinas pró-inflamatórias, em especial a IL-1β, sensibilizam nociceptores culminando no fenótipo altamente doloroso. Importantemente, as funções dos neutrófilos vão além do aumento da resposta inflamatória neste contexto. Esta célula com papel duplo, através da formação de NETs (SCHAUER et al., 2014) limitam a progressão da doença e iniciam o processo resolutivo da AG. Além disso, a expressão da proteína anexina-1, potente inibidora da fosfolipase A2, exerce importante papel na limitação da inflamação e na promoção da resolução (PERRETTI; D'ACQUISTO, 2009). Ela exerce importante papel na troca de classe de mediadores pró-inflamatórios para pró-resolutivos (LEVY et al., 2001). Tema que será revisado com mais detalhe no próximo tópico.

O tratamento da gota consiste principalmente em terapias que visam reduzir os níveis plasmáticos de urato e controlar os ataques agudos. No entanto, o principal motivo que leva os pacientes a procurar auxílio médico são os episódios de dor intensa (REES; HUI; DOHERTY, 2014). Basicamente, o controle dos episódios agudos consistem no uso de anti-inflamatórios esteroidais, não-esteroidais, colchicina e agentes biológicos (SO; MARTINON, 2017). O efeito da colchicina em desestabilizar os microtúbulos tem papel fundamental como inibidor da montagem do inflamassoma, impedindo a maturação da IL-1β e sua liberação (MARTINON et al., 2006). Recentemente, o controle dos sintomas também pode ser atingido com agentes biológicos que tem como alvo a IL-1β. Anticorpos contra IL-1β (Canakinumab) e proteínas recombinantes antagonista do receptor do receptor IL-1R (Anakinra) estão disponíveis no mercado (SO; MARTINON, 2017). Infelizmente, os medicamentos propostos para o tratamento e controle dos ataques agudos não são seguros para pacientes comorbidades (AINEs), usualmente geram efeitos colaterais (AINEs, AIEs e colchicina), apresentam custo elevado (agentes biológicos), além de não possuírem efeito analgésico satisfatório (REES; HUI; DOHERTY, 2014). Desta forma, existe uma constante necessidade do desenvolvimento de novas terapias que tenham como alvo a inibição da dor, principalmente para garantir melhor qualidade de vida àqueles que são acometidos pela AG. Por isso, o principal objetivo dessa tese foi explorar o processo de resolução da inflamação para obter novos

possíveis candidatos para o tratamento da dor induzida por cristais de MSU. Para isso, avaliamos os efeitos e mecanismos de ação da Resolvina D1 um mediador lipídico pro-resolução, e do inibidor de sEH, TPPU, na AG em camundongos.

2.4 MEDIADORES LIPÍDICOS PRÓ-RESOLUÇÃO

Conforme mencionado anteriormente, a compreensão contemporânea da resolução do processo inflamatório é pautada na ação de mediadores pro-resolutivos especializados (*specialized pro-resolving mediators*, SPMs). Essas moléculas, orquestram de maneira ativa e temporal a resolução da inflamação, restaurando a homeostase tecidual. Desde a primeira descrição sobre a troca de classe de mediadores lipídicos na resolução da inflamação (LEVY et al., 2001), os conhecimentos a cerca dos efeitos biológicos estão em constante evolução. Através da análise de exudados inflamatórios as lipoxinas foram as primeiras a serem descritas (SERHAN, 2004). Posteriormente as resolvinas, protectinas, e maresinas foram incluídas às principais famílias de mediadores (SERHAN, 2014).

Esses mediadores são biossintetizados pela ação de enzimas lipoxigenases (LOX), cicloxigenases (COX) acetiladas pela aspirina, ou por enzimas do citocromo P450, que agem sobre metabólitos dos ácidos graxos ômega-3 e ômega 6. A **Figura 2** resume o mecanismo de síntese dos SPMs e suas principais famílias (HONG et al., 2003; CHIANG; SERHA, 2020). A partir do ácido araquidônico, derivado do ômega-6, as lipoxinas A4 e B4 (LxA4, LxB4) são sintetizadas pela ação de lipoxigenases. Quando acetilada pela aspira a enzima COX produz o epímero 15-epi-LxA4, também conhecida como *aspirin-triggered* (AT-)LxA4. Por outo lado, enzimas do citocromo P450 catabolizam a formação de ácidos epoxieicosatrienoicos (EET). Os ácidos graxos essenciais do ômega-3, como ácido eicosapentaenóico (EPA) e ácido docosaexaenóico (DHA) também são matéria prima prara as demais famílias de SPM. Por exemplo, as resolvinas (Rv) da série D (RvD) são derivadas do DHA, assim como maresinas e protectinas (SERHAN, 2014; CHIANG; SERHA, 2020). Enquanto as Rv da série E, são derivadas do EPA (**Figura 2**). Estudos recentes demonstraram as resolvinas da série T, também derivadas do DHA (CHIANG et al., 2022). Um denominador comum de todos esses mediadores é a ativação de macrófagos não-flogísticos. Estes macrófagos irão realizar a eferocitose dos corpos apoptóticos de neutrófilos e induzirão os sinais da resolução do processo inflamatório. Processos estes que incluem a redução de citocinas pró-inflamatórias, retirada dos neutrófilos da superfície epitelial, fagocitose dos neutrófilos em apoptose e a

remoção dos debris inflamatórios e infecciosos (SERHAN, 2014).

Em adição às características analgésicas, anti-inflamatórias e resolutivas, os SPMs não possuem atividade imunossupressora, o que coloca essas moléculas como fortes candidatas a testes clínicos. De fato, a Resolvina E1, derivada do EPA, atingiu a clínica como RX-10045® para testes no tratamento da síndrome dos olhos ressecados. Os pacientes apresentaram melhora significativa na condição de maneira dose-dependente (Clinicaltrials.gov identificação NCT00799552) (LEE, 2012; NORLING; PERRETTI, 2013). Além disso, embora os SPMs tenham uma meia-vida extremamente curta (AURSNES et al., 2015), eles apresentam um efeito biológico duradouro, na faixa de dias (RECCHIUTI; SERHAN, 2012; FATTORI et al., 2019; ZANINELLI et al., 2022), demonstrando mecanismos secundários à interação SPM-receptor.

Em linhas gerais, os SPMs desempenham seus efeitos biológico, incluindo analgesia, agindo como agonistas, agonistas alostéricos ou inibidores (FATTORI et al., 2020). Além disso, existe uma relação bem estabelecida entre os níveis dos SPMs em tecidos com os sinais e sintomas de doenças reumáticas, demonstrando o importante papel desses mediadores no bem-estar e qualidade de vida. Por outra lado ainda, esses importantes dados em conjunto com os achados científicos nessa tese, indicam que explorar o processo de resolução da inflamação pode ser uma alternativa terapêutica para inúmeras doenças (ZANINELLI; FATTORI; VERRI, 2021).

Portanto, o conjunto de dados acerca do efeito protetivo desses mediadores e o fato que os eles apresentam atividade terapêutica na faixa de pictogramas, encorajam e dão suporte para o uso de outros SPMs isolados em testes clínicos. Nos próximos tópicos serão revisados a biologia do SPM Resolvina D1 e do sEHi TPPU, para fundamentar o racional para o desenvolvimento dos trabalhos incluídos nessa tese.

Figure 2 – Biossíntese de SPMs e EEts a partir das moléculas provenientes do metabolismo dos ácidos graxos do ômega-6 e ômega 3.

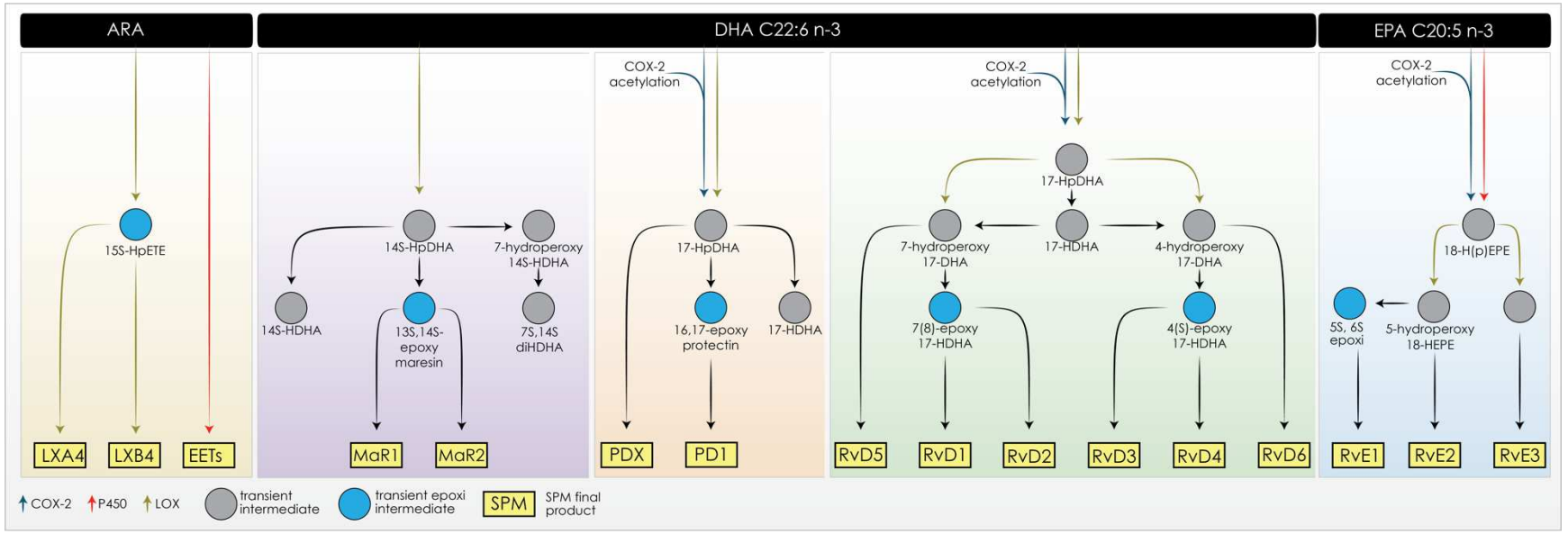

Fonte: adaptado de Fattori *et. al.,* 2022 (FATTORI et al., 2022)

2.5 RESOLVINA D1

A Resolvina D1 (ácido 7S, 8R, 17S-tri-hidroxi-4Z, 9E, 11E, 13Z, 15E, 19Z-docosahexaenóico, RvD1[**Figura 3**]) é sintetizada fisiologicamente pela ação de 15-lipoxigenase, 5-lipoxigenase e hidrolase na molécula de DHA (**Figura 4**) (SERHAN; PETASIS, 2011). Portanto, este SPM faz parte da família das Resolvinas da série D. A RvD1 foi isolada de exsudatos inflamatórios na fase resolutiva decorrentes da inflamação aguda em ambos roedores e humanos (SERHAN et al., 2000, 2002a; HONG et al., 2003). O efeito biológico da RvD1 é obtido principalmente a partir da interação com seus receptores associados a proteína G (GPCR), em murinos o receptor da LXA_4 (ALX/FPR2), e em humanos o GPR32 (MCQUALTER et al., 2010). O papel fisiológico endógeno da RvD1 e outros SPMs são essenciais para o processo resolutivo e controle da inflamação. Por exemplo, em um modelo de inflamação induzido por LPS na glândula submandibular de camundongos, animais nocaute para ALX/FPR2 apresentam maior degradação tecidual quando comparada à animais selvagens (*i.e.,* aqueles com receptor funcional) (WANG et al., 2016). Portanto, embora os mecanismos pelos quais a RvD1 age não são totalmente conhecidos, é racional investigar o papel exógeno dessa molécula no controle dos sinais e sintomas de doenças de caráter inflamatório.

Figura 3 – Estrutura química da RvD1.

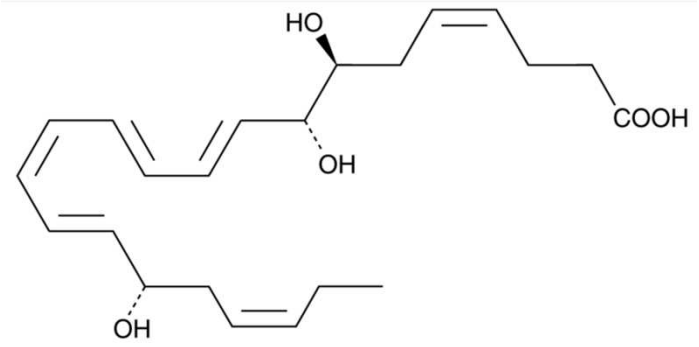

Fonte: PubChem.

Figure 4 – Biossíntese da RvD1.

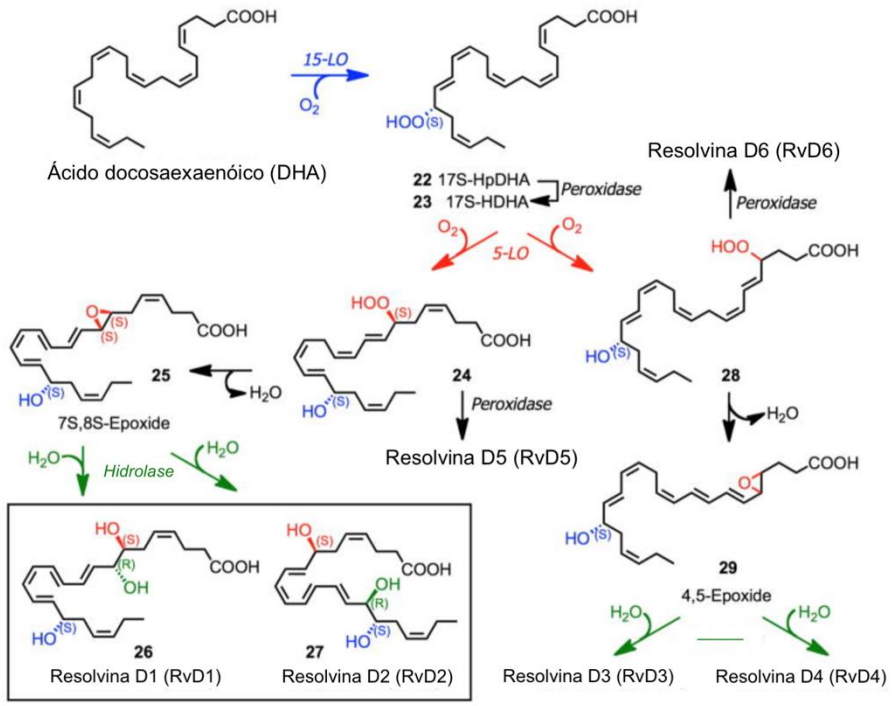

Fonte: Adaptado de *Serhan e Petasis*, 2011

Em modelos de inflamação aguda, tratamentos exógenos com a RvD1 apresentam efeitos analgésicos e anti-inflamatórios. Os efeitos anti-inflamatórios compreendem a regulação da função de macrófagos (DUFFIELD et al., 2006), inibem o recrutamento neutrofílico (SERHAN et al., 2002b; RECCHIUTI et al., 2011; ZANINELLI et al., 2022) e proteção renal contra danos induzidos pela isquemia e reperfusão (DUFFIELD et al., 2006). RvD1 também tem efeito sobre a ativação do NF-κB através de diferentes vias de sinalização, este fato confere a este SPM grande parte de suas propriedades anti-inflamatórias. De fato, em modelo de miocardite induzida por isquemia-reperfusão, o tratamento com RvD1 inibe a via PI3K/AKT e impede a ativação do NF-κB, contribuindo assim para a redução da lesão cardíaca (GILBERT et al., 2015). Neste contexto, o artigo 2 dessa tese (item 3.2) demonstrou que o tratamento *in vivo* com RvD1 reduz a fosforilação do NF-κB em neurônios nociceptores do gânglio da raiz dorsal em um modelo de gota artrite em camundongos (ZANINELLI et al., 2022). Além disso, o tratamento *in vitro* em macrófagos derivados da medula óssea (BMDM) reduziu a fosforilação e translocação desse fator nuclear para o núcleo, acarretando a redução da expressão da proteína adaptadora ASC, componente essencial do inflamassoma NLRP3 (ZANINELLI et al., 2022). Outro

mecanismo do efeito da RvD1 sob a ativação do NF-κB está relacionado ao eixo de sinalização PPAR-γ/NF-κB (LIAO et al., 2012). Este mecanismo foi descrito em um modelo animal de inflamação pulmonar induzido por LPS. Neste contexto, o papel da RvD1 em diminuir o dano tecidual foi revertido a partir da administração do inibidor PPAR-γ (GW9662). Além do mais, a ativação de PPAR-γ, neste contexto, acarretou a diminuição da degradação de IκBα, mecanismo responsável pela diminuição da ativação de NF-κB (LIAO et al., 2012). A ativação de PPAR-γ também tem como efeito a diminuição da hiperalgesia por vias subjacentes. Desta forma, um dos mecanismos da RvD1 em reduzir a dor inflamatória pode ser dependente da via PPAR-γ/NF-κB.

Com relação aos efeitos analgésicos desse mediador, os mecanismos pelos quais a dor é reduzida podem estar relacionados a ações dependentes das características anti-inflamatórias ou diretamente na inibição da sensibilização de neurônios nociceptores. A RvD1 mostrou ser efetora na redução da dor inflamatória induzida por estímulos nóxicos como carragenina, CFA e PGE2 (XU et al., 2010; PARK et al., 2011; XU; JI, 2011). Importantemente, a RvD1 não interfere na percepção normal da dor. Por outro lado, o tratamento com RvD1 também reduz a ativação de canais iônicos TRPA1, TRPV3 e TRPV4 em fibras nociceptivas perante seus respectivos agonistas, em estudos de influxo de Ca2+ in vitro (BANG et al., 2010). De forma similar, no mesmo estudo, RvD1 reduziu a hiperalgesia mecânica e alodinia induzidas por estímulos inflamatórios in vivo (BANG et al., 2010). Além da ativação neuronal, nessa tese foi demonstrado que a RvD1 também reduz a liberação do neuropeptídeo CGRP *in vivo* e *in vitro*, demonstrando um importante papel na modulação de interações neuroimunes (ZANINELLI et al., 2022). Mais efeitos analgésicos e anti-inflamatórios da RvD1 foram revisados minunciosamente em outros trabalhos (FATTORI et al., 2020; ZANINELLI; FATTORI; VERRI, 2021).

Outra importante característica dos SPMs é o efeito analgésico prolongado, um mecanismo que sugere tempo-dependência (HUANG et al., 2011; FATTORI et al., 2018; ZANINELLI et al., 2022). No caso da RvD1, em um modelo de dor pós-operatória induzida por incisão cirúrgica na pata de camundongos, um tratamento intratecal (administração que consiste na injeção de substâncias no canal raquidiano, diretamente no espaço subaracnóide, entre as vértebras) com RvD1 induziu um período de analgesia de 10 dias (HUANG et al., 2011). Os dados apresentados no artigo 2 (item 3.2), corroboram com esse estudo, no qual o pré-tratamento intratecal com RvD1, 72hrs antes do estímulo com MSU foi mais eficaz em

reduzir a dor induzida por cristais de MSU (ZANINELLI et al., 2022). Interessantemente, estudos farmacocinéticos com a RvD1 demonstraram que após a administração intravenosa (i.v.) a meia vida desse mediador é e 4.77 horas em camundongo, e indetectáveis após 8 horas (YELLEPEDDI et al., 2021). Por outro lado, em 5 minutos os níveis desse SPM já tinha atingido os tecidos, nesse caso a glândula salivar submandibular (YELLEPEDDI et al., 2021). De maneira similar o SPM Maresina 1 (MaR1) apresentou um efeito analgésico de 5 dias com um único tratamento intratecal em um modelo de inflamação induzido por adjuvante completo de Freund (CFA) (FATTORI et al., 2018). Todos esses dados dão suporte para mecanismos analgésicos secundários, por exemplo, modificações nos perfis de expressão, que culminam nos efeitos observados. Portanto, conferindo aos SPMs mais uma vantagem para o tratamento de doenças inflamatórias.

De forma geral, é evidente o potencial da RvD1 em controlar a inflamação e coordenar o processo resolutivo (WANG et al., 2016) e analgesia (BANG et al., 2010). Portanto, racionalmente nos propusemos a avaliar a eficácia da RvD1 neste modelo de AG induzida por cristais de MSU *in vivo* e em *in vitro*.

2.6 TPPU

O metabolismo do ácido araquidônico (AA), perante estímulos inflamatórios, é realizado por três vias principais: a via prostaglandina-endoperóxido sintase/cicloxigenase (PTGS/COX), a via lipoxigenase (LOX), e a via do citocromo P450 (CYP). As vias da ciclooxigenase (COX) e lipoxigenase (LOX), com exceção da formação das lipoxinas e AT-lipoxina A4, em grande parte biossintetizam mediadores pró-inflamatórios, enquanto a cascata do citocromo P450 produz tanto metabolitos pró-inflamatórios (WILLIAMS et al., 2010), quanto anti-inflamatórios (IMIG, 2012; SPECTOR; KIM, 2015). Dentre os produtos desta via estão os ácidos epóxieicosatrienóicos (EET [5,6-EET, 8,9-EET, 11,12-EET, e 14,15-EET]) (**Figure 5**) com atividades biológicas anti-inflamatórias (IMIG, 2012; GUAN et al., 2015). No entanto, todos os EET são rapidamente metabolizados em ácidos dihidroxi-eicosatrienóico (DHET) menos ativos pela epóxi hidrolase solúvel (sEH) (WANG; DUBOIS, 2012). Desta forma, o papel anti-inflamatório dos EETs, como a redução da ativação de NF-κB e o aumento da expressão da molécula VCAM – 1 (NODE et al., 1999; CHIAMVIMONVAT et al., 2007), foram demonstrados através da utilização de inibidores de epóxi hidrolase solúvel (sEHi) (AN et al., 2021). Apesar do potente perfil anti-inflamatórios dos metabolitos, esta via não tem sido explorada como um alvo farmacêutico (MARNETT, 2009; HAEGGSTRÖM et al., 2010).

Figura 5 - Biossíntese dos EETs via citocromo P450.

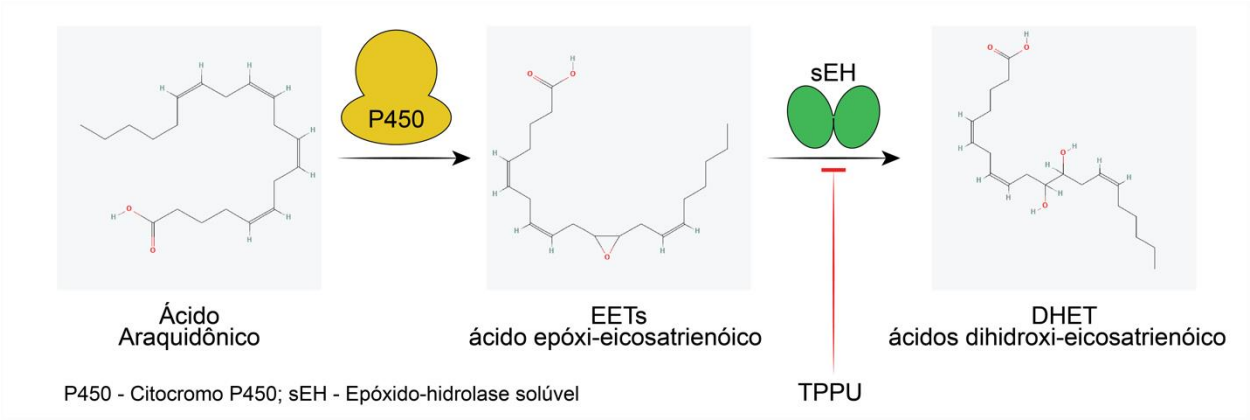

Fonte: o próprio autor.

Diante disso, Rose e colaboradores (2010) desenvolveram e patentearam um composto inibidor de enzimas epóxi hidrolases solúveis, o TPPU (1-

trifluoromethoxyphenyl-3-[1-propionylpiperidin- 4-yl] urea [**Figura 7**]), (ROSE et al., 2010). De fato, a administração do TPPU reduziu a reabsorção óssea induzida por periodontopatógenos (TRINDADE-DA-SILVA et al., 2017). Esses resultados também foram observados em animais nocaute para sEH (sEH-/-). Além disso, estudos para avaliação da farmacocinética, toxicologia e farmacodinâmica deste composto em diferentes animais (roedores, galináceos e primatas) mostrando-se seguros para uso (TSAI et al., 2010; ULU et al., 2012). Ademais, este composto também foi testado em diferentes modelos pré-clinicos apresentando atividade analgésica, anti-inflamatória e protetiva (SASSO et al., 2015; TRINDADE-DA-SILVA et al., 2017, 2020; LUO et al., 2020; TEIXEIRA et al., 2020). O TPPU também foi capaz de diminuir significantemente o comportamento relacionado com a dor em função da expressiva supressão dos marcadores de estresse do reticulo endoplasmático após 30 min da sua administração (INCEOGLU et al., 2015).

Figura 6 – Estrutura química do TPPU.

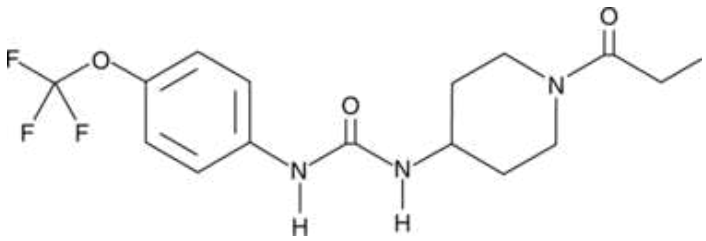

Fonte: PubChem

Contudo, todas essas evidências apontam que o TPPU pode ser eficaz em reduzir a dor e inflamação induzida por cristais de urato monossódico. Portanto, o terceiro artigo desta tese (item 3.3) investigou os efeitos do tratamento com TPPU no modelo de gota em camundongos.

3 METODOLOGIA, RESULTADOS E DISCUSSÃO

Os resultados obtidos que fazem parte dessa tese estão descritos em 4 artigos científicos, sendo que 2 deles já estão publicados, 1 está submetido e 1 está em andamento. Dentre os artigos publicados, 1 foi publicado em periódico Qualis A1 e 1 em Qualis A2. O artigo demonstrando o efeito da RvD1 na artrite gotosa (3.3) foi classificado em 2º Lugar no 24º Prêmio José Ribeiro do Valle da Sociedade Brasileira de Farmacologia e Terapêutica Experimental (SBFTE).

3.1 HARNESSING INFLAMMATION RESOLUTION IN ARTHRITIS: CURRENT UNDERSTANDING OF SPECIALIZED PRO-RESOLVING LIPID MEDIATORS' CONTRIBUTION TO ARTHRITIS PHYSIOPATHOLOGY AND FUTURE PERSPECTIVES. (DOI: 10.3389/FPHYS.2021.729134, PMID: 34539449). PUBLICADO NO PERIÓDICO INTERNACIONAL *FRONTIERS IN PHYSIOLOGY* (FI: 4.134, QUALIS A2, ANEXO I)

3.3 NEW DRUG TARGETS FOR THE TREATMENT OF GOUT: WHAT'S NEW? SUBMETIDO NO PERIÓDICO INTERNACIONAL EXPERT OPINION ON THERAPEUTIC TARGETS (FI: 6.797, QUALIS A1, ANEXO II).

3.3 RVD1 DISRUPTS NOCICEPTOR NEURON AND MACROPHAGE ACTIVATION, AND NEUROIMMUNE COMMUNICATION REDUCING PAIN AND INFLAMMATION IN GOUTY ARTHRITIS IN MICE. (DOI: : 10.1111/BPH.15897, PMID: 35716378) PUBLICADO NO PERIÓDICO INTERNACIONAL *BRITISH JOURNAL OF PHARMACOLOGY* (FI: 9.473, QUALIS A1, ANEXO III)

3.4 INHIBITION OF SOLUBLE EPOXIDE HYDROLASE WITH TPPU AMELIORATES MSU-INDUCED PAIN IN A MOUSE MODEL OF GOUTY ARTHRITIS. ARTIGO EM ANDAMENTO.

Review

3.1 Harnessing inflammation resolution in arthritis: current understanding of specialized pro-resolving lipid mediators' contribution to arthritis physiopathology and future perspectives

Tiago H. Zaninelli[1], Victor Fattori[2], and Waldiceu A. Verri Jr.[1, *]

[1]Laboratory of Pain, Inflammation, Neuropathy, and Cancer, Department of Pathology, Londrina State University, Londrina, PR, Brazil.

[2]Vascular Biology Program, Boston Children's Hospital, Department of Surgery, Harvard Medical School, Boston, MA, United States.

*** Correspondence:** Waldiceu A. Verri Jr. Departamento de Ciências Patológicas, Universidade Estadual de Londrina-UEL, Rod. Celso Garcia Cid, km 380, PR 445, 86057-970, PO Box 10.011, Londrina, Paraná, Brazil. Fax: +55 43 33714387, Phone: +55 43 33714979; waldiceujr@yahoo.com.br; waverri@uel.br.

ORCID

Zaninelli T.H – https://orcid.org/0000-0001-7233-477X

Fattori V. – https://orcid.org/0000-0002-4565-7706

Verri Jr. W.A. – https://orcid.org/0000-0003-2756-9283

Abstract

The concept behind the resolution of inflammation has changed in the past decades from a passive to an active process, which reflects in novel avenues to understand and control inflammation-driven diseases. The time-dependent and active process of resolution phase is orchestrated by the endogenous biosynthesis of specialized pro-resolving lipid mediators (SPMs). Inflammation and its resolution are two forces in rheumatic diseases that affect millions of people worldwide with pain as the most common experienced symptom. The pathophysiological role of SPMs in arthritis has been demonstrated in pre-clinical and clinical studies (no clinical trials yet), which highlight their active orchestration of disease control. The endogenous roles of SPMs also give rise to the opportunity of envisaging these molecules as novel candidates to improve the life quality of rhematic diseases patients. Herein, we discuss the current understanding of SPMs endogenous roles in arthritis as pro-resolutive, protective, and immunoresolvent lipids.

Keywords

rheumatic diseases; DMARDs; SPMs; rheumatoid arthritis; osteoarthritis

1. Introduction

Rheumatic diseases, represented by varied forms of arthritis and other musculoskeletal disorders, affect millions of people around the world. Rheumatoid arthritis (RA), osteoarthritis (OA), septic arthritis, and gouty arthritis are some examples of this painful group of diseases [1] and the focus of this review. Historically, pain in rheumatic disease is mostly attributed to tissue damage mainly due to neutrophil recruitment during the active phase of the diseases [2]. These immune cells are equipped with a vast arsenal of molecules that are released with the aim of protecting the host during infections, for example, but at the same time cause inflammation and pain. The release of pro-inflammatory cytokines such as TNF-α, IL-1β, IL-33, and the process of NETosis are widely known to aggravate arthritis disease status and pain [2]. Recent evidence also suggests that antibody immunocomplex activates nociceptors. By acting on FcγRI and FcγRIIb receptors expressed by mouse $TRPV1^+$ dorsal root ganglion (DRG) neurons, these immunocomplexes induce the release of neuropeptide and activation of nociceptors to produce pain [3].

Arthritis, in their different forms, are traditionally regarded as a life-long disease. As for diabetes, hypertension, and certain forms of cancer, current therapies for arthritis focus on disease control as cure still seems out of reach. Therefore, life-long treatment to control the inflammatory process is required to effectively prevent further cartilage and bone destruction. To the date, disease-modifying anti-rheumatic drugs (DMARDs) are one the current choice (alone or in combination) for the treatment of different types of arthritis [14; 15]. DMARDs can be categorized into conventional synthetic (cs) DMARDs (e.g. methotrexate), biologic (b) DMARDs (anakinra, etanercept) and, most recently introduced, targeted synthetic (ts) DMARDs [Janus Kinase (JAK) inhibitor] [16]. While many patients experience good disease control with DMARDs, a fraction of patients continues to experience significant pain even with low disease activity [17; 18] or in remission [19]. In addition, typical side effects such as increase susceptibility to infections, development of adaptive immunity against the biological agents [2; 14; 15], relapse of active disease, and the concomitant increase of joint pain are not uncommon [20]. Infectious arthritis are treated with a combination of broad-spectrum antibiotic with corticosteroids, immunobiological agents, or opioids for pain management, which might facilitate pathogen spread due to immunosuppression [21; 22; 23]. The high cost and wide range of side effects of these drugs frequently restricts their usage, which highlights this unmet need of new compounds to treat arthritis.

Exogenous administration of different SPMs at low doses has been shown effectiveness at treating pain and infection in experimental models [28; 29; 30]. In oppose to the current

clinically active drugs for arthritis treatment, SPMs present long lasting analgesic and anti-inflammatory effects and are not immunosuppressive compounds [28; 29; 30]. This characteristic of SPMs of blocking pain without immunosuppression rendered the term "immunoresolvent" to this class of molecules. Therefore, we review pre-clinical and clinical data involving SPMs in arthritis as well as the potential outcomes of this knowledge to arthritis therapeutics.

1.1 Specialized pro-resolving lipid mediators (SPMs) and resolution of inflammation

While it is commonly attributed to Hippocrates the use of willow bark to treat the signs of inflammation around 400 Before Common Era (BCE), it is known that the use of willow extracts dates from around 4000 BCE by ancient civilization such as the Assyrians [24]. From then, to the total organic synthesis of salicylic acid (1850s), and later to the acetylation of salicylic acid (1900s), aspirin remains one of the most used drugs [24]. Part of that is attributed to the seminal discoveries of Prof Sergio H. Ferreira and Sir John R. Vane in the field of pharmacology by showing how aspirin works and why it reduces inflammation and inflammatory pain [25; 26; 27]. Drug discovery to treat inflammation and pain, therefore, mainly focused on mimicking aspirin mechanism of action giving rise to the COX-blockers. However, COX-2 acetylation by aspirin changes the activity of this enzyme leading to the production of specialized pro-resolving lipid mediators (SPMs), which are responsible, in part, for the anti-inflammatory and analgesic mechanisms of aspirin. This knowledge makes clear now that stimulation of endogenous pathways involved in the resolution of inflammation can lead to a new road for drug discovery.

The resolution of inflammation is controlled by a time-dependent mechanism of SPM production [31; 32]. A seminal study using an air-pouch model of inflammation induced by TNF-α shows the occurrence of a biosynthetic shift from pro-inflammatory to pro-resolving lipid mediators [31]. This work demonstrates that an increase of lipoxin A_4 (LXA_4) levels correlates with the reduction in PGE_2 production, neutrophil recruitment, and consequently, the resolution of inflammation [31]. SPMs are divided into four main families: the LX, the maresin (MaR), the resolvin (Rv), and the protectin (PD) [28; 33; 34]. Endogenous biosynthesis of SPMs depends on the action of different enzymes to convert arachidonic acid (AA), eicosapentaenoic acid (EPA), docosapentaenoic acid (DPA), or docosahexaenoic acid (DHA) into distinct molecule within the different SPM classes [28; 29; 30]. The biological effects of SPMs are receptor-dependent and occurs via the activation of specific G protein-couple receptors. The receptors and expressing cellular types are summarized in **Table 1.** The

pharmacology of SPMs has been widely explored since several studies demonstrate these molecules might produce an enduring effect. Treatment with LXA_4 72h before stimulus increases the efficacy of this mediator against skin damage induced by ultraviolet B radiation. For RvD1, when treatment is performed before the development of tactile allodynia, RvD1 produces 30 days of analgesic effect in opposed to its limited analgesic effect with treatment at later time points provide limited analgesia [35]. MaR1, on the other hand, upon a single treatment, displays five days of analgesic effect when treatment is performed before stimulus with CFA and three days of analgesia when treatment is performed 24h after the stimulus [36]. In corroboration to our study, Allen and colleagues demonstrated that MaR1 presents 14 days of analgesia after repeated treatments [37]. These sets of data show that isolated SPMs demonstrate time-dependent and long-term efficacy even upon single treatment, which might be useful for the treatment of inflammatory diseases.

Further studies focusing on the immune cell side of the resolution, show that the initial production of SPMs are followed by the recruitment of a distinct subpopulation of pro-resolving macrophages, which correlates with the resolution of inflammation [32]. This was demonstrated using the self-resolving model of peritonitis induced by zymosan (1 mg, ip) [32]. Subsequent studies using the same self-resolving model of peritonitis induced by zymosan (but now using 0.1 mg, ip) by Derek Gilroy's group, shed light on the role and phenotype of these pro-resolving macrophages [38; 39; 40]. These cells possess a unique phenotype that is controlled by cAMP while sharing some markers with M1 macrophages such as iNOS and COX-2 [38]. Transcriptomic analysis reveals that, while the resolution was also achieved after injection of 10 mg of zymosan, a higher number of M1-like macrophages without the acquisition of the pro-resolving phenotype were generated when compared to stimulus with 0.1 mg of zymosan [39]. These results might indicate that hyperinflammatory states possibly compromise host response against subsequent injury and complete resolution [39]. Subsequent analysis 60 days after injection of zymosan (0.1 mg, ip) shows that resolving inflammation changes the immune cell landscape of the peritoneal cavity. This new immune cell landscape provides a more rapid and effective response against secondary tissue injury, indicating the existence of a possible tissue memory mediated by pro-resolving macrophages [40]. Therefore, in addition to the production of SPMs, complete resolution might be only achieved after this third phase of leukocyte recruitment that is mainly dominated by tissue memory-generating macrophages [38; 39; 40].

Table 1 – SPMs and their receptors

SPM Family		SPM	Receptor	Cell type	References
Lipoxins		LXA_4 AT-LXA4	GPR32 ALX/FPR_2	**ALX/FPR2** – macrophage, neutrophil, lymphocyte, natural killer, ILC2. **GPR32** – macrophage, neutrophil, and lymphocyte.	[106]
Resolvins	D-series	RvD1			[107]
		AT-RvD1			
		RvD2	GPR18	Macrophage, neutrophil, neurons, and astrocytes	[108; 109]
		RvD3	ALX/FPR_2	Macrophage, neutrophil, lymphocytes, natural killer, ILC2.	[48]
		RvD5	GPR101	Macrophages, neutrophils and monocytes.	[82]
	E-series	RvE1	ChemR23	Macrophage, dendritic cell, natural killer, ILC2, and neurons.	[110; 111; 112]
		RvE2			
Protectins		PD1/NPD1	GPR37	Macrophage and Neutrophil	[113; 114]
Maresins		MaR1	LGR6	macrophage and neutrophil	[84]

SPMs, Specialized pro-resolving mediators; LXA4, Lipoxin A4; AT-LXA4, aspirin-triggered lipoxin A4; RvD1, resolvin D1; AT-RvD1, aspirin-triggered resolvin D1; GRP32, G Protein-Coupled Receptor 32; ALX/FPR2, G-protein coupled formyl peptide receptor 2; ILC2, type 2 innate lymphoid cells; RvD2, resolvin D2; GPR18, G Protein-Coupled Receptor 18; RvD3, resolvin D3; RvD5, resolvin D5; GRP101, G Protein-Coupled Receptor 101;RvE1, resolvin E1; RvE2, resolvin E2; ChemR23, Chemerin Receptor 23; PD1, protectin D1; NPD1, neuroprotectin D1; GRP37, G Protein-Coupled Receptor 37; MaR1, maresin 1; LGR6, leucine rich repeat containing G protein-coupled receptor 6.

2. SPM levels and arthritis status

2.1. SPM levels and arthritis status in humans

In this section, we discuss the profile and role of SPMs in arthritis. Figures 1 and 2, and **Table 2** summarize our discussion. Despite the common sense of arthritis patients' abilities to predict weather changes, the balance between pro-inflammatory and SPMs could be closely related to this phenotype. Previous studies have shown that the deficiency of 12/15-lipoxigenase, a key enzyme in the synthesis of SPMs, are related to worsened outcome in an arthritis model of K/BxN serum transfer in mice [41]. In corroboration, the overexpression of 15-lipoxigenase reduces inflammation, tissue damage, and increases SPM levels [42]. Those

evidence contributed to the advances in lipidomic research in the last decade, and useful methodologies have been placed to identify and determine levels of lipid mediators in serum or synovial fluid, paving new paths towards understanding its physiological role [43]. In fact, the development of enzyme immunoassay [44] and the application of LC-MS/MS [43] for SPM or their precursors detection were key steps for the understanding of the role and temporal profiling of lipids in diseases in humans and rodents. They might be also used to stratify patients in different phases of disease or even be used as predictive for drug responsiveness. A recent study highlights that plasma levels of SMP are a potential biomarker for DMARD responsiveness in patients with RA [45]. It was found, using supervised machine-learning methodologies, that increased levels of RvD4, 10S,17S-diHDPA, 15R-LXA4, and MaR1 are linked to DMARD (methotrexate, mono or co-therapy) responsiveness in RA patients. If confirmed in a larger clinical study (the comparison in that study was conducted by assessing 36 DMARD responders vs 26 non-responders), these results might provide important insights for clinicians in terms of disease activity, therapy choice and efficacy [45].

Compelling evidence have shown, in fact, that there is a sharp edge between arthritis disease status and lipid mediator levels [44; 46; 47; 48; 49] **(Table 2).** A disbalance in SPMs correlates with the disease aggressiveness or pathogenesis, indicating SPMs might control disease status [48]. In patients with active RA, lower plasma levels of MaR1 are found when compared to patients with inactive RA or the healthy control [46]. Similarly, the levels of RvD1 are decreased in the serum of RA patients and negatively correlated with the connective tissue growth factor (CTGF), which have increased levels in RA patients [47]. In a lipidomic study, serum levels of SPMs are disrupted in patients with RA when compared to healthy controls, levels of RvD3, RvD4, RvE3, 15-epi-LXA_4 (AT- LXA_4), and PGD_2 in healthy controls are increased, whereas in RA patients higher TxB_2 levels were found [48]. This set of data indicate that higher levels of circulating SPMs are found in healthy controls when compared to RA patients (Figure 1). In the synovial fluid, however, patients with osteoarthritis (OA, usually used as negative controls in studies with RA patients) have lower levels of SPMs or pro-resolving precursors when compared to RA patients [44]. Specifically, lower levels of LXA_4, AT-LXA_4, ALX/FPR2 mRNA, and 15-LOX, were observed in comparison to RA patients [44]. Of interest, no heathy subjects were considered in that study and despite patients under treatment were considered, no drastic medication influences were noted [44]. In a similar comparison study, in spite of RA patients have higher levels of SPMs (PD1, LXA_4, and LXB_4) when compared to OA, the levels of LTB_4, and LTB_5 were also higher in RA patients [49]. Furthermore, patients under treatment with NSAIDs, in particular loxoprofen, have higher levels of PGE_2 in

comparison to patients taking celecoxib [49]. These data indicate that while circulating SPM levels are reduced in RA patients (when compared to healthy controls), in the inflammatory foci (joint synovial fluid) higher levels of these lipid mediators can be found (when compared to OA patients) (Figure 1).

Importantly, not only the levels of SPMs are effective in reducing disease symptoms, but also the precursors of those molecules might be related to analgesic and anti-inflammatory outcome. In a cohort study, higher levels of 17-HDHA is negatively correlated to thermic pain in patients with OA and healthy controls, whereas there are no changes in E- or D-series SPM levels [50]. These shed light in the fact that the whole metabolism of polyunsaturated fatty acids and their metabolites play a crucial role in the disease establishment, progression, and control. For instance, in patients with different forms of arthritis the supplementation with n-3 long chain polyunsaturated fatty acids (n-3FA) increases the levels of SPM, which negatively correlates with pain score [51]. This strong evidence demonstrates the endogenous role of SPMs and the importance of these mediators to arthritis. However, there are still several limitations regarding to temporal determination of SPMs in the disease course in human patients.

Table 2 – SPM and other lipid mediator levels in patients with arthritis and healthy subjects

Disease	*n*	Medication	Sample	Method	SPM measured	Observations	References
Rheumatoid arthritis	HC – 30 RA – 30	-	Serum	UPLC-MS/MS	MaR1	Patients with active RA have lower levels of MaR1 than healthy controls, or patients with inactive arthritis.	[46]
	HC – 30 RA – 30	-	Serum	UPLC-MS/MS	RvD1	RA patients have lower levels of RvD1 in the serum compared to healthy controls. RvD1 levels is negatively correlated to connective tissue growth factor, which is elevated in the serum of RA patients.	[47]
	HC – 3 RA – 3	-	Serum	LC-MS/MS	Lipidomic	RA patients have a disruption in SPM levels. Lower levels of RvD3, RvD4, RvE3, AT- LXA_4, and PGD_2, and high levels of TxB_2.	[48]
Rheumatoid Arthritis/ Osteoarthritis	RA – 30	Prednisolone (90%) NSAIDs (83%) Aspirin (13%)	Synovial fluid	ELISA	LXA_4, 15-epi- LXA_4, PGE_2, and LTB_4	OA patients have lower levels of LXA_4, 15-epi-LXA_4, mRNA expression of ALX/FPR2, and 15-LOX, compared to RA patients.	[44]
	OA - 15	Prednisolone (0%) NSAIDs (6%) Aspirin (1%) Statin (1%)					
	RA – 18	NSAIDs (27%) Prednisolone (50%) Other (23%)	Synovial fluid	ESI-MS	Lipidomic	OA patients have lower levels of PD1, LXA_4, and LXB_4. RA patients show higher levels of LTB_4, and LTB_5. Patients under treatment with NSAIDs, in particular Loxoprofen	[49]
	OA – 26	NSAIDs (70%)					

		Acetaminophen (30%)				have higher levels of PGE_2 when compared to patients taking celecoxib.	
Osteoarthritis	HC – 52 OA – 62	-	Serum	LC-MS/MS	Lipidomic	No changes in E-series and D-series SPMs between groups. Thermic pain is associated with the levels of the precursor 17-HDHA.	[50]

17-HDHA, 17-hydroxy docosahexaenoic acid; AT-LXA_4, aspirin-trigged lipoxin A_4; ELSA, enzyme-linked immunosorbent assay; ESI-MS, electrospray ionization-tandem mass spectrometry; HC, Healthy control; LC-MS/MS, liquid chromatography– tandem mass spectrometry; 15-LOX, 15-lipoxygenase; LTB_4, leukotriene B_4, LXB_4, lipoxin B_4; MaR1, maresin 1; NSAIDs, non-steroidal anti-inflammatory drugs; OA, osteoarthritis; PD1, protectin D1; PGD_2, prostaglandin D_2, PGE_2, prostaglandin E_2, RA: Rheumatoid arthritis; RvD1, resolvin D1, RvD3, resolvin D3; RvD4, resolvin D4; RvE3, resolvin E3; UPLC-MS/MS, ultra-performance liquid chromatography-tandem mass spectrometry.

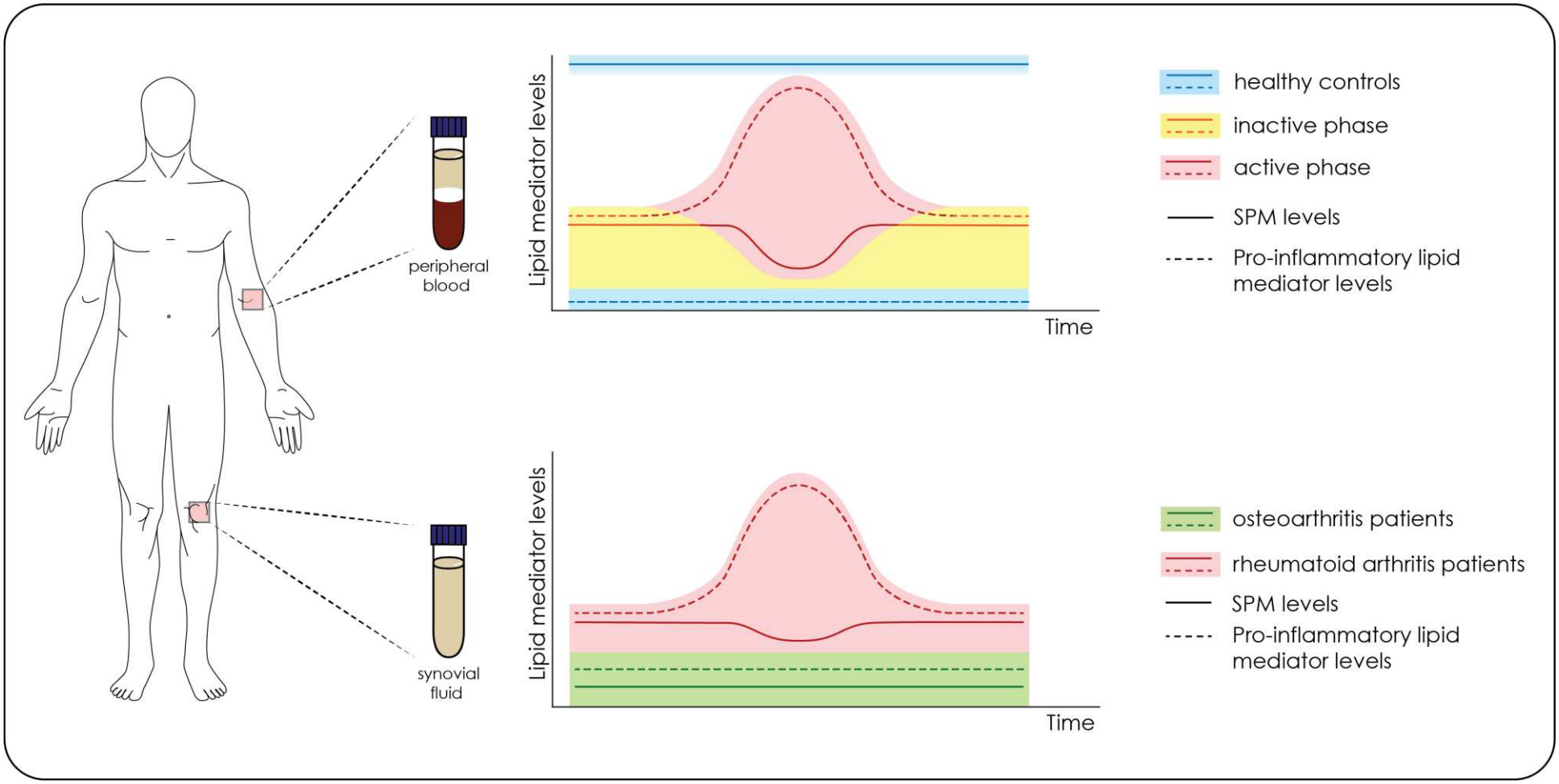

Figure 1. Fluctuation in the levels of SPMs and pro-inflammatory mediators in human samples of serum and synovial fluid. Schematic representation of the fluctuation in the levels of lipid mediators according to the authors' interpretation. In serum samples of healthy controls (in

blue), there are high levels of SPMs and low levels of pro-inflammatory mediators. In arthritic patients, the levels of SPM fluctuate according to the disease phase, which varies between inactive (yellow) and active (red). In the synovial fluid (bottom panel), the levels of SPMs are higher in RA patients (red) in comparison to osteoarthritis patients (green). In contrast, the levels of pro-inflammatory mediators are also higher in RA patients, especially in the active phase.

2.2. *SPM levels and arthritis status in mice*

There are several models (acute and chronic) used to study the pathogenesis of arthritis as well as the mechanisms of novel anti-inflammatory and anti-rheumatic compounds. **Table 3** summarizes the best-known models to study different forms of arthritis with the human symptomatic features phenocopied by them. Serum-transfer of K/BxN mice induces polyarthritis with a T- and B cell-independent component and a major role of neutrophils [4]. This mouse strain expresses the T cell receptor (TCR) transgene KRN and MHC class II molecule A(g7) and spontaneously develop inflammatory arthritis alongside high titers of autoantibodies to glucose-6-phosphate isomerase [4]. Transfer of serum or anti-glucose-6-phosphate isomerase antibodies from K/BxN mice into wild-type mice induces polyarthritis [4]. By contrast, active immunization induces adaptive immunity responsible to the development of polyarthritis in collagen-induced arthritis (CIA) model, which is initiated through intradermal immunization with type II collagen emulsified in complete Freund's adjuvant (CFA) [5; 6]. Another polyarthritis model, the collagen antibody-induced arthritis (CAIA) model is induced by the passive transfer of antibodies, in this case a cocktail of monoclonal antibodies that are directed against conserved autoantigenic epitopes in type II collagen, followed by injection of LPS [6; 7]. The antigen-induced arthritis (AIA) model is another one that is induced by an immunization of the animal. Ovalbumin or, mainly, methylated bovine serum albumin (mBSA) mixed in CFA are the most frequently used antigens. Monoarthritis is induced after a local challenge (usually the knee joint is chosen) with the same antigen [8; 9]. Septic arthritis is highly aggressive and with rapidly progression type of infectious arthritis. *Staphylococcus aureus* is the most common causative agent of septic arthritis. Knee joint injection of *S. aureus* induces chronic pain and extensive joint damage and can be used to study this type of infectious arthritis [10; 11]. Intravenous injection of the bacteria is also used to induce transient bacteremia or sepsis with a percentage of animals developing septic arthritis [12; 13]. However, the induction of sepsis due to systemic bacterial injection might be a confounder for studying the analgesic effect of new compounds.

In mice, a temporal regulation of lipid mediators was also recently established [48]. This study demonstrates the resolution phase lipid class switch, and more importantly, the role of the SPMs in arthritis resolution and regulation [48] (Figure 2). In the K/BxN RA model, local joint inflammation starts after the second serum injection, and is accompanied with joint leukocyte recruitment, redness, and edema. Because this is a self-resolving model, 11 days after serum challenge, the resolution phase starts with the reduction of inflammation and clinical score [48]. Lipidomic analysis reveals that after challenge, an increase in pro-inflammatory

eicosanoids and concomitant decrease in most SPMs is observed [48]. In fact, as clinical manifestation starts, the levels of PGE_2, PGD_2, TXB_2, and LTB_4 increases in the paw tissue. Interestingly, 16 days after challenge, a robust lipid mediator class switch restores the levels of SPMs found in the naïve animals, healthy controls. In the resolution phase, D-series Rv (such as RvD1, RvD2, RvD3 and RvD4), MaR1, and PD1, have their levels restored [48]. Moreover, a second K/BxN serum challenge disrupts resolution phase, maintains the clinical score, and levels of pro-inflammatory lipid mediators, limiting the temporal class switch and delaying resolution (Figure 2).

In conclusion, pre-clinical and clinical data **(Table 2)** demonstrate that the fluctuation in SPMs levels has an inverse correlation to arthritis status and associated symptoms. Therefore, boosting SPM levels might be a potential approach for the treatments of rheumatic diseases.

Table 3 – Animal models of arthritis

Duration	Model	Stimulus (route)/Previous immunization	Mono or polyarthritis	Human phenocopied symptoms	References
Acute	Gout	MSU crystals (intra-articular, knee joint)	Monoarthritis	Increased pro-inflammatory cytokine production in the knee joint Synovial inflammation Pain	[115]
	Zymosan	Zymosan (intra-articular, knee joint)	Monoarthritis		[116]
	LPS	LPS (intra-articular, knee joint)	Monoarthritis		[117; 118]
Chronic	AIA	mBSA (intra-articular, knee joint)/immunization with CFA	Monoarthritis	Adaptive and innate component Cartilage destruction Increased cytokine production in the knee joint Synovial inflammation	[3; 9]
	CAIA	Cocktail of monoclonal antibodies (intravenous)	Polyarthritis	Adaptive and innate component Antibodies against cartilage epitopes Cartilage destruction Chronic synovial inflammation	[7; 119]

			Increased cytokine production in the knee joint	
CIA	Type II collagen (intravenous)/immunization with CFA	Polyarthritis	Adaptive immune component Antibodies against Bone and cartilage destruction Chronic synovial inflammation Joint-specific epitopes Synovial inflammation	[5; 120]
K/BxN	Serum transfer containing anti-GPI antibodies (intraperitoneal)	Polyarthritis	Cartilage and bone destruction Innate component Pain Synovial inflammation	[4; 121]
Prosthesis-related	TiO_2 (intra-articular, knee joint)	Monoarthritis	Cartilage destruction Increased cytokine production in the knee joint Innate component Pain Synovial inflammation	[122]
Septic arthritis	*Staphylococcus aureus* (intra-articular, knee joint)	Monoarthritis	Bacterial growth and spread Cartilage and bone destruction Chronic synovial inflammation Pain Synovial inflammation	[10]
	Staphylococcus aureus (intravenous)	Polyarthritis		[12; 13; 123]

AIA, adjuvant-induced arthritis; CAIA, collagen antibody-induced arthritis; CFA, complete Freund adjuvant; CIA, collagen-induced arthritis, LPS, lipopolysaccharide; MSU, monosodium urate; TiO_2, titanium dioxide.

3. Endogenous SPM's role and levels in arthritis guiding possible therapeutic approaches

The contemporary understanding of the inflammation resolution process transformed the field and opened novel avenues to a diverse niche of therapeutic possibilities. Also, The publication of web-based resource named as Atlas of Inflammation Resolution [52] is also an important step toward elucidating the process during the resolution process. This website provides a molecular interaction map that allows users to visualize molecular pathways relevant to inflammation and its resolution. These tools might allow a better understanding of the resolution process and the potential uses and properties of SPMs. The endogenous SPMs play important roles in the course of rheumatic diseases, as described above. Endogenous SPMs are effective in limiting inflammation, protecting joint damage, therefore decreasing arthritis pain. In fact, supplementation with omega-3 fatty acids or SPM precursors have shown efficacy in clinical trials [30]. Altogether, those facts elicited the possibilities of SPM exogenous administration in therapeutic approaches. In fact, there were attempts to test clinically the role of RvE1 in the dry eye syndrome (clinicaltrials.gov identifier: NCT01675570, NCT00799552). Despite the completion of the clinical studies, up to this point, no final results were published. Focusing on pain, a major symptom in rheumatic conditions, evidence have shown that SPMs can block nociceptor activation, hence decreasing pain (revised [30; 36; 37].

Although peripheral inflammation fluctuates between asymptomatic and symptomatic periods, the pain is still commonly persistent between those phases [37]. In the K/BxN-induced self-resolving rheumatoid arthritis model, even after resolution of joint inflammation, pain is persistent [37; 53]. By establishing the lipid profile in the dorsal root ganglia (DRG) neurons (where the cell body of joint-innervated nociceptors are located), Allen and colleagues show that after arthritis resolution there is a decrease in the levels of MaR1 in the DRG. This is followed by M1 macrophage infiltration in the DRG and cytokine production (IL-1β and TNF-α) leading to neuronal activation and hyperalgesia. Treatment with MaR1 reduces mechanical hyperalgesia, DRG M1 macrophage infiltration, and decreases cytokine expression in a receptor-dependent manner [37]. Similarly, persistent hyperalgesia is also observed after diseases resolution in the animal model of mBSA antigen-induced monoarthritis [54]. This phenotype is due to elevated levels of TNF-α in the knee joint-innervated DRG, which might possibly be modulated by pro-resolving molecules. Although limited, the literature supports the important role of endogenous SPMs in the control of arthritis. Furthermore, these findings suggest the use of SPMs in therapeutic approaches, and its suitability for the development of novel treatments to arthritis (Figure 2). Thus, in this section, we focus on preclinical data showing the endogenous physiopathological role and therapeutic potential of SPMs in arthritis-

driven inflammation and pain. The pro-resolving properties are described based in the precursor molecule, *i.e.,* AA, DPA, DHA, or EPA. **Table 4** summarizes our discussion.

3.1. AA-derived SPMs

The AA is rapidly correlated to inflammation and fever. However, under the action of different enzymes, AA is metabolized in lipids with anti-inflammatory, analgesic, and pro-resolutive proprieties, such as, epoxyeicosatrienoic acids (EETs) [55], prostaglandin D_2 (PGD_2), 15deoxy-$\Delta^{12,14}$-prostaglandin J2 (15d-PGJ_2), and lipoxins.

EETs are precursors for several SPMs [56], including lipoxins. Administration of 14,15-EET inhibits bone resorption and osteoclastogenesis in ovariectomy-induced bone loss in rats. In addition, treatment with it decreases RANKL:OPG ratio and inflammatory cytokine. *In vitro*, 14,15-EET treatment in RAW264.7 and bone marrow mononuclear cells, suppresses RANKL-induced osteoclast differentiation, and reduces the activation of several osteoclastogenesis pathways. Altogether, the data points to this lipid as possible therapeutic strategy for osteoclast-related disorders, such as arthritis [57].

In spite the potent effects, ETTs are rapidly metabolized by soluble epoxy hydrolase (sEH) in ineffective molecules. Considering the instability of the compound, a therapeutic approach relaying in the use of soluble epoxy hydrolase inhibitors (sEHi), which potentialize endogenous ETT effects and SPM synthesis, can be useful. Interestingly, the administration of ETT, or sEHi have similar effects in suppressing RANKL-induced osteoclast [57]. In dogs with self-occurring osteoarthritis, pain was reduced upon administration of the sEHi EC1728 [58]. In addition, the administration of a mixture of EETs to canine chondrocytes increases cell viability and reduces IL-6 and TNF-α expression. In another study, the effects of daily treatment with the sEHi 1-trifluoromethoxyphenyl-3-(1-propionylpiperidin-4-yl) urea (TPPU) ameliorates mechanical hyperalgesia, edema, histopathological score, and cartilage destruction in the CIA model. In addition, the administration of TPPU reduces Th1- and Th17-related pro-inflammatory cytokines, while increasing Treg cells cytokine profile expression [59], demonstrating the therapeutic potential and immunoresolvent proprieties of ETTs in arthritis.

Downstream AA metabolization, prostanoids are a major group comprehending for example, prostaglandin E_2 (PGE_2), prostaglandin D_2 (PGD_2), and its degradation product, the 15-deoxy-$\Delta^{12,14}$-PGJ2 (15d-PGJ2). PGD_2 has been described to have a complex role in inflammation, with pro- and anti-inflammatory effects in differences circumstances [60]. In a model of CIA, the levels of PGD_2 increase in a time-dependent manner, accompanied by the

increase in the expression levels of its metabolization enzymes (hematopoietic PGD synthase and lipocalin-type PGD synthase), and its receptors (PD1 and PD) [61]. In corroboration, the administration of PD1 antagonist (MK0524) augments arthritis incidence and severity, increases levels of IL-1β, CXCL-1, and PGE_2, whereas reduces the levels of IL-10. On the other hand, the administration of PGD_2, or PD1 agonist (BW245C) significantly reduce arthritis incidence, inflammation response and joint damage, indicating the contribution of anti-inflammatory AA metabolites to the control of pain.

15d-PGJ_2 is a natural and potent agonist of peroxisome proliferator–activated receptor γ (PPARγ) and is well described to have anti-inflammatory actions [62; 63]. In the arthritis perspective, 15d-PGJ_2 ameliorates the outcome of CIA in rats by decreasing paw volume, arthritis score, mononuclear cell infiltration, and pannus invasion [64]. In a similar study, the cyclopentenone administration also reduces CIA clinical, histopathological and radiographic scores, edema, and CIA-induced lipid peroxidation [65]. In human synovial fibroblast, the treatment with 15d-PGJ_2 reduces TNF-α-induced matrix mieloproteinase-13 expression in culture. While an agonist of PPARγ the lipid inhibits NF-κB translocation to nucleus in a PPARγ-independent manner by acting on IKK activation, indicating it can promote anti-inflammatory effect by targeting multi-pathways [66]. In human osteoarthritic chondrocytes, treatment with 15d-PGJ_2 blocks PGE_2 production with a milder effect on COX-2 expression. Interestingly, in the presence of 15d-PGJ_2 independent of a COX-2 inducer, the enzyme levels are increased [67]. Interestingly, pharmaceutical formulation with 15d-PGJ_2 have proven to be even more effective [68; 69; 70; 71]. Nanocapsules loaded with 15d-PGJ_2 ameliorate MSU-induced pain and inflammation in a model of gouty arthritis. The treatment reduces mechanical hyperalgesia, edema, leucocyte recruitment to the knee joint, pro-inflammatory cytokines, and oxidative stress. The effects were all PPARγ-dependent [68]. These data support that 15d-PGJ_2 resolves inflammation by acting in different pathways in relevant cells in the context of arthritis.

The lipoxins are the first described SPMs [72], and the first lipid mediators of the endogenous anti-inflammatory and resolutive machinery [73]. In fact, in a model of CIA, the levels of Lipoxin A_4 (LXA_4) increase according to diseases progression achieving its peak on the resolution phase onset [74]. Although, endogenous levels are important, the treatment with LXA_4 has a protective effect in a model of zymosan-induced arthritis [75]. Local treatment with LXA_4 reduces edema and leucocyte recruitment in a receptor-dependent manner as treatment with BOC-1, an ALX/FPR2 receptor antagonist, abrogates LXA_4 effects. In addition, treatment with BML-111, a potent ALX/FPR2 agonist, also decreases immune cell recruitment to the

knee joint [75; 76]. Complementarily, the administration of aspirin increases the levels of lipoxins (*i.e.,* AT-LXA_4), thus reducing the inflammation also in a receptor-dependent fashion. The potent anti-inflammatory and analgesic effects of AA-derived SPMs and their receptor-mediated action allows the development of new formulations and novel drug candidates for the control of arthritis symptoms and progression.

In conclusion, AA-derived SPMs include EETs, prostaglandins, and lipoxins, have been shown to have pro-resolving effects in arthritic-related psychopathological events, by decreasing inflammation, cytokine and chemokine levels, osteoclast activation, bone degradation, and importantly reducing arthritis-related pain.

3.2. DPA/DHA-derived SPMs

The D-serie lipid mediators comprehend Rvs, MaRs, and PDs, which have been shown to act in the reduction of inflammation, activation of non-phlogistic macrophages, or direct blockage of neuronal activity [77]. In arthritis, the effect of RvD1, AT-RvD1, RvD3, RvD5, and MaR1 were tested in animal models.

In arthritis, the persistent inflammation could lead to extended joint destruction, bone resorption, and function loss [78]. As such, the relevance of RvD1, an agonist of GPR32 and ALX/FPR, was primarily described by its *in vitro* action in human osteoarthritic chondrocytes [79]. Treatment with it suppresses IL-1β-induced expression of COX-2, inducible nitric oxide synthase (iNOS) and metalloproteinase-13 (MMP-13), which results in lower levels of PGE_2 and nitric oxide (NO) production accompanied by the reduction in of NF-κB-p65, p38/MAPK, and JNK phosphorylation [79]. In addition to act reducing inflammation, RvD1 also reduces 4-hydroxynonenal (HNE)-induced apoptosis, suppressing caspase-3 activation and lactate dehydrogenase (LDH) release and increases Bcl2, AKT, and GSH [79]. RvD1 reduces the differentiation of macrophages in osteoclasts inhibiting the expression of tartrate resistant acid phosphatase (TRAP) and cathepsin-K [80]. Treatment with it also decreases the expression of inflammatory molecules such as, TNF-a, RANK, and PGE_2, and increases IL-10 [80]. In summary, the data indicate that *in vitro* experiments in the context of arthritis, RvD1 reduces inflammatory pathways while increase anti-apoptotic ones, giving confidence for a novel *in vivo* therapeutic approach.

In vivo, RvD1 reduces CIA clinical score, inflammation, bone and joint destructions [80] while other study show that this SPM reduces angiogenesis and decreases the expression of connective tissue growth factor (CTGF), and levels of IL-6, TNF-α, and IL-1β [47; 80].

Using fibroblast-like synoviocyte culture, treatment with RvD1 lowers the levels of CTGF and reduces the cellular proliferation. Mechanistically, RvD1 upregulates the expression of miRNA-146a-5p, which was proven to decrease the levels of inflammatory molecules and CTGF, *in vivo* and *in vitro* via the inhibition of STAT3 activation [47]. Altogether, this data shed light in the protective effect of RvD1 to arthritis progression and related bone disorders [80]. The systemic delivery of aspirin-trigged analog, AT-RvD1, or 17(R)-RvD1 is also described to reduced CFA-induced arthritis hyperalgesia and cytokines expression (TNF-α and IL-1β) [81].

RvD3 is another GPR32 and ALX/FPR agonist that is also described to resolve preclinical arthritis [48]. In the K/BxN arthritis model, treatment with RvD3 decreases the arthritis clinical score, edema, and leucocyte recruitment. Importantly, the exogenous administration, was also effective to reduce the levels of LTB_4, PGE_2, PGD_2, $PGF_{2\alpha}$, TXB_2, and 8-iso-$PGF_{2\alpha}$. In animals lacking ALX/FPR2/3 receptor, the effects of RvD3 were abolished, indicating its effects are dependent on that receptor [48]. Similarly, RvD5 reduces prostaglandin and LTB_4 levels and improves arthritis clinical score, edema and weight loss, by signaling via its receptor GPR101 in the K/BxN model [82]. However, an important point regarding RvD5 is the demonstration of its lack of analgesic effect in female mouse [83] . Considering the higher incidence of rheumatoid arthritis in women, treatment with RvD5 would have this drawback compared to other analgesic SPMs.

Compelling evidence have shown that MaR1, an agonist of LGR6 receptor [84], have analgesic, anti-inflammatory, and neuroprotective proprieties [36; 85; 86; 87]. In the K/BxN model, lower endogenous levels of MaR1 in the DRG correlates with persistent mechanical hyperalgesia and systemic delivery of it, either before or after the clinical signs of self-resolution, significatively reduces mechanical hyperalgesia [37]. In addition, MaR1 inhibits macrophage recruitment to the DRG and reduces the population of M1 macrophages, contributing to pain reduction [37]. Regarding its effect on neurons, previous work of our group demonstrated that MaR1 reduces CGRP release in cultured DRG and TRPV1 activation-induced calcium influx *in vivo* [36]. By this neuronal regulation, intrathecal treatment with MaR1 reduces the peripheral recruitment of inflammatory neutrophils and macrophages, reducing in addition to pain, peripheral inflammation [36]. In corroboration, Allen and colleagues demonstrated that MaR1 also reduces calcium influx induced by capsaicin (TRPV1 agonist) in a GPCR-dependent manner and CGRP release [37]. In another study, CIA-associate clinical score and cytokine profile were abrogated with MaR1 treatment [46]. The

administration of MaR1 reduces the levels of TNF-α, IL-β, IL-6, IFN-γ, IL-17, and increases the levels of IL-10 and TGF-β. Further, the number of Th17 cells were reduced, whereas the number of Treg cells were increase with the treatment. There are strong evidence that RA patients have increased number of Th17 cells and decreased proportion of Treg cells [88; 89]. The unbalance in Treg/Th17 ratio contributes to triggering autoimmunity and inducing inflammation [88]. In terms of mechanism, treatment with MaR1 induces the overexpression of miR-21, which increases Treg cell number and restore Treg/Th17 balance, therefore improving disease outcome [46].

In addition to the isolated D-serie SPMs biologic activity, here reviewed, metabolomic pathways also generate pro-resolving sulfido-conjugates, which are effective in elicit pro-resolving phagocyte functions and tissue regeneration [90; 91; 92; 93]. Despite the effect that MaRs-, PDs-, or Rvs-conjugates in tissue regenerations (CTR) were not explored in rheumatic diseases, this recent described branch of pro-resolving mediators might add to novel approaches for the treatment of arthritis, enlarging clinical perspectives of these classes.

In summary, the presented pre-clinical data highlight the important endogenous role of D-serie Rvs, MaRs, and PDs in the control of arthritis symptoms. The current literature demonstrates a series of protective effects, in which the SPMs orchestrate the resolution of the inflammatory process, by decreasing the expression and/or release of pro-inflammatory cytokines, chemokines, and lipid mediators. Furthermore, *in vitro* or *in vivo* treatment diminish the differentiation and activation of osteoclasts, which decrease bone degradation. Combined, the pro-resolutive, protective, immunoresolvent and analgesic properties of D-serie SPMs improve the overall disease outcome.

3.3. EPA-derived SPMs

The E-serie resolvins include RvE1, RvE2, and RvE3. While their anti-inflammatory effects have been demonstrated in models of asthma [94], atherogenesis [95], and dry eye syndrome [96], and analgesic effects in models of inflammatory pain [97]; these mediators have not been tested in rheumatic disease models. *In vitro*, however, treatment with RvE1 suppresses RANK-L-induced RAW264.7 differentiation in osteoclasts, reduces the expression of osteoclast-related genes, and decreases the process of bone reabsorption. Furthermore, RvE1 inhibits IL-17-induced expression of RANK-L, COX-2, and PGE_2 synthesis. These data indicate that RvE1 act on pathways that interfere with osteoclast differentiation and bone reabsorption, which might indicate that E-serie Rv could be effective in reducing arthritis

symptoms. However, it remains to be determined whether *in vivo* effects during arthritis are observed with any of the RvE.

4. Conclusions and future perspectives

Focusing on the therapeutic point of view, we envision at least 4 different SPM-based therapeutic approaches based on their pathophysiological roles in arthritis: **1)** Development of more stable SPM analogues. BML-111 (a LXA4 analog) and benzo-diacetylenic-17R-RvD1-methyl ester (RvD1 analog) are examples that we can highlight. These compounds are the agonists of ALX/FPR2 and GPR32, respectively. BML-111 has demonstrated activity in two different models of arthritis [76] and therefore the development of novel and stabler analogues might help overcome the issue of SPM half-life. RX-10045 is an example that reached clinical trials. RX-10045 is a pro-drug for a RvE1 analogue that has been tested for dry eye syndrome. **2)** Development of pharmaceutical formulations to improve the effect of SPMs or their analogues. Since SPM can be rapidly metabolized, the development of systems aiming at protecting or enabling targeted delivery of SPM might be useful. For instance, SPM-loaded nano capsules or ectosomes in addition to the use of polymeric nanoparticles might help overcome this issue. For instance, 17(R)-RvD1- or a lipoxin analogue (benzo-LXA4)-loaded ectosomes accelerates wound healing and reduces CFA-induced temporomandibular joint [98]. Another example is the utilization of an engineered polymeric nanoparticle containing the Ac2-26 (an ANXA1 mimetic peptide). This system has demonstrated efficacy by promoting wound repair in a model of colitis [99]. **3)** Development of pro-resolving small molecules. Given SPM receptors are G protein-coupled receptors (GPCRs), the discovery of novel orthosteric agonists (binds to the same site as the endogenous ligand), positive allosteric modulators (binds to a different site and increases the activity of the endogenous ligand), or small molecules with the ability of inducing biased agonism (activates a specific signaling pathway of a given GPCR) are also interesting and promising alternative for stimulating resolution pathways. **4)** Development of SPM catabolism blockers. Like monoamine oxidase inhibitor (MAOI) drugs used for depression and in some cases chronic pain, the discovery of compounds with the ability of targeting enzymes that promote SPM catabolism might be useful to increase endogenous or exogenous SPM availability and thereby their effect. As we discussed above, evidence supports that disease severity correlates with low levels of SPMs, thus, enhancing their levels might be a manner of improving patient well-being by enhancing endogenous SPMs levels.

Interestingly, SPMs might be also useful for infectious arthritis. If not by bactericidal effect *per se*, SPMs stimulate the phagocytosis and clearance of different pathogens. For

instance, RvD1 synergizes with ciprofloxacin to promote the non-phlogistic phagocytosis of *Pseudomonas aeruginosa* during lung infection [100] and against *Escherichia coli* [101]. Similarly, other SPMs such as RvD2 [102], MaR1 [103], or PDX [104] decrease local and systemic bacterial burden, which leads to increased survival in model of sepsis. These effects could be helpful because: **i)** new resistant mechanisms are constantly being developed by microorganisms, and therefore, compounds that block pain and actively fight infection are likely to be more effective. **ii)** Some antibiotics, such as the β-lactam, induce bacteriolysis releasing LPS and LTA that can induce post-infectious sequalae due persistent activation of immune cells [105]. Therefore, in addition to block pain, SPMs enhance bacterial clearance, lower antibiotic requirements, and shorten resolution time interval [101]. These effects can contribute to reduce antibiotic resistance and post-infectious sequelae.

Concluding, in the past decades, the advent of SPM characterization allowed the establishment of their pivotal endogenous role in different disease status and symptomatology. There are pre-clinical and clinical evidence that arthritis initiation, symptoms development, and its resolution line up well with the fluctuation in endogenous SPMs levels in a manner that low levels of SPMs correlate with disease severity. In turn, using the reverse approach, treatment with/replenishing/diminishing the metabolization of AA-, DHA/DPA-derived SPMs was demonstrated to improve overall disease outcome, effectively reducing inflammation, pain, and bone destruction. Those lipids reprogram immune cells, block neuronal activity, or modulate the host response, without compromising the immune system or offering undesired side effects. Thus, the understanding of SPMs endogenous roles in arthritis has open novel venues for better understanding the disease itself, therapeutic approaches, and monitoring disease activity and treatment efficac

1

Table 4 – Pre-clinical effects of SPMs in rheumatic conditions

	Mediator	Species	Model/Stimulus	Dose or concentration	Route	Outcome	Reference
AA	14,15-EET	Mouse	Ovariectomy-induced bone loss	17 mg/kg	i.p.	Inhibits osteoclastogenesis and bone loss. Decreases RANKL:OPG ratio and inflammatory cytokines	[57]
		in vitro – Raw264.7 macrophages	RANKL	2 μM	-	Suppresses RANKL-induced osteoclast differentiation, phosphorylation of NF-kB, ERK, and JNK. Prevents the production of reactive oxygen species.	
	EC1728 (sEHi – EET indirect)	Dog	Self-occurring arthritis	5 mg/kg	p.o.	Decreases pain.	[58]
	ETT mixture	*in vitro* – canine chondrocytes	IL-1β	0.4 μg/mL	-	Increases cell viability and decreases levels of TNF-a and IL-6.	

TPPU (sEHi – EET indirect)	Mouse	CIA	10 mg/kg	p.o.	Ameliorates hyperalgesia, histopathological score, and cartilage destruction. Decreases Th1- and Th17-related cytokine levels and increases Treg-related ones.	[59]
PGD_2	Mouse	CIA	0.6 mg/kg	i.pl.	Reduces immune cell infiltration, bone erosion, and arthritis incidence.	[61]
15d-PGJ2	Rat	CIA	10 μg/kg	i.p.	Decreases paw volume, arthritis score, mononuclear cell infiltration, and pannus invasion.	[64]
	Mouse	CIA	30 μg/kg	i.p.	Decreases clinical, histopathological and radiographic scores, edema, and lipid peroxidation.	[65]
	in vitro – human synovial fibroblasts	TNF-α	1-3 μM	-	Reduces MMP-13 expression and NF-kB activation.	[66]

		in vitro – human osteoarthritic chondrocytes	IL-1β	10 μM	-	Blocks PGE_2 synthesis, and partially reduces the expression of COX-2.	[67]
	15d-PGJ2 nanocapsule	Mouse	Gouty arthritis/MSU crystals	30 ug/kg	s.c.	Reduces mechanical hyperalgesia, edema, leucocyte recruitment, oxidative stress, pro-inflammatory cytokines, and mRNA expression of NLRP3 inflammasome components. Increases levels of IL-10.	[68]
		in vitro – bone marrow-derived macrophages.	MSU crystal	3 μM	-	Decreases IL-1β release.	
	LXA_4	Mouse	Zymosan-induced	20 ng	i.a.	Reduces edema and leucocyte recruitment.	[75]
DPA/DHA	RvD1	*in vitro* – human	IL-1β	10 μM	-	Suppress COX-2, iNOS, and MMP-13 expression. Reduces PGE2 and NO levels.	[79]

osteoarthritic chondrocytes.	HNE	10 μM	-	Reduces apoptosis, caspase-3 activation and lactate LDH release. Increases the levels of Bcl2, AKT, and GSH.	
Mouse	CIA	100 ng	i.v.	Decreases angiogenesis and CTGF levels. Increases miRNA-146a-5p expression.	[47]
in vitro – fibroblast-like synoviocyte	-	100 nM	-	Decreases the expression of pro-inflammatory cytokines and CTGF by upregulating the expression of miRNA-146a-5p and inhibiting STAT3 activation.	
Mouse	CIA	500 ng	i.p.	Attenuates clinical score, cartilage degradation, and bone resorption. Decreases synovial proliferation, serum markers of cartilage and bone damage, and inflammatory mediators.	[80]
In vitro – Raw264.7	LPS M-CSF	500 nM	-	Reduces osteoclast differentiation, expression of	

		RANK-L			inflammatory mediators, and bone erosion.	
AT-RvD1	Rat	CFA-induced arthritis	100 ng	i.p.	Decreases mechanical hyperalgesia and levels of pro-inflammatory cytokines (TNF-α and IL-1β).	[81]
RvD3	Mouse	K/BxN serum	100 ng	i.p.	Decreases arthritis clinical score, edema, and leucocyte recruitment. Reduces local eicosanoid levels (e.g. LTB_4, PGE_2, and TXB_2) in an ALX/FPR2-deperndent manner.	[48]
RvD5	Mouse	K/BxN serum	150 ng	i.p.	Reduces arthritis clinical score, edema, arthritis-induced weight loss, and levels of prostaglandin and LTB_4. The effects were dependent of GPR101 receptor.	[82]
MaR1	Mouse	K/BxN serum	100 ng	i.p.	Attenuates mechanical hypersensitivity; reduces	[37]

						monocyte/macrophage infiltration in the DRG.	
		Mouse	CIA	100 ng	i.v.	Reduces arthritis clinical score, and pro-inflammatory cytokine levels (TNF-α, IL-β, IL-6, IFN-γ, IL-17A). Increases levels of IL-10, TGF-β, and miR-21. Regulates Treg/Th17 balance.	[46]
EPA	RvE1	*in vitro* – Raw264.7	RANKL	100 nM	-	Reduces osteoclast differentiation, bone resorption, and expression of osteoclast-related genes. Decreases IL-17-induced expression of RANKL, COX-2 mRNA, and synthesis of PGE_2.	[124]

AA, arachidonic acid; AKT, protein kinase B; AT-RvD1, aspirin-trigged Resolvin D1; Bcl2, B-cell lymphoma 2; EET, epoxyeicosatrienoic acid; 15d-PGJ_2, 15-deoxy-delta-12,14-prostaglandin J_2; CIA, collagen-induced arthritis; COX-2, cyclooxygenase-2; CTGF, connective tissue growth factor; DHA, docosahexaenoic Acid; DPA, docosapentaenoic acid; DRG, dorsal root ganglia; ERK, extracellular-signal-regulated kinase; GSH, reduced glutathione; HNE, 4-hydroxy-2-nonenal; i.a., intra-articular; i.p., intraperitoneal; i.pl., intraplatar; i.v. intravenous; IFN-γ, interferon-gamma; IL-10, interleukin-10; IL-17, interleukin-17; IL-1β, interleukin-1β; IL-6, interleukin-6; iNOS, inducible nitric oxide synthase; JNK, c-Jun N-terminal kinase; LDH, lactate dehydrogenase; LPS, lipopolysaccharide; LTB4, leukotriene B4; M-CSF, macrophage colony-stimulating factor; MaR1, maresin 1; MMP-13, matrix metalloproteinase-13; MSU, monosodium urate; NF-κB, nuclear factor-κB; NLRP3, NLR Family Pyrin

Domain Containing 3; NO, nitric oxide; OPG, osteoprotegerin; p.o., per oral; PGD_2, prostaglandin D_2; PGE_2, prostaglandin E_2; RANKL, receptor activator of nuclear factor-kappa B ligand; RvD1, resolvin D1, RvD3, resolvin D3; RvD5, resolvin D5; RvE1, resolvin E1; s.c., subcutaneously; sEHi, soluble epoxy hydrolase; STAT3, signal transducer and activator of transcription 3; TGF- β, transforming growth factor beta; TNF-α, tumor necrosis factor-α; TPPU, N-[1-(1-oxopropyl)-4-piperidinyl]-N'-[4-(trifluoromethoxy)phenyl)-urea; TXB_2, thromboxane B_2.

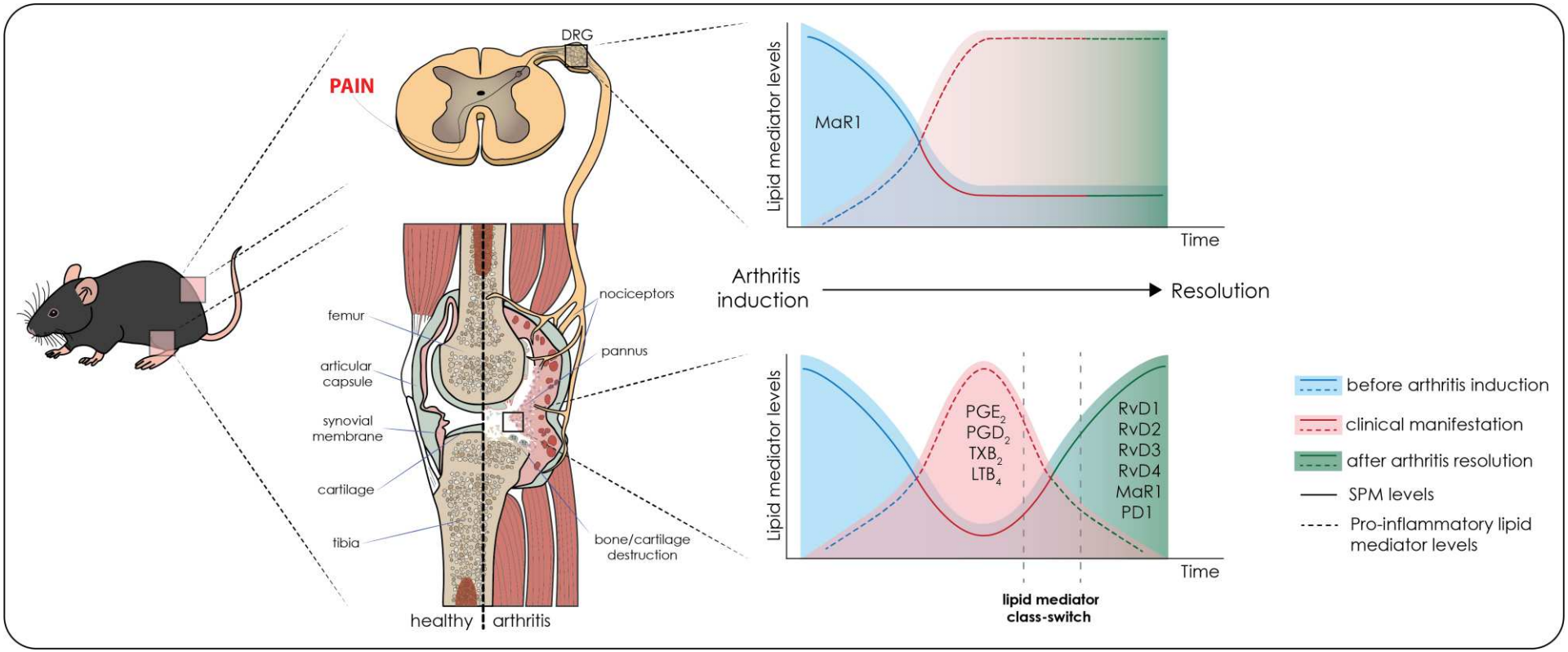

Figure 2. Pre-clinical levels of lipid mediators and their correlation with arthritis status. Schematic representation of the fluctuation in the levels of lipid mediators, *i.e.* pro-inflammatory lipid mediators and SPMs, in arthritis initiation, resolution, and associated pain in the K/BxN-induced arthritis model. The time-dependent resolution process is singular and tissue-specific; therefore, there is a variation in the resolution

between the joint and DRG. In the joint, the inflammatory events lead to an increase in pro-inflammatory lipid mediators and decrease in SPM levels. In the resolution phase, the lipid class switch supports the inflammation resolution and restore the levels of SPMs (Arnardottir, Dalli, Norling, Colas, Perretti & Serhan, 2016). While the joint has the health status restored, in the DRG, the class switch does not occur at the same pace, and the imbalance between pro-inflammatory mediators and SPMs in the dorsal root ganglia (DRG) result in persistent pain (Allen et al., 2020).

Author contributions

All Authors contributed significantly to the writing and conception of this review article as well as approved the final version of the manuscript.

Declaration of Competing Interest

The authors declare no conflict of interest. All financial support was disclosed in the manuscript.

Funding

This work was supported by grants from the Department of Science and Technology from the Science, Technology and Strategic Inputs Secretariat of the Ministry of Health (Decit/SCTIE/MS, Brazil) inter- mediated by National Council for Scientific and Technological Development (CNPq, Brazil) with support of Araucária Foundation and State Health Secretariat, Paraná (SESA-PR, Brazil; PPSUS Grant agreement 041/2017, protocol 48.095); Programa de Apoio a Grupos de Excelência (PRONEX) grant supported by SETI/Araucária Foundation and MCTI/CNPq; and Paraná State Government (agreement 014/2017, protocol 46.843). THZ acknowledges the PhD scholarship from Coordination for the Improvement of Higher Education Personnel (CAPES, Brazil, finance code 001). WAVJ acknowledges the CNPq Senior Research fellowship.

References

[1] M. Gourley, and F.W. Miller, Mechanisms of disease: Environmental factors in the pathogenesis of rheumatic disease. Nat Clin Pract Rheumatol 3 (2007) 172-80.

[2] V. Fattori, F.A. Amaral, and W.A. Verri, Jr., Neutrophils and arthritis: Role in disease and pharmacological perspectives. Pharmacol Res 112 (2016) 84-98.

[3] A. Bersellini Farinotti, G. Wigerblad, D. Nascimento, D.B. Bas, C. Morado Urbina, K.S. Nandakumar, K. Sandor, B. Xu, S. Abdelmoaty, M.A. Hunt, K. Angeby Moller, A. Baharpoor, J. Sinclair, K. Jardemark, J.T. Lanner, I. Khmaladze, L.E. Borm, L. Zhang, F. Wermeling, M.S. Cragg, J. Lengqvist, A.J. Chabot-Dore, L. Diatchenko, I. Belfer, M. Collin, K. Kultima, B. Heyman, J.M. Jimenez-Andrade, S. Codeluppi, R. Holmdahl, and C.I. Svensson, Cartilage-binding antibodies induce pain through immune complex-mediated activation of neurons. The Journal of experimental medicine 216 (2019) 1904-1924.

[4] P. Monach, K. Hattori, H. Huang, E. Hyatt, J. Morse, L. Nguyen, A. Ortiz-Lopez, H.J. Wu, D. Mathis, and C. Benoist, The K/BxN mouse model of inflammatory arthritis: theory and practice. Methods in molecular medicine 136 (2007) 269-82.

[5] J.S. Courtenay, M.J. Dallman, A.D. Dayan, A. Martin, and B. Mosedale, Immunisation against heterologous type II collagen induces arthritis in mice. Nature 283 (1980) 666-8.

[6] D.L. Asquith, A.M. Miller, I.B. McInnes, and F.Y. Liew, Animal models of rheumatoid arthritis. European journal of immunology 39 (2009) 2040-4.

[7] K. Terato, K.A. Hasty, R.A. Reife, M.A. Cremer, A.H. Kang, and J.M. Stuart, Induction of arthritis with monoclonal antibodies to collagen. Journal of immunology 148 (1992) 2103-8.

[8] W.A. Verri, Jr., A.T. Guerrero, S.Y. Fukada, D.A. Valerio, T.M. Cunha, D. Xu, S.H. Ferreira, F.Y. Liew, and F.Q. Cunha, IL-33 mediates antigen-induced cutaneous and articular hypernociception in mice. Proceedings of the National Academy of Sciences of the United States of America 105 (2008) 2723-8.

[9] W.A. Verri, Jr., F.O. Souto, S.M. Vieira, S.C. Almeida, S.Y. Fukada, D. Xu, J.C. Alves-Filho, T.M. Cunha, A.T. Guerrero, R.B. Mattos-Guimaraes, F.R. Oliveira, M.M. Teixeira, J.S. Silva, I.B. McInnes, S.H. Ferreira, P. Louzada-Junior, F.Y. Liew, and F.Q. Cunha, IL-33 induces neutrophil migration in rheumatoid arthritis and is a target of anti-TNF therapy. Annals of the rheumatic diseases 69 (2010) 1697-703.

[10] L. Staurengo-Ferrari, S.C. Trevelin, V. Fattori, D.C. Nascimento, K.A. de Lima, J.S. Pelayo, F. Figueiredo, R. Casagrande, S.Y. Fukada, M.M. Teixeira, T.M. Cunha, F.Y. Liew, R.D. Oliveira, P. Louzada-Junior, F.Q. Cunha, J.C. Alves-Filho, and W.A. Verri, Interleukin-33 Receptor (ST2) Deficiency Improves the Outcome of Staphylococcus aureus-Induced Septic Arthritis. Frontiers in immunology 9 (2018) 962.

[11] L. Staurengo-Ferrari, K.W. Ruiz-Miyazawa, F.A. Pinho-Ribeiro, T.P. Domiciano, V. Fattori, S.S. Mizokami, J.S. Pelayo, J. Bordignon, F. Figueiredo, R. Casagrande, K.M. Miranda, and W.A. Verri, Jr., The nitroxyl donor Angeli's salt ameliorates Staphylococcus aureus-induced septic arthritis in mice. Free radical biology & medicine 108 (2017) 487-499.

[12] A. Jarneborn, M. Mohammad, C. Engdahl, Z. Hu, M. Na, A. Ali, and T. Jin, Tofacitinib treatment aggravates Staphylococcus aureus septic arthritis, but attenuates sepsis and enterotoxin induced shock in mice. Scientific reports 10 (2020) 10891.

[13] S. Sultana, and B. Bishayi, Potential anti-arthritic and anti-inflammatory effects of TNF-alpha processing inhibitor-1 (TAPI-1): A new approach to the treatment of S. aureus arthritis. Immunobiology 225 (2020) 151887.
[14] S.L. Kolasinski, T. Neogi, M.C. Hochberg, C. Oatis, G. Guyatt, J. Block, L. Callahan, C. Copenhaver, C. Dodge, D. Felson, K. Gellar, W.F. Harvey, G. Hawker, E. Herzig, C.K. Kwoh, A.E. Nelson, J. Samuels, C. Scanzello, D. White, B. Wise, R.D. Altman, D. DiRenzo, J. Fontanarosa, G. Giradi, M. Ishimori, D. Misra, A.A. Shah, A.K. Shmagel, L.M. Thoma, M. Turgunbaev, A.S. Turner, and J. Reston, 2019 American College of Rheumatology/Arthritis Foundation Guideline for the Management of Osteoarthritis of the Hand, Hip, and Knee. Arthritis & rheumatology 72 (2020) 220-233.
[15] J.A. Singh, K.G. Saag, S.L. Bridges, Jr., E.A. Akl, R.R. Bannuru, M.C. Sullivan, E. Vaysbrot, C. McNaughton, M. Osani, R.H. Shmerling, J.R. Curtis, D.E. Furst, D. Parks, A. Kavanaugh, J. O'Dell, C. King, A. Leong, E.L. Matteson, J.T. Schousboe, B. Drevlow, S. Ginsberg, J. Grober, E.W. St Clair, E. Tindall, A.S. Miller, T. McAlindon, and R. American College of, 2015 American College of Rheumatology Guideline for the Treatment of Rheumatoid Arthritis. Arthritis care & research 68 (2016) 1-25.
[16] D. De Cock, and K. Hyrich, Malignancy and rheumatoid arthritis: Epidemiology, risk factors and management. Best practice & research. Clinical rheumatology 32 (2018) 869-886.
[17] P.M. Welsing, J. Fransen, and P.L. van Riel, Is the disease course of rheumatoid arthritis becoming milder? Time trends since 1985 in an inception cohort of early rheumatoid arthritis. Arthritis and rheumatism 52 (2005) 2616-24.
[18] Y.C. Lee, M.L. Frits, C.K. Iannaccone, M.E. Weinblatt, N.A. Shadick, D.A. Williams, and J. Cui, Subgrouping of patients with rheumatoid arthritis based on pain, fatigue, inflammation, and psychosocial factors. Arthritis & rheumatology 66 (2014) 2006-14.
[19] Y.C. Lee, J. Cui, B. Lu, M.L. Frits, C.K. Iannaccone, N.A. Shadick, M.E. Weinblatt, and D.H. Solomon, Pain persists in DAS28 rheumatoid arthritis remission but not in ACR/EULAR remission: a longitudinal observational study. Arthritis research & therapy 13 (2011) R83.
[20] L.G. Schipper, L.T. van Hulst, R. Grol, P.L. van Riel, M.E. Hulscher, and J. Fransen, Meta-analysis of tight control strategies in rheumatoid arthritis: protocolized treatment has additional value with respect to the clinical outcome. Rheumatology (Oxford) 49 (2010) 2154-64.
[21] K. Orlicka, E. Barnes, and E.L. Culver, Prevention of infection caused by immunosuppressive drugs in gastroenterology. Therapeutic advances in chronic disease 4 (2013) 167-85.
[22] V.P. Cabral, C.A. Andrade, S.R. Passos, M.F. Martins, and Y.H. Hokerberg, Severe infection in patients with rheumatoid arthritis taking anakinra, rituximab, or abatacept: a systematic review of observational studies. Revista brasileira de reumatologia 56 (2016) 543-550.
[23] L.M. Plein, and H.L. Rittner, Opioids and the immune system - friend or foe. British journal of pharmacology 175 (2018) 2717-2725.
[24] J.G. Mahdi, Medicinal potential of willow: A chemical perspective of aspirin discovery. Journal of Saudi Chemical Society 14 (2010) 317-322.
[25] J.R. Vane, Inhibition of prostaglandin synthesis as a mechanism of action for aspirin-like drugs. Nature: New biology 231 (1971) 232-5.

[26] S.H. Ferreira, Prostaglandins, aspirin-like drugs and analgesia. Nature: New biology 240 (1972) 200-3.
[27] S.H. Ferreira, S. Moncada, and J.R. Vane, Indomethacin and aspirin abolish prostaglandin release from the spleen. Nature: New biology 231 (1971) 237-9.
[28] C.N. Serhan, Treating inflammation and infection in the 21st century: new hints from decoding resolution mediators and mechanisms. FASEB J 31 (2017) 1273-1288.
[29] C.D. Buckley, D.W. Gilroy, and C.N. Serhan, Proresolving lipid mediators and mechanisms in the resolution of acute inflammation. Immunity 40 (2014) 315-27.
[30] V. Fattori, T.H. Zaninelli, F.S. Rasquel-Oliveira, R. Casagrande, and W.A. Verri, Jr., Specialized pro-resolving lipid mediators: A new class of non-immunosuppressive and non-opioid analgesic drugs. Pharmacological research 151 (2020) 104549.
[31] B.D. Levy, C.B. Clish, B. Schmidt, K. Gronert, and C.N. Serhan, Lipid mediator class switching during acute inflammation: signals in resolution. Nat Immunol 2 (2001) 612-9.
[32] G.L. Bannenberg, N. Chiang, A. Ariel, M. Arita, E. Tjonahen, K.H. Gotlinger, S. Hong, and C.N. Serhan, Molecular circuits of resolution: formation and actions of resolvins and protectins. Journal of immunology 174 (2005) 4345-55.
[33] N. Chiang, and C.N. Serhan, Structural elucidation and physiologic functions of specialized pro-resolving mediators and their receptors. Mol Aspects Med 58 (2017) 114-129.
[34] C.N. Serhan, N. Chiang, J. Dalli, and B.D. Levy, Lipid mediators in the resolution of inflammation. Cold Spring Harb Perspect Biol 7 (2015) a016311.
[35] L. Huang, C.F. Wang, C.N. Serhan, and G. Strichartz, Enduring prevention and transient reduction of postoperative pain by intrathecal resolvin D1. Pain 152 (2011) 557-65.
[36] V. Fattori, F.A. Pinho-Ribeiro, L. Staurengo-Ferrari, S.M. Borghi, A.C. Rossaneis, R. Casagrande, and W.A. Verri, Jr., The specialised pro-resolving lipid mediator maresin 1 reduces inflammatory pain with a long-lasting analgesic effect. British journal of pharmacology 176 (2019) 1728-1744.
[37] B.L. Allen, K. Montague-Cardoso, R. Simeoli, R.A. Colas, S. Oggero, B. Vilar, P.A. McNaughton, J. Dalli, M. Perretti, E. Sher, and M. Malcangio, Imbalance of pro-resolving lipid mediators in persistent allodynia dissociated from signs of clinical arthritis. Pain (2020).
[38] J. Bystrom, I. Evans, J. Newson, M. Stables, I. Toor, N. van Rooijen, M. Crawford, P. Colville-Nash, S. Farrow, and D.W. Gilroy, Resolution-phase macrophages possess a unique inflammatory phenotype that is controlled by cAMP. Blood 112 (2008) 4117-27.
[39] M.J. Stables, S. Shah, E.B. Camon, R.C. Lovering, J. Newson, J. Bystrom, S. Farrow, and D.W. Gilroy, Transcriptomic analyses of murine resolution-phase macrophages. Blood 118 (2011) e192-208.
[40] J. Newson, M. Stables, E. Karra, F. Arce-Vargas, S. Quezada, M. Motwani, M. Mack, S. Yona, T. Audzevich, and D.W. Gilroy, Resolution of acute inflammation bridges the gap between innate and adaptive immunity. Blood 124 (2014) 1748-64.
[41] G. Kronke, J. Katzenbeisser, S. Uderhardt, M.M. Zaiss, C. Scholtysek, G. Schabbauer, A. Zarbock, M.I. Koenders, R. Axmann, J. Zwerina, H.W. Baenckler, W. van den Berg, R.E. Voll, H. Kuhn, L.A. Joosten, and G. Schett, 12/15-lipoxygenase counteracts

inflammation and tissue damage in arthritis. Journal of immunology 183 (2009) 3383-9.

[42] C.N. Serhan, A. Jain, S. Marleau, C. Clish, A. Kantarci, B. Behbehani, S.P. Colgan, G.L. Stahl, A. Merched, N.A. Petasis, L. Chan, and T.E. Van Dyke, Reduced inflammation and tissue damage in transgenic rabbits overexpressing 15-lipoxygenase and endogenous anti-inflammatory lipid mediators. Journal of immunology 171 (2003) 6856-65.

[43] M. Giera, A. Ioan-Facsinay, R. Toes, F. Gao, J. Dalli, A.M. Deelder, C.N. Serhan, and O.A. Mayboroda, Lipid and lipid mediator profiling of human synovial fluid in rheumatoid arthritis patients by means of LC-MS/MS. Biochimica et biophysica acta 1821 (2012) 1415-24.

[44] A. Hashimoto, I. Hayashi, Y. Murakami, Y. Sato, H. Kitasato, R. Matsushita, N. Iizuka, K. Urabe, M. Itoman, S. Hirohata, and H. Endo, Antiinflammatory mediator lipoxin A4 and its receptor in synovitis of patients with rheumatoid arthritis. The Journal of rheumatology 34 (2007) 2144-53.

[45] E.A. Gomez, R.A. Colas, P.R. Souza, R. Hands, M.J. Lewis, C. Bessant, C. Pitzalis, and J. Dalli, Blood pro-resolving mediators are linked with synovial pathology and are predictive of DMARD responsiveness in rheumatoid arthritis. Nature communications 11 (2020) 5420.

[46] S. Jin, H. Chen, Y. Li, H. Zhong, W. Sun, J. Wang, T. Zhang, J. Ma, S. Yan, J. Zhang, Q. Tian, X. Yang, and J. Wang, Maresin 1 improves the Treg/Th17 imbalance in rheumatoid arthritis through miR-21. Annals of the rheumatic diseases 77 (2018) 1644-1652.

[47] W. Sun, J. Ma, H. Zhao, C. Xiao, H. Zhong, H. Ling, Z. Xie, Q. Tian, H. Chen, T. Zhang, M. Chen, S. Jin, and J. Wang, Resolvin D1 suppresses pannus formation via decreasing connective tissue growth factor caused by upregulation of miRNA-146a-5p in rheumatoid arthritis. Arthritis research & therapy 22 (2020) 61.

[48] H.H. Arnardottir, J. Dalli, L.V. Norling, R.A. Colas, M. Perretti, and C.N. Serhan, Resolvin D3 Is Dysregulated in Arthritis and Reduces Arthritic Inflammation. Journal of immunology 197 (2016) 2362-8.

[49] Y. Sano, S. Toyoshima, Y. Miki, Y. Taketomi, M. Ito, H. Lee, S. Saito, M. Murakami, and Y. Okayama, Activation of inflammation and resolution pathways of lipid mediators in synovial fluid from patients with severe rheumatoid arthritis compared with severe osteoarthritis. Asia Pac Allergy 10 (2020) e21.

[50] A.M. Valdes, S. Ravipati, C. Menni, A. Abhishek, S. Metrustry, J. Harris, A. Nessa, F.M.K. Williams, T.D. Spector, M. Doherty, V. Chapman, and D.A. Barrett, Association of the resolvin precursor 17-HDHA, but not D- or E- series resolvins, with heat pain sensitivity and osteoarthritis pain in humans. Scientific reports 7 (2017) 10748.

[51] A.E. Barden, M. Moghaddami, E. Mas, M. Phillips, L.G. Cleland, and T.A. Mori, Specialised pro-resolving mediators of inflammation in inflammatory arthritis. Prostaglandins Leukot Essent Fatty Acids 107 (2016) 24-9.

[52] C.N. Serhan, S.K. Gupta, M. Perretti, C. Godson, E. Brennan, Y. Li, O. Soehnlein, T. Shimizu, O. Werz, V. Chiurchiu, A. Azzi, M. Dubourdeau, S.S. Gupta, P. Schopohl, M. Hoch, D. Gjorgevikj, F.M. Khan, D. Brauer, A. Tripathi, K. Cesnulevicius, D. Lescheid, M. Schultz, E. Sarndahl, D. Repsilber, R. Kruse, A. Sala, J.Z. Haeggstrom, B.D. Levy, J.G. Filep, and O. Wolkenhauer, The Atlas of Inflammation Resolution (AIR). Mol Aspects Med 74 (2020) 100894.

[53] S. Rifbjerg-Madsen, A.W. Christensen, R. Christensen, M.L. Hetland, H. Bliddal, L.E. Kristensen, B. Danneskiold-Samsoe, and K. Amris, Pain and pain mechanisms in patients with inflammatory arthritis: A Danish nationwide cross-sectional DANBIO registry survey. PLoS One 12 (2017) e0180014.
[54] W.A. Goncalves, B.M. Rezende, M.P.E. de Oliveira, L.S. Ribeiro, V. Fattori, W.N. da Silva, P. Prazeres, C.M. Queiroz-Junior, K.T.O. Santana, W.C. Costa, V.A. Beltrami, V.V. Costa, A. Birbrair, W.A. Verri, Jr., F. Lopes, T.M. Cunha, M.M. Teixeira, F.A. Amaral, and V. Pinho, Sensory Ganglia-Specific TNF Expression Is Associated With Persistent Nociception After Resolution of Inflammation. Frontiers in immunology 10 (2019) 3120.
[55] D.W. Gilroy, M.L. Edin, R.P. De Maeyer, J. Bystrom, J. Newson, F.B. Lih, M. Stables, D.C. Zeldin, and D. Bishop-Bailey, CYP450-derived oxylipins mediate inflammatory resolution. Proc Natl Acad Sci U S A 113 (2016) E3240-9.
[56] K.R. Schmelzer, L. Kubala, J.W. Newman, I.H. Kim, J.P. Eiserich, and B.D. Hammock, Soluble epoxide hydrolase is a therapeutic target for acute inflammation. Proc Natl Acad Sci U S A 102 (2005) 9772-7.
[57] H. Guan, L. Zhao, H. Cao, A. Chen, and J. Xiao, Epoxyeicosanoids suppress osteoclastogenesis and prevent ovariectomy-induced bone loss. FASEB journal : official publication of the Federation of American Societies for Experimental Biology 29 (2015) 1092-101.
[58] C.B. McReynolds, S.H. Hwang, J. Yang, D. Wan, K. Wagner, C. Morisseau, D. Li, W.K. Schmidt, and B.D. Hammock, Pharmaceutical Effects of Inhibiting the Soluble Epoxide Hydrolase in Canine Osteoarthritis. Front Pharmacol 10 (2019) 533.
[59] C.A. Trindade-da-Silva, J.T. Clemente-Napimoga, H.B. Abdalla, S.M. Rosa, C. Ueira-Vieira, C. Morisseau, W.A. Verri, Jr., V.A.M. Montalli, B.D. Hammock, and M.H. Napimoga, Soluble epoxide hydrolase inhibitor, TPPU, increases regulatory T cells pathway in an arthritis model. FASEB journal : official publication of the Federation of American Societies for Experimental Biology (2020).
[60] M.N. Ajuebor, A. Singh, and J.L. Wallace, Cyclooxygenase-2-derived prostaglandin D(2) is an early anti-inflammatory signal in experimental colitis. Am J Physiol Gastrointest Liver Physiol 279 (2000) G238-44.
[61] N. Maicas, L. Ibanez, M.J. Alcaraz, A. Ubeda, and M.L. Ferrandiz, Prostaglandin D2 regulates joint inflammation and destruction in murine collagen-induced arthritis. Arthritis and rheumatism 64 (2012) 130-40.
[62] R. Rajakariar, M. Hilliard, T. Lawrence, S. Trivedi, P. Colville-Nash, G. Bellingan, D. Fitzgerald, M.M. Yaqoob, and D.W. Gilroy, Hematopoietic prostaglandin D2 synthase controls the onset and resolution of acute inflammation through PGD2 and 15-deoxyDelta12 14 PGJ2. Proc Natl Acad Sci U S A 104 (2007) 20979-84.
[63] J. Li, C. Guo, and J. Wu, 15-Deoxy--(12,14)-Prostaglandin J2 (15d-PGJ2), an Endogenous Ligand of PPAR-gamma: Function and Mechanism. PPAR Res 2019 (2019) 7242030.
[64] Y. Kawahito, M. Kondo, Y. Tsubouchi, A. Hashiramoto, D. Bishop-Bailey, K. Inoue, M. Kohno, R. Yamada, T. Hla, and H. Sano, 15-deoxy-delta(12,14)-PGJ(2) induces synoviocyte apoptosis and suppresses adjuvant-induced arthritis in rats. J Clin Invest 106 (2000) 189-97.
[65] S. Cuzzocrea, N.S. Wayman, E. Mazzon, L. Dugo, R. Di Paola, I. Serraino, D. Britti, P.K. Chatterjee, A.P. Caputi, and C. Thiemermann, The cyclopentenone prostaglandin 15-

250 deoxy-Delta(12,14)-prostaglandin J(2) attenuates the development of acute and
251 chronic inflammation. Mol Pharmacol 61 (2002) 997-1007.
252 [66] T.H. Lin, C.H. Tang, K. Wu, Y.C. Fong, R.S. Yang, and W.M. Fu, 15-deoxy-Delta(12,14) -
253 prostaglandin-J2 and ciglitazone inhibit TNF-alpha-induced matrix
254 metalloproteinase 13 production via the antagonism of NF-kappaB activation in
255 human synovial fibroblasts. J Cell Physiol 226 (2011) 3242-50.
256 [67] H. Fahmi, J.P. Pelletier, F. Mineau, and J. Martel-Pelletier, 15d-PGJ(2) is acting as a 'dual
257 agent' on the regulation of COX-2 expression in human osteoarthritic chondrocytes.
258 Osteoarthritis Cartilage 10 (2002) 845-8.
259 [68] K.W. Ruiz-Miyazawa, L. Staurengo-Ferrari, F.A. Pinho-Ribeiro, V. Fattori, T.H. Zaninelli,
260 S. Badaro-Garcia, S.M. Borghi, K.C. Andrade, J.T. Clemente-Napimoga, J.C. Alves-Filho,
261 T.M. Cunha, L.F. Fraceto, F.Q. Cunha, M.H. Napimoga, R. Casagrande, and W.A. Verri,
262 Jr., 15d-PGJ2-loaded nanocapsules ameliorate experimental gout arthritis by
263 reducing pain and inflammation in a PPAR-gamma-sensitive manner in mice.
264 Scientific reports 8 (2018) 13979.
265 [69] C. Alves, N. de Melo, L. Fraceto, D. de Araujo, and M. Napimoga, Effects of 15d-PGJ(2)-
266 loaded poly(D,L-lactide-co-glycolide) nanocapsules on inflammation. British journal
267 of pharmacology 162 (2011) 623-32.
268 [70] M.H. Napimoga, C.A. da Silva, V. Carregaro, T.S. Farnesi-de-Assuncao, P.M. Duarte, N.F.
269 de Melo, and L.F. Fraceto, Exogenous administration of 15d-PGJ2-loaded
270 nanocapsules inhibits bone resorption in a mouse periodontitis model. Journal of
271 immunology 189 (2012) 1043-52.
272 [71] J.T. Clemente-Napimoga, J.A. Moreira, R. Grillo, N.F. de Melo, L.F. Fraceto, and M.H.
273 Napimoga, 15d-PGJ2-loaded in nanocapsules enhance the antinociceptive properties
274 into rat temporomandibular hypernociception. Life Sci 90 (2012) 944-9.
275 [72] C.N. Serhan, M. Hamberg, and B. Samuelsson, Lipoxins: novel series of biologically active
276 compounds formed from arachidonic acid in human leukocytes. Proc Natl Acad Sci U
277 S A 81 (1984) 5335-9.
278 [73] C.N. Serhan, Lipoxins and aspirin-triggered 15-epi-lipoxins are the first lipid mediators
279 of endogenous anti-inflammation and resolution. Prostaglandins, leukotrienes, and
280 essential fatty acids 73 (2005) 141-62.
281 [74] M.M. Chan, and A.R. Moore, Resolution of inflammation in murine autoimmune arthritis
282 is disrupted by cyclooxygenase-2 inhibition and restored by prostaglandin E2-
283 mediated lipoxin A4 production. Journal of immunology 184 (2010) 6418-26.
284 [75] F.P. Conte, O. Menezes-de-Lima, Jr., W.A. Verri, Jr., F.Q. Cunha, C. Penido, and M.G.
285 Henriques, Lipoxin A(4) attenuates zymosan-induced arthritis by modulating
286 endothelin-1 and its effects. British journal of pharmacology 161 (2010) 911-24.
287 [76] L. Zhang, X. Zhang, P. Wu, H. Li, S. Jin, X. Zhou, Y. Li, D. Ye, B. Chen, and J. Wan, BML-111,
288 a lipoxin receptor agonist, modulates the immune response and reduces the severity
289 of collagen-induced arthritis. Inflamm Res 57 (2008) 157-62.
290 [77] C.N. Serhan, Pro-resolving lipid mediators are leads for resolution physiology. Nature
291 510 (2014) 92-101.
292 [78] D.L. Scott, F. Wolfe, and T.W. Huizinga, Rheumatoid arthritis. Lancet 376 (2010) 1094-
293 108.

[79] H. Benabdoune, E.P. Rondon, Q. Shi, J. Fernandes, P. Ranger, H. Fahmi, and M. Benderdour, The role of resolvin D1 in the regulation of inflammatory and catabolic mediators in osteoarthritis. Inflamm Res 65 (2016) 635-45.
[80] H.A. Benabdoun, M. Kulbay, E.P. Rondon, F. Vallieres, Q. Shi, J. Fernandes, H. Fahmi, and M. Benderdour, In vitro and in vivo assessment of the proresolutive and antiresorptive actions of resolvin D1: relevance to arthritis. Arthritis research & therapy 21 (2019) 72.
[81] J.F. Lima-Garcia, R.C. Dutra, K. da Silva, E.M. Motta, M.M. Campos, and J.B. Calixto, The precursor of resolvin D series and aspirin-triggered resolvin D1 display anti-hyperalgesic properties in adjuvant-induced arthritis in rats. British journal of pharmacology 164 (2011) 278-93.
[82] M.B. Flak, D.S. Koenis, A. Sobrino, J. Smith, K. Pistorius, F. Palmas, and J. Dalli, GPR101 mediates the pro-resolving actions of RvD5n-3 DPA in arthritis and infections. J Clin Invest 130 (2020) 359-373.
[83] X. Luo, Y. Gu, X. Tao, C.N. Serhan, and R.R. Ji, Resolvin D5 Inhibits Neuropathic and Inflammatory Pain in Male But Not Female Mice: Distinct Actions of D-Series Resolvins in Chemotherapy-Induced Peripheral Neuropathy. Front Pharmacol 10 (2019) 745.
[84] N. Chiang, S. Libreros, P.C. Norris, X. de la Rosa, and C.N. Serhan, Maresin 1 activates LGR6 receptor promoting phagocyte immunoresolvent functions. J Clin Invest 129 (2019) 5294-5311.
[85] T. Yang, G. Xu, P.T. Newton, A.S. Chagin, S. Mkrtchian, M. Carlstrom, X.M. Zhang, R.A. Harris, M. Cooter, M. Berger, K.R. Maddipati, K. Akassoglou, and N. Terrando, Maresin 1 attenuates neuroinflammation in a mouse model of perioperative neurocognitive disorders. Br J Anaesth 122 (2019) 350-360.
[86] J. Gao, C. Tang, L.W. Tai, Y. Ouyang, N. Li, Z. Hu, and X. Chen, Pro-resolving mediator maresin 1 ameliorates pain hypersensitivity in a rat spinal nerve ligation model of neuropathic pain. Journal of pain research 11 (2018) 1511-1519.
[87] Y.H. Wang, Y. Li, J.N. Wang, Q.X. Zhao, S. Wen, S.C. Wang, and T. Sun, A Novel Mechanism of Specialized Proresolving Lipid Mediators Mitigating Radicular Pain: The Negative Interaction with NLRP3 Inflammasome. Neurochem Res 45 (2020) 1860-1869.
[88] Q. Niu, B. Cai, Z.C. Huang, Y.Y. Shi, and L.L. Wang, Disturbed Th17/Treg balance in patients with rheumatoid arthritis. Rheumatol Int 32 (2012) 2731-6.
[89] M. Samson, S. Audia, N. Janikashvili, M. Ciudad, M. Trad, J. Fraszczak, P. Ornetti, J.F. Maillefert, P. Miossec, and B. Bonnotte, Brief report: inhibition of interleukin-6 function corrects Th17/Treg cell imbalance in patients with rheumatoid arthritis. Arthritis and rheumatism 64 (2012) 2499-503.
[90] X. de la Rosa, P.C. Norris, N. Chiang, A.R. Rodriguez, B.W. Spur, and C.N. Serhan, Identification and Complete Stereochemical Assignments of the New Resolvin Conjugates in Tissue Regeneration in Human Tissues that Stimulate Proresolving Phagocyte Functions and Tissue Regeneration. The American journal of pathology 188 (2018) 950-966.
[91] N. Chiang, I.R. Riley, J. Dalli, A.R. Rodriguez, B.W. Spur, and C.N. Serhan, New maresin conjugates in tissue regeneration pathway counters leukotriene D4-stimulated vascular responses. FASEB journal : official publication of the Federation of American Societies for Experimental Biology 32 (2018) 4043-4052.

[92] C.C. Jouvene, A.E. Shay, M.A. Soens, P.C. Norris, J.Z. Haeggstrom, and C.N. Serhan, Biosynthetic metabolomes of cysteinyl-containing immunoresolvents. FASEB journal : official publication of the Federation of American Societies for Experimental Biology 33 (2019) 13794-13807.
[93] B.D. Levy, R.E. Abdulnour, A. Tavares, T.R. Bruggemann, P.C. Norris, Y. Bai, X. Ai, and C.N. Serhan, Cysteinyl maresins regulate the prophlogistic lung actions of cysteinyl leukotrienes. The Journal of allergy and clinical immunology 145 (2020) 335-344.
[94] A. Siddiquee, M. Patel, S. Rajalingam, D. Narke, M. Kurade, and D.S. Ponnoth, Effect of omega-3 fatty acid supplementation on resolvin (RvE1)-mediated suppression of inflammation in a mouse model of asthma. Immunopharmacol Immunotoxicol 41 (2019) 250-257.
[95] H. Hasturk, R. Abdallah, A. Kantarci, D. Nguyen, N. Giordano, J. Hamilton, and T.E. Van Dyke, Resolvin E1 (RvE1) Attenuates Atherosclerotic Plaque Formation in Diet and Inflammation-Induced Atherogenesis. Arterioscler Thromb Vasc Biol 35 (2015) 1123-33.
[96] N. Li, J. He, C.E. Schwartz, P. Gjorstrup, and H.E. Bazan, Resolvin E1 improves tear production and decreases inflammation in a dry eye mouse model. J Ocul Pharmacol Ther 26 (2010) 431-9.
[97] Z.Z. Xu, L. Zhang, T. Liu, J.Y. Park, T. Berta, R. Yang, C.N. Serhan, and R.R. Ji, Resolvins RvE1 and RvD1 attenuate inflammatory pain via central and peripheral actions. Nature medicine 16 (2010) 592-7, 1p following 597.
[98] L.V. Norling, M. Spite, R. Yang, R.J. Flower, M. Perretti, and C.N. Serhan, Cutting edge: Humanized nano-proresolving medicines mimic inflammation-resolution and enhance wound healing. Journal of immunology 186 (2011) 5543-7.
[99] G. Leoni, P.A. Neumann, N. Kamaly, M. Quiros, H. Nishio, H.R. Jones, R. Sumagin, R.S. Hilgarth, A. Alam, G. Fredman, I. Argyris, E. Rijcken, D. Kusters, C. Reutelingsperger, M. Perretti, C.A. Parkos, O.C. Farokhzad, A.S. Neish, and A. Nusrat, Annexin A1-containing extracellular vesicles and polymeric nanoparticles promote epithelial wound repair. J Clin Invest 125 (2015) 1215-27.
[100] M. Codagnone, E. Cianci, A. Lamolinara, V.C. Mari, A. Nespoli, E. Isopi, D. Mattoscio, M. Arita, A. Bragonzi, M. Iezzi, M. Romano, and A. Recchiuti, Resolvin D1 enhances the resolution of lung inflammation caused by long-term Pseudomonas aeruginosa infection. Mucosal immunology 11 (2018) 35-49.
[101] N. Chiang, G. Fredman, F. Backhed, S.F. Oh, T. Vickery, B.A. Schmidt, and C.N. Serhan, Infection regulates pro-resolving mediators that lower antibiotic requirements. Nature 484 (2012) 524-8.
[102] M. Spite, L.V. Norling, L. Summers, R. Yang, D. Cooper, N.A. Petasis, R.J. Flower, M. Perretti, and C.N. Serhan, Resolvin D2 is a potent regulator of leukocytes and controls microbial sepsis. Nature 461 (2009) 1287-91.
[103] Y. Hao, H. Zheng, R.H. Wang, H. Li, L.L. Yang, S. Bhandari, Y.J. Liu, J. Han, F.G. Smith, H.C. Gao, and S.W. Jin, Maresin1 Alleviates Metabolic Dysfunction in Septic Mice: A (1)H NMR-Based Metabolomics Analysis. Mediators of inflammation 2019 (2019) 2309175.
[104] H. Xia, L. Chen, H. Liu, Z. Sun, W. Yang, Y. Yang, S. Cui, S. Li, Y. Wang, L. Song, A.F. Abdelgawad, Y. Shang, and S. Yao, Protectin DX increases survival in a mouse model

385 of sepsis by ameliorating inflammation and modulating macrophage phenotype.
386 Scientific reports 7 (2017) 99.
387 [105] I. Ginsburg, The role of bacteriolysis in the pathophysiology of inflammation, infection
388 and post-infectious sequelae. APMIS : acta pathologica, microbiologica, et
389 immunologica Scandinavica 110 (2002) 753-70.
390 [106] R.R. Hodges, D. Li, M.A. Shatos, J.A. Bair, M. Lippestad, C.N. Serhan, and D.A. Dartt,
391 Lipoxin A4 activates ALX/FPR2 receptor to regulate conjunctival goblet cell secretion.
392 Mucosal immunology 10 (2017) 46-57.
393 [107] S. Krishnamoorthy, A. Recchiuti, N. Chiang, G. Fredman, and C.N. Serhan, Resolvin D1
394 receptor stereoselectivity and regulation of inflammation and proresolving
395 microRNAs. The American journal of pathology 180 (2012) 2018-27.
396 [108] N. Chiang, J. Dalli, R.A. Colas, and C.N. Serhan, Identification of resolvin D2 receptor
397 mediating resolution of infections and organ protection. The Journal of experimental
398 medicine 212 (2015) 1203-17.
399 [109] L.Y. Zhang, Z.H. Liu, Q. Zhu, S. Wen, C.X. Yang, Z.J. Fu, and T. Sun, Resolvin D2 Relieving
400 Radicular Pain is Associated with Regulation of Inflammatory Mediators, Akt/GSK-
401 3beta Signal Pathway and GPR18. Neurochemical research 43 (2018) 2384-2392.
402 [110] S. Deyama, K. Shimoda, H. Suzuki, Y. Ishikawa, K. Ishimura, H. Fukuda, N. Hitora-
403 Imamura, S. Ide, M. Satoh, K. Kaneda, S. Shuto, and M. Minami, Resolvin E1/E2
404 ameliorate lipopolysaccharide-induced depression-like behaviors via ChemR23.
405 Psychopharmacology 235 (2018) 329-336.
406 [111] M. Herova, M. Schmid, C. Gemperle, and M. Hersberger, ChemR23, the receptor for
407 chemerin and resolvin E1, is expressed and functional on M1 but not on M2
408 macrophages. Journal of immunology 194 (2015) 2330-7.
409 [112] M.P. Motwani, R.A. Colas, M.J. George, J.D. Flint, J. Dalli, A. Richard-Loendt, R.P. De
410 Maeyer, C.N. Serhan, and D.W. Gilroy, Pro-resolving mediators promote resolution in
411 a human skin model of UV-killed Escherichia coli-driven acute inflammation. JCI
412 insight 3 (2018).
413 [113] V.L. Marcheselli, P.K. Mukherjee, M. Arita, S. Hong, R. Antony, K. Sheets, J.W. Winkler,
414 N.A. Petasis, C.N. Serhan, and N.G. Bazan, Neuroprotectin D1/protectin D1
415 stereoselective and specific binding with human retinal pigment epithelial cells and
416 neutrophils. Prostaglandins, leukotrienes, and essential fatty acids 82 (2010) 27-34.
417 [114] S. Bang, Y.K. Xie, Z.J. Zhang, Z. Wang, Z.Z. Xu, and R.R. Ji, GPR37 regulates macrophage
418 phagocytosis and resolution of inflammatory pain. The Journal of clinical
419 investigation 128 (2018) 3568-3582.
420 [115] F.A. Amaral, V.V. Costa, L.D. Tavares, D. Sachs, F.M. Coelho, C.T. Fagundes, F.M. Soriani,
421 T.N. Silveira, L.D. Cunha, D.S. Zamboni, V. Quesniaux, R.S. Peres, T.M. Cunha, F.Q.
422 Cunha, B. Ryffel, D.G. Souza, and M.M. Teixeira, NLRP3 inflammasome-mediated
423 neutrophil recruitment and hypernociception depend on leukotriene B(4) in a
424 murine model of gout. Arthritis and rheumatism 64 (2012) 474-84.
425 [116] A.T. Guerrero, W.A. Verri, Jr., T.M. Cunha, T.A. Silva, F.A. Rocha, S.H. Ferreira, F.Q. Cunha,
426 and C.A. Parada, Hypernociception elicited by tibio-tarsal joint flexion in mice: a novel
427 experimental arthritis model for pharmacological screening. Pharmacol Biochem
428 Behav 84 (2006) 244-51.

[117] A.T. Guerrero, L.G. Pinto, F.Q. Cunha, S.H. Ferreira, J.C. Alves-Filho, W.A. Verri, Jr., and T.M. Cunha, Mechanisms underlying the hyperalgesic responses triggered by joint activation of TLR4. Pharmacological reports : PR 68 (2016) 1293-1300.
[118] W.T. Chen, U. Mahmood, R. Weissleder, and C.H. Tung, Arthritis imaging using a near-infrared fluorescence folate-targeted probe. Arthritis research & therapy 7 (2005) R310-7.
[119] K.S. Nandakumar, L. Svensson, and R. Holmdahl, Collagen type II-specific monoclonal antibody-induced arthritis in mice: description of the disease and the influence of age, sex, and genes. The American journal of pathology 163 (2003) 1827-37.
[120] J.J. Inglis, C.A. Notley, D. Essex, A.W. Wilson, M. Feldmann, P. Anand, and R. Williams, Collagen-induced arthritis as a model of hyperalgesia: functional and cellular analysis of the analgesic actions of tumor necrosis factor blockade. Arthritis and rheumatism 56 (2007) 4015-23.
[121] H. Jonsson, P. Allen, and S.L. Peng, Inflammatory arthritis requires Foxo3a to prevent Fas ligand-induced neutrophil apoptosis. Nature medicine 11 (2005) 666-71.
[122] S.M. Borghi, S.S. Mizokami, F.A. Pinho-Ribeiro, V. Fattori, J. Crespigio, J.T. Clemente-Napimoga, M.H. Napimoga, D.L. Pitol, J.P.M. Issa, S.Y. Fukada, R. Casagrande, and W.A. Verri, Jr., The flavonoid quercetin inhibits titanium dioxide (TiO2)-induced chronic arthritis in mice. The Journal of nutritional biochemistry 53 (2018) 81-95.
[123] F. Fatima, Y. Fei, A. Ali, M. Mohammad, M.C. Erlandsson, M.I. Bokarewa, M. Nawaz, H. Valadi, M. Na, and T. Jin, Radiological features of experimental staphylococcal septic arthritis by micro computed tomography scan. PloS one 12 (2017) e0171222.
[124] Y. Funaki, Y. Hasegawa, R. Okazaki, A. Yamasaki, Y. Sueda, A. Yamamoto, M. Yanai, T. Fukushima, T. Harada, H. Makino, and E. Shimizu, Resolvin E1 Inhibits Osteoclastogenesis and Bone Resorption by Suppressing IL-17-induced RANKL Expression in Osteoblasts and RANKL-induced Osteoclast Differentiation. Yonago Acta Med 61 (2018) 8-18.

Review

3.2 New drug targets for the treatment of gout: What's new?

Tiago H. Zaninelli[1], Geovana M. Cebinelli[1], Telma Saraiva-Santos[1], Victor Fattori[1,2], Sergio M. Borghi[1,3], Rubia Casagrande[4], Waldiceu A. Verri Jr[1]*

[1]Laboratory of Pain, Inflammation, Neuropathy, and Cancer, Department of Pathology, Centre of Biological Sciences, Londrina State University, Londrina, Paraná, Brazil.

[2]Vascular Biology Program, Department of Surgery, Boston Children's Hospital-Harvard Medical School, Karp Research Building, 300 Longwood Ave. 02115, Boston, Massachusetts, United States.

[3]Center for Research in Health Sciences, University of Northern Londrina, Londrina 86041-120, PR, Brazil.

[4]Laboratory of Antioxidants and Inflammation, Department of Pharmaceutical Sciences, Centre of Health Sciences, Londrina State University, Londrina, Paraná, Brazil.

* Corresponding author.

Present address: Departamento de Ciências Patológicas, Universidade Estadual de Londrina, Rodovia Celso Garcia Cid Km480 PR445, 86057-970, Post-office box 10.011, Londrina, Paraná, Brazil. E-mail address: waverri@uel.br

Abstract

Introduction: Gout arthritis (GA) is an intermittent inflammatory disease affecting approximately 10% of worldwide population. Symptomatic phases (acute flares) are timely spaced by asymptomatic periods. During acute attack, redness, joint swelling, limited movement, and excruciating pain are common symptoms. However, the currently available therapies are not fully effective in reduce symptoms and offered numerous side effects. Therefore, unveiling new drug targets and effector molecules are required in developing novel GA therapeutics.

Areas covered: This review discusses the pathophysiological mechanisms of GA and explore potential pharmacological targets to ameliorate disease outcome. In addition, we listed promising pre-clinical studies demonstrating effector molecules with therapeutical potential. Among those we emphasized the importance of natural products, including traditional Chinese medicine formulas, and their multitarget mechanisms of action.

Expert opinion: In our search, we observed that there is a massive gap between the pre-clinical and clinical knowledge. Only a minority (4.4%) of clinical trials aimed to intervene applying natural products, or current hot targets described herein. In this sense, we envisage four possibilities for GA therapeutics, which includes the repurposing of existing therapies, ALX/FPR2 agonism for improvement in disease outcome, the use of multitarget drugs (*e.g.,* natural products), and targeting the neuroinflammatory component of GA.

Key words: natural products, specialized pro-resolving lipid mediators, drug repurposing, multitargeting drug.

Highlights

- Current therapies for GA are not fully effective in control its symptom.
- The side-effects of available drugs are associated to the treatment discontinuance or are not safe for patients with comorbidity.
- There is a huge gap in translational studies from pre-clinical to clinical research.
- In this review we highlight 15 mechanisms-based drug targets for GA prevention, incidence, and treatment.
- Lipid mediator production and signaling are effective targets for GA therapeutics: blockage of pro-inflammatory mediators and endogenous production of specialized pro-resolving mediators (SPMs) or pharmacological treatment restore tissue homeostasis in MSU-induced animal models of GA.
- Natural products with antioxidant and multitarget mechanisms are highly effective in ameliorate MSU-induced GA in pre-clinical studies, thus are suitable candidates for drug development or repurposing.

1. Introduction

Gouty arthritis (GA) is an inflammatory disease that affects approximately 10% of worldwide population [1]. Diet habits and unbalanced metabolism of purines are triggers for hyperuricemia (*e.g.,* increased plasma levels of uric acid). In this condition, saturation of uric acid leads to the formation of monosodium urate crystals (MSU) deposits in the articular cavities and periarticular tissues, and their sensing by the immune system [2]. The recognition of MSU crystals by resident immune cells triggers an acute inflammatory crises (gout flare) accompanied by heat, redness, joint swelling, limited movement, and, most importantly, excruciating and debilitating pain [3].

The first reports on GA were made by the Egyptian civilizations and dated from 2,640 b.C. Although the vast majority of GA pathophysiological mechanism was described in the XXI century [4], disease management is yet a great challenge. Although MSU crystals induce a self-limited inflammation, this acute condition can become chronic, and may lead to the formation of gouty tophi, massive MSU crystals formations that can reach sizes to be visualized without the need of a microscope. By chronic stimulation of the immune system, there is induction of changes in the cellular profile leading to the formation of giant cells derived from the fusion of macrophages as usual in granulomas [5]. In fact, a fully effective therapeutic approach is one of the biggest challenges in this millenary disease.

The complexity of GA pathophysiological mechanisms, at the same time it offers several targets for drug development also trickers the outcome response with undesired side effects and poor analgesic phenotype. Currently, the preventive management of GA lays on diet habits and control of uric acid levels. During acute flares, non-steroidal anti-inflammatory drugs (NSAIDs), steroidal anti-inflammatory drugs (SAIDs), and colchicine are often prescribed. More recently, GA patients also may take advantage of immunotherapies, such as anti-IL-1β humanized antibodies or IL-1 receptor antagonist (IL-1ra). However, as most of the pharmacological approaches, those therapies also have limited efficacy accompanied by significant side effects, and high costs in the case of immunobiologicals. Therefore, the focus of this review is to discuss the current pre-clinical scenario for GA therapies and list novel drug targets for this old disease.

2. Current knowledge on gout arthritis pathophysiology

Uric acid is a weak acid formed at the last steps of the purine metabolism. Under physiological pH, uric acid is ionized and presented in the form of urate. The elevation of the serum uric acid level above 6.8 mg/dL (pathological threshold of hyperuricemia) promotes the formation and deposition of MSU crystals in tissues [6]. The most common cause of hyperuricemia in patients with GA is the renal underexcretion, decreasing two-thirds of the urate excretion, or extrarenal underexcretion, responsible for the remained urate excretion [7]. About 10% of the urate filtered by the kidneys is excreted, the other 90% are reabsorbed through specific anion transporters, such as resorptive urate-anion exchangers (URAT1/SLC22A12, OAT4/SLC22A11, OAT10/SLC22A3) and resorptive urate transporter (GLUT9/SLC2A9) [8].

Most hyperuricemic patients remain asymptomatic and don't develop gout [9]. Previous studies have already shown the correlation of genetic factors related to the function of transporters with the development of GA. For instance, dysfunctional variants of renal urate transporter URAT1/SLC22A12 have been described to have protective actions and decrease susceptibility to GA [10]. Thirteen single nucleotide polymorphisms (SNPs) in genes of urate transporters (ABCG2, SLC2A9, SLC22A11, GCKR, MEPE, PPM1K-DT, LOC105377323, and ADH1B) were identified as predictors for the progression of hyperuricemia to GA, demonstrating the participation of urate transporters in the GA pathophysiology [11].

In the context of hyperuricemia, the formation and deposition of MSU crystals in tissues is dependent on several factors that could interfere with the solubility and local concentration of urate, such as low temperatures, pH, concentration of water and cations, and components of the extracellular matrix (i.e., proteoglycans, collagens) [12]. The presence of these factors explains the deposition of crystals in peripheral joints, such as the metatarsophalangeal joint and osteoarthritic joints [12]. Temperature also influences the activation of the inflammasome. Lower temperatures (*i.e.*, peripheral joints) favor the release of IL-1β and GA development [13].

After formation and deposition of MSU crystals in the synovial fluid, it is phagocytosed by resident mononuclear phagocytes (*e.g.,* synoviocyte) triggering the production of reactive oxygen species (ROS) and reactive nitrogen species (RNS) [5]. In addition to activate inflammasomal NLRP3, the response to MSU crystals can also induces cytotoxicity, inflammation, and cellular necrosis, such as the process of necroptosis [5]. In this case, crystal-induced cell necrosis is

mediated by the receptor-interacting protein kinase-3 (RIPK3) and the pseudokinase mixed-lineage kinase domain-like (MLKL), which together form a necrosome complex that interacts with mitochondrial membranes, leading to cell death [14]. Necrotic cells also amplify the local inflammatory response by releasing DAMPs (*i.e.,* ATP, histones, alarmins, and IL-1α) [5], which bind to pattern recognition receptors (PRR), such as toll-like receptor (TRLs) and purine and purinergic receptors (e.g., P2X7R), leading to further activation of the immune system [5].

The hallmark mechanism of GA is the assembly and activation of the NLRP3 inflammasome upon MSU crystals phagocytosed by macrophages. The NLRP3 machinery is a multi-protein complex that responds to danger signals, such as, mitochondrial ROS, potassium efflux, and lysosomal proteins [5,15]. The assembly and activation of the inflammasome is divided into two steps; the priming (signal 1) and the activation (signal 2), which ensures the specificity of the response [4,16]. During the priming, the cell activates the downstream signaling pathway of NF-κB and promotes the expression of all functional components necessary for the assembly and activation of the NLRP3 inflammasome, which occurs upon signal 2 [16]. NLRP3 inflammasome composition includes NLRP3, an adaptor protein ASC, and pro-caspase-1 [16]. Pro-caspase-1 is then activated in CASPASE-1 promoting proteolytic cleavage of pro-IL-1β in biologically active IL-1β [5].

In GA, the priming is dependent on the activation of TLRs, especially TLR2 and TLR4 [4]. The role of these receptors may be due to the involvement of endogenous ligands (such as proteins S100A8/ S100A9, and long chain free fatty acids) in preparing immune cells to producing pro-IL-1β [17,18]. Previous studies have demonstrated the activity of cold-inducible RNA-binding protein (CIRP) in activating signal 1 in human neutrophils. CIRP is an endogenous molecule with pro-inflammatory properties released during cellular stress situations [19]. For instance, neutrophils pre-treated with CIRP produce IL-1β in response to MSU stimulation, indicating that this protein may also act as a signal 1, by increasing the expression levels of pro-IL-1β, collaborating to inflammasome assembly and release of active IL-1β in response to MSU crystals [19].

The inflammasome activation occurs from the interaction of MSU crystals with the plasma membrane of competent cells, and this signal is necessary for aggregation and polymerization of the components of the inflammasome and release of IL-1β. This interaction promotes a cellular response that is poorly understood, but which includes the efflux of potassium and calcium through ionic channels, and mitochondrial perturbations that lead to the production and release of ROS

602 [20,21]. Activating factors such as Nek7, a member of the Ser/Thr kinases (Nek) family related
603 mammalian to NIMA [22]. Nek7 promotes NLRP3 oligomerization and inflammasome assembly,
604 which is composed by the NLRP3 [16].

605 GA pathology is intimately connected to the release of IL-1β, which orchestrates the
606 development of acute inflammatory episodes promoting vasodilation and neutrophil recruitment
607 [16]. The recruitment of neutrophils into the inflammatory microenvironment contributes to the
608 production and release of more pro-inflammatory cytokines and chemokines (*i.e.,* IL-8, IL-6 and
609 CXCL8), ROS, and lipidic mediators such as PGE_2 and LTB_4 [2,23]. It is also known that MSU
610 crystals induce neutrophils to produce and release neutrophil extracellular traps (NETs) [24],
611 leading to the death of these cells and contributing to the amplification of necroinflammation in
612 acute cases of the disease [5]. Furthermore, IL-1β release results in the activation of varied cell
613 types via IL-1 receptor (IL-1R), and also contribute to the production of other pro-inflammatory
614 cytokines and chemokines, as well as the activation of pro-inflammatory transcription factors (*i.e.,*
615 NF-κB and JNK) (SO; MARTINON, 2017).

616 In addition to IL-1β, the participation of other cytokines in GA pathophysiology, such as
617 IL-33 and IL-17, has also been demonstrated. High levels of IL-33 are found in the synovial fluid
618 of GA patients [23]. IL-33 is a member of the IL-1 family that, upon release, acts as a cytokine
619 activating the ST2 receptors, promoting leukocytes recruitment in rheumatic diseases [25], and
620 foment immune response activation in GA [26]. The major mechanisms of IL-33 in GA is through
621 the enhancement of pro-inflammatory cytokines release by macrophages, specially IL-1β [23].
622 Similarly, studies have also shown an increase in serum levels of IL-17 at the beginning of acute
623 GA flares, due to T-cell activation, which contributes to the development of the disease [27]. IL-
624 17 is a pro-inflammatory cytokine produced by T helper 17 (Th17) cells, playing an important role
625 in exacerbating autoimmune diseases, such as rheumatoid arthritis [28].

626 Both the abundant recruitment of neutrophils and the production of pro-inflammatory
627 mediators (*i.e.,* PGE_2, bradykinin, cytokines, substance P) sensitize and activate nociceptor
628 neurons, playing an important role in the development of excruciating pain, as reported by GA
629 patients [29–31]. MSU crystals do not directly activates sensory nociceptor neurons, however, its
630 deposition in the joint cavities and the cell-dependent inflammatory response induce pain [31]. In
631 this process, pro-inflammatory mediators, especially IL-1β, sensitize nociceptor sensory neurons
632 causing the release and activation of cytokines, prostanoids, kinins, complement system

components, and neuropeptides that contribute to the development of pain. In fact, IL-1β can also act directly on nociceptors through neural receptors such as IL-1R1, and transient receptor potential (TRP) family members such as vanilloid subtype 1 (TRPV1) and ankyrin 1 (TRPA1) [31].

For instance, TRPV1 activation causes depolarization of the nociceptors and subsequent release of neuropeptides, contributing to the production of nociceptive and edematogenic responses in response to the stimulus with MSU [32]. TRPA1 is also expressed in peptidergic sensory fibers, and is activated by ROS compounds (*i.e.,* H_2O_2). In fact, MSU crystals increase H_2O_2 production, thus promoting the activation of TRPA1 channels, contributing to pain response [33].

Although much have evolved in the understanding of GA pathophysiology, a massive gap is still present in its treatment. Current treatments for GA were reviewed elsewhere [34–37]. Nevertheless, the control of uric acid serum levels is crucial to avoid acute flares or disease aggravation over time generating chronic inflammation. Chronic cases of the disease are characterized by the presence of chronic gouty synovitis, structural joint damage and the presence of gouty tophi [9]. The gouty tophi consists of a nucleus where the MSU crystals are compacted, a surrounding cell coronal zone and an external fibrovascular zone, representing a chronic granulomatous inflammation [9]. Cells that participate in the innate and adaptive immunity, such as multinucleated giant cells, and pro-inflammatory cytokines (i.e., IL-1β, TNF-α, TGF-β1) are also present in the chronic phase of GA [38]. Nevertheless, in all scenarios of the disease, the control of excruciating pain is still an unmet need. **Figure 1** pictures the GA pathophysiology.

3. Mechanism-based targeting of gout arthritis pathology

The GA pathophysiological mechanism is plenished of components, going beyond of IL-1β system. Although the broad spectrum of involved components and signaling pathways limit pain management, it also increases the possibility for drug targets. In addition, it might also indicate that GA therapeutics should consider the use of multiple drug targets or drugs that have multiple mechanisms of action. Thus, in this topic we focus to discuss and list some potential novel drug candidates organized by their mechanism of action. The intention is to discuss potential candidates considering their mechanism of action and not to provide an exhaustive list of drugs that act by each mechanism since there is a limitation of citations as per journal style. We will also base our discussion on the following types of approaches antagonism, agonism, or neutralization, for the control of hypouricemia, pain, and inflammation in pre-clinical settings. Tables 1 – 15 summarize our discussion.

3.1. Inducers of the uric acid exporter ABCG2

Studies have shown that ATP-binding cassette subfamily G member 2 (ABCG2), a higher-capacity urate exporter, play a fundamental role in hyperuricemia and gout susceptibility, what is presumed to be used as managers of GA pathophysiology. Loss-of-function mutations in this protein are related to GA development, through disturbances in urinary, biliary, and fecal excretion mechanisms [39–41]. For instance, SNP in rs72552713 gene was previously demonstrated to be distinct in gouty arthritis patients and control individuals, with the allele T related with an increased risk of gout by carriers [42]. In pediatric patients with early onset of hyperuricemia/gout, genetic dysregulated ABCG2 variant was demonstrated to be a crucial risk familial factor component for the disease [43,44]. Additionally, single nucleotide polymorphisms in ABCG2 rs2231142 can predict nephrolithiasis and chronic kidney disease is Asian man [41]. Therefore, ABCG2 transporters are promising target candidates for GA treatment. **Table 1** brings details of the studies cited in our briefly discussion.

3.2. Modulators of phagocytosis and autophagy

Recognition and phagocytosis of MSU crystals is an essential event of GA. This process leads to the formation of phagolysosome that aim to particulate and inactivate crystals [45]. However, due to the shape and physical characteristics, MSU crystals are not digested, to the contrary, they cause the rupture of phagolysosomes and drive the inflammatory response since cathepsins are sensed by and activate NLRP3 inflammasome assembling resulting in IL-1β and IL-18 maturation and release [4]. In fact, the reduction in crystals phagocytosis decreases NLRP3 inflammasome activation, IL-1β maturation [46]. A clinical study also demonstrated that the levels of pro-inflammatory mediators, including IL-1β and IL-18, are correlated with crystal phagocytosis index in samples of synovial fluid (SF) from patients with GA [47].

In an *in vitro* study with normal human osteoblasts, the phagocytosis of MSU crystals triggers – not only the activation of the inflammasome NLRP3 – but also the activation of a NLRP3-dependent autophagy mechanism [48]. Differently from professional phagocytes (*e.g.* macrophages) the engulfment of MSU microcrystals by osteoblast causes autophagy, which although dependent on NLRP3, is not associate to the inflammasome-dependent production of IL-1β, thus ameliorating the inflammatory response [48]. Therefore, autophagy is a well conserved mechanism – dependent on phagocytosis – to the complete removal of particles without exacerbating the production of pro-inflammatory mediators [45,48]. Nevertheless, in the GA context, the phagocytosis followed by autophagy are not effective in eliminate the particles [48].

Unfortunately, although very effective in GA, systemic or chronic blockage of phagocytosis might be a double-edged sword. Those mechanisms are also important for tissue homeostasis, including immune response and pathogens killing. Therefore, the schedule of treatment, dose, and application route should be carefully determined to avoid susceptibility to infections. There are compounds whose activity depends on reducing phagocytosis or inducing autophagy in GA (**Table 2**)**.** Nevertheless, all the compounds discussed in this topic have been described to have multitarget mechanisms including effects in the modulation of phagocytosis or autophagy. Thus, allowing the development, repurposing, or supplementation to reduce GA flares.

3.3. Inhibitors of ATP signaling and purinergic receptors

The inflammatory response is often associated to cell damage and the release of danger-associate molecular patter (DAMP). For instance, during the formation of extracellular traps ATP, HMGB1, histones, and genetic material are expose to the extracellular inflammatory milieu. During this process, ATP, and other DAMPs signals via specific receptor to foment inflammation. Importantly, ATP signaling via purinergic receptor P2X ligand-gated ion channel 7 (P2X7R) also culminates in the activation of NLRP3 inflammasome and IL-1β maturation, a signaling pathway shared with MSU-induced inflammation. In fact, during GA, ATP signaling via P2X7R seams to synergistically induce the production of IL-1β, since extracellular ATP changes might also contribute to disease initiation and maintenance [49]. In a culture of blood monocytes-derived macrophages obtained from gout patients, MSU crystals or ATP induced the release of IL-1β when compared to non-treated cells [50]. However, combined treatment with MSU and ATP enhances in approximately 10-fold the release of IL-1β [50]. In a model of MSU-induced GA in rats, the administration of ATP in combination with MSU crystal accelerates the development of acute gout symptoms, parameters that were decreased with pre-treatment with BBG treatment, a P2X7R antagonist [51]. Moreover, ATP increase the release of pro-inflammatory cytokines and decrease the Treg/Th17 ratio, exacerbating inflammation [51].

In humans, the gene that codifies P2X7R is described to have several SNP. Those polymorphisms are, in some cases, associated to a spontaneous increase in IL-1β release [52]. Patients with two or more SNP in the gene loci rs1653624 and rs7958316, presented higher propension to develop GA [53]. Corroborating these results, in a rat model of self-occurring GA, MSU and ATP are synergistic related to polymorphisms in a allele of P2X7R gene, which increase the susceptibility to disease development [50]. Those compelling evidence not only shed light in the synergetic role of P2X7R in GA, but also a potential drug target for the disease therapeutics. **Table 2** also summarizes the molecules candidates for ATP receptor antagonists.

3.4. Modulators of mitochondrial damage and mitophagy

Mitophagy characterizes a process in which cells selectively remove injured mitochondria via the specific sequestration and engulfment of this organelle, and subsequent degradation by lysosomal activity [54,55]. It is a fundamental process for mediating cell survival and viability in response to both stress conditions and regular physiological processes, aiming to reinstate

homeostasis [55]. This cellular phenomenon is triggered by the upstream effector of NLRP3 activation, mitochondrial oxidative stress, ROS generation, or in case of mitochondrial damaged mitophagy is often in place [56]. In fact, mitophagy represents a critical process for the retainment of the NLRP3 inflammasome activation in macrophages via p62 signaling [56,57].

In experimental models of GA, the investigation about whether the induction of mitophagy is beneficial for GA treatment has been observed in some studies. For instance, the polyphenols resveratrol [58] and curcumin [59], and the iridoid monoterpenoid loganin [60], were described to reduce NLRP3 inflammasome activation, and the levels of IL-1β/IL-18, by mechanisms also related to the modulation of mitochondrial damage and mitophagy. The detailed mechanism and experimental conditions are summarized in **Table 2**. In summary, those reports suggest that mitochondrial distress participates in GA pathogenesis, and it is a targetable phenomenon, because it contributes to NLRP3 assemble and IL-1β production. In addition, resveratrol, curcumin, and loganin are promising candidates to treat GA symptoms via mitochondrial protective effects.

3.5. Inhibitors of inflammasome NLRP3

The inflammasome NLRP3 represents a crucial mechanism of GA physiopathology, and each of its components – NLRP3, caspase-1, and the adaptor molecule ASC – have pivotal roles in IL-1β maturation, which explain they are also drug targets for GA therapeutics. In this section, we will review studies that described the inhibition of the NLRP3 to limit GA pathology.

3.5.1. NLRP3

The NLRP3 is the primary molecule for sensing and triggering the inflammasome molecular platform assembly to maturate pro-IL-1β and pro-IL-18. However, inhibiting NLRP3 is, by far, not the only approach to reduce inflammasome activity. Targeting NF-κB activation has also consequences such as preventing the induction of NLRP3 expression, and the components of NLRP3 inflammasome. We have listed molecules that target this important molecular mechanism in GA, as per inhibition of NF-κB and impairment of NLRP3 expression, or the reduction in NLRP3 and other components of this inflammasome (**Table 3**).

3.5.2. ASC-speck

NLRP3 inflammasome assembly requires the adapter protein apoptosis associated speck-like protein containing a CARD (ASC) [4,61]. ASC oligomerization provides the generation of large intracellular protein scaffold, creating a unique structure called ASC "speck" [62]. After inflammasome NLRP3 activation, ASC protein polymerization contributes to the inflammatory activity and is fundamental to pro-caspase-1 recruitment and further cleavage in its active form, CASPASE-1 [63]. Therefore, targeting ASC expression or its assembling might contribute to GA outcome. **Table 3** curates molecules that inhibit ASC-speck formation, ASC mRNA expression, NLRP3 and ASC interaction, and upstream molecules involved in NLRP3 activation such as TRAF1 (tumor necrosis factor receptor associated factor 1) in vitro or in MSU murine GA.

3.5.3. Caspase-1

IL-1β maturation depends on CASPASE-1 proteolytic activity [4]. Therefore, targeting CASPASE-1 is also a key to novel therapeutic approaches for GA. In the pre-clinical scenario impairment of CASPASE-1 activity has been described to improve GA outcome [64,65]. Currently, the described approaches consist on the inhibition of its proteolytic activity and the impairment of pro-caspase-1 interaction with NLRP3-associated components [64,65]. Specifically, there are molecules – listed in **Table 3** – that block CAPASE-1 activity by biding in the active pocket [64,65]. In addition, this specificity contributes not only to protein function but also to CASPASE-1 interaction with other components and signaling pathways [64,65]. For instance, the inhibition of CASPASE-1 activity by the small molecule NSC697923, suppressed NF-κB activation, blocked the interaction between receptor interacting protein-2 and pro-caspase-1, thereby impairing NLRP3 priming and MSU-induced edema and IL-1b release [65]. Therefore, blocking CASPASE-1 activity may involve the impairment of other processes necessary for NLRP3 inflammasome activity.

3.6. Inhibitors of cytokines, complement system, Toll-like receptor 4 (TLR4) and related signaling pathways

Neutrophil recruitment to joint cavity and periarticular tissue is a hallmark of GA [61]. Neutrophil recruitment in GA depends on the production of chemotactic cytokines [61]. In fact, pharmacological treatment with DF2162 [61] or reparixin [66], allosteric antagonists of CXCR2 and CXCR1/2, respectively, and the selectin inhibitor, fucoidin [61] reduce neutrophil influx to the knee joint cavity in models of GA. In addition to neutrophils, macrophages also contribute to GA pathology. During GA, levels of macrophage migration inhibitory factor (MIF) are increased in the synovial fluid of patients and in MSU-induced GA in mice. Those levels correlate positively with IL-1β levels in patients, [66]. Administration of recombinant MIF (rMIF) triggers the expression of IL-1β mRNA, which increases leukocytes recruitment, IL-1β and CXCL1 production, and histological changes in a similar manner to MSU-induced GA [66]. MIF knockout, pharmacological inhibition ((S,R)-3-(4-hydroxyphenyl)-4,5-dihydro-5-isoxazole acetic acid), or antibody neutralization reduced all observed events [66]. Thus, demonstrating that MIF is a drug target to reduce leukocytes recruitment and IL-1β expression in GA.

Similarly, the level of the cytokine/alarmin IL-33 is described to be elevated in the synovial fluid of patients with GA and correlates significantly with the number of total leukocytes and neutrophils, in comparison to synovial fluid samples of osteoarthritis patients [23]. IL-33 has been demonstrated to orchestrate the recruitment of neutrophils in other rheumatic diseases such as rheumatoid arthritis [67]. The knockout of IL-33 receptor (ST2) decreased MSU-induced inflammation, leukocyte recruitment, and pain [23]. Moreover, functionally, IL-33 potentiates the maturation of IL-1β in BMDM cells culture [23]. Mechanistically this also might indicate that anti-IL-33 therapies (e.g., Itepekimab) or blockers for ligand-receptor signaling might be repurposed to GA treatment, however pre-clinical and clinical studies are required.

Other cytokines, such as IL-17A, also contribute to GA pathophysiology. In fact, there are Th17 cells in the MSU inflammatory milieu and treatment with anti-IL-17A monoclonal antibody reduced MSU-induced joint inflammation [68]. These findings suggest that repurposing of IL-17 humanized monoclonal antibodies, such as secukinumab, used for the treatment of psoriasis and psoriatic arthritis, might also be beneficial for GA patients.

Importantly, proteins from the complement system also participates in MSU-induced inflammation in mice [69]. In a culture of peritoneal macrophages, the proteins C3a and C5a increase in a concentration-dependent manner the release of IL-1β in comparison to LPS-primed cells, therefore suggesting a priming-like effect [69,70]. In fact, MSU crystals rapidly induce the

activation of complement system and increase the levels of C3a and C5a in mice peritoneal exsudates [69]. C5a contributes to the increase in ROS production, which drives the expression of NLRP3 components and IL-1β maturation upon MSU stimulus [69]. Therefore, targeting the complement system might be an important approach for GA therapeutics.

The production of IL-1β and the inflammatory response caused by MSU crystals is also dependent on TLR4, which guides downstream signaling to MSU-induced inflammation and pain. For instance, TLR4 signaling can be blocked by lipopolysaccharide from *Rhodobacter sphaeroides* (LPS-RS). Inhibition of spleen tyrosine kinase (SYK) with OXSI 2 also reduced the release IL-1β leading to the reduction of pain and inflammation in GA [71]. In another study, Phosphoinositide-3 kinase gamma (PI3Kγ) inhibition or knockout, reduced MSU-induced inflammation, and pain [72], indicating a relevant role in gout arthritis physiopathology. However, considering the complex involvement of PI3Kγ in several signaling process, potential side effects upon chronic treatment should be considered. For instance, it has been shown that the analgesic drug morphine activates PI3Kγ in the DRG neurons to inhibit nociceptive neurons activation [73]. As endogenous opioids and other drugs such as diclofenac and dipyrone likely share a PI3Kγ-dependent mechanism [74,75], it is uncertain the extend that PI3Kγ inhibition would have over endogenous analgesic mechanisms. **Table 3** summarizes our discussion.

3.7. Regulatory T lymphocyte (T_{reg})

As mentioned earlier, adaptive immunity cells such as Th17 cells are relevant in GA pathology. Tregs also represent a specialized group of T cells with the attribution of suppressing the immune response, aiming homeostasis and self-tolerance. Tregs induced by B cells (Treg-of-B cells) is a distinct $Foxp3^-$ subpopulation active in inflammatory conditions. During *in vitro* settings, Treg-of-B cells blocked the activation of NLRP3 inflammasome induced by MSU or ATP in macrophages, and consequently, inhibited caspase-1 activation and IL-1β production. Moreover, in a mouse model of air pouch gouty inflammation, Treg-of-B reduced the influx of inflammatory cells, as well as cytokine and chemokine production, therefore suggesting this subset of regulatory immune cell represents a potential target for gouty arthritis control [76]

3.8. Inducers of Nrf2 activation

The activation of Nrf2-antioxidant responsive elements (ARE) transcriptional signaling confers protective effects for cells through the induction of detoxification pathways and ROS elimination, which ultimately, leads to a well-known anti-antioxidant, anti-inflammatory, and analgesic effects. Thus, the modulation of this pathways can render control of GA. Activation of Nrf2 orchestrated resolution of GA by inhibiting MSU-induced articular edema, leukocytes recruitment, NLRP3 activation and increased the expression of antioxidant molecules, such as heme oxigenase-1 [77–79]. **Table 3** details the experimental conditions and possible drugs targeting this pathway.

3.9. Inducers of protein kinase A (PKA)

PKA belongs to a family of enzymes whose activity is dependent on the cellular levels of cyclic adenosine monophosphate (cAMP). PKA is characterized as a serine protein kinase that phosphorylates serine and threonine (Ser/Thr) residues on its targets [80]. Regarding NLRP3 inflammasome activity, PKA is known to phosphorylate Ser/Thr residue, leading to NLRP3 ubiquitination and consequently, the suppression of NLRP3 activation [81,82]. Furthermore, the PKA inhibitor, H89, favors NLRP3 inflammasome assembly and activation [82]. This result suggests that PKA induction might be a potential target to treat NLRP3-dependent inflammatory diseases. Example of PKA inducer can be found at **Table 4**.

3.10. miRNAs and circRNAs

Micro RNAs (miRNAs) are short non-coding RNA molecules that play important roles in controlling gene expression. miRNAs are effective in modulating gene expression via mRNA interaction, mRNA degradation, or translational repression [83]. Studies have evaluated the effects of miRNA as therapeutical tools in experimental models of GA. For instance, miR-223-3p is described to possess immunomodulatory and anti-inflammatory properties, and its dysregulated expressions is related to infection [84] and rheumatic diseases [85]. It was demonstrated that miR-223-3p can inhibit NLRP3 inflammasome activation and IL-1β release in rodent macrophages [86] and neutrophils [87]. In MSU-induced GA, miR-223-3p is downregulated in joint samples of rats

899 [88]. In addition, in fibroblast-like synoviocytes (FLS), treatment with miR-223-3p reduces
900 NLRP3, caspase-1, and IL-1β at mRNA and protein levels [88].
901 Similarly, circular RNAs (circRNAs) represents a type of single-stranded RNA that forms
902 covalently closed continuous loop and are also related to transcriptional regulation [89]. For
903 instance, the levels of circHIPK3 have been shown to be increased in synovial fluid mononuclear
904 cells (SFMCs) from gouty arthritis patients and in MSU-stimulated THP-1 cells [90]. Increases in
905 circHIPK3 contributes to inflammation by sponging miRNA-192 and miRNA-561, which in turn
906 results in the promotion of toll-like receptor 4 (TLR4) and NLRP3 signaling [90]. Interestingly,
907 genetic deletion of CircHIPK3 reverted gouty arthritis in mice [90]. Altogether, these data
908 highlight the therapeutic potential of miRNA and circRNA modulation for the treatment of GA.
909 Examples of miRNA and circRNA that are active in GA or that activity has not been tested yet in
910 GA can be found at **Table 4**.
911
912 **3.11. Mediators and molecules regulating inflammation resolution**
913
914 The contemporary comprehension of resolution of inflammation has attributed to pro-
915 resolving lipid mediators an important function, and the fact that these molecules have analgesic,
916 anti-inflammatory, and pro-resolutive properties shed light in therapeutic approaches [91–93].
917 15d-PGJ2 is a cyclopentenone prostaglandin with peroxisome proliferator-activated receptor-
918 gamma (PPAR-γ) dependent and independent signaling mechanisms with pro-resolution effects
919 [94]. The treatment with 15d-PGJ2-loaded nanocapsules inhibited MSU-induced joint mechanical
920 hyperalgesia, edema, leukocyte recruitment, and oxidative stress in a PPAR-γ-dependent manner
921 [95].
922 Other pro-inflammatory mediators, such as leukotriene B4 (LTB_4), were described to be
923 involved in MSU-induced nociception [61]. Blocking 5-LOX activity with the five-lipoxygenase
924 activating protein inhibitor MK886, reduced mechanical hyperalgesia, neutrophil recruitment, and
925 the levels of IL-1β and CXCL1, indicating a lipid mediator related nociception mechanism [61].
926 Similarly, the same effects were obtained by treating mice with LTB_4 receptor (BLT1) antagonist,
927 CP105696 [61]. Moreover, in vitro, CP105696 treatment reduces both LTB_4- and MSU-induced
928 ROS production [61]. 5-LOX is also important for the synthesis of specialized pro-resolving
929 mediators (SPMs), which have been described to exert anti-inflammatory and analgesic proprieties

930 in experimental gouty arthritis [96]. In the context of resolution pharmacology, Annexin A1 signals
931 through ALX/FPR2, a G protein-coupled receptor (G-PCR), which has the SPM LXA_4 and RvD1
932 as agonists. The treatment with the AnxA1-active N-terminal peptide (Ac_{2-26}), reduced MSU-
933 induced inflammation in the knee joint [97]. In addition, synthetic LXA_4 mimetics (sLXms), AT-
934 01-KG, also agonist of ALX/FPR2 reduced MSU-induced associated inflammation [98]. These
935 data indicated that the resolution process of inflammation might be an effective target via
936 ALX/FPR_2 [96–98]. Therefore, in summary targeting 5-LOX can reduce gout inflammation.
937 However, it must be verified in clinical settings whether this approach will interfere with the
938 endogenous production of pro-resolution lipid mediators and the extend that this will affect the
939 effectiveness of treatment. At least by exogenous administration, SPM such as LXA_4 and RvD1
940 reduce gout inflammation and pain [96–98]. **Table 4** summarizes the detailed mechanisms and
941 experimental settings.
942
943 **3.12. Targeting neuroinflammation and neuro-immune communication**
944
945 The recognition and phagocytosis of MSU crystal by resident cells is fundamental to trigger
946 GA. Despite colchicine partially inhibits this phenomenon, treatment is accompanied with severe
947 gastrointestinal side-effect [99]. The neuropeptide calcitonin gene-related peptide (CGRP), which
948 is abundant in the synovial fluid of GA patients [100] was observed to enhance crystal
949 phagocytosis and IL-1β maturation [96]. Quite interestingly, resolving D1 (RvD1), a SPM,
950 disrupted nociceptor neuron activation and CGRP release in *vivo* and *in vitro*, thus, RvD1 blocked
951 CGRP-induced enhancement of MSU crystals phagocytosis and IL-1β release. These results reveal
952 that RvD1 can inhibit neuro-immune communication to reduce GA [96]. This study also sheds
953 light that anti-CGRP therapies available for the treatment of migraine (*e.g.,* atogepant, erenumab,
954 eptinezumab, fremanezumab, and galcanezumab) or its receptor antagonism (*e.g.,* rimegepant),
955 might be repurposed for GA treatment, however complementary studies are yet necessary.
956 Another possible targetable approach is by modulating nociceptor neuron activation. TRP
957 channels are well known to participate in GA physiopathology contributing to edema and pain
958 [32,71,101,102]. In fact, blockade of TRPA1, TRPV1, and TRPV4 resulted in overall reduction in
959 MSU-triggered disease [32,101,102]. The blockade of TRPA1 by HC-030031 reduced disease
960 outcome and the expression of TRPA1 and TRPV1 in DRG neurons [101]. Similarly, TRPV1

961 antagonism with SB366791 also results in analgesic effect and the reduction of inflammatory
962 markers [71,103]. This pharmacological approach is in line with the detection of increased TRPV1
963 in the DRGs of gout arthritis rats compared to negative controls indicating a gain of function of
964 this channel [32,103]. In addition, GSK219, a TRPV4 antagonist was described to reduced GA-
965 related symptoms in mice [102]. On the other hand, neuronal hyperpolarization is another possible
966 approach [104]. Treatment with Retigabine and Flupirtine, agonists of the potassium channel
967 family Kv7/M (potassium channels family) reduced mechanical and thermal hyperalgesia [104].
968 Another analgesic mechanism related to neuronal hyperpolarization is dependent on neuronal
969 production of NO followed by activation of cGMP/PKG/ATP-sensitive K^+ channels signaling
970 pathway [105]. In fact, in a study the effects of an NO donor were tested in mice [106]. The NO
971 donor administration decreased primary afferent neuronal activation, articular mechanical
972 hyperalgesia and knee joint edema [106]. Treatment also reduced leukocyte recruitment, oxidative
973 stress, NF-κB activation, and the production of pro-inflammatory cytokine [106]. These
974 mechanisms are detailed in **Table 4**. In summary, neuroimmune interactions and neuronal
975 modulation might also be pursued in the treatment of GA.
976
977 **3.13. Antioxidants and multitarget drugs**
978
979 Natural products such as flavonoids, polyphenols, terpenoids and sesquiterpene lactones are
980 well known compounds with pronounced anti-inflammatory and analgesic actions in different
981 experimental conditions [107,108], including GA. In **Table 5** we list the compounds and their
982 detailed mechanisms of action in GA signs and symptoms. In general, the outcome observed in
983 experimental mice models upon treatment with antioxidants are multiples mechanisms
984 culminating in symptoms improvement.
985 Flavonoids present antioxidant proprieties by reducing oxidative stress [79,109–112] and by
986 increasing endogenous antioxidant systems, *e.g.* increase in glutathione levels [79,109,110].
987 Among the effects, reduction in leukocytes recruitment to joint tissue [79,109,110,113,114],
988 blockade of NF-κB activation [79,110,114], decrease in mRNA expression and protein levels of
989 chemokines and cytokines, especially IL-1β [79,110,113,114] are often observed. In addition to
990 the shared mechanisms, the analgesic, antioxidant, anti-inflammatory effects of the flavonoid
991 quercetin were blocked by opioid antagonist, naloxone [109]. In this sense, quercetin exert its

analgesic effects in a similar mechanism as opioids [109]. Moreover, flavonoids have a low toxicity profile and also exert effects in downregulated hyperuricemia [115].

The triterpenoids are other class of natural products that have been described to exert anti-gouty effects. Mechanistically those compounds on the inhibition of leukocytes recruitment [115], paw edema [115], and reduced the levels of pro-inflammatory cytokines [116]. Sesquiterpene lactones are abundant in plant extracts and have anti-inflammatory and analgesic proprieties [117]. In fact, experimental GA mice present treated with sesquiterpenoids have been described to also inhibited leukocyte recruitment to the synovial tissue [118,119] and improve GA signs in rodents [120,121]. Particularly, the sesquiterpene lactone budelein A, reduced MSU crystal phagocytosis, decreased NF-κB activation, and NLRP3 inflammasome-dependent IL-1β maturation, contributing to inhibit a crucial pathophysiological step in gout [119]. Isoquinoline alkaloids are also natural products belonging to the family of phytochemicals [122]. In a model of GA in mice, isoquinone alkaloid treatment reduced MSU-induced pain, edema, leukocyte recruitment, and the production of pro-inflammatory cytokines [121]. In addition, *in vitro* (RAW 264.7 macrophages)*/vivo* data also evidenced that this compound exerts its anti-GA properties by targeting ROS-NLRP3-ASC speck-capsase-1 signaling and inducing antioxidant enzymes [121]. Thus, revealing its various mechanisms and targets to counteracts the GA pathology.

Plants extracts, such as from *Coffea arabica* and *Lychnophora pinaster* were described to have analgesic proprieties in GA [115][123] [124], by targeting leukocyte recruitment, cytokine production (*i.e.,* IL-1β and TNF-α) [123,124]. Importantly different organic fractions from *Lychnophora pinaster* have an additional mechanism, regulating hyperuricemia by inhibiting xanthine oxidase (XOD) activity [115]. Therefore, those and other natural products and plant extracts (Table 14) should be further considered as potential candidates to gouty therapeutics.

The protein phosphatase A2 (PPA2) mediates a wide range of cellular activity, including GA [112]. In BMDM cells, MSU or nigericin stimulation reduced the expression of PPA2, while the anti-hyperuricemic drug febuxostat and the PPA2 activator fingolimod phosphatase restored PPA2 levels [112]. Changes in expression levels were accompanied by inhibition of leukocyte recruitment and IL-1β production, whereas increased the recruitment of anti-inflammatory non-classical monocytes [112]. These effects were mechanistically attributed to the inhibitory activity of PPA2 upon xanthine oxidase-derived ROS in M1 macrophages [112]. Therefore, this study

highlights that PPA2 participates in GA pathophysiology, and its activation (e.g., using fingolimod), might be a promisor multi target drug for GA treatment.

The inflammatory milieu in gout arthritis is also composed by kinins and angiotensin II, which are described to be involved in pain perception and inflammation in several diseases. They have a common step in their synthesis/metabolism since the angiotensin converting enzyme that converts angiotensin I in angiotensin II, degrades bradykinin [125,126]. In a model of MSU-induced gout in rats antagonism of kinin receptor B1, reduced pain behavior and edema [127]. In another study, the antagonism of Angiotensin receptor type 2 (AT_2R) ameliorates gout arthritis outcome in mice, reducing pain, edema, leukocyte recruitment [128]. Therefore, the anti-inflammatory effects of kinin receptor B1 and AT_2R antagonists might be further explored as multitarget drugs in gout arthritis therapeutics.

3.14. Traditional Chinese medicine (TCM)

Herbal formulas comprehend the base of TMC. Despite TCM and herbal extracts have shared multitarget mechanism with antioxidant molecules (Table 14), we have designated this section to reinforce the cultural importance of TCM and its effects in in experimental GA. The herbal formulas, experiment details, and mechanisms are listed in **Table 5**. In summary, centenary TCM herbal formulas have been described to exert protective effects by reducing hypouricemia [129–131]. In addition, most formulas are described to reduce leukocytes recruitment [129,130,132–134], the levels of pro-inflammatory lipid mediators (*i.e.* PGE_2 and LTB_4), and production of pro-inflammatory cytokines (*i.e.* IL-1β, IL-6, and TNF-α) [129,130,134].

3.15. Gout and Gut microbiota

In the past decade, significant progression was made towards understanding the effects and roles of gut microbiota in health and disease. Most importantly, how dysbiosis might interfere in disease initiation or outcome. In a study with two independent cohorts analyzing 1392 subjects, microbiota dysbiosis is associated with increased serum levels of urate [135]. In particular, the increase levels are observed with low relative abundances of genus *Coprococcus*, demonstrating a direct effect of gut microbiota in disease propension [135]. In addition, microbiota dysbiosis in

GA patients is also associated with enriched function on carbohydrate metabolism but a lower potential for purine metabolism, increasing the susceptivity to higher urate plasma levels and GA occurrence [136].

Importantly, the influence in urate levels gut microbiota is also associated to individual response to urate-lowering therapies [137]. A cohort study analyzed stool samples from health and GA patients [137]. The study also divided GA patients in two groups, those that respond to urate-lowering therapy (febuxostat), and patients with uncontrolled urate levels even under febuxostat treatment [137]. The study demonstrated, using 16S rRNA gene-based microbiota analysis, that the diversity gut microbiota was reduced in GA patients compared to health controls [137]. Furthermore, this difference was more accentuated in patients that do not respond to urate-lowering therapies [137]. Corroborating these data, in another cohort study, patients treated with febuxostat have more diversity and increased potential for purine metabolism [136]. To the contrary, oral administration of colchicine also induces gut microbiota dysbiosis in mice [138]. These results associated to functional metagenomics predictions and exploration functional biomarkers indicate that modulation of gut microbiome may also serve as a tool to treat and predict responsiveness of patients to the treatment and drug efficacy [136,137,139]. **Table 5** lists the influence of microbiota products to GA outcome and possible therapeutic approaches using microbiota enrichment (probiotics administration) for the control of hyperuricemia [140,141]. Therefore, the current literature supports that gut microbiota might be modulated biologically or pharmacologically to improve organism responses to inflammatory diseases, including GA.

4. Conclusions

The present review discusses the current knowledge on gout arthritis disease mechanisms and treatments under pre-clinical investigation. This scenario allows to identify disease mechanisms indicating novel potential targets to develop gout arthritis treatments. Novel treatments are needed on the basis of molecules that present lessened side effects or other types of side effect, which allows selecting the treatment drug that is the most adequate to the co-morbidities of a specific patient. Lowering the treatment cost is also relevant since biologicals are effective, but the cost is too high. Drugs that target the signaling pathways involved in IL-1β maturation and are not biologicals, could represent a great advance for the patients. Effectively, just a low number of patients can afford an anti-IL-1β treatment that costs around $250,000 (USD) per year and is considered to have the lower cost-effectiveness acceptability probability [142]. Higher efficacy is also desirable since the gout inflammation is not well-controlled in most cases and in the acute flares. In fact, the management of acute flares needs improvement since the patient feels excruciating pain that is not fully controlled. Considering this rationale, we sieve the literature to present the current targets for drug development as well as some examples of molecules with promising activity against the disease mechanisms of gout arthritis. **Figure 2** depicts the GA signaling pathways that are targeted by mechanism-specific drug groups (bold numbers) discussed herein.

5. Expert Opinion

Since GA first reports more than 2,000 b.C. and until today, the humanity has struggle to control its symptoms and impacts in life quality. It is not that there are not available therapies, but the lack in fully active anti-inflammatory and analgesic therapies during GA flares, or the innumerous undesired side effects discourage patients' adherence to treatment. Unfortunately, GA therapeutics are yet an echoing question. An echo questioning what is new, how should it be improved, and how patients could beneficiate from more effective therapies? One important point is that patient's response to treatment vary, which means a portion of patients report reasonable analgesic effects from currently available therapies. However, even with heterogeneity of population, most therapies offer undesired side effects (*e.g.,* colchicine), are expensive (e.g., immunobiologicals), upon chronic usage might induce toxicity (e.g., NSAIDs), or interfere in the immune system response (*e.g.,* SAIDs, immunobiologicals). Therefore, we focused on discussing GA pathophysiological mechanisms that might be used for drug targeting, and reviewed pre-clinical data from promising drug candidates in GA treatment based on their mechanisms of action.

In the big picture in this review, we explored dozens of published studies demonstrating mechanisms of action and pharmacological proprieties of molecules from varied classes with analgesic, anti-inflammatory, and antioxidant activity in experimental models of GA in rodents (Table 1 - 5). In comparison, using "gout flare" as search parameter in the clinicaltrials.gov platform, resulted in only 67 studies listed. From those, 36 trials with completed status have canakinumab, anakinra, and rilonacept (*i.e.,* drugs targeting IL-1β signaling), and alternatives to colchicine delivery as the most used interventions. Targeting IL-1β would be a promising approach in GA since it has been demonstrated initially in pre-clinical settings showing the role of NLRP3 inflammasome in IL-1β maturation and disease [4]. Only 4.4% of listed clinical trials aimed to intervene with natural products, or current hot targets described herein. Thus, clinical trials and pre-clinical research are not entirely aligned with each other. The massive gap between pre-clinical discovery and the clinical studies it is still an issue to GA therapeutic development and novel pharmacological approaches. Nevertheless, our review brought several drug targets and drug candidates that might contribute to the future of GA treatment. More importantly, our approach aimed at highlighting promising mechanisms of action or targets in GA to allow the rational development of novel molecules.

Despite of the challenges in GA treatment, according to our review, herein we envisage novel possibilities and drug targets. Among possibilities we highlight the I) repurposing of existing therapies; II) ALX/FPR2 agonism for improvement in disease outcome; III) the use of multitarget drugs; and IV) targeting the neuroinflammatory component of GA. GA pathophysiology, specifically gout flare, is dependent of several components that contribute to disease development and symptoms. Among those components, crystal precipitation and phagocytosis, NF-κB activation, NLRP3 inflammasome engagement, IL-1β release [4] and neutrophils recruitment [61].

Discussing those possibilities, the approach I would involve seeking for drugs that are not used for gout treatment, but that have been shown to present potential as anti-inflammatory drugs with low side effects or side effects different from the current therapies, *i.e.* drugs that inhibit phagocytosis, NF-κB activation, and IL-1β pathway (Tables 2, 5-8). The approach II is related to stimulating the resolution of inflammation that is induced by annexin A1 and SPMs (*e.g.,* LXA4 and RvD1), both agonists of the ALX/FPR2 receptor. As described above, activating these receptors will have varied beneficial consequences in GA disease such as inhibition of neutrophil recruitment, cell profile modulation, and reducing NF-kB activation [96–98]. The potential drug candidates are summarized in Table 4.

Approach III considers the use of multitarget molecules (Table 5). For instance, natural products that are described to reduce GA parameters by targeting varied inflammatory pathways (Table 3, 5). In our experience, flavonoids are promising molecules, which are antioxidants as per their chemical structure [107,108]. However, evidence also supports that they inhibit NF-κB activation, in some cases by directly interacting with it or binding to some cytokines preventing their actions. Hesperidin methyl-chalcone (HMC) has analgesic and anti-inflammatory effects [79]. HMC in combination with another flavonoid, diosmin, is approved for the treatment of certain blood vessel problems and hemorrhoids. In fact, there are clinical trials testing this combination for other diseases, such as metabolic syndrome and diabetic neuropathy (clinicaltrials.gov NCT05243238), in which combined treatment improved disease outcome [143]. This combination has also been evaluated for treatment of COVID-19 (clinicaltrials.gov NCT04452799). Therefore, both pre-clinical and clinical evidence suggest the use of HMC for the treatment of GA. Furthermore, the discussed pre-clinical data also have highlighted other flavonoids, terpenes, and herbal extracts with analgesic and anti-inflammatory proprietress that would be the leading point to develop novel therapeutical approaches (Table 5). Sesquiterpene lactones are known to reduce NF-kB activation. However,

in addition to that, budlein A also reduces the phagocytosis of MSU crystals [119]. Thus, budlein A likely interferes with signals 1 and 2 of the GA pathology [119]. The multitarget drugs do not need to abolish a single pathway to be pharmacologically active, and this is an advantage since physiological process can continue. The opposite occurs with single target drugs such as NSAIDs that need to inhibit at least 80% of COX activity to be pharmacologically active.

Discussing the approach IV. During gout flares, CGRP levels are increased in the synovial fluid [100]. Recently, our group demonstrated that CGRP enhance MSU phagocytosis and IL-1β release by macrophages. Despite the SPM RvD1 reduced CGRP enhancement of MSU crystal phagocytosis and IL-1β maturation, this study shed light in the possibility to target CGRP in gout arthritis [96]. It is known that CGRP plays an important role in migraine. Moreover, there are several anti-CGRP humanized antibodies FDA approved and commercially available, such as atogepant, erenumab, eptinezumab, fremanezumab, and galcanezuma. Although those immunobiologicals present considerable analgesic effects, they also fit in the scope of expense medications. In this sense, Rimegepant, an orally available CGRP receptor (RAMP1) antagonist might overcome the high costs of immunobiologicals and the need of assisted delivery since it is orally available and therefore, different from other anti-CGRP therapies (intravenous).

These are some potential approaches to evolve the field based on what has been shown in terms of disease pathophysiological mechanisms and targets, offering approaches to improve the rationale for medication prescription. Chinese herbal medicine has also been used for the treatment of GA and we highlighted some pre-clinical data (Table 5). To expand those ethnopharmacological knowledge, there is need of further proof-of-concept evidence and randomized controlled clinical trials. The use of other plant extracts that have been used in folk medicine is still a potential approach. However, isolating and identifying active compounds seems to be a more updated approach for the most part of the biomedical field since the composition would be fixed as well as the adverse side effects. Altogether, the current data support that there is much to advance in GA treatment, and this review discusses some possibilities of how to evolve in this regard.

Acknowledgement

Authors thank the funding of Brazilian grants from CNPq (#309633/2021-4; #307852/2019-9; #307689/2022-0; #405027/2021-4; #427946/2018-2), Fundação Araucária/ MCTI/ CNPq/

SESA-PR/ Parana State Government (PPSUS agreement #041/2017; PRONEX agreement #014/2017) and CAPES (finance code 001).

Author contributions

All authors contributed significantly to the writing and conception of this review article as well as approved the final version of the manuscript.

Funding

This work was supported by grants from the Department of Science and Technology from the Science, Technology and Strategic Inputs Secretariat of the Ministry of Health (Decit/SCTIE/MS, Brazil) intermediated by the National Council for Scientific and Technological Development (CNPq, Brazil) with support of Araucária Foundation and State Health Secretariat, Paraná (SESA−PR, Brazil; PPSUS Grant agreement 041/2017, protocol 48.095); Programa de Apoio a Grupos de Excelência (PRONEX) grant supported by SETI/Araucária Foundation and MCTI/CNPq; and Paraná State Government (agreement 014/2017, protocol 46.843). TZ acknowledges the Ph.D. scholarship from Coordination for the Improvement of Higher Education Personnel (CAPES, Brazil, finance code 001). WV acknowledges the CNPq Senior Research fellowship.

References

[1] Kuo CF, Grainge MJ, Zhang W, et al. Global epidemiology of gout: Prevalence, incidence and risk factors [Internet]. Nat. Rev. Rheumatol. Nature Publishing Group; 2015 [cited 2021 Apr 10]. p. 649–662. Available from: https://pubmed.ncbi.nlm.nih.gov/26150127/.

[2] Dalbeth N, Merriman TR, Stamp LK. Gout. Lancet [Internet]. 2016/10/30. 2016;388:2039–2052. Available from: http://www.sciencedirect.com/science/article/pii/S0140673616003469.

[3] Wu B, Mottola G, Chatterjee A, et al. Perivascular delivery of resolvin D1 inhibits neointimal hyperplasia in a rat model of arterial injury. J Vasc Surg [Internet]. Mosby Inc.; 2017 [cited 2021 Apr 16]. p. 207-217.e3. Available from: https://pubmed.ncbi.nlm.nih.gov/27034112/.

[4] Martinon F, Pétrilli V, Mayor A, et al. Gout-associated uric acid crystals activate the NALP3 inflammasome. Nature [Internet]. 2006 [cited 2021 Apr 1];440:237–241. Available from: https://pubmed.ncbi.nlm.nih.gov/16407889/.

[5] Desai J, Steiger S, Anders HJ. Molecular Pathophysiology of Gout. Trends Mol Med. 2017;23:756–768.

[6] Benn CL, Dua P, Gurrell R, et al. Physiology of hyperuricemia and urate-lowering treatments. Front Med. 2018;5:1–28.

[7] Perez-Ruiz F, Calabozo M, García Erauskin G, et al. Renal underexcretion of uric acid is present in patients with apparent high urinary uric acid output. Arthritis Care Res. 2002;47:610–613.

[8] Bahn A, Hagos Y, Reuter S, et al. Identification of a new urate and high affinity nicotinate transporter, hOAT10 (SLC22A13). J Biol Chem. 2008;283:16332–16341.

[9] Dalbeth N, Gosling AL, Gaffo A, et al. Gout. Lancet. 2021;397:1843–1855.

[10] Toyoda Y, Kawamura Y, Nakayama A, et al. Substantial anti-gout effect conferred by common and rare dysfunctional variants of URAT1/SLC22A12. Rheumatol. 2021;60:5224–5232.

[11] Sandoval-Plata G, Morgan K, Abhishek A. Variants in urate transporters, ADH1B, GCKR and MEPE genes associate with transition from asymptomatic hyperuricaemia to gout: Results of the first gout versus asymptomatic hyperuricaemia GWAS in Caucasians using data from the UK Biobank. Ann Rheum Dis. 2021;80:1220–1226.

[12] Richette P, Bardin T. Gout. Lancet. 2010;375:318–328.

[13] Ahn H, Lee G. Lower Temperatures Exacerbate NLRP3 Inflammasome Activation by

Promoting Monosodium Urate Crystallization, Causing Gout. 2021;

[14] Mulay SR, Desai J, Kumar S V., et al. Cytotoxicity of crystals involves RIPK3-MLKL-mediated necroptosis. Nat Commun. 2016;7.

[15] Pétrilli V, Papin S, Dostert C, et al. Activation of the NALP3 inflammasome is triggered by low intracellular potassium concentration. Cell Death Differ [Internet]. 2007 [cited 2022 Oct 30];14:1583–1589. Available from: https://pubmed.ncbi.nlm.nih.gov/17599094/.

[16] So AK, Martinon F. Inflammation in gout: mechanisms and therapeutic targets. Nat Rev Rheumatol [Internet]. 2017/09/30. 2017;13:639–647. Available from: https://www.ncbi.nlm.nih.gov/pubmed/28959043.

[17] Holzinger D, Nippe N, Vogl T, et al. Myeloid-related proteins 8 and 14 contribute to monosodium urate monohydrate crystal-induced inflammation in gout. Arthritis Rheumatol (Hoboken, NJ) [Internet]. 2014 [cited 2022 Oct 30];66:1327–1339. Available from: https://pubmed.ncbi.nlm.nih.gov/24470119/.

[18] Joosten LAB, Netea MG, Mylona E, et al. Engagement of fatty acids with Toll-like receptor 2 drives interleukin-1β production via the ASC/caspase 1 pathway in monosodium urate monohydrate crystal-induced gouty arthritis. Arthritis Rheum [Internet]. 2010 [cited 2022 Oct 30];62:3237–3248. Available from: https://pubmed.ncbi.nlm.nih.gov/20662061/.

[19] Fujita Y, Yago T, Matsumoto H, et al. Cold-inducible RNA-binding protein (CIRP) potentiates uric acid-induced IL-1β production. Arthritis Res Ther. 2021;23:1–9.

[20] Strowig T, Henao-Mejia J, Elinav E, et al. Inflammasomes in health and disease. Nature. 2012;481:278–286.

[21] Yaron JR, Gangaraju S, Rao MY, et al. K(+) regulates Ca(2+) to drive inflammasome signaling: dynamic visualization of ion flux in live cells. Cell Death Dis [Internet]. 2015 [cited 2022 Oct 30];6. Available from: https://pubmed.ncbi.nlm.nih.gov/26512962/.

[22] Shi H, Wang Y, Li X, et al. NLRP3 activation and mitosis are mutually exclusive events coordinated by NEK7, a new inflammasome component. Nat Immunol [Internet]. 2016 [cited 2022 Oct 30];17:250–258. Available from: https://pubmed.ncbi.nlm.nih.gov/26642356/.

[23] Fattori V, Staurengo-Ferrari L, Zaninelli TH, et al. IL-33 enhances macrophage release of IL-1β and promotes pain and inflammation in gouty arthritis. Inflamm Res [Internet]. 2020 [cited 2022 Aug 1];69:1271–1282. Available from:

https://pubmed.ncbi.nlm.nih.gov/32886146/.

[24] Desai J, Kumar S V., Mulay SR, et al. PMA and crystal-induced neutrophil extracellular trap formation involves RIPK1-RIPK3-MLKL signaling. Eur J Immunol. 2016;46:223–229.

[25] Verri WA, Souto FO, Vieira SM, et al. IL-33 induces neutrophil migration in rheumatoid arthritis and is a target of anti-TNF therapy. Ann Rheum Dis [Internet]. 2010 [cited 2023 Feb 23];69:1697–1703. Available from: https://ard.bmj.com/content/69/9/1697.

[26] Martin NT, Martin MU. Interleukin 33 is a guardian of barriers and a local alarmin. Nat Immunol. 2016;17:122–131.

[27] Liu Y, Zhao Q, Yin Y, et al. Serum levels of IL-17 are elevated in patients with acute gouty arthritis. Biochem Biophys Res Commun. 2018;497:897–902.

[28] Gaffen SL. The role of interleukin-17 in the pathogenesis of rheumatoid arthritis. Curr Rheumatol Rep. 2009;11:365–370.

[29] Inoue A, Ikoma K, Morioka N, et al. Interleukin-1β induces substance P release from primary afferent neurons through the cyclooxygenase-2 system. J Neurochem. 1999;73:2206–2213.

[30] Samad TA, Moore KA, Sapirstein A, et al. Interleukin-1 β-mediated induction of Cox-2 in the CNS contributes to inflammatory pain hypersensitivity. Nature. 2001;410:471–475.

[31] Ramonda R, Oliviero F, Galozzi P, et al. Best Practice & Research Clinical Rheumatology Molecular mechanisms of pain in crystal-induced arthritis. Best Pract Res Clin Rheumatol. 2015;29:98–110.

[32] Hoffmeister C, Trevisan G, Rossato MF, et al. Role of TRPV1 in nociception and edema induced by monosodium urate crystals in rats. Pain [Internet]. 2011 [cited 2021 May 6];152:1777–1788. Available from: https://pubmed.ncbi.nlm.nih.gov/21550723/.

[33] Trevisan G, Hoffmeister C, Rossato F, et al. Author ' s Accepted Manuscript. Free Radic Biol Med. 2014;

[34] Pascart T, Richette P. Current and future therapies for gout. Expert Opin Pharmacother [Internet]. 2017 [cited 2023 Jan 23];18:1201–1211. Available from: https://pubmed.ncbi.nlm.nih.gov/28689430/.

[35] Cicero AFG, Fogacci F, Kuwabara M, et al. Therapeutic Strategies for the Treatment of Chronic Hyperuricemia: An Evidence-Based Update. Medicina (Kaunas) [Internet]. 2021 [cited 2023 Jan 23];57:1–18. Available from:

https://pubmed.ncbi.nlm.nih.gov/33435164/.

[36] Edwards NL, So A. Emerging therapies for gout. Rheum Dis Clin North Am [Internet]. 2014 [cited 2023 Jan 23];40:375–387. Available from: https://pubmed.ncbi.nlm.nih.gov/24703353/.

[37] Pillinger MH, Mandell BF. Therapeutic approaches in the treatment of gout. Semin Arthritis Rheum [Internet]. 2020 [cited 2023 Jan 23];50:S24–S30. Available from: https://pubmed.ncbi.nlm.nih.gov/32620199/.

[38] Dalbeth N, Pool B, Gamble GD, et al. Cellular characterization of the gouty tophus: A quantitative analysis. Arthritis Rheum. 2010;62:1549–1556.

[39] Wrigley R, Phipps-Green AJ, Topless RK, et al. Pleiotropic effect of the ABCG2 gene in gout: Involvement in serum urate levels and progression from hyperuricemia to gout. Arthritis Res Ther [Internet]. 2020 [cited 2023 Mar 8];22:1–10. Available from: https://arthritis-research.biomedcentral.com/articles/10.1186/s13075-020-2136-z.

[40] Ristic B, Sikder MOF, Bhutia YD, et al. Pharmacologic inducers of the uric acid exporter ABCG2 as potential drugs for treatment of gouty arthritis. Asian J Pharm Sci. 2020;15:173–180.

[41] Zhang K, Li C. ABCG2 gene polymorphism rs2231142 is associated with gout comorbidities but not allopurinol response in primary gout patients of a Chinese Han male population. Hereditas [Internet]. 2019 [cited 2023 Mar 8];156:26. Available from: https://hereditasjournal.biomedcentral.com/articles/10.1186/s41065-019-0103-y.

[42] Duong NT, Ngoc NT, Thang NTM, et al. Polymorphisms of ABCG2 and SLC22A12 Genes Associated with Gout Risk in Vietnamese Population. Med 2019, Vol 55, Page 8 [Internet]. 2019 [cited 2023 Mar 8];55:8. Available from: https://www.mdpi.com/1648-9144/55/1/8/htm.

[43] Toyoda Y, Pavelcová K, Klein M, et al. Familial early-onset hyperuricemia and gout associated with a newly identified dysfunctional variant in urate transporter ABCG2. Arthritis Res Ther [Internet]. 2019 [cited 2023 Mar 8];21:1–3. Available from: https://arthritis-research.biomedcentral.com/articles/10.1186/s13075-019-2007-7.

[44] Stiburkova B, Pavelcova K, Pavlikova M, et al. The impact of dysfunctional variants of ABCG2 on hyperuricemia and gout in pediatric-onset patients. Arthritis Res Ther [Internet]. 2019 [cited 2023 Mar 8];21:1–10. Available from: https://arthritis-research.biomedcentral.com/articles/10.1186/s13075-019-1860-8.

[45] Stuart LM, Ezekowitz RAB. Phagocytosis: elegant complexity. Immunity [Internet]. 2005 [cited 2023 Feb 18];22:539–550. Available from:

https://pubmed.ncbi.nlm.nih.gov/15894272/.

[46] Zamudio-Cuevas Y, Fernández-Torres J, Martínez-Nava GA, et al. Phagocytosis of monosodium urate crystals by human synoviocytes induces inflammation. Exp Biol Med (Maywood) [Internet]. 2019 [cited 2023 Feb 18];244:344–351. Available from: https://pubmed.ncbi.nlm.nih.gov/30739483/.

[47] Baggio C, Sfriso P, Cignarella A, et al. Phagocytosis and inflammation in crystal-induced arthritis: a synovial fluid and in vitro study. Clin Exp Rheumatol [Internet]. 2021 [cited 2023 Feb 18];39:494–500. Available from: https://pubmed.ncbi.nlm.nih.gov/32828141/.

[48] Allaeys I, Marceau F, Poubelle PE. NLRP3 promotes autophagy of urate crystals phagocytized by human osteoblasts. Arthritis Res Ther [Internet]. 2013;15:R176–R176. Available from: http://www.ncbi.nlm.nih.gov/pubmed/24456929.

[49] Tao JH, Zhang Y, Li XP. P2X7R: a potential key regulator of acute gouty arthritis. Semin Arthritis Rheum [Internet]. 2013 [cited 2023 Feb 18];43:376–380. Available from: https://pubmed.ncbi.nlm.nih.gov/23786870/.

[50] Li X, Wan A, Liu Y, et al. P2X7R Mediates the Synergistic Effect of ATP and MSU Crystals to Induce Acute Gouty Arthritis. Oxid Med Cell Longev [Internet]. 2023 [cited 2023 Feb 19];2023. Available from: https://pubmed.ncbi.nlm.nih.gov/36686377/.

[51] Dai X, Fang X, Xia Y, et al. ATP-Activated P2X7R Promote the Attack of Acute Gouty Arthritis in Rats Through Activating NLRP3 Inflammasome and Inflammatory Cytokine Production. J Inflamm Res [Internet]. 2022 [cited 2023 Feb 19];15:1237–1248. Available from: https://pubmed.ncbi.nlm.nih.gov/35845088/.

[52] Gong Q yao, Chen Y. Correlation between P2X7 receptor gene polymorphisms and gout. Rheumatol Int [Internet]. 2015 [cited 2023 Feb 19];35:1307–1310. Available from: https://pubmed.ncbi.nlm.nih.gov/25800962/.

[53] Tao JH, Cheng M, Tang JP, et al. Single nucleotide polymorphisms associated with P2X7R function regulate the onset of gouty arthritis. PLoS One [Internet]. 2017 [cited 2023 Feb 19];12:e0181685. Available from: https://journals.plos.org/plosone/article?id=10.1371/journal.pone.0181685.

[54] Gkikas I, Palikaras K, Tavernarakis N. The Role of Mitophagy in Innate Immunity. Front Immunol [Internet]. 2018 [cited 2023 Feb 24];9. Available from: https://pubmed.ncbi.nlm.nih.gov/29951054/.

[55] Ma K, Chen G, Li W, et al. Mitophagy, Mitochondrial Homeostasis, and Cell Fate. Front cell Dev Biol [Internet]. 2020 [cited 2023 Feb 24];8. Available from:

https://pubmed.ncbi.nlm.nih.gov/32671064/.

[56] Biasizzo M, Kopitar-Jerala N. Interplay Between NLRP3 Inflammasome and Autophagy. Front Immunol [Internet]. 2020 [cited 2023 Feb 24];11. Available from: https://pubmed.ncbi.nlm.nih.gov/33163006/.

[57] Zhong Z, Sanchez-Lopez E, Karin M. Autophagy, NLRP3 inflammasome and auto-inflammatory/immune diseases. Clin Exp Rheumatol [Internet]. 2016 [cited 2023 Feb 24];34:12–16. Available from: https://www.clinexprheumatol.org/abstract.asp?a=10865.

[58] Fan W, Chen S, Wu X, et al. Resveratrol Relieves Gouty Arthritis by Promoting Mitophagy to Inhibit Activation of NLRP3 Inflammasomes. J Inflamm Res [Internet]. 2021 [cited 2022 Nov 19];14:3523–3536. Available from: https://pubmed.ncbi.nlm.nih.gov/34335041/.

[59] Chen B, Li H, Ou G, et al. Curcumin attenuates MSU crystal-induced inflammation by inhibiting the degradation of IκBα and blocking mitochondrial damage. Arthritis Res Ther [Internet]. 2019 [cited 2023 Feb 24];21:1–15. Available from: https://arthritis-research.biomedcentral.com/articles/10.1186/s13075-019-1974-z.

[60] Choi N, Yang G, Jang JH, et al. Loganin Alleviates Gout Inflammation by Suppressing NLRP3 Inflammasome Activation and Mitochondrial Damage. Mol 2021, Vol 26, Page 1071 [Internet]. 2021 [cited 2023 Feb 24];26:1071. Available from: https://www.mdpi.com/1420-3049/26/4/1071/htm.

[61] Amaral FA, Costa V V, Tavares LD, et al. NLRP3 inflammasome-mediated neutrophil recruitment and hypernociception depend on leukotriene B(4) in a murine model of gout. Arthritis Rheum [Internet]. 2012;64:474–484. Available from: http://www.ncbi.nlm.nih.gov/pubmed/21952942.

[62] Stutz A, Horvath GL, Monks BG, et al. ASC speck formation as a readout for inflammasome activation. Methods Mol Biol [Internet]. 2013 [cited 2023 Feb 24];1040:91–101. Available from: https://pubmed.ncbi.nlm.nih.gov/23852599/.

[63] Nagar A, DeMarco RA, Harton JA. Inflammasome and Caspase-1 Activity Characterization and Evaluation: An Imaging Flow Cytometer-Based Detection and Assessment of Inflammasome Specks and Caspase-1 Activation. J Immunol [Internet]. 2019 [cited 2023 Feb 24];202:1003–1015. Available from: https://pubmed.ncbi.nlm.nih.gov/30598512/.

[64] Wu J, Luo Y, Jiang Q, et al. Coptisine from Coptis chinensis blocks NLRP3 inflammasome activation by inhibiting caspase-1. Pharmacol Res [Internet]. 2019

[cited 2023 Mar 9];147. Available from: https://pubmed.ncbi.nlm.nih.gov/31336157/.

[65] Cao D yi, Zhang Z hui, Li R ze, et al. A small molecule inhibitor of caspase-1 inhibits NLRP3 inflammasome activation and pyroptosis to alleviate gouty inflammation. Immunol Lett. 2022;244:28–39.

[66] Galvão I, Dias ACF, Tavares LD, et al. Macrophage migration inhibitory factor drives neutrophil accumulation by facilitating IL-1β production in a murine model of acute gout. J Leukoc Biol [Internet]. 2016 [cited 2022 Nov 21];99:1035–1043. Available from: https://pubmed.ncbi.nlm.nih.gov/26868525/.

[67] Verri Jr. WA, Souto FO, Vieira SM, et al. IL-33 induces neutrophil migration in rheumatoid arthritis and is a target of anti-TNF therapy. Ann Rheum Dis [Internet]. 2010;69:1697–1703. Available from: http://www.ncbi.nlm.nih.gov/pubmed/20472598.

[68] Raucci F, Iqbal AJ, Saviano A, et al. IL-17A neutralizing antibody regulates monosodium urate crystal-induced gouty inflammation. Pharmacol Res [Internet]. 2019 [cited 2022 Nov 14];147. Available from: https://pubmed.ncbi.nlm.nih.gov/31315067/.

[69] Khameneh HJ, Ho AWS, Laudisi F, et al. C5a Regulates IL-1β Production and Leukocyte Recruitment in a Murine Model of Monosodium Urate Crystal-Induced Peritonitis. Front Pharmacol [Internet]. 2017 [cited 2022 Oct 30];8. Available from: https://pubmed.ncbi.nlm.nih.gov/28167912/.

[70] An LL, Mehta P, Xu L, et al. Complement C5a potentiates uric acid crystal-induced IL-1β production. Eur J Immunol [Internet]. 2014 [cited 2022 Oct 30];44:3669–3679. Available from: https://pubmed.ncbi.nlm.nih.gov/25229885/.

[71] Rossato MF, Hoffmeister C, Trevisan G, et al. Monosodium urate crystal interleukin-1β release is dependent on Toll-like receptor 4 and transient receptor potential V1 activation. Rheumatology (Oxford) [Internet]. 2020 [cited 2022 Nov 14];59:233–242. Available from: https://pubmed.ncbi.nlm.nih.gov/31298290/.

[72] Tavares LD, Galvão I, Costa V V., et al. Phosphoinositide-3 kinase gamma regulates caspase-1 activation and leukocyte recruitment in acute murine gout. J Leukoc Biol [Internet]. 2019 [cited 2022 Nov 20];106:619–629. Available from: https://pubmed.ncbi.nlm.nih.gov/31392775/.

[73] Cunha TM, Roman-Campos D, Lotufo CM, et al. Morphine peripheral analgesia depends on activation of the PI3Kgamma/AKT/nNOS/NO/KATP signaling pathway. Proc Natl Acad Sci U S A [Internet]. 2010;107:4442–4447. Available from: http://www.ncbi.nlm.nih.gov/pubmed/20147620.

[74] Cunha TM, Souza GR, Domingues AC, et al. Stimulation of peripheral Kappa opioid

receptors inhibits inflammatory hyperalgesia via activation of the PI3Kγ/AKT/nNOS/NO signaling pathway. Mol Pain. 2012;8.

[75] Cecílio NT, Souza GR, Alves-Filho JC, et al. The PI3Kγ/AKT signaling pathway mediates peripheral antinociceptive action of dipyrone. Fundam Clin Pharmacol [Internet]. 2021 [cited 2023 Feb 25];35:364–370. Available from: https://pubmed.ncbi.nlm.nih.gov/32979233/.

[76] Huang JH, Chiang BL. Regulatory T cells induced by B cells suppress NLRP3 inflammasome activation and alleviate monosodium urate-induced gouty inflammation. iScience. 2021;24:102103.

[77] Cheng JJ, Ma XD, Ai GX, et al. Palmatine Protects Against MSU-Induced Gouty Arthritis via Regulating the NF-κB/NLRP3 and Nrf2 Pathways. Drug Des Devel Ther [Internet]. 2022 [cited 2023 Mar 8];16:2119–2132. Available from: https://pubmed.ncbi.nlm.nih.gov/35812134/.

[78] Lin Y, Luo T, Weng A, et al. Gallic Acid Alleviates Gouty Arthritis by Inhibiting NLRP3 Inflammasome Activation and Pyroptosis Through Enhancing Nrf2 Signaling. Front Immunol [Internet]. 2020 [cited 2023 Mar 8];11. Available from: https://pubmed.ncbi.nlm.nih.gov/33365024/.

[79] Ruiz-Miyazawa KW, Pinho-Ribeiro FA, Borghi SM, et al. Hesperidin Methylchalcone Suppresses Experimental Gout Arthritis in Mice by Inhibiting NF-κB Activation. J Agric Food Chem [Internet]. 2018 [cited 2022 Nov 16];66:6269–6280. Available from: https://pubmed.ncbi.nlm.nih.gov/29852732/.

[80] Morrison H. Protein kinase A. Enzym Act Sites their React Mech [Internet]. 2021 [cited 2023 Feb 25];173–178. Available from: https://books.google.com/books/about/Enzyme_Active_Sites_and_their_Reaction_M.html?hl=pt-BR&id=EeP7DwAAQBAJ.

[81] Mortimer L, Moreau F, MacDonald JA, et al. NLRP3 inflammasome inhibition is disrupted in a group of auto-inflammatory disease CAPS mutations. Nat Immunol [Internet]. 2016 [cited 2023 Feb 25];17:1176–1186. Available from: https://pubmed.ncbi.nlm.nih.gov/27548431/.

[82] Pan H, Lin Y, Dou J, et al. Wedelolactone facilitates Ser/Thr phosphorylation of NLRP3 dependent on PKA signalling to block inflammasome activation and pyroptosis. Cell Prolif [Internet]. 2020 [cited 2023 Feb 25];53:e12868. Available from: https://onlinelibrary.wiley.com/doi/full/10.1111/cpr.12868.

[83] O'Brien J, Hayder H, Zayed Y, et al. Overview of MicroRNA Biogenesis, Mechanisms

of Actions, and Circulation. Front Endocrinol (Lausanne) [Internet]. 2018 [cited 2023 Feb 25];9. Available from: https://pubmed.ncbi.nlm.nih.gov/30123182/.

[84] Yuan S, Wu Q, Wang Z, et al. miR-223: An Immune Regulator in Infectious Disorders. Front Immunol. 2021;12:5346.

[85] Dunaeva M, Blom J, Thurlings R, et al. Circulating serum miR-223-3p and miR-16-5p as possible biomarkers of early rheumatoid arthritis. Clin Exp Immunol [Internet]. 2018 [cited 2023 Feb 25];193:376–385. Available from: https://onlinelibrary.wiley.com/doi/full/10.1111/cei.13156.

[86] Bauernfeind F, Rieger A, Schildberg FA, et al. NLRP3 Inflammasome Activity Is Negatively Controlled by miR-223. J Immunol [Internet]. 2012 [cited 2023 Feb 25];189:4175–4181. Available from: https://journals.aai.org/jimmunol/article/189/8/4175/85859/NLRP3-Inflammasome-Activity-Is-Negatively.

[87] Feng Z, Qi S, Zhang Y, et al. Ly6G+ neutrophil-derived miR-223 inhibits the NLRP3 inflammasome in mitochondrial DAMP-induced acute lung injury. Cell Death Dis 2017 811 [Internet]. 2017 [cited 2023 Feb 25];8:e3170–e3170. Available from: https://www.nature.com/articles/cddis2017549.

[88] Tian J, Zhou D, Xiang L, et al. MiR-223-3p inhibits inflammation and pyroptosis in monosodium urate-induced rats and fibroblast-like synoviocytes by targeting NLRP3. Clin Exp Immunol [Internet]. 2021 [cited 2023 Feb 25];204:396–410. Available from: https://onlinelibrary.wiley.com/doi/full/10.1111/cei.13587.

[89] Zhou WY, Cai ZR, Liu J, et al. Circular RNA: metabolism, functions and interactions with proteins. Mol Cancer [Internet]. 2020 [cited 2023 Feb 25];19. Available from: https://pubmed.ncbi.nlm.nih.gov/33317550/.

[90] Lian C, Sun J, Guan W, et al. Circular RNA circHIPK3 Activates Macrophage NLRP3 Inflammasome and TLR4 Pathway in Gouty Arthritis via Sponging miR-561 and miR-192. Inflammation [Internet]. 2021 [cited 2023 Feb 25];44:2065–2077. Available from: https://link.springer.com/article/10.1007/s10753-021-01483-2.

[91] Serhan CN. Novel Pro-Resolving Lipid Mediators in Inflammation Are Leads for Resolution Physiology. Nature. 2014;510:92–101.

[92] Fattori V, Zaninelli TH, Rasquel-Oliveira FS, et al. Specialized pro-resolving lipid mediators: A new class of non-immunosuppressive and non-opioid analgesic drugs [Internet]. Jan 1, 2020. Available from: https://pubmed.ncbi.nlm.nih.gov/31743775/.

[93] Zaninelli TH, Fattori V, Verri WAJ. Harnessing Inflammation Resolution in Arthritis:

Current Understanding of Specialized Pro-resolving Lipid Mediators' Contribution to Arthritis Physiopathology and Future Perspectives. Front Physiol [Internet]. 2021 [cited 2021 Oct 17];0:1444. Available from: https://pubmed.ncbi.nlm.nih.gov/34539449/.

[94] Li J, Guo C, Wu J. 15-Deoxy-Δ-12,14-Prostaglandin J2 (15d-PGJ2), an Endogenous Ligand of PPAR- γ: Function and Mechanism. PPAR Res [Internet]. 2019 [cited 2023 Mar 8];2019. Available from: https://pubmed.ncbi.nlm.nih.gov/31467514/.

[95] Ruiz-Miyazawa KW, Staurengo-Ferrari L, Pinho-Ribeiro FA, et al. 15d-PGJ 2-loaded nanocapsules ameliorate experimental gout arthritis by reducing pain and inflammation in a PPAR-gamma-sensitive manner in mice. Sci Rep [Internet]. 2018 [cited 2022 Aug 1];8. Available from: https://pubmed.ncbi.nlm.nih.gov/30228306/.

[96] Zaninelli TH, Fattori V, Saraiva-Santos T, et al. RvD1 disrupts nociceptor neuron and macrophage activation, and neuroimmune communication reducing pain and inflammation in gouty arthritis in mice. Br J Pharmacol [Internet]. 2022 [cited 2022 Aug 1]; Available from: https://pubmed.ncbi.nlm.nih.gov/35716378/.

[97] Galvao I, Vago JP, Barroso LC, et al. Annexin A1 promotes timely resolution of inflammation in murine gout. Eur J Immunol [Internet]. 2017;47:585–596. Available from: http://www.ncbi.nlm.nih.gov/pubmed/27995621.

[98] Galvão I, Melo EM, de Oliveira VLS, et al. Therapeutic potential of the FPR2/ALX agonist AT-01-KG in the resolution of articular inflammation. Pharmacol Res [Internet]. 2021 [cited 2022 Dec 4];165. Available from: https://pubmed.ncbi.nlm.nih.gov/33493655/.

[99] Rees F, Hui M, Doherty M. Optimizing current treatment of gout. Nat Rev Rheumatol [Internet]. 2014;10:271–283. Available from: http://www.ncbi.nlm.nih.gov/pubmed/24614592.

[100] Hernanz A, De Miguel E, Romera N, et al. Calcitonin gene-related peptide II, substance p and vasoactive intestinal peptide in plasma and synovial fluid from patients with inflammatory joint disease. Rheumatology [Internet]. 1993 [cited 2021 Apr 16];32:31–35. Available from: https://pubmed.ncbi.nlm.nih.gov/7678534/.

[101] Trevisan G, Hoffmeister C, Rossato MF, et al. Transient receptor potential ankyrin 1 receptor stimulation by hydrogen peroxide is critical to trigger pain during monosodium urate-induced inflammation in rodents. Arthritis Rheum [Internet]. 2013 [cited 2022 Nov 14];65:2984–2995. Available from: https://pubmed.ncbi.nlm.nih.gov/23918657/.

[102] Lan Z, Chen L, Feng J, et al. Mechanosensitive TRPV4 is required for crystal-induced inflammation. Ann Rheum Dis [Internet]. 2021 [cited 2022 Nov 14];80:1604–1614. Available from: https://pubmed.ncbi.nlm.nih.gov/34663597/.

[103] Hoffmeister C, Silva MA, Rossato MF, et al. Participation of the TRPV1 receptor in the development of acute gout attacks. Rheumatol (United Kingdom) [Internet]. 2014 [cited 2021 Apr 5];53:240–249. Available from: https://pubmed.ncbi.nlm.nih.gov/24185761/.

[104] Zhang F, Liu S, Jin L, et al. Antinociceptive Efficacy of Retigabine and Flupirtine for Gout Arthritis Pain. Pharmacology [Internet]. 2020 [cited 2022 Nov 19];105:471–476. Available from: https://pubmed.ncbi.nlm.nih.gov/32062659/.

[105] Zaninelli TH, Mizokami SS, Bertozzi MM, et al. Kaurenoic Acid Reduces Ongoing Chronic Constriction Injury-Induced Neuropathic Pain: Nitric Oxide Silencing of Dorsal Root Ganglia Neurons. Pharm 2023, Vol 16, Page 343 [Internet]. 2023 [cited 2023 Mar 8];16:343. Available from: https://www.mdpi.com/1424-8247/16/3/343/htm.

[106] Rossaneis AC, Longhi-Balbinot DT, Bertozzi MM, et al. [Ru(bpy) 2(NO)SO 3](PF 6), a Nitric Oxide Donating Ruthenium Complex, Reduces Gout Arthritis in Mice. Front Pharmacol [Internet]. 2019 [cited 2022 Aug 1];10. Available from: https://pubmed.ncbi.nlm.nih.gov/30914954/.

[107] Hohmann MSN, Longhi-Balbinot DT, Guazelli CFS, et al. Sesquiterpene Lactones: Structural Diversity and Perspectives as Anti-Inflammatory Molecules. Stud Nat Prod Chem. 2016;49:243–264.

[108] Ferraz CRR, Carvalho TTT, Manchope MFF, et al. Therapeutic Potential of Flavonoids in Pain and Inflammation: Mechanisms of Action, Pre-Clinical and Clinical Data, and Pharmaceutical Development. Molecules [Internet]. 2020;25. Available from: http://www.ncbi.nlm.nih.gov/pubmed/32050623.

[109] Ruiz-Miyazawa KW, Staurengo-Ferrari L, Mizokami SS, et al. Quercetin inhibits gout arthritis in mice: induction of an opioid-dependent regulation of inflammasome. Inflammopharmacology [Internet]. 2017 [cited 2022 Nov 16];25:555–570. Available from: https://pubmed.ncbi.nlm.nih.gov/28508104/.

[110] Staurengo-Ferrari L, Ruiz-Miyazawa KW, Pinho-Ribeiro FA, et al. Trans-Chalcone Attenuates Pain and Inflammation in Experimental Acute Gout Arthritis in Mice. Front Pharmacol [Internet]. 2018 [cited 2022 Nov 16];9. Available from: https://pubmed.ncbi.nlm.nih.gov/30333752/.

[111] Ruiz-Miyazawa KW, Borghi SM, Pinho-Ribeiro FA, et al. The citrus flavanone

naringenin reduces gout-induced joint pain and inflammation in mice by inhibiting the activation of NFκB and macrophage release of IL-1β. J Funct Foods [Internet]. 2018;48:106–116. Available from: http://www.sciencedirect.com/science/article/pii/S1756464618303219.

[112] Elsayed S, Elsaid KA. Protein phosphatase 2A regulates xanthine oxidase-derived ROS production in macrophages and influx of inflammatory monocytes in a murine gout model. Front Pharmacol [Internet]. 2022 [cited 2023 Feb 25];13. Available from: https://pubmed.ncbi.nlm.nih.gov/36467056/.

[113] Pereira M, Oliveira D, Oliveira V, et al. Ouratea spectabilis and its biflavanone ouratein D exert potent anti-inflammatory activity in MSU crystal-induced gout in mice. Planta Med [Internet]. 2023 [cited 2023 Feb 25]; Available from: https://pubmed.ncbi.nlm.nih.gov/36626932/.

[114] Lee WY, Chen HY, Chen KC, et al. Treatment of rheumatoid arthritis with traditional chinese medicine. Biomed Res Int [Internet]. 2014 [cited 2023 Feb 25];2014. Available from: https://pubmed.ncbi.nlm.nih.gov/24991562/.

[115] De Souza MR, De Paula CA, Pereira De Resende ML, et al. Pharmacological basis for use of Lychnophora trichocarpha in gouty arthritis: anti-hyperuricemic and anti-inflammatory effects of its extract, fraction and constituents. J Ethnopharmacol [Internet]. 2012 [cited 2022 Nov 19];142:845–850. Available from: https://pubmed.ncbi.nlm.nih.gov/22732730/.

[116] Chen L, Mola M, Deng X, et al. Dolichos falcata Klein attenuated the inflammation induced by monosodium urate crystals in vivo and in vitro. J Ethnopharmacol [Internet]. 2013 [cited 2022 Nov 19];150:545–552. Available from: https://pubmed.ncbi.nlm.nih.gov/24060409/.

[117] Chadwick M, Trewin H, Gawthrop F, et al. Sesquiterpenoids lactones: benefits to plants and people. Int J Mol Sci [Internet]. 2013;14:12780–12805. Available from: http://www.ncbi.nlm.nih.gov/pubmed/23783276.

[118] Bernardes ACFPF, Matosinhos RC, de Paula Michel Araújo MC, et al. Sesquiterpene lactones from Lychnophora species: Antinociceptive, anti-inflammatory, and antioxidant pathways to treat acute gout. J Ethnopharmacol [Internet]. 2021 [cited 2022 Nov 17];269. Available from: https://pubmed.ncbi.nlm.nih.gov/33359866/.

[119] Fattori V, Zarpelon AC, Staurengo-Ferrari L, et al. Budlein A, a Sesquiterpene Lactone From Viguiera robusta, Alleviates Pain and Inflammation in a Model of Acute Gout Arthritis in Mice. Front Pharmacol [Internet]. 2018 [cited 2022 Aug 1];9. Available

from: https://pubmed.ncbi.nlm.nih.gov/30319413/.

[120] Dinesh P, Rasool MK. Berberine, an isoquinoline alkaloid suppresses TXNIP mediated NLRP3 inflammasome activation in MSU crystal stimulated RAW 264.7 macrophages through the upregulation of Nrf2 transcription factor and alleviates MSU crystal induced inflammation in rats. Int Immunopharmacol [Internet]. 2017 [cited 2022 Nov 19];44:26–37. Available from: https://pubmed.ncbi.nlm.nih.gov/28068647/.

[121] Wang Y, Zhu W, Lu D, et al. Tetrahydropalmatine attenuates MSU crystal-induced gouty arthritis by inhibiting ROS-mediated NLRP3 inflammasome activation. Int Immunopharmacol [Internet]. 2021 [cited 2022 Nov 17];100. Available from: https://pubmed.ncbi.nlm.nih.gov/34482265/.

[122] Khan AY, Suresh Kumar G. Natural isoquinoline alkaloids: binding aspects to functional proteins, serum albumins, hemoglobin, and lysozyme. Biophys Rev [Internet]. 2015 [cited 2023 Feb 25];7:407–420. Available from: https://pubmed.ncbi.nlm.nih.gov/28510102/.

[123] Matosinhos RC, Bezerra JP, Barros CH, et al. Coffea arabica extracts and their chemical constituents in a murine model of gouty arthritis: How they modulate pain and inflammation. J Ethnopharmacol. 2022;284:114778.

[124] Barros CH, Matosinhos RC, Bernardes ACFPF, et al. Lychnophora pinaster's effects on inflammation and pain in acute gout. J Ethnopharmacol [Internet]. 2021 [cited 2022 Nov 17];280. Available from: https://pubmed.ncbi.nlm.nih.gov/34324952/.

[125] Pulakat L, Sumners C. Angiotensin Type 2 Receptors: Painful, or Not? Front Pharmacol. 2020;11:2180.

[126] Calixto JB, Medeiros R, Fernandes ES, et al. Kinin B 1 receptors: key G-protein-coupled receptors and their role in inflammatory and painful processes. Br J Pharmacol [Internet]. 2004 [cited 2023 Jan 16];143:803–818. Available from: www.nature.com/bjp.

[127] Silva CR, Oliveira SM, Hoffmeister C, et al. The role of kinin B1 receptor and the effect of angiotensin I-converting enzyme inhibition on acute gout attacks in rodents. Ann Rheum Dis [Internet]. 2016 [cited 2022 Nov 15];75:260–268. Available from: https://pubmed.ncbi.nlm.nih.gov/25344431/.

[128] Shepherd AJ, Mickle AD, Golden JP, et al. Macrophage angiotensin II type 2 receptor triggers neuropathic pain. Proc Natl Acad Sci U S A [Internet]. 2018 [cited 2023 Jan 17];115:E8057–E8066. Available from: /pmc/articles/PMC6112686/.

[129] Lee YM, Son E, Kim DS. Comparative Study of Anti-Gouty Arthritis Effects of Sam-

Myo-Whan according to Extraction Solvents. Plants (Basel, Switzerland) [Internet]. 2021 [cited 2022 Nov 17];10:1–13. Available from: https://pubmed.ncbi.nlm.nih.gov/33535406/.

[130] Lin X, Shao T, Huang L, et al. Simiao Decoction Alleviates Gouty Arthritis by Modulating Proinflammatory Cytokines and the Gut Ecosystem. Front Pharmacol [Internet]. 2020 [cited 2022 Nov 18];11. Available from: https://pubmed.ncbi.nlm.nih.gov/32670069/.

[131] Chen W Di, Zhao YL, Sun WJ, et al. "Kidney Tea" and Its Bioactive Secondary Metabolites for Treatment of Gout. J Agric Food Chem [Internet]. 2020 [cited 2022 Nov 18];68:9131–9138. Available from: https://pubmed.ncbi.nlm.nih.gov/32786873/.

[132] Shi L, Xu L, Yang Y, et al. Suppressive effect of modified Simiaowan on experimental gouty arthritis: an in vivo and in vitro study. J Ethnopharmacol [Internet]. 2013 [cited 2022 Nov 19];150:1038–1044. Available from: https://pubmed.ncbi.nlm.nih.gov/24184191/.

[133] Deng J, Wu Z, Chen C, et al. Chinese Medicine Huzhen Tongfeng Formula Effectively Attenuates Gouty Arthritis by Inhibiting Arachidonic Acid Metabolism and Inflammatory Mediators. Mediators Inflamm [Internet]. 2020 [cited 2022 Nov 18];2020. Available from: https://pubmed.ncbi.nlm.nih.gov/33132756/.

[134] Wu ZC, Xue Q, Zhao ZL, et al. Suppressive Effect of Huzhentongfeng on Experimental Gouty Arthritis: An In Vivo and In Vitro Study. Evid Based Complement Alternat Med [Internet]. 2019 [cited 2023 Jan 19];2019. Available from: https://pubmed.ncbi.nlm.nih.gov/31871475/.

[135] Wei J, Zhang Y, Dalbeth N, et al. Association Between Gut Microbiota and Elevated Serum Urate in Two Independent Cohorts. Arthritis Rheumatol (Hoboken, NJ) [Internet]. 2022 [cited 2023 Feb 22];74:682–691. Available from: https://pubmed.ncbi.nlm.nih.gov/34725964/.

[136] Lin S, Zhang T, Zhu L, et al. Characteristic dysbiosis in gout and the impact of a uric acid-lowering treatment, febuxostat on the gut microbiota. J Genet Genomics. 2021;48:781–791.

[137] ul-Haq A, Lee KA, Seo H, et al. Characteristic alterations of gut microbiota in uncontrolled gout. J Microbiol [Internet]. 2022 [cited 2023 Feb 22];60:1178–1190. Available from: https://link.springer.com/article/10.1007/s12275-022-2416-1.

[138] Shi Y, Cai H, Niu Z, et al. Acute oral colchicine caused gastric mucosal injury and disturbance of associated microbiota in mice. Toxicology [Internet]. 2021 [cited 2023

Feb 23];461. Available from: https://pubmed.ncbi.nlm.nih.gov/34453961/.
[139] Wang Z, Li Y, Liao W, et al. Gut microbiota remodeling: A promising therapeutic strategy to confront hyperuricemia and gout. Front Cell Infect Microbiol [Internet]. 2022 [cited 2023 Feb 23];12. Available from: https://pubmed.ncbi.nlm.nih.gov/36034697/.
[140] Li Y, Zhu J, Lin G, et al. Probiotic effects of Lacticaseibacillus rhamnosus 1155 and Limosilactobacillus fermentum 2644 on hyperuricemic rats. Front Nutr [Internet]. 2022 [cited 2023 Feb 23];9. Available from: https://pubmed.ncbi.nlm.nih.gov/36245501/.
[141] Cao J, Liu Q, Hao H, et al. Lactobacillus paracasei X11 Ameliorates Hyperuricemia and Modulates Gut Microbiota in Mice. Front Immunol [Internet]. 2022 [cited 2023 Feb 23];13. Available from: https://pubmed.ncbi.nlm.nih.gov/35874662/.
[142] van de Laar CJ, Janssen CA, Janssen M, et al. Model-based cost-effectiveness analyses comparing combinations of urate lowering therapy and anti-inflammatory treatment in gout patients. PLoS One [Internet]. 2022 [cited 2023 Feb 25];17. Available from: https://pubmed.ncbi.nlm.nih.gov/35089941/.
[143] Osama H, Hamed EO, Mahmoud MA, et al. The Effect of Hesperidin and Diosmin Individually or in Combination on Metabolic Profile and Neuropathy among Diabetic Patients with Metabolic Syndrome: A Randomized Controlled Trial. J Diet Suppl [Internet]. 2022 [cited 2023 Jan 23]; Available from: https://pubmed.ncbi.nlm.nih.gov/35946912/.
[144] Piao MH, Wang H, Jiang YJ, et al. Taxifolin blocks monosodium urate crystal-induced gouty inflammation by regulating phagocytosis and autophagy. Inflammopharmacology [Internet]. 2022 [cited 2023 Feb 18];30:1335–1349. Available from: https://pubmed.ncbi.nlm.nih.gov/35708797/.
[145] Xu R, Zhao L, Liu J, et al. Natural Adrenocorticotropic Hormone (ACTH) Relieves Acute Inflammation in Gout Patients by Changing the Function of Macrophages. J Healthc Eng [Internet]. 2022 [cited 2023 Mar 12];2022. Available from: https://pubmed.ncbi.nlm.nih.gov/35646298/.
[146] Zhao L, Zhao T, Yang X, et al. IL-37 blocks gouty inflammation by shaping macrophages into a non-inflammatory phagocytic phenotype. Rheumatology (Oxford) [Internet]. 2022 [cited 2023 Mar 12];61:3841–3853. Available from: https://pubmed.ncbi.nlm.nih.gov/35015844/.
[147] Lou D, Zhang X, Jiang C, et al. 3 β,23-Dihydroxy-12-ene-28-ursolic Acid Isolated from Cyclocarya paliurus Alleviates NLRP3 Inflammasome-Mediated Gout via PI3K-

AKT-mTOR-Dependent Autophagy. Evid Based Complement Alternat Med [Internet]. 2022 [cited 2023 Mar 20];2022. Available from: https://pubmed.ncbi.nlm.nih.gov/35047046/.

[148] Shin SH, Jeong J, Kim JH, et al. 1-Palmitoyl-2-Linoleoyl-3-Acetyl-rac-Glycerol (PLAG) Mitigates Monosodium Urate (MSU)-Induced Acute Gouty Inflammation in BALB/c Mice. Front Immunol. 2020;11:710.

[149] Li X, Liu Y, Luo C, et al. Z1456467176 alleviates gouty arthritis by allosterically modulating P2X7R to inhibit NLRP3 inflammasome activation. Front Pharmacol [Internet]. 2022 [cited 2023 Feb 19];13. Available from: https://pubmed.ncbi.nlm.nih.gov/36052144/.

[150] Xue Y, Li R, Fang P, et al. NLRP3 inflammasome inhibitor cucurbitacin B suppresses gout arthritis in mice. J Mol Endocrinol [Internet]. 2021 [cited 2023 Mar 20];67:27–40. Available from: https://pubmed.ncbi.nlm.nih.gov/34047713/.

[151] Lin X, Wang H, An X, et al. Baeckein E suppressed NLRP3 inflammasome activation through inhibiting both the priming and assembly procedure: Implications for gout therapy. Phytomedicine [Internet]. 2021 [cited 2023 Mar 20];84. Available from: https://pubmed.ncbi.nlm.nih.gov/33667838/.

[152] Chang WC, Chu MT, Hsu CY, et al. Rhein, An Anthraquinone Drug, Suppresses the NLRP3 Inflammasome and Macrophage Activation in Urate Crystal-Induced Gouty Inflammation. Am J Chin Med [Internet]. 2019 [cited 2023 Mar 20];47:135–151. Available from: https://pubmed.ncbi.nlm.nih.gov/30612459/.

[153] Wei H, Hu C, Xie J, et al. Doliroside A attenuates monosodium urate crystals-induced inflammation by targeting NLRP3 inflammasome. Eur J Pharmacol [Internet]. 2014 [cited 2023 Mar 20];740:321–328. Available from: https://pubmed.ncbi.nlm.nih.gov/25064339/.

[154] He M, Hu C, Chen M, et al. Effects of Gentiopicroside on activation of NLRP3 inflammasome in acute gouty arthritis mice induced by MSU. J Nat Med [Internet]. 2022 [cited 2023 Mar 20];76:178–187. Available from: https://pubmed.ncbi.nlm.nih.gov/34586567/.

[155] Yadav VR, Prasad S, Sung B, et al. The role of chalcones in suppression of NF-κB-mediated inflammation and cancer. Int Immunopharmacol [Internet]. 2011;11:295–309. Available from: http://www.pubmedcentral.nih.gov/articlerender.fcgi?artid=3058688&tool=pmcentrez&rendertype=abstract.

[156] Li W, Xu H, Shao J, et al. Discovery of alantolactone as a naturally occurring NLRP3 inhibitor to alleviate NLRP3-driven inflammatory diseases in mice. Br J Pharmacol [Internet]. 2023 [cited 2023 Mar 20]; Available from: https://pubmed.ncbi.nlm.nih.gov/36668704/.

[157] Luo T, Zhou X, Qin M, et al. Corilagin Restrains NLRP3 Inflammasome Activation and Pyroptosis through the ROS/TXNIP/NLRP3 Pathway to Prevent Inflammation. Oxid Med Cell Longev [Internet]. 2022 [cited 2023 Mar 22];2022. Available from: https://pubmed.ncbi.nlm.nih.gov/36299604/.

[158] Li WY, Yang F, Chen JH, et al. β-Caryophyllene Ameliorates MSU-Induced Gouty Arthritis and Inflammation Through Inhibiting NLRP3 and NF-κB Signal Pathway: In Silico and In Vivo. Front Pharmacol [Internet]. 2021 [cited 2023 Mar 22];12. Available from: https://pubmed.ncbi.nlm.nih.gov/33967792/.

[159] Hao K, Jiang W, Zhou M, et al. Targeting BRD4 prevents acute gouty arthritis by regulating pyroptosis. Int J Biol Sci [Internet]. 2020 [cited 2023 Mar 22];16:3163–3173. Available from: https://pubmed.ncbi.nlm.nih.gov/33162822/.

[160] Domiciano TP, Wakita D, Jones HD, et al. Quercetin Inhibits Inflammasome Activation by Interfering with ASC Oligomerization and Prevents Interleukin-1 Mediated Mouse Vasculitis. Sci Reports 2017 71 [Internet]. 2017 [cited 2023 Feb 24];7:1–11. Available from: https://www.nature.com/articles/srep41539.

[161] Lee HE, Yang G, Kim ND, et al. Targeting ASC in NLRP3 inflammasome by caffeic acid phenethyl ester: a novel strategy to treat acute gout. Sci Reports 2016 61 [Internet]. 2016 [cited 2023 Feb 24];6:1–11. Available from: https://www.nature.com/articles/srep38622.

[162] Ren L, Li Q, Li H, et al. Polysaccharide extract from Isatidis Radix inhibits multiple inflammasomes activation and alleviate gouty arthritis. Phyther Res [Internet]. 2022 [cited 2023 Feb 24];36:3295–3312. Available from: https://onlinelibrary.wiley.com/doi/full/10.1002/ptr.7514.

[163] Zhang AH, Liu W, Jiang N, et al. Spirodalesol, an NLRP3 Inflammasome Activation Inhibitor. Org Lett [Internet]. 2016 [cited 2023 Feb 25];18:6496–6499. Available from: https://pubs.acs.org/doi/full/10.1021/acs.orglett.6b03435.

[164] Liu W, Yang J, Fang S, et al. Spirodalesol analog 8A inhibits NLRP3 inflammasome activation and attenuates inflammatory disease by directly targeting adaptor protein ASC. J Biol Chem [Internet]. 2022 [cited 2023 Feb 25];298:102696. Available from: http://www.jbc.org/article/S0021925822011395/fulltext.

[165] Mirzaesmaeili A, Zangiabadi S, Raspanti J, et al. Cutting Edge: Negative Regulation of Inflammasome Activation by TRAF1 Can Limit Gout. J Immunol [Internet]. 2023 [cited 2023 Feb 25];210:531–535. Available from: https://journals.aai.org/jimmunol/article/210/5/531/237653/Cutting-Edge-Negative-Regulation-of-Inflammasome.

[166] Santos PD, Vieira TN, Gontijo Couto AC, et al. Stephalagine, an aporphinic alkaloid with therapeutic effects in acute gout arthritis in mice. J Ethnopharmacol [Internet]. 2022 [cited 2022 Nov 17];293. Available from: https://pubmed.ncbi.nlm.nih.gov/35427727/.

[167] Feng Y, Yu Y, Chen Z, et al. Effects of β-Carotin and Green Tea Powder Diets on Alleviating the Symptoms of Gouty Arthritis and Improving Gut Microbiota in C57BL/6 Mice. Front Microbiol [Internet]. 2022 [cited 2022 Nov 17];13. Available from: https://pubmed.ncbi.nlm.nih.gov/35145506/.

[168] Pragasam SJ, Rasool M. Dietary component p-coumaric acid suppresses monosodium urate crystal-induced inflammation in rats. Inflamm Res [Internet]. 2013 [cited 2022 Nov 21];62:489–498. Available from: https://pubmed.ncbi.nlm.nih.gov/23420453/.

[169] De Oliveira DP, Garcia EDF, De Oliveira MA, et al. cis-Aconitic Acid, a Constituent of Echinodorus grandiflorus Leaves, Inhibits Antigen-Induced Arthritis and Gout in Mice. Planta Med [Internet]. 2022 [cited 2022 Nov 20];88. Available from: https://pubmed.ncbi.nlm.nih.gov/34763354/.

[170] Vieira TN, Saraiva ALL, Guimarães RM, et al. Angiotensin type 2 receptor antagonism as a new target to manage gout. Inflammopharmacology [Internet]. 2022 [cited 2022 Nov 14]; Available from: https://pubmed.ncbi.nlm.nih.gov/36173505/.

[171] Lee YM, Shon EJ, Kim OS, et al. Effects of Mollugo pentaphylla extract on monosodium urate crystal-induced gouty arthritis in mice. BMC Complement Altern Med [Internet]. 2017 [cited 2022 Nov 19];17. Available from: https://pubmed.ncbi.nlm.nih.gov/28874151/.

[172] Lv H, Chen J, Liu F, et al. A Traditional Clinic Chinese Medicine Prescription Qu-Zhuo-Tong-Bi (QZTB) Alleviates Gouty Arthritis in Model Rats. Evid Based Complement Alternat Med [Internet]. 2019 [cited 2022 Nov 19];2019. Available from: https://pubmed.ncbi.nlm.nih.gov/31885675/.

[173] Han J, Xie Y, Sui F, et al. Zisheng Shenqi decoction ameliorates monosodium urate crystal-induced gouty arthritis in rats through anti-inflammatory and anti-oxidative effects. Mol Med Rep [Internet]. 2016 [cited 2022 Nov 19];14:2589–2597. Available

from: https://pubmed.ncbi.nlm.nih.gov/27432278/.

[174] Wang X, Long H, Chen M, et al. Modified Baihu decoction therapeutically remodels gut microbiota to inhibit acute gouty arthritis. Front Physiol [Internet]. 2022 [cited 2023 Feb 23];13. Available from: https://pubmed.ncbi.nlm.nih.gov/36589463/.

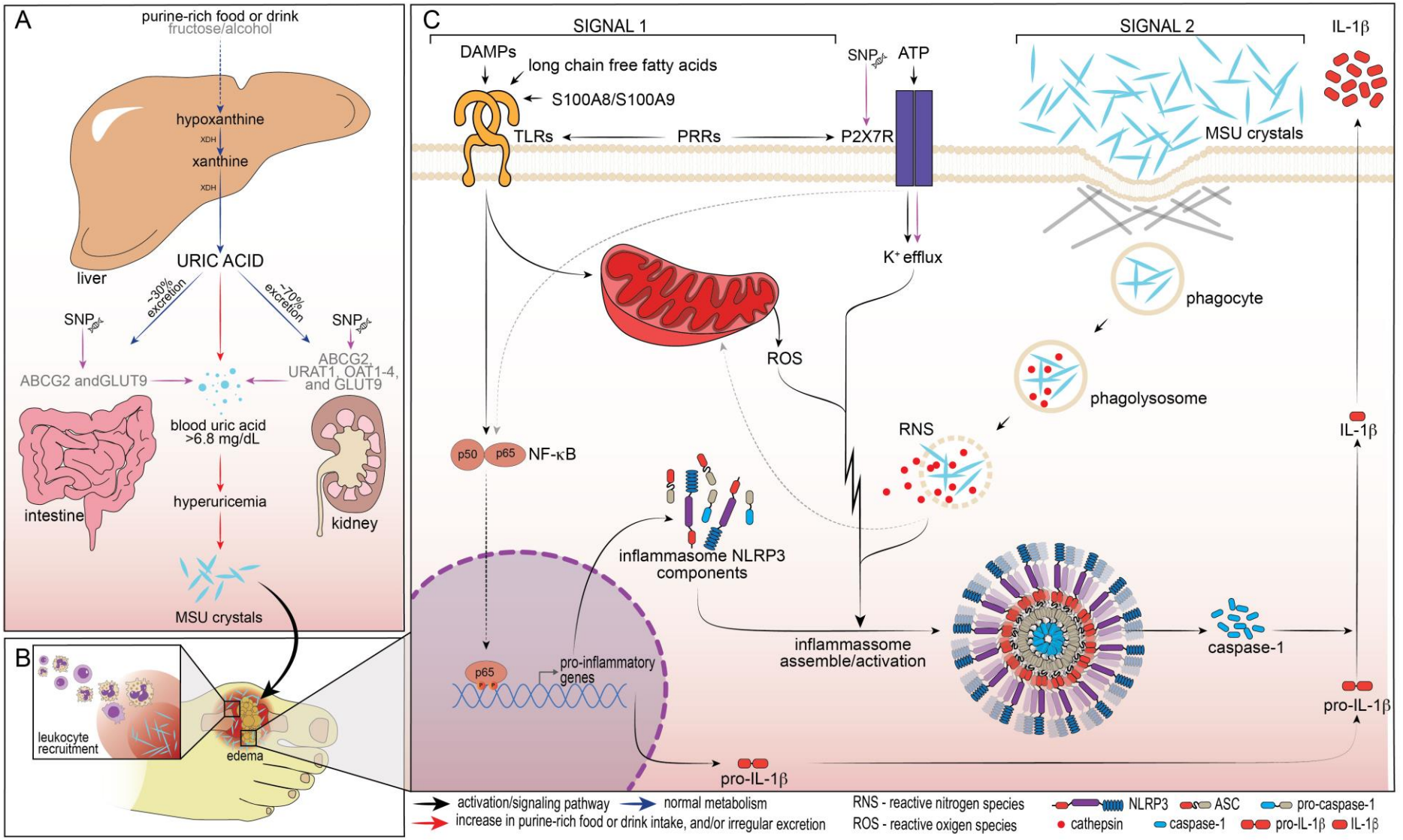
A
purine-rich food or drink
fructose/alcohol
hypoxanthine
XDH
xanthine
XDH
liver
URIC ACID
~30% excretion
~70% excretion
SNP
SNP
ABCG2 andGLUT9
ABCG2, URAT1, OAT1-4, and GLUT9
blood uric acid >6.8 mg/dL
hyperuricemia
intestine
kidney
MSU crystals
B
leukocyte recruitment
edema
C
SIGNAL 1
DAMPs
long chain free fatty acids
S100A8/S100A9
TLRs
PRRs
SNP
ATP
P2X7R
SIGNAL 2
IL-1β
MSU crystals
K+ efflux
phagocyte
ROS
phagolysosome
RNS
IL-1β
p50
p65
NF-κB
inflammasome NLRP3 components
inflammassome assemble/activation
caspase-1
p65
pro-inflammatory genes
pro-IL-1β
pro-IL-1β
activation/signaling pathway
normal metabolism
increase in purine-rich food or drink intake, and/or irregular excretion
RNS - reactive nitrogen species
ROS - reactive oxigen species
NLRP3
ASC
pro-caspase-1
cathepsin
caspase-1
pro-IL-1β
IL-1β

Figure 1. Schematic representation of GA causes, symptoms, and pathophysiological mechanism. (A) normal metabolism (blue arrows) of purine rich food or drink occurs in the liver and the product, uric acid, is excreted by the intestine and kidneys. Increase in purine-rich food or drink intake and/or irregular excretion, results in higher levels of uric acid in the blood, causing hyperuricemia. In the blood concentrations of uric acid above 6.8 mg/dL saturates and precipitates in the articular and periarticular tissue in the form of MSU crystals. (B) The precipitated MSU crystals induce inflammation, leukocytes recruitment, edema, and pain, classical symptoms of GA. (C) In the joint tissue, resident macrophages (synoviocyte) are naturally activated by endogenous proteins (S100A8/A9), long chain free fatty acids, or danger associated molecular patterns (DAMPs) (Signal 1) by toll-like and purinergic receptors, leading to NF-κB activation and the expression of pro-inflammatory genes. Among expressed genes are the components from the inflammasome NLRP3 (NLRP3, ASC, pro-caspase-1, and pro-IL-1β), cytokines, and chemokines. MSU crystals are recognized and phagocytize, which triggers phagolysosome rupture, due to its physical proprieties, cathepsin release, oxidative stress, and receptor-triggered potassium efflux, culminating in the assemble and activation of NLRP3 inflammasome machinery. The NLRP3 inflammasome catabolizes the cleavage of pro-caspase-1 to active caspase-1, resulting in pro-IL-1β activation and release. IL-1β is a key cytokine in GA, which with other cytokines, chemokines, and lipid mediators, play an important role in the disease symptoms and progression. Pink arrows points to single nucleotide polymorphism (SNP) that contribute to disease onset and progression

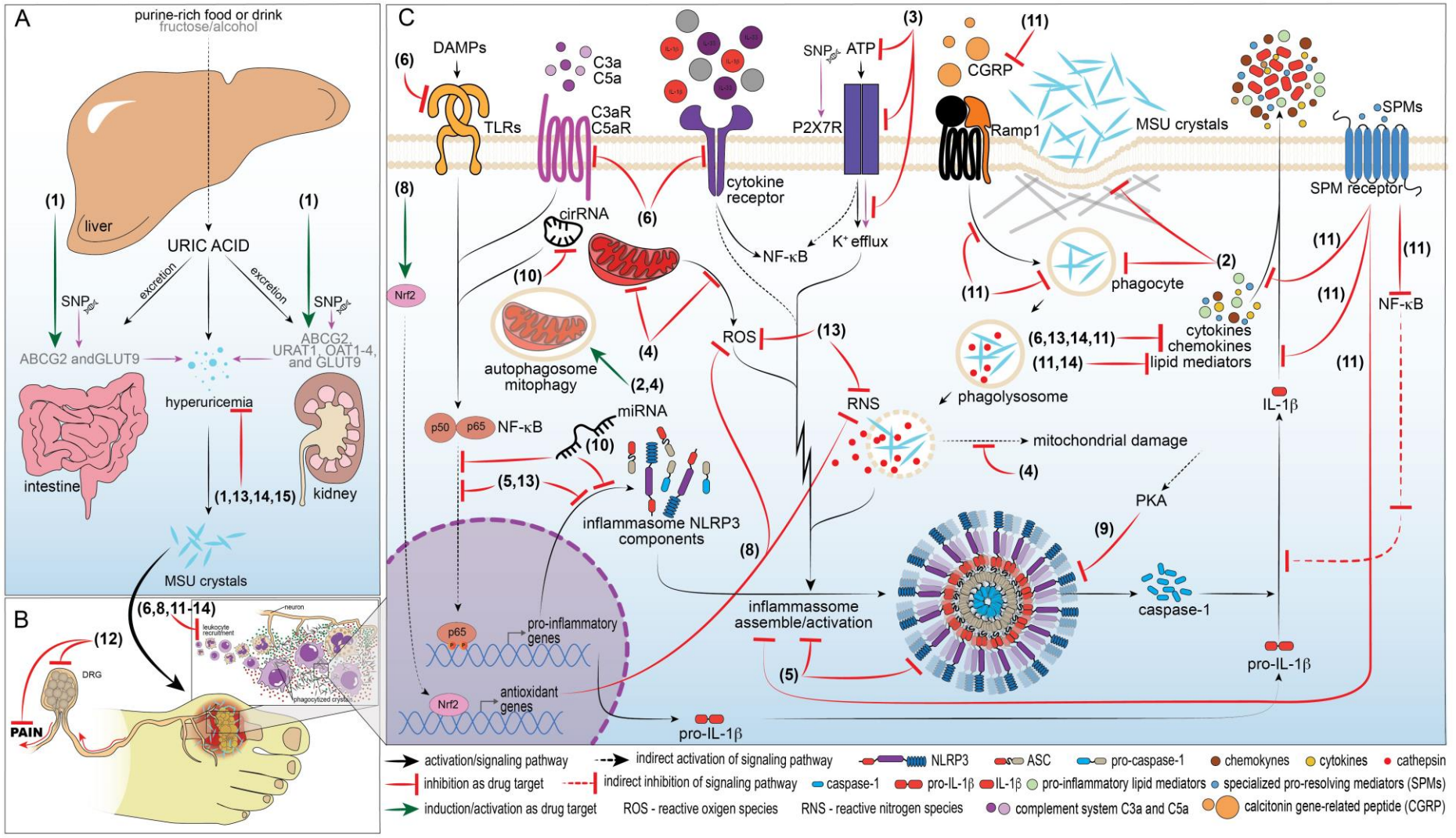
A
purine-rich food or drink
fructose/alcohol
liver
URIC ACID
excretion
excretion
(1)
(1)
SNP
SNP
ABCG2 andGLUT9
ABCG2, URAT1, OAT1-4, and GLUT9
hyperuricemia
intestine
kidney
(1,13,14,15)
MSU crystals
B
(6,8,11-14)
(12)
DRG
PAIN
neuron
leukocyte recruitment
phagocytized crystal
C
DAMPs
(6)
TLRs
C3a
C5a
C3aR
C5aR
cytokine receptor
SNP
ATP
(3)
P2X7R
CGRP
(11)
Ramp1
MSU crystals
SPMs
SPM receptor
(8)
Nrf2
cirRNA
(6)
(10)
NF-κB
K+ efflux
(11)
phagocyte
(2)
(11)
(11)
NF-κB
autophagosome mitophagy
(4)
(2,4)
ROS
(13)
(6,13,14,11)
(11,14)
cytokines
chemokines
lipid mediators
(11)
phagolysosome
RNS
IL-1β
p50
p65
NF-κB
miRNA
(10)
(5,13)
mitochondrial damage
(4)
PKA
(9)
inflammasome NLRP3 components
(8)
inflammassome assemble/activation
caspase-1
p65
pro-inflammatory genes
Nrf2
antioxidant genes
pro-IL-1β
(5)
pro-IL-1β
activation/signaling pathway
indirect activation of signaling pathway
NLRP3
ASC
pro-caspase-1
chemokynes
cytokines
cathepsin
inhibition as drug target
indirect inhibition of signaling pathway
caspase-1
pro-IL-1β
IL-1β
pro-inflammatory lipid mediators
specialized pro-resolving mediators (SPMs)
induction/activation as drug target
ROS - reactive oxigen species
RNS - reactive nitrogen species
complement system C3a and C5a
calcitonin gene-related peptide (CGRP)

Figure 2. GA signaling pathways that are targeted by mechanism-specific drug groups (bold numbers). Green arrows indicate potential drug targets that induction leads to GA diseases status improvement. Red arrows indicate potential drug targets that by inhibition/blockage improve GA outcome. Each arrow is accompanied by bold numbers corresponding to the mechanism-specific drug target, that are described as follows: **(1)** Inducers of the uric acid exporter ABCG2, **(2)** Modulators of phagocytosis and autophagy, **(3)** Inhibitors of ATP signaling and purinergic receptors, **(4)** Modulators of mitochondrial damage and mitophagy, **(5)** Inhibitors of NLRP3, ASC-speck, or Caspase-1, **(6)** Inhibitors of cytokines, complement system, Toll-like receptor 4 (TLR4) and related signaling pathways, **(8)** Inducers of Nrf2 and antioxidants, **(9)** Inducers of protein kinase A (PKA), **(10)** miRNAs and circRNAs, **(11)** Mediators and molecules regulating inflammation resolution, **(12)** Targeting neuroinflammation and neuro-immune communication, **(13)** Antioxidants and multitarget drugs, and **(14)** Traditional Chinese medicine (TCM). Tables 2-5 summarize described effective molecules in modulate the target mechanism. Pink arrows points to single nucleotide polymorphism (SNP) that contribute to disease onset and progression.

Table 1 – Inducers of uric acid exporters ABCG2

Condition	Study	Observed Outcome	Reference
ABCG2 Q141K variants (*rs2231142* and rs*10011796*)	Evaluated the association of ABCG2 exporters allele polymorphism and GA susceptibility.	Presence of the allele Q141K (*rs2231142)* and the genotype rs*10011796* increases the GA risk in patients with hyperuricemia in 21.5-fold in Polynesians and 2.6-fold in Europeans. The allele 141K increases GA flares frequency in Polynesian.	[39]
Familiar GA and mutations in ABCG2	Investigated the polymorphism variants in ABCG2 exporters and early familiar hyperuricemia and GA onset in a European family.	Non-synonymous allelic variants of ABCG2—c.34G>A (p.V12 M) and c.725T>C (p.I242T, a novel variant) are related to the development of early onset of hyperuricemia/gout in a European pedigree.	[43]
ABCG2 SNP and GA comorbidities association	Evaluated the association between ABCG2 SNP *rs2231142* affecting common comorbidities	There is a strong association between ABCG2 SNP *rs2231142* and GA comorbidities including nephrolithiasis and chronic kidney disease.	[41]
ABCG2 mutation and pediatric hypouricemia/GA	Investigated the dysfunctional variants of ABCG2 (SNP *rs2231142*) on hyperuricemia and gout in pediatric-onset patients.	The common (p.V12M, p.Q141K) and three very rare (p.K360del, p.T421A, p.T434M) allelic ABCG2 variants were detected in the study. Those variants are associated with early-onset GA and hyperuricemia. Patients with those mutations have affected first degree relatives (*i.e.,* with hyperuricemia/GA).	[44]
ABCG2 mutation in a Vietnamese cohort	Assessed the relationship between polymorphisms in ABCG2 and SLC22A12 and gout susceptibility	The SNP rs72552713 (ABCG2) and rs11231825 (SLC22A12) are associated with GA in the Vietnamese population.	[42]
Drug targets for ABCG2 transporters	Reviewed possible drug targets for activation of ABCG2 transporters and their potential drugs for GA treatment.	In summary, the potential drug targets are listed with their respective drugs between bracts. The transcription factors: PPARγ (pioglitazone, rosiglitazone); PPARα (clofibrate, gemfibrozil); Nrf2 (Fumarate esters, sulphoraphane, astemizole); AhR (omeprazole, carbidopa); and DNA methyltransferases: DNMT1 (Laccaic acid, epigallocatechin-3-gallate)	[40]

GA – Gout Arthritis; SNP – single nucleotide polymorphism; PPAR – peroxisome proliferator-activated receptor; NRF2 – nuclear factor erythroid 2-related factor 2; AhR, aryl hydrocarbon receptor; DNMT1, DNA methyltransferase 1

Table 2 - Modulators of phagocytosis and autophagy, Inhibitors of ATP signaling and purinergic receptors, and Modulators of mitochondrial damage and mitophagy

Drug target	Compound	Animal	Dose/concentration and Administration Route	Observed Outcome	Reference
Modulators of phagocytosis and autophagy	Resolvin D1 (RvD1)	Mouse BMDM	100 ng/mL (*in vitro*)	Reduces the phagocytosis index of MSU crystal accompanied by the decrease in NF-κB activation and IL-1β levels in the culture supernatant	[96]
	Budlein-A	Mice	10 mg/kg, p.o.	Reduces the phagocytosis index of MSU crystals in neutrophils and macrophages recruited to the knee joint.	[119]
	Taxifolin	Mice	100 mg/kg 200 mg/kg	Upregulates phagocytosis of MSU crystals and induces autophagy by increasing the expression of the autophagy-related protein LC3. Taxifolin decreases IL-1β production and the levels of Caspase-1 and HMGB1. In this case increase in phagocytosis followed by autophagy ameliorates GA in mice.	[144]
	Natural Adrenocorticotropic Hormone (ACTH)	Mice *in vitro*	2.5 U/mL $1.25\text{-}2.5\times10^{-4}$ U/mL	Reduces edema and joint inflammation. Inhibits phagocytosis of MSU and latex beads in THP-1 cells, converts M1 to M2 macrophages as per iNos/Arginase 1 ration, and downregulates ROS production in macrophages.	[145]

	IL-37	*in vitro*	10 ng/mL (recombinant)	Shapes macrophages into a 'silent' non-inflammatory phagocytic cell, promotes MSU phagocytosis, decrease cytokines production via GSK-3β modulation. in IL-37 non-inflammatory phagocytosis.	[146]
	3 β,23-Dihydroxy-12-ene-28-ursolic Acid	*In vitro*	5 μM	Reduces the expression of NLRP3, pro-caspase-1, CASPASE-1, pro-IL-1β, and IL-1β at protein level. Decreases NLRP3-associated ROS production via AKT-mTOR-Dependent upregulation of autophagy-related proteins (*i.e.,* LC3 and p62).	[147]
Inhibitors of ATP signaling and purinergic receptors	Brilliant Blue G (BBG)	Rat	50 mg/kg, i.v.	Treatment significantly reduced the severity of acute gouty arthritis.	[51]
	1-palmitoyl-2-linoleoyl-3-acetyl-rac-glycerol	Mice	250 mg/kg, p.o.	Reduces edema and neutrophil recruitment *in vivo* and *in vitro*. Moreover, reduces the intracellular endosomal trafficking of P2Y6 purinergic receptors.	[148]
	Z1456467176	Mice	1, 10, 50, and 100 μM (*in vitro*)	Inhibited ATP-induces activation of the NLRP3, caspase-1, and IL-1β.	[149]
	Mutation	**Sample**	**Condition**	**Observed Outcome**	**Reference**
	non-synonymous SNP and gout	Human cohort	One or more SNP in the loci *rs1653624* and *rs7958316*	Increases APT synergic response and increases propension to develop GA.	[53]
	non-synonymous SNP and gout	Rat – self occurring GA model	SNP in an allele of P2X7R gene	Increase MSU and ATP synergistic action (in only 30% of injected rats). The SNP	[50].

				increases the susceptibility to disease development.	
Modulators of mitochondrial damage and mitophagy	Resveratrol	Rat	50 mg/kg, p.o.	Improves gait score and reduces MSU-induced synovitis. In MSU-induced peritonitis, resveratrol reduces neutrophil recruitment, IL-1β and IL-18 levels, and increases macrophage recruitment to the peritoneal cavity. *In vitro*, reduces IL-1β maturation by decreasing levels of cleaved caspase and IL-1β via mitophagy.	[58].
	Curcumin	Rat	150 mg/kg, i.p. 1, 5 and 10 μM (*in vitro*)	*In vivo*, curcumin reduces edema, inflammatory cell infiltration, and NLRP3 inflammasome activation. *In vitro*, curcumin inhibits NF-κB and pro-inflammatory mediators, prevents mitochondrial-derived oxidative stress and damage, and inhibits NLRP3 activation after MSU stimulation.	[59]
	Loganin	Mice	5 and 30 mg/kg, p.o. 25, 50 and 100 μM (*in vitro*)	*In vivo*, loganin reduces MSU-induced NLRP3 inflammasome activation and mitochondrial stress. *In vitro*, loganin inhibits ASC-speck formation, caspase-1 and IL-1β production, and mitochondrial dysfunction.	[60]

BMDM – Bone marrow-derived macrophages; MSU – monosodium urate; p.o. – per oral; LC3 -Microtubule-associated protein 1A/1B-light chain 3; HMGB1 - High Mobility Group Box 1; GA – Gout Arthritis; ROS – Reactive oxygen species; i.v. intravenous; ATP - Adenosine 5′-triphosphate; P2Y6 - P2Y purinoceptor 6; NLRP3 - NOD-, LRR- and pyrin domain-containing protein 3; SNP – single nucleotide polymorphism; i.p. – intraperitoneal; NF-kB – Nuclear factor kappa B; ASC – apoptosis-associated speck-like protein containing a CARD.

1

Table 3 – Inhibitors of inflammasome NLRP3, cytokines, complement system, Toll-like receptor 4 (TLR4) and related signaling pathways NLRP3, and inducers of Nrf2 and antioxidant genes

Drug target	Compound	Animal	Dose/concentration and Administration Route	Observed Outcome	Reference
Inhibitors of NLRP3	Cucurbitacin B	mouse	2.5 mg/kg, i.p. 0.1 μmol/L (*in vitro*)	Reduces edema and leukocyte recruitment. *In vitro*, cucurbitacin B reduces the expression of NLRP3 inflammasome components (*i.e.* NLRP3, ASC, pro-caspase-1, and por-IL-1β. Inhibit ATP and MSU-induced production of por-IL-1β.	[150]
	Baeckein E	mouse	50 mg/kg, p.o. 1.6 μM (*in vitro*)	Inhibits MSU-induced edema, leukocyte recruitment, and NF-kB activation, resulting in the reduction of NLRP3, pro-caspase-1, and IL-1β at mRNA and protein levels. *In vitro*, baeckein E suppresses ATP-induced IL-1β maturation in J774A.1 LPS-primed macrophages. Impairs NLRP3 inflamassoma assemble by inhibition of NF-κB and MAPKs signaling pathways. Inhibits ROS production and mitochondrial damage in macrophages.	[151]
	Rhein	*In vitro*	2.5 – 5.0 μg/mL	Suppresses ASC-speck formation and NLRP3 inflammasome activation through the reduction in the levels of activated caspase-1 and mature IL-1β. Rhein also	[152]

			reduces MSU-induced TNF-α production in macrophages.	
Doliroside A	Rat	10- 40 mg/kg, p.o. 15 – 60 μM (*in vitro*)	Reduces edema, thermal hyperalgesia, and restores weight-bearing asymmetry. Decreases MSU-induced leukocyte recruitment, synovial inflammation, and hyperplasia. *In vitro*, doliroside A, inhibits caspase-1 activation and IL-1β maturation, impairing LPS-induced priming and inflammasome activation.	[153]
Gentiopicroside	mouse	200 mg/kg, i.p. 5000 μM (*in vitro*)	Reduces edema, mechanical and thermal hyperalgesia, and leukocytes recruitment. Inhibits NLRP3, ASC, and pro-caspase-1 expression, and CASPASE-1 activity. Treatment also decreases the levels of TNF-α, IL-1β, and IL-6 *in vivo*. *In vitro*, gentiopicroside reduce the expression of NLRP3, ASC, and pro-caspase-1, accompanied by the reduction in IL-1β, IL-18, and IL-6.	[154]
Cardamonin	mouse	2.5 mg/kg, i.p. 5 μM (*in vitro*)	Pre- or post-MSU injection treatment reduces MSU-induced edema and leukocytes recruitment to the knee joint. In J774A.1 macrophage cardamonin reduces NLRP3 expression, activated CASPASE-1 and mature IL-1β.	[155]

Alantolactone	mouse	20 mg/kg, i.p. 2 μM (*in vitro*)	Alleviates MSU-induced edema, leukocytes recruitment, and IL-1β levels in the articular tissue in mice. In vitro, in BMDM culture, alantolactone inhibits ATP-induced production of IL-1β in macrophages, suppresses IL-1β secretion, caspase-1 activation, and pyroptosis by directly bound to the NACHT domain of NLRP3 and blocking NLRP3 inflammasome assembly. Alan of NLRP3 inflammasomes. Alantolactone probably targets the Arg335 residues in NLRP3 leading to suppression of NLRP3-NEK7 interaction.	[156]
Corilagin	mouse	20 mg/kg, i.p. 40 μM (*in vitro*)	Reduces MSU-induced leukocyte recruitment, activated caspase-1, IL-1β, and TNF-α levels in articular tissue. *In vitro*, corilagin reduces ATP-, Nigericin-, and MSU-induced pyroptosis, LDH release, ASC-speck formation, and the levels of activated CASPASE-1, gasdermin D N-terminal fragment (GSDMD-NT), and IL-1β in BMDM culture through the reduction of mtROS levels and the blockage of NLRP3-TXNIP interaction.	[157]
β-Caryophyllene	Rat	100 – 400 mg/kg	Reduces leukocyte recruitment, edema, and mechanical hyperalgesia. Inhibits the activation of NLRP3 inflammasome by	[158]

				reducing the expression levels of all its components via the modulation of NF-κB activation.	
	JQ-1 (bromodomain-containing protein 4 inhibitor)	Rat	25 mg/kg, i.a. 1 μM (*in vitro*)	Reduces leukocyte recruitment, edema, mechanical hyperalgesia and IL-1β in the articular tissue. Reduces pro-caspase-1 expression and activation *in vivo* and *in vitro* (THP-1 human monocytes). Blocks pyroptosis, inhibits NF-κB activation and the expression of NLRP3 inflammasome components.	[159]
Inhibitors of ASC and ASC-speck formation	Quercetin	-	100 μM (*in vitro*)	Inhibits ASC speck formation and oligomerization in BMDM cells *in vitro*.	[160].
	Quercetin	Mice	100 mg/kg, s.c.	Reduces mechanical hyperalgesia, leukocyte recruitment, TNF-α, IL-1β, and NF-κB phosphorylation. Decreases oxidative stress and increases endogenous antioxidants, including the expression of Nrf2 and HO-1 mRNA. All observed effects were blocked by Naloxone, thus indicating an opioid-similar mechanism.	[109]
	Caffeic acid phenetyl ester	-	0.5, 1, 5 or 10 μM (*in vitro*)	Blocks MSU-induces interaction between inflammasome components NLRP3 and ASC *in vitro*. Suppressed MSU crystal-induced formation of ASC oligomers.	[161]

Polysaccharide extract from *Isatidis Radix*	-		Reduces ASC oligomerization induced by nigericin, ATP, poly (I:C), MSU, and intracellular LPS. Reduces the number of nigericin-induced specks. Inhibited inflammasome formation.	[162]
Spirodalesol	Mice	0.25, 0.50, or 1 μM (in vitro) 5 or 10 mg/kg	Reduces LPS+ATP-induced NLRP3 activation and caspase-1 cleavage, IL-1β release. Increases LPS-induced endotoxemia survival in mice and decreases IL-1β production.	[163]
Spirodalesol analog 8A	-	0.3, 1.0, or 3.0 μM (in vitro) 5 or 10 mg/kg	Reduce ASC speck formation and prevents its recruitment by NLRP3. In consequence, inhibited the activation of caspase-1 and the maturation of IL-1β *in vitro*. *In vivo* increases LPS-induced endotoxemia survival in mice and decreases IL-1β production.	[164]
TRAF1	Mice	Knockout	TRAF1 inhibits NLRP3 activation by inducing ASC linear ubiquitination and degradation, thus reducing inflammasome assembly. Importantly, the knockout for *Traf1* (*Traf1*$^{-/-}$) enhanced the release of IL-1β on human macrophages *in vitro*, and MSU-induce GA symptoms in mice. *Traf1*$^{-/-}$ mice presented enhanced edema formation, increased leukocytes infiltration, and cytokines production.	[165]

Inhibitors of caspase-1	NSC697923	Mice	10 mg/kg, i.p. 5 μM (*in vitro*)	Blocks CAPASE-1 activity by biding in a favorable conformation in the active pocket, suppress NF-κB activation, and inhibits its interaction with receptor interacting protein-2, impairing NLRP3 primming and IL-1β maturation. *In vivo*, NSC697923 reduces MSU-induced edema, NLRP3 expression, pro-caspase-1 activation, and IL-1β maturation.	[65]
	Coptisine	Mice	11.61 mg/kg, i.v. 1–30 μM (*in vitro*)	Blocks CASPASE-1 also by biding in a favorable conformation in the active pocket. Inhibits the binding between pro-caspase-1 and ASC, reduced NLRP3 expression, and ATP- and MSU-induced IL-1β maturation, in vitro and in vivo, respectively.	[64]
Inhibitors and role of cytokines, complement system, Toll-like receptor 4 (TLR4) and related signaling pathways	DF2162 (DF) CXCR1/2 allosteric antagonist	Mice	15 mg/kg, p.o.	Reduces mechanical hyperalgesia, neutrophil recruitment, MPO activity, and cell adhesion in synovial vasculature.	[61].
	Fucoidin		20 mg/kg, i.v.		
	Reparixin	Mice	30 mg/kg, s.c.	Reduces the accumulation of neutrophils and the amount IL-1β in the joints.	[66].
	(S,R)-3-(4-hydroxyphenyl)-4,5-dihydro-5-isoxazole acetic acid		150 μg/site, i.a.		
	Macrophage Migration Inhibitory factor (MIF)		1 mg/kg, i.p.		

	IL-33	Mice	IL-33 receptor (ST2) knockout ($ST2^{-/-}$)	$ST2^{-/-}$ reduces evoked and non-evoked pain behaviors. *In vitro*, IL-33 enhances the release of IL-1β and TNF-α in BMDM culture, which are decreased in $ST2^{-/-}$ culture.	[23]
	Anti-IL-17A	Mice	10 mg/joint, i.a.	Reduces MSU-induced inflammation, including leukocyte recruitment, MPO activity, and edema. Reduces the levels of MCP-1. IL-1α, IL-1β, IL-16, IL-17, the complement protein C5a, and B lymphocyte chemoattractant (BLC). Pain was not measured.	[68]
	Complement system	Mice	knockout^{-}	C3a and C5a receptors knockout (*C3ar*$^{-/-}$, *C5ar*$^{-/-}$) reduces MSU-induced leukocyte recruitment and IL-1β production.	[69].
	Lipopolysaccharide from *Rhodobacter sphaeroides* (LPS-RS)	Mice	25 mg/joint, i.a.	Reduces nociception and inflammation, decreases IL-1β and nitric oxide production.	[71]
	iSYK (OXSI 2)		25 nmol/joint, i.a.		
	Aminoguanidine (AMG)		100 mg/joint, i.a.		
	AS605240	Mice	50 mg/kg, s.c.	Reduces mechanical hyperalgesia, neutrophil recruitment, CXCL1 and ROS levels. Reduces NLRP3 activation, capase-1 cleavage, and IL-1β maturation.	[72]
Inducers of Nrf2 and antioxidant genes	Gallic Acid	Mice	20-80 μM (*in vitro*) 100 mg/kg, i.a.	Inhibits LPS-primed macrophages ATP-, nigericin-, or MSU-induced LDH release and pyroptosis. Blocks NLRP3 by decreasing	[78]

			NLRP3-NEK7 interaction, ASC oligomerization, thereby reducing CASPASE-1 and IL-1β levels. Increases the expression of Nrf2 and blocks mitochondrial ROS production. Nrf2 antagonism (ML385) or expression inhibition (siRNA) revert the protective effects of Gallic Acid *in vitro*. *In vivo*, Gallic acid treatment reduces edema, leukocyte recruitment, and inhibits inhibit IL-1β and caspase 1 (p20) production.	
Palmatine (PAL)	Mice	20, 40 and 80 μM (*in vitro*) 25 – 100 mg/kg, p.o.	In LPS-primed THP-1 macrophages, PAL inhibits MSU-induced mRNA expression and levels of pro-inflammatory cytokines (IL-1β, IL-6, IL-18, and TNF-α) in a dose-dependent manner. PAL increases the levels of endogenous antioxidants (SOD and GSH) and decreases lipid peroxidation (reduces MDA levels). PAL reduces NF-κB/NLRP3 signaling pathways through inhibiting the phosphorylation of p-65 and IκBα, blocking the expression of NLRP3, ASC, IL-1β and Caspase-1, which was accompanied by increase in antioxidant protein expression of Nrf2 and HO-1. *In vivo,* PAL reduces MSU-induced edema, leukocytes recruitment, the production of pro-inflammatory cytokines	[77]

			(IL-1β, IL-6, IL-18, and TNF-α), and MDA, while increases the levels of SOD and GSH.	
Hesperidin Methylchalcone	Mice	30 mg/kg, p.o.	Reduces MSU-induced hyperalgesia, edema, and leukocyte recruitment in a dose-dependent manner. Modulates MSU-induced oxidative stress by increasing the levels of GSH, FRAP and ABTS, and decreasing superoxide anion and NO levels in the knee joint. Reduces the levels of pro-inflammatory cytokines (IL-1β, TNF-α, IL-6) and IL-10, while increases the levels of TGF-β. Importantly, the treatment induces the expression of Nrf2 and HO-1 and decreases the mRNA levels of NLRP3, ASC, pro-caspase-1, and pro-IL-1 β.	[79]

p.o. – per oral; i.p. – intraperitoneal; i.a. – intraarticular; MSU – monosodium urate; NLRP3 - NACHT, LRR, and PYD domains-containing protein 3; ASC – apoptosis-associated speck-like protein containing a CARD; ATP - Adenosine triphosphate; MAPK - mitogen-activated protein kinases (MAPK); LPS - Lipopolysaccharides; BMDM – Bone marrow-derived macrophages; NEK7 - Ser/Thr kinase NEK7; TXNIP - thioredoxin-interacting protein; mtROS – mitochondrial reactive oxygen species; LDH – lactate dehydrogenase; NF-κB – Nuclear factor kappa B; Nrf2 - NF-E2–related factor 2; HO-1 - Heme oxygenase-1; ATP – Adenosine 5′-triphosphate; TRAF1 - Tumor necrosis factor receptor associated factor 1; i.v. – intravenous; s.c. – subcutaneous; CXCR1/2 - C-X-C chemokine receptor 1/2; MPO – myeloperoxidase; CCL1 – Chemokine (C-C motif) ligand 1; ROS – Reactive oxygen species; siRNA - small interfering RNA; SOD - superoxide dismutase; GSH – glutathione , MDA - malondialdehyde; IκBα - nuclear factor of kappa light polypeptide gene enhancer in B cells inhibitor, alpha; FRAP assay – ferric reducing antioxidant power; ABTS assay - relative ability of antioxidants to scavenge the ABTS; NO – nitric oxide.

1

Table 4 – Inducers of protein kinase A (PKA), miRNA and cirRNA, Mediators and molecules regulating inflammation resolution, and neuroinflammation and neuro-immune communication

Drug target	Compound	Animal	Dose/concentration and Administration Route	Observed Outcome	Reference
Inducers of PKA	Wedelolactona	-	40 µmol/L (*in vitro*)	Inhibited ASC protein oligomerization, and consequently, speck formation during NLRP3 inflammasome assembly. This condition has been reversed by PKA inhibitor H89, evidencing a modulatory effect of treatment upon catalytic activity of PKA.	[82].
miRNA and cirRNA	miR-223	-	*In vitro*	Inhibited NLRP3 inflammasome activation and IL-1β in macrophages.	[86]
	miR-223	-	*In vitro*	Inhibited NLRP3 inflammasome activation and IL-1β in neutrophils.	[87]
	miR-223-3p	-	*In vitro*	Reduces NLRP3, caspase-1, and IL-1β at mRNA and protein levels in fibroblast-like synoviocytes.	[88]
	circHIPk3	Mice	*In vivo/in vitro*	Increases inflammation by sponging miRNA-192 and miRNA-561 and promotes toll-like receptor 4 (TLR4)-NLRP3 signaling. Genetic deletion of circHIPK3 reverted gouty arthritis in mice.	[90]

Mediators and molecules regulating inflammation resolution	Resolvin D1 (RvD1)	Mice	3 ng/animal, i.p. or i.t. 100 ng/mL (*in vitro*)	Reduced mechanical hyperalgesia, edema, and restore rear member weight distribution. Disrupted nociceptor neuron activation and CGRP release. Reduced leucocyte recruitment, macrophage activation and IL-1β maturation (*in vivo and in vitro*). Blocked CGRP-induced enhancement of MSU crystal phagocytosis and IL-1b release.	
	15d-PGJ2-loaded nanocapsules	Mice	30 mg/kg, s.c.	Reduces mechanical hyperalgesia, edema, leukocyte recruitment, and oxidative stress. Decrease the levels of IL-1β, TNF-α, IL-6, IL-17, IL-33, and increases the levels of IL-10 in the knee joint. Blocks IL-1β release in macrophages culture *in vitro.* All observe effects were PPAR-γ dependent.	[95]
	Stigmasterol	Mice	15 mg/kg, p.o.	Reduces mechanical hyperalgesia, neutrophil recruitment, and IL-1β levels.	[124]
	β-sitosterol	Mice	25 mg/kg, p.o.	Reduces edema.	[115]
	MK886	Mice	3 mg/kg, p.o.	Reduces mechanical hyperalgesia, neutrophil recruitment, and the levels of IL-1β and CXCL1.	[61]
	CP105696	Mice	-	Reduces mechanical hyperalgesia, neutrophil recruitment, and the levels of IL-1β and CXCL1. *In vitro,* reduces	

				LTB_4- or MSU-induced ROS production.	
	AnxA1-active N-terminal peptide (Ac_{2-26})	Mice	150 mg/mice, i.p.	Pre-treatment decreases neutrophil recruitment, IL-1β, and CXCL1 production in periarticular joint tissue. Post-treatment decreases neutrophil accumulation, IL-1β, and mechanical hyperalgesia, and improves the histopathological score. Increases neutrophils apoptosis and shortens resolution phase interval.	[97]
	AT-01-KG	Mice	1.7 μg/kg, i.p.	Reduces neutrophil recruitment, IL-1β and CXCL1 production, and tissue damage. Diminishes hypernociception. Induces neutrophil apoptosis and increases subsequent efferocytosis. Effects were dependent of ALX/FPR_2.	[98]
Neuroinflammation and neuro-immune communication	Resolvin D1 (RvD1)	Mice	3 ng/animal, i.p. or i.t. 100 ng/mL (*in vitro*)	Disrupted nociceptor neuron activation and CGRP release. Reduced leucocyte recruitment, macrophage activation and IL-1b maturation (*in vivo and in vitro*). Blocked CGRP-induced enhancement of MSU crystal phagocytosis and IL-1β release.	[96]
	SB366791	Mice	10 nmol/joint, i.a.	Inhibits pain-like behavior, hyperalgesia, allodynia, and articular oedema. Reduces leucocyte infiltration and IL-1β production.	[32]
	HC-030031	Mice	300 nmol/paw, i.pl.	Decreases thermal hyperalgesia, non-evoke pain like behavior, and edema. Reduces the expression of TRPA1 and	[101]

			TRPV1, leukocyte recruitment, and IL-1β levels.	
GSK219	Mice	5 mg/kg, i.p. 1 μM (*in vitro*)	Reduces mechanical and thermal hyperalgesia, edema, leukocyte recruitment, and MPO activity. Reduces MSU-induced IL-1β release in cultured synovial macrophages.	[102]
SB366791	Mice	100 nmol/joint, i.a.	Reduces nociception and inflammation.	[71]
Retigabine	Rat	15 mg/kg, i.p.	Reduced mechanical and thermal hyperalgesia.	[104]
Flupirtine	Rat	20 mg/kg, i.p.		
[Ru(bpy)2(NO)SO3](PF6)	Mice	1 mg/kg, s.c.	Reduces mechanical hyperalgesia, edema, leukocytes recruitment, oxidative stress, and cytokine levels (IL-1β, TNF-α, and IL-6). Inhibits NF-κB activation and IL-1β maturation. Decreases neuronal activation and capsaicin induced Ca^{2+} influx.	[106]

ASC – apoptosis-associated speck-like protein containing a CARD; NLRP3 - NACHT, LRR, and PYD domains-containing protein 3; CGRP – calcitonin gene-related peptide; MSU – monosodium urate; PPAR-γ – proliferator-activated receptor γ; CXCL1 – Chemokine (C-C motif) ligand 1; LTB_4 – leukotriene B_4; ROS – reactive oxygen species; ALX/FPR_2 - formyl peptide receptor 2; i.p. – intraperitoneal; i.t. – intrathecal; i.a. intraarticular; i.pl. – intraplanar; TRPA1 - potential do receptor transitório, subfamília A, membro 1; TRPV1 – transient receptor potential vanilloid 1; MPO – myeloperoxidase; NF-κB – Nuclear Factor kappa B; s.c. subcutaneous

1

Table 5 – Antioxidants, multitarget drugs, and plants extracts, traditional Chinese medicine, and gut microbiota.

Drug target	Compound	Animal	Dose/concentration and Administration Route	Observed Outcome	Reference
Antioxidants, multitarget drugs, and plants extracts	Quercetin	Mice	15 mg/kg, p.o.	Reduces mechanical hyperalgesia, neutrophil recruitment, and IL-1β levels.	[124]
	Phenolic chlorogenic acid	Mice	15 mg/kg, p.o.		
	Cinnamic acid	Mice	15 mg/kg, p.o.		
	Quercetin	Mice	100 mg/kg, s.c.	Reduces mechanical hyperalgesia, leukocyte recruitment, TNF-α, IL-1β, and NF-κB phosphorylation. Decreases oxidative stress and increases endogenous antioxidants, including the expression of Nrf2 and HO-1 mRNA. All observed effects were blocked by Naloxone, thus indicating an opioid-dependent mechanism.	[109]
	Ouratea spectabilis stems extract	Mice	10, 30 and 100 mg/kg, p.o.	Inhibited recruitment of leukocytes, and IL-1β and CXCL1 levels.	[113]
	Calycosin	Mice		Reduces articular pain, edema, and neutrophils recruitment. Inhibited the expression of AIM2 inflammasome, caspase-1, ASC, and IL-1β, also	[114]

			blocking the phosphorylation of NF-κB. The treatment also inhibited p62-keap-1 pathway.	
Hesperidin Methyl chalcone	Mice	30 mg/kg, p.o.	Reduces mechanical hyperalgesia, edema, leukocyte recruitment, cytokine production (IL-1β, TNF-α, IL-6, and IL-10), and oxidative stress. Restores the levels of endogenous antioxidants. Increases the levels of TGF-β. Reduces NF-κB activation and the expression of mRNA for the components of NLRP3. Diminished the maturation of IL-1β *in vitro*.	[79]
Trans-chalcone	Mice	30 mg/kg, p.o.	Reduces mechanical hyperalgesia, edema, leukocytes recruitment, IL-1β, TNF-α, and IL-6 levels, phosphorylation of NF-κB, and oxidative stress. Restores the levels of endogenous antioxidants. Increases the levels of TGF-β. Reduces the expression of mRNA for the components of NLRP3. Diminished the maturation of IL-1β *in vitro*.	[110]
Naringenin	Mice	150 mg/kg, p.o.	Inhibited mechanical hyperalgesia and edema, leukocyte infiltration to the synovial tissue, citokines production (IL-1β, TNF-α, IL-6, and IL-17).	[111]

			Reduced NF-κB activation, oxidative stress, and the expression of NLRP3 inflammasome components.	
Apigenin	Mice	25 mg/kg, p.o.	Inhibit paw edema and reduces XOD activity.	[115]
Luteolin	Mice	25 mg/kg, p.o.	Reduces edema.	
Eremantholide C	Mice	25 mg/kg, p.o.		
Triterpernoid luteol	Mice	25 mg/kg, p.o.	Inhibited MSU-induced mechanical hyperalgesia, neutrophils recruitment and edema.	
Acid-3-O-β-D-glucopyranoside	-	10 – 40 μg/mL (*in vitro*)	Reduces MSU-induced IL-1β, TNF-α, and IL-6 production.	[116]
Budlein-A	Mice	10 mg/kg, p.o.	Reduced mechanical hyperalgesia, edema, leukocyte recruitment, and MSU crystal phagocytosis. Decreases the activation of NF-κB (*in vitro and in vivo*), the expression of mRNA for pro-IL-1β and TNF-α. Inhibits TNF-α and IL-1β release *in vitro* suggesting NF-κB- and NLRP3-related mechanisms.	[119]
Lychnopholide	Mice	5 mg/kg, p.o.	Reduces mechanical hyperalgesia, neutrophils recruitment, oxidative stress, and TNF-α levels.	[118]
Eremantholide C	Mice	2.5 – 10 mg/kg, p.o.		
Goyazensolide	Mice	2.5 mg/kg, p.o.		
Stephalagine	Mice	1 mg/kg, p.o.	Reduces mechanical and thermal hyperalgesia, non-evoked pain	[166]

			behavior, leukocytes recruitment, and IL-1β levels.	
Berberine	Rat	50 mg/kg, i.p.	Reduced thermal hyperalgesia and edema. *In vitro*, increases Nrf2 and endogenous antioxidants mRNA expression. Decreases caspase-1 activation and IL-1β maturation.	[120]
Tetrahydropalmatine	Mice	40 mg/kg, i.p.	Reduces mechanical and thermal hyperalgesia, edema, leukocytes recruitment, levels of pro-inflammatory cytokines (IL-1β, IL-18, IL-6, and TNF-α). Decreases the expression of all inflamassoma NLRP3 components at mRNA and protein level. Inhibits oxidative stress and restores the levels of endogenous antioxidants.	[121]
β-carotin	Mice	Diet *ad libitum*	Reduces mechanical hyperalgesia, edema, and uric acid levels in the plasma. Decreases leukocyte recruitment, and the levels of pro-inflammatory cytokines in the footpad and serum (IL-1β, TNF-α, and IL-6).	[167]
Resveratrol	Rat	50 mg/kg, p.o.	Improves gait score and reduces MSU-induced synovitis. In MSU-induced peritonitis, resveratrol reduces neutrophil recruitment, levels of IL-1β	[58]

			and IL-18, and increases macrophage recruitment to the peritoneal cavity. *In vitro*, reduces IL-1β maturation by decreasing levels of cleaved caspase and IL-1β via mitophagy.	
Caffeic acid	Mice	10 mg/kg, p.o.	Reduces hyperalgesia, leukocytes recruitment, and pro-inflammatory cytokines (IL-1β, IL-6 and TNF-α).	[123]
p-Coumaric acid	Mice	100 mg/kg, p.o.	Reduces edema and oxidative stress. Restore endogenous antioxidants. Reduces pain in acid acetic-induced peritonitis.	[168]
Cis-Aconitic Acid	Mice	30 mg/kg, p. o.	Reduces leukocyte recruitment and NF-κB activation.	[169]
Fingolimod phosphate	Mice	5 mg/kg, i.p. 2.5 μM (*in vitro*)	Activates PPA2 and inhibits inflammatory monocytes and neutrophils, and the production of IL-1β. Increased the recruitment of anti-inflammatory non-classical monocytes macrophages. Activation of PPA2 inhibits xanthine oxidase (XOD)-induced ROS production in M1 macrophages.	[112].
Coffea arabica extract (caffeic and chlorogenic acid)	Mice	25 – 225 mg/kg, p.o.	Reduces hyperalgesia, leukocytes recruitment, and pro-inflammatory cytokines (IL-1β, IL-6, and TNF-α).	

	Lychnophora pinaster aerial athanolic extract (rutin, quercetin, lupeol, stigmasterol, caffeic acid, and chlorogenic acid)	Mice	375 mg/kg, p.o.	Reduces mechanical hyperalgesia, leukocyte recruitment, and the levels of pro-inflammatory cytokines (TNF-α and IL-1β).	[112].
	Lychnophora trichocarpha extract (luteolin, apigenin, lupeol, eremantholide C, and licnopholide)	Mice	250 mg/kg, p.o.	Reduces MSU-induced edema. Decreases oxonate-induced hyperuricemic in mice.	[170]
	PD123319	Mice	10 pmol/joint, i.a.	AT_2R antagonisms reduces evoked and non-evoked pain behaviors, edema formation, leukocyte recruitment, IL-1β levels, NO concentrations, and AT_2R mRNA expression.	[170]
	SSR240612	Rat	10 nmol/articulation	Reduces evoked and non-evoked pain behaviors and edema.	[127]
Traditional Chinese medicine (TCM)	Huzhen Tongfeng Formula	Rabbit	0.7 g/kg, p.o.	Reduces leukocyte recruitment. The study also indicates a mechanism related to the inhibition of arachidonic acid metabolism.	[133]
	Huzhen Tongfeng Formula	Rat	0.25, 0.50, and 1 g/kg, p.o.	Reduces edema and leukocyte recruitment, accompanied by the reduction of 1L-1β, IL-6, and TNF-α levels.	[134].
	Clerodendranthus spicatus (kidney tea)	Mice	200 mg/kg, p.o.	Reduces edema in the gouty arthritis model. Reduces pain in acetic-acid-induced writhing test. From 32	[131]

			isolated compounds, 9 presents anti-gouty proprieties, 4 of those have analgesic effects.	
Simiao	Mice	4, 8, and 16 g/kg/day, p.o.	Reduces pain, edema, neutrophils recruitment, uric acid levels in the plasma and the related enzymes. Decreases serum levels of pro-inflammatory cytokines (IL-1β, IL-9, IFN-γ, MIP-1α and MIP-1β).	[130]
Modified Simiaowan	Rat	10 g/kg, p.o.	Reduces edema and neutrophil recruitment. Presents analgesic effects in acetic acid-induced writhing in mice.	[132]
Mollugo pentaphylla extract	Mice	300 mg/kg, p.o.	Restores rear member weight distribution. Reduces edema, cytokines levels in the paw tissue (IL-1β and TNF-α), and the mRNA expression of NF-κB and components of inflamassoma NLRP3.	[171]
Qu-Zhuo-Tong-Bi (QZTB)	Rat	500 mg/kg, p.o.	Reduces edema, evoked and non-evoked pain behaviors. Decreases the expression of NLRP3 at mRNA and protein levels. Reduces IL-1β and TNF-α levels in the ankle tissue.	[172]
Zisheng Shenqi	Rat	40 mg/kg, p.o.	Reduces edema, inflammation, the levels of IL-1β and TNF-α. Decreases the activation of NF-kB, and the	[173]

				expression of NLRP1 and NLRP6. Increases endogenous antioxidants (SOD, GSH, GSH-Px).	
	Dolichos falcata Klein etanol extract (acid-3-O-β-D-glucopyranoside and doliroside A)	Rat	40 mg/kg, p.o.	Reduces mechanical hyperalgesia, edema, and restores rear member weight distribution. Decreases the levels of pro-inflammatory cytokines (IL-1β, TNF-α, and IL-6) in the serum and synovial fluid. The observed effects are attributed to two isolated compounds acid-3-O-β-D-glucopyranoside and doliroside A.	[116]
	Sam-Myo-Whan	Mice	200 mg/kg, p.o.	Restores changes in rear limbs weight distribution. Reduces edema, leukocyte recruitment (MPO activity), IL-1β, and TNF-α levels.	[129]
Gut microbiota	Febuxostat	Clinical	Under treatment – no dose specification.	Restores gut microbiota diversity and its potential for purine metabolism.	[136]
	Lacticaseibacillus rhamnosus 1155 *Limosilactobacillus fermentum* 2644	Hypouricemic rats	1.5×10^8 CFU/day, p.o. Alone or in combination.	Restore gut diversity, resulting in the reduction of plasma uric acid. Increase in urate secretion in the feces.	[140]
	Lactobacillus paracasei X111	Mice	1.5×10^9 CFU, p.o.	Decreases serum levels of urate and restored gut microbiota diversity	[141]
	Baihu decoction	Rat	5.84 and 35 g/kg/d, p.o.	Restored gut microbiota and reduced GA symptoms.	[174]

p.o. – per oral; HO-1 – heme oxigenasse-1; s.c. – subcutaneous; CXCL1 – Chemokine (C-C motif) ligand 1; AIM2 - Interferon-inducible protein AIM2; ASC - Apoptosis-associated speck-like protein containing a CARD; Keap-1 – Kelch-like ECH-associated protein 1; NF-κB – nuclear factor kappa B; NLRP3 - NOD-, LRR- and pyrin domain-

containing protein 3; XOD – xanthine oxidase; MSU – monosodium urate; i.p. – intraperitoneal; i.a. – intraarticular; Nrf2 - nuclear factor erythroid 2–related factor 2; AT_2R - angiotensin II type 2 receptor; NLRP1 - NLR Family Pyrin Domain Containing 1; NLRP6 - NOD-like receptor family pyrin domain containing 6; SOD - superoxide dismutase; GSH – Glutathione; GSH-Px – Glutathione peroxidase; MPO – myeloperoxidase; GA – gouty arthritis.

Research article

3.3 RvD1 disrupts nociceptor neuron and macrophage activation, and neuroimmune communication reducing pain and inflammation in gouty arthritis in mice

Tiago H. Zaninelli[1], Victor Fattori[1,4], Telma Saraiva-Santos[1], Stephanie Badaro-Garcia[1], Larissa Staurengo-Ferrari[1], Ketlem C. Andrade[1], Nayara A. Artero[1], Camila R. Ferraz[1], Mariana M. Bertozzi[1], Fernanda Rasquel-Oliveira[1], Marilia F. Manchope[1], Flávio A. Amaral[3], Mauro M. Teixeira[3], Sergio M. Borghi[1], Michael S. Rogers[4], Rubia Casagrande[2], Waldiceu A. Verri Jr[1]*

[1]Laboratory of Pain, Inflammation, Neuropathy, and Cancer, Department of Pathology, Centre of Biological Sciences, Londrina State University, Londrina, Paraná, Brazil.
[2]Laboratory of Antioxidants and Inflammation, Department of Pharmaceutical Sciences, Centre of Health Sciences, Londrina State University, Londrina, Paraná, Brazil.
[3]Department of Biochemistry and Immunology, Biological Sciences Institute, Federal University of Minas Gerais, Belo Horizonte, Brazil.
[4]Vascular Biology Program, Department of Surgery, Boston Children's Hospital-Harvard Medical School, Karp Research Building, 300 Longwood Ave. 02115, Boston, Massachusetts, United States.

* Corresponding author.
Present address: Departamento de Ciências Patológicas, Universidade Estadual de Londrina, Rodovia Celso Garcia Cid Km480 PR445, 86057-970, Post-office box 10.011, Londrina, Paraná, Brazil. E-mail address: waverri@uel.br

Data availability statement

The data that support the findings of this study are available from the corresponding author upon reasonable request.

Funding statement

All funding sources are described in the Acknowledgments section, which mentions the following: PRONEX grant supported by SETI/Araucária Foundation and MCTI/CNPq; and Paraná State Government (agreement 014/2017, protocol 46.843); Funding Authority for Studies and Projects and State Secretariat of Science, Technology and Higher Education (MCTI/FINEP/CT-INFRA-PROINFRA, Brazil (grant agreements 01.12.0294.00 and 01.13.0049.00); Grants from The J. Willard and Alice S. Marriott Foundation and Marriott Daughters Foundation. T.H.Z., T.S.-S., S.B.-G., M.M.B., F.R.O., N.A.A., and M.F.M. F.A.P.-R. acknowledge PhD scholarship from Coordination for the Improvement of Higher Education Personnel (CAPES, Brazil, finance code 001), K.C.A. acknowledge master's degree scholarship from CAPES. C.R.F. received CNPq Post-Doc fellowship. S.M.B. thanks the fellowship from FUNADESP. F.A.A., M.M.T., R.C. and W.A.V.J. acknowledge the CNPq Researcher fellowship. We also thank the support of CMLP-UEL for the access to equipment free of charge.

Author contribution statement

Authors' contribution is disclosed in the manuscript and described as follows: **Conceptualization:** T.H. Zaninelli, V. Fattori, and W.A. Verri; **investigation and data curation:** T.H. Zaninelli, V. Fattori, T. Santos-Saraiva, S. Badaro-Garcia, L. Staurengo-Ferrari, K.C. Andrade, N. A. Artero, C.R. Ferraz, M.M. Bertozzi, F. Rasquel-Oliveira, M.F. Manchope, F.A. Amaral, M.M. Teixeira, S.M. Borghi, M.S. Rogers, R. Casagrande, W.A. Verri; **funding acquisition:** M.S. Rogers, R. Casagrande, and W.A. Verri; **methodology:** T.H. Zaninelli, V. Fattori, and W.A. Verri; **resources:** F.A. Amaral, M.M. Teixeira, M.S. Rogers, R. Casagrande, and W.A. Verri; **project administration:** T.H. Zaninelli; **supervision:** V. Fattori, M.S. Rogers, and W.A. Verri; **visualization:** T.H. Zaninelli, V. Fattori, and W.A. Verri; **writing–original draft:** T.H. Zaninelli, V. Fattori, and W.A. Verri; **writing – editing and reviewing:** all authors. **All authors have read and approved the final version of the manuscript.**

Conflict of interest disclosure

The authors declare no conflicts of interest.

Ethics approval statement

All authors acknowledge that all animal experiments were approved by the Londrina State University ethics committee (CEUA-UEL) under process number 22186.2016.37, which is an Institutional representative and works under the Brazilian law regulations by the Brazilian National Council for the Control of Animal Experimentation (CONCEA). Moreover, as described in the *Methods* section under *Compliance with requirements for studies using animals* (subtopic 2.2) all experiments were conducted in accordance with the International Association for Study of Pain (IASP) and ARRIVE 2.0 guidelines.

Permission to reproduce material from other sources.

This manuscript did not reproduce any material from other sources.

List of authors' information

Tiago Henrique Zaninelli, tiagozaninelli@gmail.com - https://orcid.org/0000-0001-7233-477X
Victor Fattori – vfattori@outlook.com – https://orcid.org/0000-0002-4565-7706
Telma Saraiva-Santos - telmasaraivasantos@gmail.com - https://orcid.org/0000-0003-3639-6441
Stephanie Badaro-Garcia - stehbgarcia@gmail.com – https://orcid.org/0000-0002-7619-1929
Larissa Staurengo-Ferrari - larissasferrari@gmail.com - https://orcid.org/0000-0003-4094-6223
Ketlem C. Andrade - ketlemandrade94@gmail.com - https://orcid.org/0000-0001-9448-3864
Nayara A. Artero - naayanitelli@hotmail.com - https://orcid.org/0000-0002-6791-6449
Camila R. Ferraz - camila_ferraz96@hotmail.com - https://orcid.org/0000-0003-4550-0773
Mariana M. Bertozzi - marianambertozzi@gmail.com - https://orcid.org/0000-0002-0551-4313

Fernanda Rasquel-Oliveira - fernandarasquel@gmail.com - https://orcid.org/0000-0001-9210-9764
Marilia F. Manchope - marilia.manchope@gmail.com - https://orcid.org/0000-0003-2882-6536
Flávio A. Amaral – famaral@icb.ufmg.br - https://orcid.org/0000-0002-1695-0612
Mauro M. Teixeira – mmtex@icb.ufmg.br - https://orcid.org/0000-0002-6944-3008
Sergio M. Borghi – sergio_borghi@yahoo.com.br - https://orcid.org/0000-0002-6978-7505
Michael S. Rogers – Michael.Rogers@childrens.harvard.edu - https://orcid.org/0000-0002-5250-8434
Rubia Casagrande – rubiacasa@uel.br - https://orcid.org/0000-0002-2296-1668
Waldiceu A. Verri Jr- waverri@uel.br - https://orcid.org/0000-0003-2756-9283

Word count:3966

Abstract

Background and purpose: Gouty arthritis is characterised by an intense inflammatory response to monosodium urate crystals (MSU), which induces severe pain. Current therapies are often ineffective in reducing gout-related pain. Resolvin D1 (RvD1) is a specialised pro-resolving lipid mediator with anti-inflammatory and analgesic proprieties. In this study, we evaluated the effects and mechanisms of action of RvD1 in an experimental mouse model of gouty arthritis, an aim that was not pursued previously in the literature.

Experimental approach: Male mice were treated with RvD1 (intrathecally or intraperitoneally) before or after intraarticular stimulation with MSU. Mechanical hyperalgesia was assessed using an electronic von Frey aesthesiometer. Leukocyte recruitment was determined by knee joint wash cell counting and immunofluorescence. IL-1β production was measured by ELISA. Phosphorylated NF-kB and apoptosis-associated speck-like protein containing CARD (ASC) were detected by immunofluorescence, and mRNA expression was determined by RT-qPCR. CGRP release was determined by EIA and immunofluorescence. MSU crystal phagocytosis was evaluated by confocal microscopy.

Key results: RvD1 inhibited MSU-induced mechanical hyperalgesia in a dose- and time-dependent manner by reducing leukocyte recruitment and IL-1β production in the knee joint. Intrathecal RvD1 reduced the activation of peptidergic neurons and macrophages as well as silenced nociceptor to macrophage communication and macrophage function. CGRP stimulated MSU phagocytosis and IL-1β production by macrophages. RvD1 downmodulated this phenomenon directly by acting on macrophages, and indirectly by inhibiting CGRP release and CGRP-dependent activation of macrophages.

Conclusions and implications: This study reveals a hitherto unknown neuro-immune axis in gouty arthritis that is targeted by RvD1.

Keywords: specialised pro-resolving lipid mediator; rheumatic diseases; gout; CGRP; neuroimmune; MSU; phagocytosis.

List of abbreviations

AITC: allyl isothiocyanate
AKT: protein kinase B
ALX/FPR2: lipoxin receptor/N-formyl peptide receptor-2
ASC: apoptosis-associated speck-like protein containing a caspase recruitment domain
BMDM: bone marrow-derived macrophages
CAIA: collagen antibody-induced arthritis
CFA: complete Freund's adjuvant
CGRP: calcitonin gene-related peptide
DAPI: 4′,6-diamidino-2-phenylindole
DRG: dorsal root ganglia
eGFP: enhanced green fluorescent protein
ELISA: enzyme-linked immunosorbent assay
GA: gouty arthritis
GM-CSF: granulocyte/monocyte colony stimulating factor
GPR18: G protein-coupled receptor 18
GPR32: G protein-coupled receptor 32
i.a.: intra-articular
i.p.: intraperitoneal
i.t.: intrathecal
I-κB: inhibitor of kappa B
Il-1β: interleukin 1-beta
IL-1R1: interleukin 1 receptor type I
IL-6: interleukin 6
LDH: lactate dehydrogenase
LPS: lipopolysaccharide
LysM: lysozyme M
MaR1: maresin 1
MSU: monosodium urate
Nav1.8: voltage-gated sodium channel 1.8
NF-κB: nuclear factor kappa B
NLRP3: NLR family pyrin domain containing 3
PI3K: phosphatidylinositol 3-kinase
pNF-κB: phosphorylated nuclear factor kappa B
PPARγ: peroxisome proliferator-activated receptor gamma
RPMI: Roswell Park Memorial Institute 1640 media
RT-qPCR: real time quantitative polymerase chain reaction
RvD1: resolvin D1
RvD2: resolvin D2
RvE1: resolvin E1
SPM: specialized pro-resolving mediator
SWB: static weight bearing
TNF-α: tumor necrosis factor alpha
TRAP: tartrate-resistant acid phosphatase
TRP: transient receptor potential channels
TRPA1: transient receptor potential ankyrin subtype 1
TRPV1: transient receptor potential vanilloid subtype 1
TRPV3: transient receptor potential vanilloid subtype 3
TRPV4: transient receptor potential vanilloid subtype 4

Bullet point summary

What is already known

- Novel therapies with improved efficacy in reducing gout pain and inflammation are needed.
- Resolvin D1 (RvD1) is an anti-inflammatory and analgesic pro-resolution lipid in other disease models.

What this study adds

- RvD1 disrupts nociceptor neuron and macrophage activation, and their CGRP-dependent neuroimmune communication.
- CGRP enhances MSU phagocytosis and IL-1β production and RvD1 downmodulated this phenomenon directly and indirectly.

Clinical significance

- RvD1 reduces gouty arthritis pathology and symptoms by mechanisms that are different from current treatments.
- A hitherto unknown disease mechanism in gouty arthritis that is targeted by RvD1 was uncovered.

1. Introduction

Gouty arthritis (GA) is an intermittent disease, the most common form of inflammatory arthritis, and gout flares are considered one of the most painful acute conditions known (Martinon et al., 2006; So and Martinon, 2017; Perna et al., 2020). The incidence and prevalence of gout have increased in developed and developing countries; gout affects approximately 10% of the worldwide population (SY et al., 2011; Kuo et al., 2015). Gout is caused by high levels of blood uric acid (hyperuricaemia) resulting in the formation and deposition of monosodium urate (MSU) crystals on articular and periarticular tissues (Dalbeth and Haskard, 2005). Resident macrophages (type A synoviocytes) phagocytose MSU crystals and produce pro-inflammatory mediators triggering neutrophil recruitment (Dinarello, 2009) and excruciating pain (Faires and Mccarty, 1962). The physiopathology of gout is dependent on NLRP3 (NLR family pyrin domain containing 3) inflammasome engagement, activation and caspase-1-mediated maturation of interleukin (IL)-1β (Martinon et al., 2006; Amaral et al., 2012). The current understanding of gout arthritis pathology highlights IL-1β as the primary pro-inflammatory cytokine in both inflammation and pain.

Even though GA flares are self-limiting in humans (up to 10 days), if left untreated, continued MSU deposition can induce joint damage, movement limitation, and increase the probability of recurrent acute flares (Schlesinger and Thiele, 2010; So and Martinon, 2017). The management of gout consists of urate-lowering therapies and control of acute flares. In fact, the main reason for patients to seek medical care is intense and debilitating pain during gout episodes (Rees et al., 2014). Currently, steroidal and non-steroidal anti-inflammatories, colchicine and biological agents are used in the control of gout flares (So and Martinon, 2017). However, these drugs lack safety in patients with comorbidities, cause side effects, present high cost, or offer non-satisfactory analgesic effect (Rees et al., 2014). Therefore, novel analgesic drugs are still needed to the treatment of gout.

Resolvin D1 (7S,8R,17S-trihydroxy-4Z,9E,11E,13Z,15E,19Z-docosahexaenoic acid, RvD1) is a specialised pro-resolving lipid mediator (SPM) derived from the metabolization of the ω-3 polyunsaturated fatty acid, docosahexaenoic acid (Bannenberg and Serhan, 2010). RvD1 actively orchestrates the process of inflammation resolution and has anti-inflammatory and analgesic proprieties described in experimental murine models (Krishnamoorthy et al., 2010; Ji et al., 2011; Liao et al., 2012; Benabdoune et al., 2016; Benabdoun et al., 2019). Notably, SPMs also exert their biological effect by modulating neuronal activation (Bang et al., 2010; Xu et al., 2010; Park et al., 2011; Fattori et al., 2019; Perna et al., 2020), which reinforce their analgesic property. Thus, the broad analgesic effect and multiple mechanisms already known position RvD1 as a candidate to be tested in the context of GA. In this study, we addressed the anti-inflammatory and analgesic effects of RvD1 in a mouse model of MSU-induced GA.

2. Methods

2.1. Experimental procedures

Male Swiss mice were treated with resolvin D1 (RvD1) (Cayman Chemicals, Ann Arbor, MI, USA, cat. # 10012554) at 0.3, 3, or 30 ng per animal or vehicle (3.2% ethanol in saline) either via intrathecal (i.t., between L4 – L6 vertebrae, 10 µL) or intraperitoneal (i.p.; 200 µL) injection 0.5 h before intra-articular injections of monosodium urate (MSU) (100 µg/10 µL, i.a.). Mechanical hyperalgesia and oedema were evaluated 1, 3, 5, 7, and 15 h after MSU stimulus. The 0.5h pre-treatment time was selected as a starting time point considering pharmacokinetic proprieties and according to previously studies from our group (Ruiz-Miyazawa et al., 2018; Staurengo-Ferrari et al., 2018; Rossaneis et al., 2019). Based on the results of this first set of experiments, mice were treated with 3 ng of RvD1 or vehicle (i.p. or i.t.) 72, 24, 48, or 0.5 h before MSU crystal injection, followed by assessment of mechanical hyperalgesia and oedema at the same time points. This pre-treatment experiment was intended to identify the protocol that achieves maximal RvD1 activity. Based on these experiments, the dose of 3 ng and pre-treatment time of 72 h were chosen for subsequent experiments. Post-treatment protocols were also performed. Mice were stimulated with MSU and treated with RvD1 (3 ng/animal, i.t. or i.p.) 0.5 or 2h later. Mechanical hyperalgesia and oedema were evaluated 0, 1, 3, 5, 7, and 15 h after MSU stimulus. For the post-treatment of 0.5h, at the end of the experiment, the knee joint cell wash was collected to determine leukocyte recruitment. The effects of intrathecal pre-treatment were evaluated at the knee joint inflammation through leukocytes recruitment, calcitonin gene-related peptide $CGRP^{+}$ fibres fluorescence intensity in the synovial tissue, and interleukin-1β (IL-1β) production. In dorsal root ganglia (DRG) neurons, the effects were evaluated by real time quantitative polymerase chain reaction (RT-qPCR) for transient receptor potential vanilloid subtype 1 (*Trpv1)*, voltage-gated sodium channel 1.8 (*Nav1.8)*, *Substance P*, and calcitonin gene-relates peptide (*Calca*) mRNA

expression, and immunofluorescence for phosphorylated nuclear factor kappa B (p-NF-κB) and CGRP. The effects of systemic RvD1 treatment (i.p.) were evaluated in leukocyte recruitment and IL-1β production. RvD1 effects were also determined *in vitro*. The role of RvD1 in CGRP release was investigate in cultured DRG neurons. NF-kB activation, maturation of IL-1β, and crystal phagocytosis were determined in bone marrow-derived macrophages (BMDM). The number of animals or biological samples used in each experimental procedure is summarised in Tables S1-S9, and figures' legends.

2.2. Compliance with requirements for studies using animals

Male healthy Swiss (25-30 g, 8 weeks old), C57BL/6 (20-25 g, 8 weeks old) mice from Londrina State University (Londrina, Parana, Brazil), and healthy LysM-eGFP (20-25 g, 8 weeks old, C57BlL/6 background) transgenic mice from University of Sao Paulo - Ribeirao Preto Medical School (Ribeirao Preto, Sao Paulo, Brazil), were used in this study. Transgenic LysM-eGFP C57BL/6 background mice express enhanced green fluorescent protein (eGFP) controlled by the lysozyme M promoter (LysM) active in neutrophils and macrophages. This mouse strain was used as a reporter mouse for leukocyte recruitment. All mice were housed in standard clear cages (6 mice per cage), with wood shavings bedding, free access to food and bottled water, light/dark cycle of 12/12h and controlled temperature (21°±1°C). In this study, we used a total of 645 animals. Block randomization was used to randomize subjects into groups resulting in equal sample sizes at all time points for each experiment. The investigators were blinded to groups in all experiments for all parameters, including behaviour analyses, all data acquisition, sample processing, and data analyses. Animals were under isoflurane anaesthesia (3% v/v in O_2) for intrathecal treatment and gout arthritis induction. Euthanasia was performed under isoflurane anaesthesia (5% v/v in O_2) followed by decapitation. Harvested samples were coded and randomised for processing. Animal care and handling procedures were approved by

Londrina State University Ethics Committee (process number 22186.2016.37) and were in accordance with the International Association for Study of Pain (IASP) and ARRIVE 2.0 guidelines (Lilley et al., 2020). Due to funding, sex was not considered as a variable in this study, therefore, whether the present results are replicated in females remains to be determined. All efforts were made to minimize the number of animals and their suffering.

2.3. MSU Crystal preparation and Induction of knee inflammation

MSU crystal preparation was adapted from Nishmura *et al.* 1997 (Nishimura et al., 1997). Briefly, 672 mg of uric acid (cat. sc-213135A, Santa Cruz Biotechnology, Dallas, TX, USA), was dissolved in 200 mL of boiling single distilled water containing 800 mg of NaOH (cat. # 01H1028.01.AH, Labsynth, Diadema, SP, Brazil). The pH was adjusted to 7.2 and the solution was gradually cooled by stirring at room temperature. The solution was filtered through a 0.22 μm membrane and incubated overnight (4ºC, under low agitation) to form the crystals. Crystals were collected by centrifugation (3000g, 2 min at 4ºC), washed twice with pure ethanol, and air dried. The crystals were sterilised by heating (180ºC, 2h) and stored at sterile environment until use. Joint inflammation was induced by the intra-articular (i.a.) administration of MSU (100 μg/10 μL of sterile saline) into the right knee joint of mice under isoflurane anaesthesia (3% v/v in O_2). Control animals received an i.a. injection of sterile saline (10μL).

2.4. Evaluation of knee joint mechanical hyperalgesia and oedema

Femur-tibial joint mechanical hyperalgesia was evaluated by an electronic version of von Frey filaments as previously described (Ruiz-Miyazawa et al., 2018). Briefly, mice were placed in acrylic cages with a wire grid floor. The measurement was performed only when the

animals were quiet and with all four paws on the grid floor. The method consists of an electronic pressure-meter, with a force transducer fitted with polypropylene tip (Insight instruments, Ribeirao Preto, SP, Brazil). To evaluate knee joint pain, we used a large tip (4.15 mm^2 area, 2.30 mm of diameter) to exclude subcutaneous effects. An increased perpendicular force was applied to the central area of the hind paw surface to induce flexion of femur-tibial joint followed by hind paw withdrawal. A digital analgesimeter recorded the intensity of the maximum force applied (in grams) when the paw was withdrawn. The test was performed at the times: 1, 3, 5, 7, and 15 h. The results are expressed as withdrawal mechanical threshold in grams. Keen joint oedema was assessed with a dial thickness gauge calliper (Mitutoyo) before (zero time), and after MSU intra-articular injections at the times 1, 3, 5, 7, and 15 h. Oedema was determined for each mouse knee joint by the difference between the indicated times and time zero. The results are expressed as Δmm.

2.5. Static weight bearing (SWB)

Unilateral peripheral inflammation produces changes in weight distribution toward the non-injured paw (Laboureyras et al., 2009). Changes in rear member weight distribution were evaluated using the SWB apparatus (model BIO-SWB-TOUCH-M, Bioseb, France). The device consists of an acrylic chamber where the animal is comfortably maintained while the hind paws rest on two individual weight sensor plates (left and right). The animal stands and makes a natural adjustment to the degree of pain by adapting weight distribution on the non-injured rear paw. The value of the weight applied on each sensor is displayed on the LCD screen of the control unit. Mice were habituated for at least four consecutive days prior to the behavioural testing. The experiment was conducted in a quiet, temperature-controlled room. The measurements were performed before (baseline values), 7 and 15 h after the MSU stimulus.

The results are expressed as right·left^{-1} paw ratio, which was calculated by using the mean of three measurements at 0 (baseline value), 7, and 15 h after MSU injection.

2.6. Leukocyte migration

The knee joint wash was collected 15h after MSU injection to measure leucocyte recruitment. The articular cavities were wash 3 times with 3.3 µL of saline with 1mM EDTA, then diluted to a final volume of 50 µL to evaluate leukocyte migration. The wash solution was diluted in Turk's solution 1:2 (used to lyse the erythrocytes) and the total number of leukocytes was determined in a Neubauer chamber (haemocytometer). Differential cell counts (mononuclear and polymorphonuclear) were determined in Rosenfeld-stained slides using a light microscope. The results are expressed in number of cells per cavity. Leukocyte recruitment was also determined using LysM-eGFP transgenic mice. Animals were pre-treated with RvD1 (i.t.) and stimulated with MSU. The knee joint was collected and processed for immunofluorescence staining. The fluorescence intensity of eGFP^{+} cells within the periarticular tissue was used as a secondary measurement of immune cells recruitment.

2.7. Immunofluorescence staining

Fifteen hours after MSU stimulus the knee joint and L4-L6 vertebrae associated DRGs were dissected and post-fixed in 4% paraformaldehyde for 24 hours. Knee joints were decalcified in 20% EDTA (m/v), under agitation (100 rpm) at 37°C for 48 h. The knee joint and DRG samples were incubated in sucrose 30% (m/v) (72 hours, 4°C) and embedded in optimum cutting temperature reagent. The blocks were sectioned in a cryostat at 20 and 15µm of thickness, respectively. All samples were blocked with 5% bovine serum albumin (BSA) in

phosphate buffered saline with 0.3% Triton 100-X. The knee joint sections were stained with rabbit anti-mouse CGRP (1:500, cat. # C8198, Millipore Sigma; RRID:AB_259091) followed by secondary goat anti-rabbit Alexa Fluor 647 (1:500, cat. # A-21235, Thermo Fisher Scientific; RRID:AB_2535804), the nuclei were stained with DAPI (1:1000, cat. # 14285, Cayman Chemicals). For DRG staining we used mouse anti-mouse phospho-NFκB (1:200, cat. # sc-136548, Santa Cruz Biotechnology; RRID:AB_10610391) and rabbit anti-mouse CGRP (1:500, cat. # C8198, Millipore Sigma; RRID:AB_259091) followed by goat anti-mouse Alexa Fluor 647 (1:500, cat. # A-21236, Thermo Fisher Scientific; RRID:AB_2535805) and goat anti-rabbit Alexa Fluor 488 (1:500, cat. # A-11008, Thermo Fisher Scientific; RRID:AB_143165), respectively. For *in vitro* immunofluorescence, bone marrow-derived macrophages were stained with anti-mouse phosphorylated-NFκB (1:200, cat. # sc-136548, Santa Cruz Biotechnology; RRID:AB_10610391), followed by goat anti-mouse Alexa Fluor 594 secondary antibody (1:500, cat. # A21125, Thermo Fisher Scientific, RRID:AB_141593); and anti-mouse ASC/TMS1 (1:75, cat. # NBP1-78977, Novus Biologicals; RRID:AB_11015255), followed by goat anti-rabbit Alexa Fluor 647 secondary (1:500, cat. # A-21235, Thermo Fisher Scientific; RRID:AB_2535804). DNA were also stained with DAPI (1:1000, cat. # 14285, Cayman Chemicals). Image acquisition and analysis of fluorescence intensity were performed using a Confocal Microscope (TCS SP8, Leica Microsystems, Mannheim, Germany).

2.8. RT-qPCR

Right rear paw innervating DRGs (L4-L6) were dissected into TRIzol™ reagent, and the total RNA was extracted following the manufacturer's instructions. The wavelength absorption ratio (260/280 nm) was between 1.8 – 2.0 for all samples, indicating good RNA purity as determined by spectrophotometry. Reverse transcription of total RNA to cDNA and

qPCR were performed using GoTaq® 2-Step RT-qPCR System (Promega, Madison, WI, USA) on a StepOnePlus™ Real-Time PCR System (Applied Biosystems®, Thermo Fisher Scientific, Waltham, MA, USA). Relative gene expression was determined using the comparative $2^{-(\Delta\Delta Ct)}$ method. The primers sequence used in this study were *Trpv1* sense: 5′-TTC CTG CAG AAG AGC AAG AAG C-3′, *Trpv1* antisense: 5′- CCC ATT GTG CAG ATT GAG CAT-3′; *Nav1.8* sense: 5′-GTG TGC ATG ACC CGA ACT GAT-3′, *Nav1.8* antisense: 5′-CAA AAC CCT CTT GCC AGT ATC T-3′; *Substance p* sense: 5'-GGT ACC GCA AAA TCG AAC-3', *Substance p* antisense: 5'-GGC ATC GAT TTC CTC TGC-3', *Calca* sense: 5'-CCC TTT CCT GGT TGT CAG CA-3', *Calca* antisense: 5'-TGG GCT GCT TTC CAA GAT TGA-3'. The expression of *Gapdh* mRNA was used as a reference gene to normalise data.

2.9. CGRP release

As previously described (Fattori et al., 2019), DRG neurons from naïve mice were cultured for 1 week in Neurobasal-A medium (Gibco™, Thermo Fisher Scientific Waltham, MA, U.S.) with half of the medium being replaced with fresh media every 2 days. On the 7th day, neurons were treated either with vehicle (0.1% ethanol in medium) or different concentrations of RvD1 (1-100 ng/mL) before stimulus with capsaicin (500 nM) for 1 h at 37ºC, in a humidified incubator with 5% CO_2. The supernatant was collected for CGRP concentration determination using a CGRP EIA kit following the manufacturer's instructions (Cayman Chemical, Ann Arbor, MI, U.S.). The results are expressed in pg/mL.

2.10. Bone marrow-derived macrophages (BMDM) preparation and IL-1β maturation assay

BMBM were obtained according previous described (Staurengo-Ferrari et al., 2018). In summary, bone marrow cells were isolated from femurs and tibiae of C57BL/6 mice (8weeks old). The flushed cells were cultured in RPMI 1640 media supplemented with 10% FBS, 2 mM L-glutamine, 100 U/mL penicillin, 100 μg/mL streptomycin and 20% of L929 cell conditioned medium as source of granulocyte/monocyte colony stimulating factor (GM-CSF). The cells were cultured for 7 days at 37ºC in a humidified incubator with 5% CO_2. On the 7th day, BMDMs were collected in PBS, washed in RPMI 1640, and seeded at 1.5x10^5 cells/well on a 96-well plate for IL-1β levels determination. BMDMs were primed with 500 ng/ml of lipopolysaccharide (LPS) from *Escherichia coli* (Santa Cruz Biotechnology, Dallas, TX, U.S.) (signal 1) and 3 h later were stimulated with MSU (450 μg/mL) (signal 2) for 5h. Cells were treated with vehicle (ethanol in media 0.1%) or RvD1 (1-100 ng/mL) prior to signal 1. For instance, in protocol 1 (P1) cells were not treated, in protocol 2 (P2) BMDMs were treated with vehicle, and in protocol 3 (P3) cells were treated with RvD1 for 0.5 hours. In the sequence, P2 and P3 were then LPS-primmed and MSU stimulated. After MSU incubation, the supernatant was collected to determine IL-1β levels by ELISA. The results are expressed as picograms (pg) per millilitre (mL). The supernatant was also used to determine cell viability as per LDH release (Promega, Madison, WI, U.S.), and the results are expressed in percentage of LDH release.

In another set of experiments, 4x10^5 cells were seeded onto a round glass cover slip (13 mm) on a 24-well plate for phospho-NF-κB and ASC immunostaining. Cells were treated either before signal 1, with 100 ng/mL of RvD1 or vehicle (P2 or P3, respectively). After incubation, cells were fixed and stained as above. Results are expressed as phospho-NF-κB fluorescence intensity and percentage of colocalization with the nucleus (DAPI staining).

The effect of CGRP in IL-1β maturation was also explored in this *in vitro* approach. In protocol 5 (P5), cells were primed with LPS (signal 1) for 2 hours, followed by CGRP (10 –

100 nM, GenScript Biotech, Piscataway, NJ, U.S) for 1 hours, and stimulated with MSU (signal 2). After 5 hours, the supernatant was collected for IL-1β level determination. The concentration of 100 nM of CGRP was chosen to for the next experiments (P1 – P7). The results are expressed as pg/mL of sample.

2.11. Phagocytosis assay

BMDMs were seeded on round glass cover slip (13 mm) onto a 24-well plate at the density of $1x10^6$ cells/well. Macrophage treatment, stimulus concentrations, and incubation period were based in the *in vitro* experimental design. Therefore, cells were treated either with RvD1 (100 ng/mL) or vehicle (0.1% ethanol) 0.5 h before LPS (500 ng/mL) or vehicle (medium) for 2 h, following CGRP (100 nM) or vehicle (media) treatment. Then, cells were stimulated with MSU crystals (450 μg/mL) and incubated at 37ºC, 5% CO_2 for 5 h. The phagocytosis index was determined by confocal microscopy (Leica, SP8, Wetzlar, Germany). Briefly, images were acquired in a random field of each one of the 8 biological samples. The number of total cells and cells with crystals (phagocytised MSU particles) were used to generate the phagocytosis index. The results are expressed as MSU phagocytosis (cells with MSU crystals inside, %).

2.12. Cytokine measurement

Knee joint samples were homogenised in 500 μL of phosphate buffered saline containing protease inhibitors. Samples were centrifuged (4500 rpm × 15 min × 4°C). The supernatant of homogenised tissue, or of *in vitro* culture supernatant were stored for further quantification. The levels of IL-1β were determined by enzyme-linked immunosorbent assay

(ELISA), using an Invitrogen kit (Thermo Fisher Scientific, Carlsbad, CA, U.S.). The results are expressed as pg/mg of protein, or pg/mL of culture supernatant.

2.13. Experimental design and statistical analysis

Data were analysed using GraphPad Prism statistical software (GraphPad Software, Inc., USA-500.288, version 8.0). The investigators were blinded to groups in all experiments for all parameters, including behaviour analyses, all data acquisition, sample processing, and data analyses. Data was submitted to Shapiro-Wilk normality test and Brown-Forsythe homogeneity test before proceeding to parametric or non-parametric analysis. Results are presented as means ±SEM (standard error of the mean, for data with Gaussian distribution) or median + range (for data with non-Gaussian distribution). The number of mice used for each experiment is as indicated in the figure legends and Tables S1-S9. Sample size was determined using G*Power3.1 (Erdfelder et al., 2009). The effect size f was determined using the population mean, power of analysis was set to 0.95, and a probability error of 0.05. The method of block randomization was used to randomize subjects into groups resulting in equal sample sizes at all time points for each experiment. The average value between two (or three for SWB, specifically) technical replicates were considered as the final value (data plotted and analysed) for each experiment for each animal or biological sample. Technical replicates were not considered as independent samples. Two-way ANOVA was used for repeated measurements, to compare groups and doses at all time-points when the parameters were measured at different time-points after the stimulus. The analysed factors were treatments, time, and time versus treatment interaction. For one time-point analysis, data with Gaussian distribution and homogeneous were analysed by one-way ANOVA followed by Tukey's post-hoc test. Kruskal-Wallis followed by Dunn's multiple comparison test was performed for non-Gaussian-

distributed data or data without variance homogeneity. $P<0.05$ was considered significant. For detailed information on statistical analysis please see Tables S1-S8, which includes information on data normality, homogeneity, one- or two-way ANOVA F and P values. The data and statistical analysis comply with the recommendations of the British Journal of Pharmacology on experimental design and analysis in pharmacology.

3. Results

3.1. RvD1 reduces mechanical hyperalgesia and oedema in a time- and dose-dependent manner.

First, we measured the efficacy of resolvin D1 (RvD1) treatment in monosodium urate (MSU)-induced mechanical hyperalgesia (**Fig. 1A**). We used the intraperitoneal (i.p.) route to evaluate systemic effects of RvD1 and the intrathecal (i.t.) route to measure neuronal inhibition. Doses of 3 and 30 ng of RvD1 administered 30 min before MSU injection reduced mechanical hyperalgesia and oedema to a similar extent, regardless of the administration route. Thus, we selected 3 ng of RvD1 for further work **(Fig. 1 B – C)**. RvD1 has a long-lasting analgesic effect in a range of days (Huang et al., 2011). Because of that, we asked whether increasing the time of pre-treatment would still allow observing analgesia by RvD1 administration. Mice were treated with RvD1 (3ng/animal), 72h, 48h, 24h, or 0.5 hours before MSU injection (**Fig. 1D**). Even though RvD1 reduced mechanical hyperalgesia and oedema at all tested time points (**Fig. 1 E – F**), 72h pre-treatment showed the best inhibition for both delivery routes (**Fig. 1 E – F**). The vehicle (3.2% ethanol in saline) showed no effect. Based on these results, the dose of 3 ng and pre-treatment time of 72 h were chosen for subsequent experiments. Rear member weight distribution using static weight-bearing (SWB) is a non-evoked measurement of pain (Laboureyras et al., 2009). RvD1 i.t. or i.p. pre-treatment restored rear leg weight-bearing distribution (**Fig. 1 G**). We next addressed if RvD1 exert analgesic and anti-inflammatory effects when administrated after MSU stimulus. RvD1 (3 ng/animal, i.t. or i.p.) post-treatment (30 min or 2h) reduced MSU-induced mechanical hyperalgesia and oedema (**Supplementary Fig. S1B, S2B**).

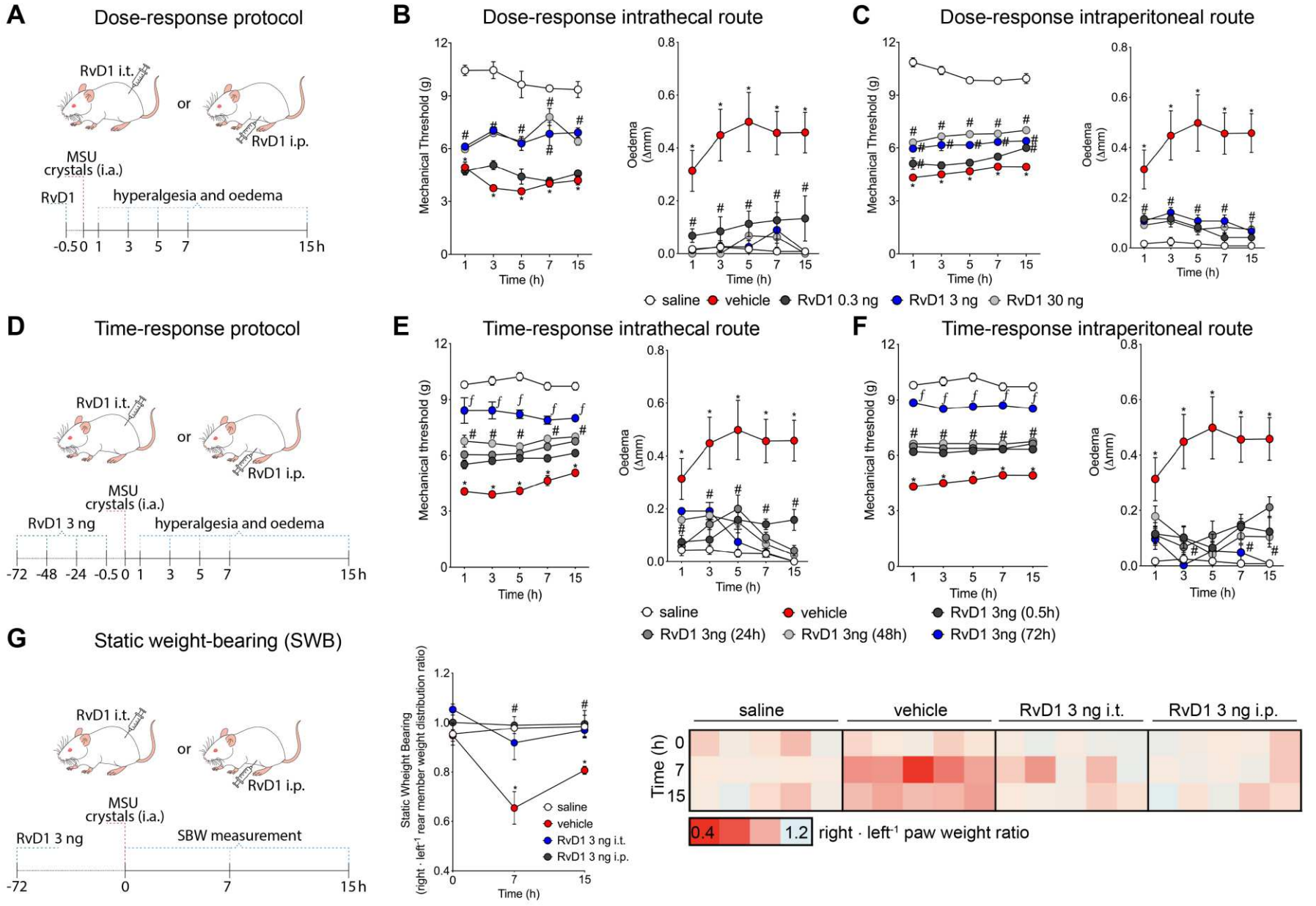
A
Dose-response protocol
RvD1 i.t.
or
RvD1 i.p.
MSU crystals (i.a.)
RvD1
hyperalgesia and oedema
-0.5 0 1 3 5 7 15 h
B
Dose-response intrathecal route
Mechanical Threshold (g)
Oedema (Δmm)
Time (h)
C
Dose-response intraperitoneal route
saline
vehicle
RvD1 0.3 ng
RvD1 3 ng
RvD1 30 ng
D
Time-response protocol
RvD1 3 ng
-72 -48 -24 -0.5 0 1 3 5 7 15 h
E
Time-response intrathecal route
Mechanical threshold (g)
F
Time-response intraperitoneal route
RvD1 3ng (0.5h)
RvD1 3ng (24h)
RvD1 3ng (48h)
RvD1 3ng (72h)
G
Static weight-bearing (SWB)
SBW measurement
Static Weight Bearing (right · left⁻¹ rear member weight distribution ratio)
RvD1 3 ng i.t.
RvD1 3 ng i.p.
saline
vehicle
Time (h)
0.4
1.2
right · left⁻¹ paw weight ratio

1

Figure 1. RvD1 reduces mechanical hyperalgesia and oedema in a time- and dose-dependent manner and restores rear leg weight distribution (A and D) dose-response treatment protocol scheme. Mechanical hyperalgesia (B and E left; C and F left) and oedema (B and E right; C and F right) were evaluated 1, 3, 5, 7, and 15h after MSU stimulus (100 μg per knee joint). Results from mechanical hyperalgesia are presented as paw withdrawal threshold (in grams) and for oedema as Δ of knee joint size (in mm). (G) SWB (Static Weight Bearing) was used as a nonreflexive method of pain measurement. The graph and heat map shows the right·left^{-1} rear leg ratio of each mouse over time. Results are presented as mean ± SEM of measurements, n = 6 (von Frey and oedema), and n = 5 (SWB) mice per group (*P < 0.05 vs. saline, # P < 0.05 vs. vehicle-treated group, *f* P< 0.05 vs. vehicle-treated and other pre-treatment groups). All statistical information and analysis are presented in Table S1 in the supplementary material.

3.2. RvD1 inhibits leukocyte recruitment and IL-1β production in the knee joint.

Leukocyte recruitment to the knee joint is a hallmark of rheumatic diseases. Treatment with RvD1 via both delivery routes (**Fig. 2A**) reduced MSU-induced recruitment of total leukocyte**,** neutrophils**,** and mononuclear cells **(Fig. 2 B – C)**. RvD1 post-treatment also reduced leukocyte recruitment (**Supplementary Fig. S1C).** Cellular recruitment is dependent on cytokine production in the inflamed tissue and the pro-inflammatory cytokine IL-1β plays a crucial role in GA (Martinon et al., 2006). Regardless of the administration route (i.p. or i.t.), RvD1 reduced IL-1β levels to a similar extent in the knee tissue (**Fig. 2D**). Of interest, RvD1 systemic treatment (i.p.) did not induce liver or kidney toxicity (**Supplementary Fig. S3**).

3.3. RvD1 decreases interleukin-1β (IL-1β) maturation, ASC protein expression, and NF-κB activation in macrophages in vitro.

The inflammasome NLRP3 (NLR family pyrin domain containing 3) machinery is composed of the NLRP3, the adaptor molecule ASC (apoptosis-associated speck-like protein containing a caspase recruitment domain), pro-caspase-1, and pro-IL-1β. It is an essential mechanism in GA pathology (Martinon et al., 2006). The transcription factor NF-kB regulates the expression of those components. Therefore, we investigated the RvD1 effect on NF-kB activation, ASC expression, and IL-1β production using bone marrow-derived macrophages (BMDMs) (Fig. 3A). In this *in vitro* system, IL-1β release is dependent on 2 signals: lipopolysaccharide (LPS) priming (signal 1) and MSU-triggered NLRP3 inflammasome assembling (signal 2) to produce mature IL-1β (Martinon et al., 2006). Treating with RvD1 at 100 ng/mL before LPS-priming (signal 1) reduced IL-1β production (Fig. 3B). None of the RvD1 concentrations or stimuli reduced cell viability as measured by LDH release (Fig. 3B). RvD1 also reduced ASC expression, NF-kB phosphorylation (Fig. 3C), and NF-kB translocation to the nucleus (Fig. 3D), indicating important anti-inflammatory mechanisms.

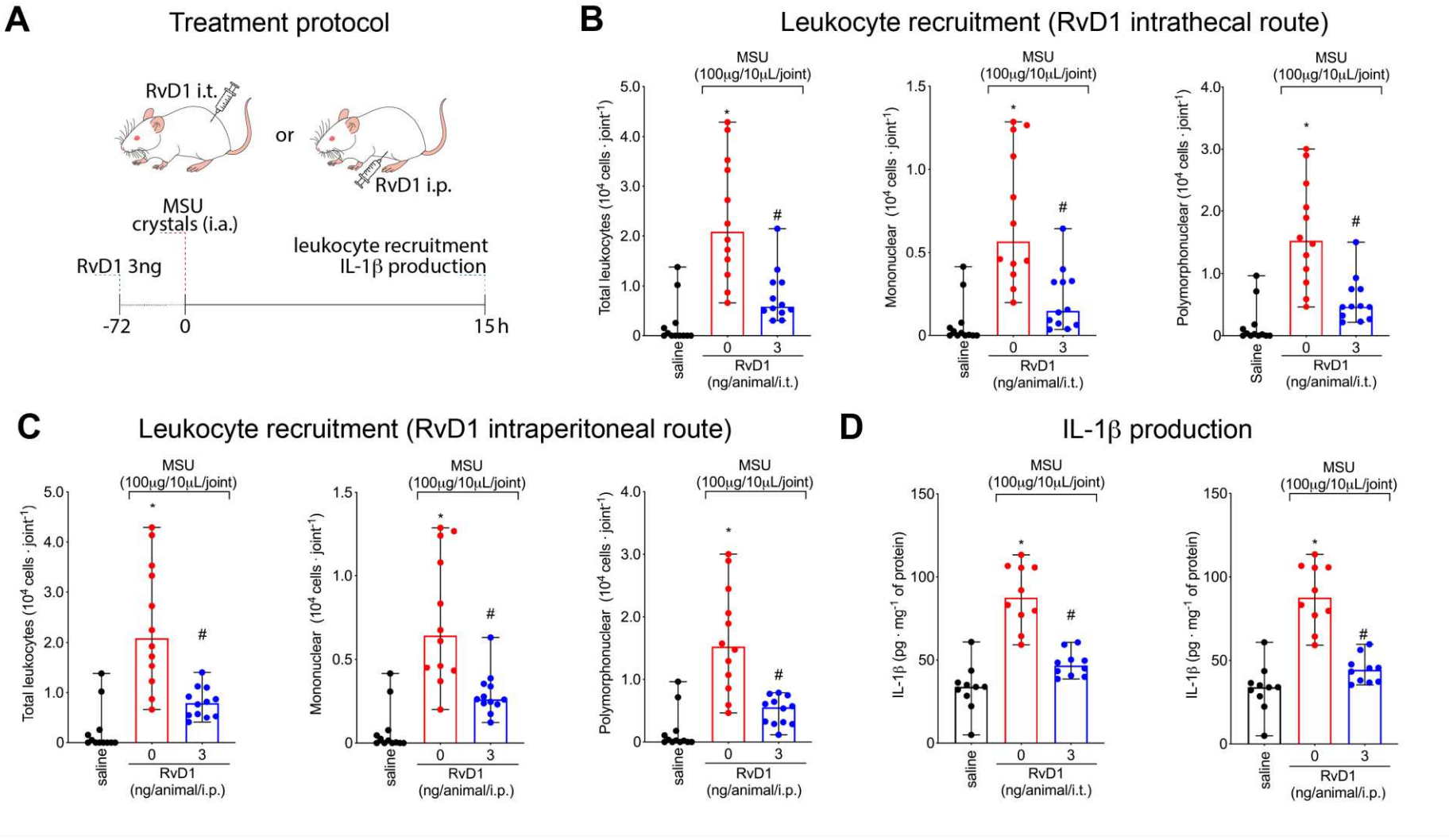
A
Treatment protocol
RvD1 i.t.
or
RvD1 i.p.
MSU
crystals (i.a.)
RvD1 3ng
leukocyte recruitment
IL-1β production
-72
0
15 h
B
Leukocyte recruitment (RvD1 intrathecal route)
MSU
(100μg/10μL/joint)
Total leukocytes (10^4 cells · joint^-1)
Mononuclear (10^4 cells · joint^-1)
Polymorphonuclear (10^4 cells · joint^-1)
saline
0
3
RvD1
(ng/animal/i.t.)
C
Leukocyte recruitment (RvD1 intraperitoneal route)
RvD1
(ng/animal/i.p.)
D
IL-1β production
IL-1β (pg · mg^-1 of protein)

Figure 2. RvD1 inhibits leukocyte recruitment and IL-1β production in the knee joint. (A) treatment protocol scheme for inflammatory infiltrate and IL-1β evaluation in the knee joint. Leukocyte recruitment to the knee joint was evaluated 15hrs after MSU injection. Results are expressed as number of cells per knee joint cavity, and are presented as median and range of measurements, n = 12 mice per group (*P < 0.05 vs. saline, # P < 0.05 vs. vehicle-treated group). (D) Fifteen hours after the stimulus the knee joint tissue was processed and the concentration of IL-1β was determined by ELISA. Results are expressed as picograms per milligram of protein, and are presented as median and range of measurements, n = 10 mice per group per experiment (*P < 0.05 vs. saline, # P < 0.05 vs. vehicle-treated group). All statistical information and analysis are presented in Table S2 in the supplementary material.

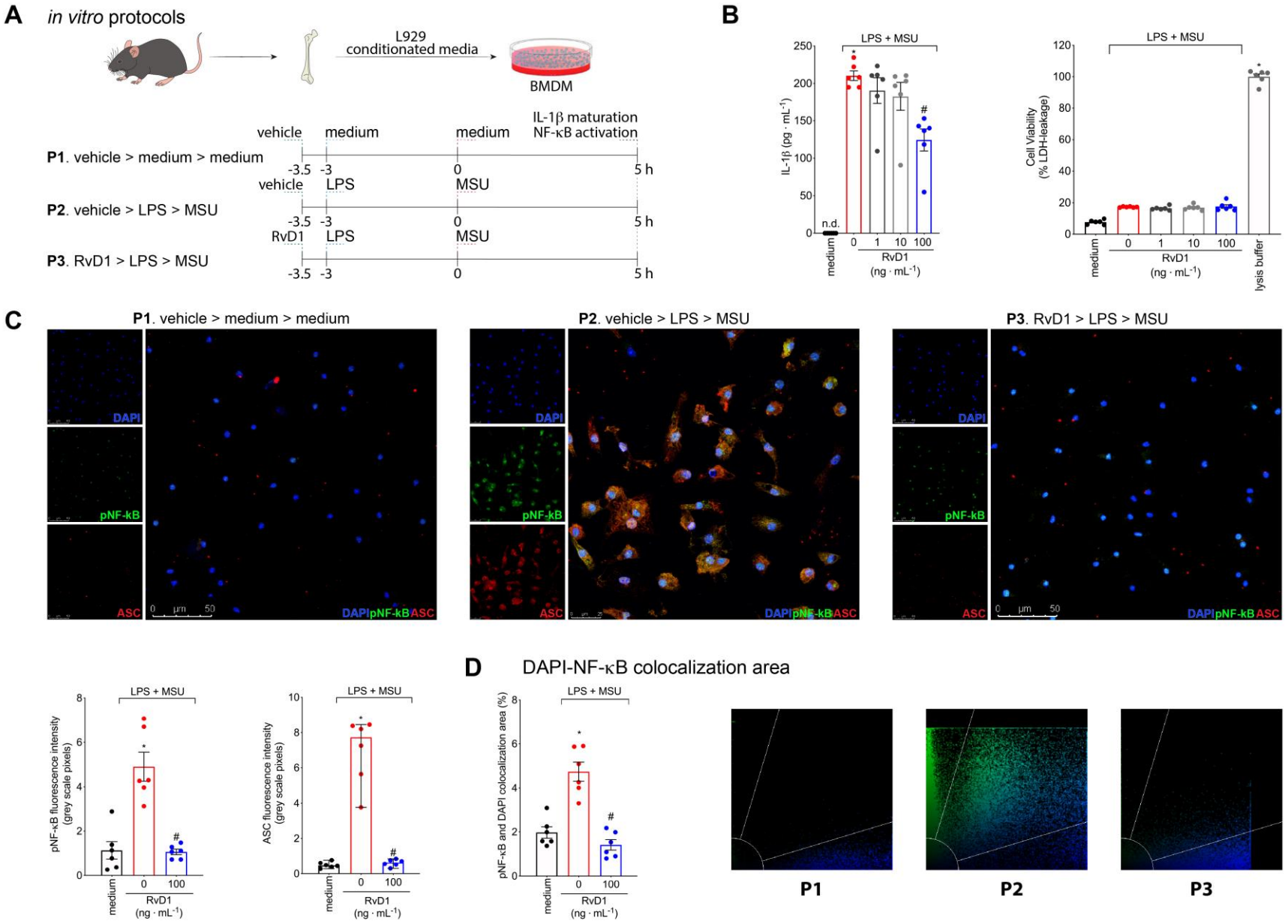
A
in vitro protocols
L929
conditionated media
BMDM
IL-1β maturation
NF-κB activation
vehicle
medium
medium
P1. vehicle > medium > medium
-3.5 -3 0 5 h
vehicle
LPS
MSU
P2. vehicle > LPS > MSU
-3.5 -3 0 5 h
RvD1
LPS
MSU
P3. RvD1 > LPS > MSU
-3.5 -3 0 5 h
B
LPS + MSU
IL-1β (pg · mL-1)
n.d.
medium
0 1 10 100
RvD1
(ng · mL-1)
LPS + MSU
Cell Viability
(% LDH-leakage)
medium
0 1 10 100
RvD1
(ng · mL-1)
lysis buffer
C
P1. vehicle > medium > medium
P2. vehicle > LPS > MSU
P3. RvD1 > LPS > MSU
DAPI
pNF-kB
ASC
0 μm 50
DAPI pNF-kB ASC
LPS + MSU
pNF-κB fluorescence intensity
(grey scale pixels)
ASC fluorescence intensity
(grey scale pixels)
medium
0 100
RvD1
(ng · mL-1)
D
DAPI-NF-κB colocalization area
pNF-κB and DAPI colocalization area (%)
P1
P2
P3

Figure 3. RvD1 decreases IL-1β maturation, ASC protein expression, and NF-κB activation in macrophages in vitro. (A) Schematic view of bone marrow-derived macrophages preparation and *in vitro* treatment protocols. (B) *in vitro* IL-1β levels and treatment cytotoxicity. Results are presented as mean ± SEM of measurements, n = 6 individual biological samples per treatment protocol (*P < 0.05 vs. medium, # P < 0.05 vs. vehicle-treated cells). (C) BMDMs were treated according to the presented protocols and were stained for ASC and phospho-NF-κB. Results of fluorescence intensity in grey scale value are expressed in mean ± SEM for phospho-NF-κB and median and range for ASC of, n = 6 (*P < 0.05 vs. medium, # P < 0.05 vs. vehicle-treated cells). (D) DAPI and phospho-NF-κB colocalization area. Results are expressed in percentage of colocalization area. Immunostaining results are presented as mean ± SEM of measurements, n = 6 individual biological samples per treatment protocol per experiment (*P < 0.05 vs. medium, # P < 0.05 vs. vehicle-treated cells). All statistical information and analysis are presented in Table S3 in the supplementary material

3.4. RvD1 reduces MSU-induced activation of CGRP⁺ nociceptors in vivo*, blocks CGRP release in the knee joint periarticular tissue and in cultured DRG neurons*

Ion channel expression is intimately related to neuronal activation and pain perception during gout flares (Hoffmeister et al., 2014; Qiu et al., 2021) (**Fig. 4A**). We observed that i.t. RvD1 reduced MSU-induced increase of *Trpv1*, *Nav1.8*, *Substance P*, and *Calca* (calcitonin gene-related peptide gene) mRNA levels (**Fig. 4B**). Furthermore, RvD1 reduced not only overall fluorescence intensity of phosphorylated-NF-κB but also its fluorescence intensity in $CGRP^+$ DRG neurons indicating lessened activation of $CGRP^+$ neurons upon RvD1 treatment (**Fig. 4C**). However, could RvD1 be acting directly on nociceptors activation or indirectly by reducing macrophage activation? We observed that capsaicin (a TRPV1 agonist) induces the release of CGRP by DRG neurons, which was reduced by RvD1 in a concentration-dependent manner. Thus, RvD1 can directly silence nociceptor sensory neurons decreasing the release of neuropeptides such as CGRP (**Fig. 4D**). Next, combining fluorescence analysis of LysM-eGFP (a reporter mouse for mature neutrophils) (Faust et al., 2000) with staining of peptidergic fibres using CGRP antibody, we determined whether RvD1 blocks leukocyte recruitment near $CGRP^+$ fibres **(Fig. 4E)**. RvD1 reduced eGFP fluorescence intensity surrounding $CGRP^+$ fibres, which might indicate a reduction of LysM-$eGFP^+$ neutrophils recruitment towards these $CGRP^+$ axons (**Fig. 4E)**. CGRP fluorescence intensity is inversely proportional to its release and can be used as an indirect measurement (Hoffmann et al., 2002). We infer that RvD1 reduces neuronal activation by reducing CGRP expression in DRG neurons and the activation of $CGRP^+$ neurons (enhanced NF-κB phosphorylation) (**Fig. 4A-C**). Moreover, RvD1 reduced CGRP release *in vitro* (**Fig. 4D**) and *in vivo*, as measured by CGRP fluorescence intensity in the axons innervating the periarticular tissue (**Fig. 4E).** CGRP in turn, exerts its peripheral functions via immune cells. Therefore, by silencing $CGRP^+$ neurons, RvD1 disrupts the communication between nociceptive neurons and immune cells.

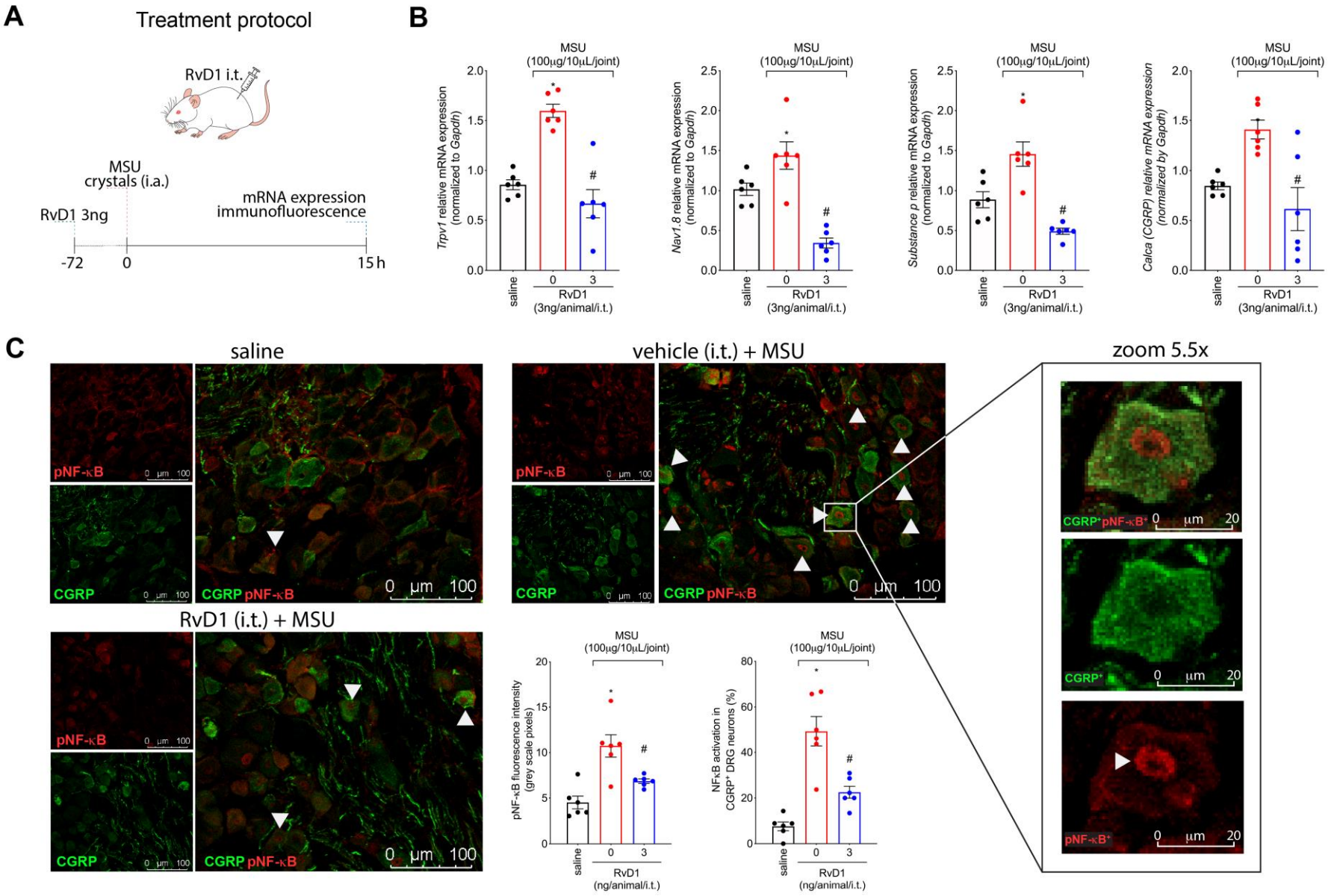
A
Treatment protocol
RvD1 i.t.
MSU
crystals (i.a.)
RvD1 3ng
mRNA expression
immunofluorescence
-72
0
15 h
B
MSU
(100µg/10µL/joint)
Trpv1 relative mRNA expression
(normalized to Gapdh)
Nav1.8 relative mRNA expression
(normalized to Gapdh)
Substance p relative mRNA expression
(normalized to Gapdh)
Calca (CGRP) relative mRNA expression
(normalized by Gapdh)
saline
RvD1
(3ng/animal/i.t.)
C
saline
vehicle (i.t.) + MSU
zoom 5.5x
RvD1 (i.t.) + MSU
pNF-κB
CGRP
CGRP pNF-κB
0 µm 100
pNF-κB fluorescence intensity
(grey scale pixels)
NFκB activation in
CGRP+ DRG neurons (%)
RvD1
(ng/animal/i.t.)
CGRP+pNF-κB+
CGRP+
pNF-κB+
0 µm 20

1

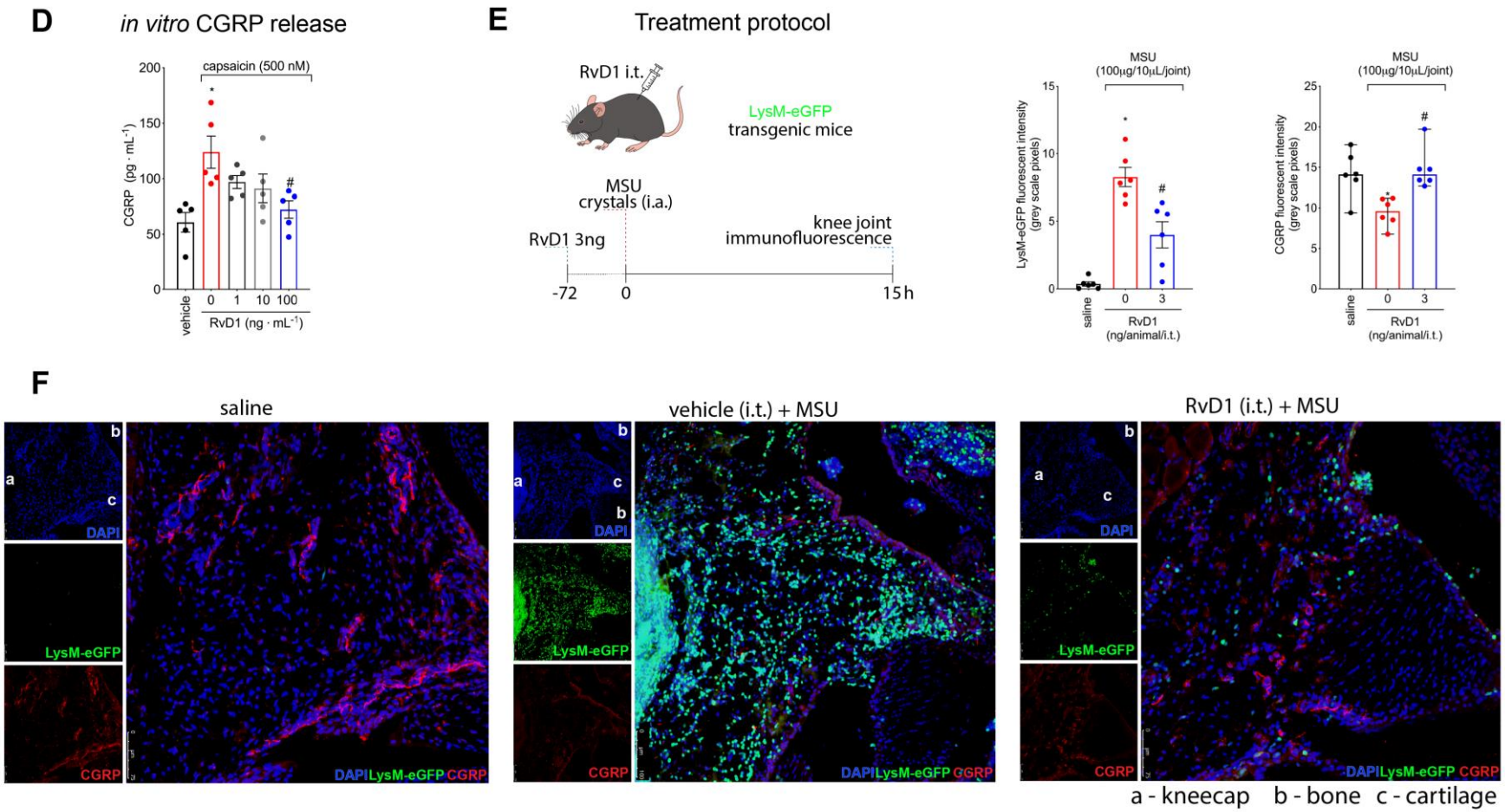

Figure 4. RvD1 reduces MSU-induced activation of CGRP+ nociceptors in vivo, blocks CGRP release in the knee joint periarticular tissue and in cultured DRG neurons (A) Schematic representation of the protocol. The DRGs (ipsilateral, vertebrae L4 – L6) were dissected and processed for RT-qPCR (B) or immunostaining (C). Results are presented as mean ± SEM of measurements, n = 6 mice per group (*P < 0.05 vs. saline, # P < 0.05 vs. vehicle-treated group). (D) CGRP release determined by EIA using cultured DRG neurons from naïve mice. Results are expressed as

picograms per millilitres of culture supernatant, are presented as mean ± SEM of measurements, n = 5 per treatment protocol (*P < 0.05 vs. saline, # P < 0.05 vs. vehicle-treated group). (E) Treatment protocol scheme of LysM-eGFP mice and determination of LysM+ cells in the knee joint. Results are expressed as fluorescence intensity in grey scale pixels and are presented as mean ± SEM of measurements, n = 6 mice per group (*P < 0.05 vs. saline, # P < 0.05 vs. vehicle-treated group; for CGRP fluorescence intensity (E right), results are presented as median and range, n = 6 mice per group (*P < 0.05 vs. saline, # P < 0.05 vs. vehicle-treated group). (F) LysM-eGFP knee joint immunofluorescence representative images. All statistical information and analysis are presented in Table S4 in the supplementary material.

3.5. RvD1 decreases CGRP enhancement of macrophage release of IL-1β and phagocytosis of MSU crystals.

Because CGRP increases the phagocytosis of other inert molecules (Ichinose and Sawada, 1996), we investigated the activity of CGRP in macrophage activation and MSU crystal phagocytosis. Since RvD1 (i.t.) reduces CGRP release, this approach would indicate whether this lipid could indirectly modulate MSU phagocytosis by reducing CGRP release. However, as RvD1 is active when injected i.p., we reason that it could also directly interfere with MSU crystals phagocytosis. Thus, BMDMs were subjected to different treatment protocols (P1 – P7) (**Fig. 5A**). CGRP increased IL-1β release in a concentration-dependent manner with the concentration of 100 nM being significantly different compared to the other lower concentrations (**Fig. 5B, P5 protocol**). Therefore, this concentration was chosen to the next experiments. CGRP increased phagocytosis of MSU crystals by macrophages (**Fig. 5C, E**). Interestingly, it also increased the phagocytosis of MSU crystals in naïve macrophages (*i.e.* non LPS-primed BMDMs) (**Fig. 5C, E, P7 protocol**) although this difference was not statistically significant. CGRP also increased IL-1β concentrations in the culture supernatant (**Fig. 5D, P1 – P7**), demonstrating that CGRP might have an important role in GA pathophysiology. Importantly, RvD1 treatment reduced not only MSU phagocytosis (P4), and CGRP potentiation of MSU crystal internalization (P6), but also IL-1β maturation (**Fig. 5C – E**). Table S9 makes a summary list of all experiments, methods, n, figures and in which table all the statistical details can be found.

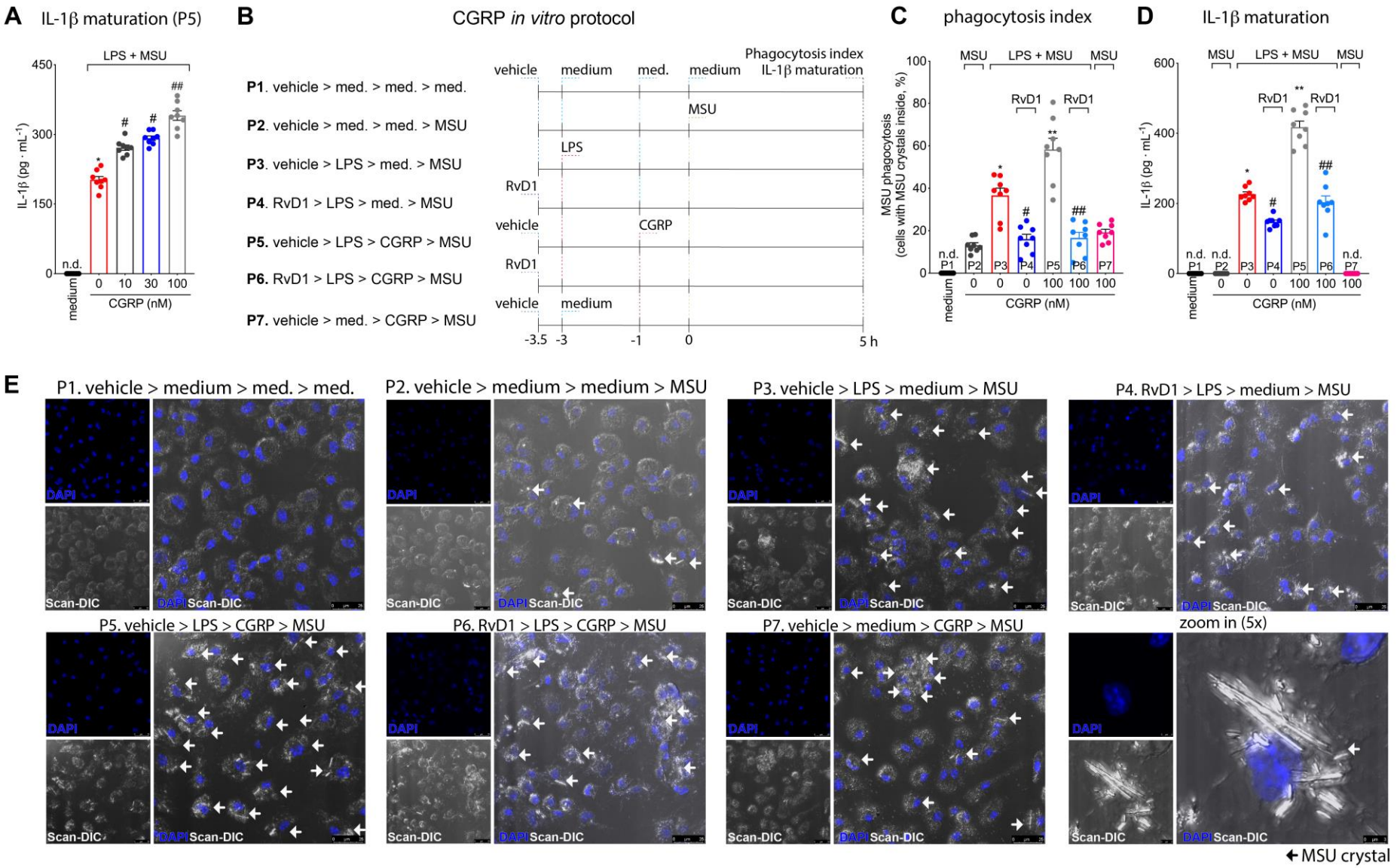
A
IL-1β maturation (P5)
LPS + MSU
IL-1β (pg · mL⁻¹)
n.d.
medium
CGRP (nM)
B
CGRP in vitro protocol
P1. vehicle > med. > med. > med.
P2. vehicle > med. > med. > MSU
P3. vehicle > LPS > med. > MSU
P4. RvD1 > LPS > med. > MSU
P5. vehicle > LPS > CGRP > MSU
P6. RvD1 > LPS > CGRP > MSU
P7. vehicle > med. > CGRP > MSU
Phagocytosis index
IL-1β maturation
vehicle
medium
med.
MSU
LPS
RvD1
CGRP
5 h
C
phagocytosis index
MSU phagocytosis (cells with MSU crystals inside, %)
MSU
LPS + MSU
RvD1
D
IL-1β maturation
E
P1. vehicle > medium > med. > med.
P2. vehicle > medium > medium > MSU
P3. vehicle > LPS > medium > MSU
P4. RvD1 > LPS > medium > MSU
P5. vehicle > LPS > CGRP > MSU
P6. RvD1 > LPS > CGRP > MSU
P7. vehicle > medium > CGRP > MSU
zoom in (5x)
DAPI
Scan-DIC
MSU crystal

Figure 5. RvD1 decreases CGRP enhancement of macrophage release of IL-1β and phagocytosis of MSU crystals. (A) *In vitro* protocols for CGRP effect in potentiate MSU-induced IL-1β production. Cells were treated according to P5. IL-1β levels were determined via ELISA, the results are expressed as picograms per millilitres of culture supernatant, and are presented as mean ± SEM of measurements, n = 8 per treatment protocol (*P < 0.05 vs. medium, # P < 0.05 vs. vehicle-treated group, ## P < 0.05 vs. CGRP 10 and 30 nM treated group). (B) *in vitro* protocol for MSU crystals phagocytosis assay (C and E) and determination of IL-1β levels (D). Results are expressed as MSU phagocytosis (cells with MSU crystals inside, %) and IL-1β levels in picograms per millilitre, for C and D respectively, and are presented as mean ± SEM of measurements, n = 8 samples per treatment protocol (*P < 0.05 vs. P1 and P2, **P<0.05 vs. P3 group, # P < 0.05 vs. P3 group; ## P< 0.05 vs. P5). (E, white arrow points to macrophages with phagocytised MSU) Representative images from the phagocytosis index. Genetic material is in blue (DAPI staining). All statistical information and analysis are presented in Table S5 in the supplementary material.

4. Discussion

We report that either intrathecal (i.t.) or intraperitoneal (i.p.) administration of RvD1 reduced MSU-induced pain and inflammation with time-dependent efficacy. RvD1 i.t. treatment reduced pain, oedema, leukocyte recruitment and IL-1β production in the knee joints of gouty mice. RvD1 i.t. treatment reduced MSU-induced mRNA expression of pain-related ion channels (*Trpv1* and *Nav1.8*), neuropeptides (*substance P and Calca*), and the activation of DRG neurons, as observed by the reduction of NF-κB activation in $CGRP^+$ neurons. Thus, i.t. RvD1 acts by silencing neurons reducing CGRP release. In turn, CGRP is the link explaining the activity of i.t. RvD1 in GA since this neuropeptide increased the phagocytosis of MSU crystals and IL-1β release by macrophages. RvD1 also acted directly on macrophages reducing MSU crystals phagocytosis and IL-1β release to stop the inflammatory response. Thus, RvD1 inhibits nociceptor neuron and macrophage activation, and interrupts the neuro-immune communication between these cells reducing the MSU crystal-induced acute flare in male mice.

Although gout is more prevalent in men (8.21%) than women (2.33%) (SY et al., 2011; Kuo et al., 2015), risk factors for developing the disease does not differ between sexes (Evans et al., 2019). While differential activation of spinal cord immune cells plays a role in pain and analgesia in males and females (Mogil and Bailey, 2010; Sorge et al., 2015), to the date, no study reports sex-dependent differences in pain during GA. Although we acknowledge the importance of sex-dependent variables and this is a limitation of our study, it was out of the scope to determine whether GA pain and RvD1's effect differ between female vs male mice.

RvD1 half-life after intravenous (i.v.) administration is of approximately 4.77 hours in mice, and indetectable after 8 h, but detectable in tissues, such as submandibular salivary gland, within 5 min after administration (Yellepeddi et al., 2021). RvD1 also increases miRNAs expression,

which explain its resolution effects at later time points (Bannenberg et al., 2005; Recchiuti and Serhan, 2012; Sun et al., 2020). Evidence also supports that RvD1 can induce the production of itself and other SPMs such as lipoxin A_4 (Bathina and Das, 2021). Thus, RvD1 activity is a time-dependent process involving the modulation of gene expression, immune cell activity and phenotype, modulation of endogenous SPM production and is not solely dependent on RvD1 presence at the time of evaluation. In fact, RvD1 analgesia with the 72h pre-treatment was higher than earlier time points before MSU injection. Our findings corroborate data demonstrating in a model of paw incision induced pain that a single i.t. treatment with RvD1 produces 10 days of analgesia (Huang et al., 2011). This time-dependent effect is also observed with other SPMs. Maresin 1 pre-treatment provides 5 days of analgesia, while post-treatment confers analgesia for 3 days (Fattori et al., 2019). Thus, the time-dependent increase in efficacy indicates that SPMs, RvD1 included, might be good candidates for prevention and treatment of chronic, painful conditions. In the case of GA, the acute flares tend to be more frequent upon the chronicity of the inflammatory process, thus, a preventive treatment with RvD1 is rational. Although post-treatment with RvD1 also provides analgesia in GA, the mechanistic studies were mostly pre-treatment protocols, and this is a limitation of our study.

NLRP3 inflammasome activation culminates in IL-1β maturation and release, a pivotal innate immune event in GA (Martinon et al., 2006; Amaral et al., 2012; So and Martinon, 2017). This mechanism consists of an auto-amplification loop that accounts for leukocyte recruitment, NF-κB activation, and the production of macrophage-derived mediators (Amaral et al., 2012, 2016). All these factors are responsible for nociceptive neurons sensitisation and unbearable pain in GA (Binshtok et al., 2008; Marcotti et al., 2018). Thus, we next investigated the effect of RvD1 on IL-1β maturation *in vitro*. In BMDM, two signals are required for IL-1β release. Signal 1 or priming,

is related to NF-κB activation and its downstream pathways, culminating in the expression of all inflammasome components (NLRP3, ASC, pro-caspase-1) and pro-IL-1β. Signal 2 or activation, is triggered by MSU crystals phagocytosis, phagolysosome lysis and NLRP3 inflammasome activation by cathepsin release (Martinon et al., 2006). Herein, we demonstrate that RvD1 (100 ng/mL, 265.6 nM) downmodulates macrophage activation by reducing NF-κB phosphorylation, its translocation to the nucleus, and the expression of the NLRP3 inflammasome adaptor molecule ASC. More importantly, these events are accompanied by a reduction in IL-1β levels in the culture supernatant, thus, demonstrating a functional outcome. Our data confirm that RvD1 reduces NF-κB activation (Krishnamoorthy et al., 2010; Liao et al., 2012; Wu et al., 2017; Yin et al., 2017) or inflammasome activation in other models (Li et al., 2017; Yin et al., 2017) as well as clinical score, oedema, leukocyte recruitment, and bone-resorption in a model of collagen antibody-induced arthritis (Benabdoun et al., 2019). Thus, the literature sustains the mechanisms observed in our *in vitro* and *in vivo* approaches in MSU arthritis.

Limbs, skin, and joints are highly innervated by a subset of sensory neurons responsible for pain perception, called nociceptors (Cai et al., 2019). Pro-inflammatory lipid mediators, chemokines, and cytokines sensitise and activate those neurons causing pain (Ji et al., 2014; Pinho-Ribeiro et al., 2017). The expression of ion channels, such as those of TRP family, are also related to the increase in neuronal activity. RvD1 blocks allyl isothiocyanate (AITC)-induced TRP ankyrin subtype 1 (TRPA1) current (Park et al., 2011). RvD1 blocks calcium influx and animal behaviours triggered by TRPA1, TRPV3, and TRPV4 agonists (Bang et al., 2010). TRPV1 plays a crucial role in GA nociceptive and inflammatory responses in rats (Hoffmeister et al., 2014). Because of this direct effect on nociceptor and $TRPV1^+$ neuron participation in gout physiopathology, we next addressed the effects of RvD1 on nociceptors *in vivo*. Our data suggest that RvD1 reduced MSU-

induced neuronal sensitisation by decreasing the mRNA expression of pain-related ion channels (*Nav1.8* and *Trpv1*) and neuropeptides (*Substance P* and *Calca*). These phenomena are also observed with other SPMs. For instance, MaR1 reduces TRPV1 and Nav1.8 mRNA expression, and capsaicin neuronal activation (Fattori et al., 2019). RvE1 reduces TNF-α-induced excitatory postsynaptic currents frequency in spinal cord neurons (Xu et al., 2010) while RvD2 reduces TRPV1 sensitisation (Payrits et al., 2020; Perna et al., 2020).

The activation of neurons upon noxious stimuli triggers the release of neuropeptides. As a result, the levels of CGRP are increased in the synovial fluid of GA patients during active flares (Hernanz et al., 1993). Because RvD1 diminished CGRP mRNA expression, we determined whether RvD1 could reduce the activation of peptidergic nociceptors. We demonstrated that RvD1 reduced CGRP release in cultured DRG neurons, corroborating a study demonstrating that RvD1 blocks CGRP release by trigeminal nociceptors (Payrits et al., 2020). *In vivo* we showed that RvD1 reduced CGRP mRNA expression in the DRG and restored CGRP staining in the axons of peripheral nociceptor neurons innervating the knee joints; this was used as a surrogate of CGRP release. RvD1 also reduced the activation of $CGRP^+$ DRG neurons as observed by reduced pNF-kB detection in $CGRP^+$ DRG neurons. The present data corroborate our group's findings showing for the first time that the SPM MaR1 blocks CGRP release (Fattori et al., 2019), which was confirmed by an independent group (Allen et al., 2020). Since in GA leukocytes are recruited to the surroundings of $CGRP^+$ neurons in the knee joints and CGRP enhances macrophage particles phagocytosis (Ichinose and Sawada, 1996), we then investigated the role of CGRP in MSU crystals phagocytosis and IL-1β maturation. To our knowledge, we demonstrate for the first time that CGRP enhances MSU phagocytosis and IL-1β release, which were reduced by RvD1. These findings indicate that RvD1 limits phagocytosis and the consequent IL-1β release through direct

and indirect mechanisms. Indirectly, RvD1 reduces neuronal activation and CGRP release, which reduces the peripheral functions of CGRP during GA such as leukocyte recruitment, MSU phagocytosis, and IL-1β maturation. RvD1 inhibits macrophage activation directly further reducing MSU phagocytosis and IL-1β release to limit pain and inflammation in GA. Therefore, we demonstrated a functional consequence of inhibiting neuronal CGRP release and its role in neuro-immune interactions in the GA disease context.

5. Conclusion

RvD1 (i.t. or i.p.) displays time-dependent analgesic effect and immunoresolvent activity in GA (**Fig. 6**) acting in the range of nanograms (3 ng per mouse). RvD1 reduces NF-κB activation decreasing MSU-induced IL-1β production in BMDM *in vitro*. I.t. treatment with RvD1 reduced DRG neuron mRNA expression and decreased activation of $CGRP^+$ neurons. *In vitro*, RvD1 blocked capsaicin-induced CGRP release. In turn, CGRP activates macrophages, enhancing MSU crystals phagocytosis and IL-1β maturation. Thus, there is a previously unrecognised neuroimmune axis in GA pathophysiology. Importantly, the inhibition of neuronal activation and CGRP release might be closely related to the observed overall disease improvement. It is also noteworthy that the safe preclinical profile, the long-lasting effect (Huang et al., 2011), and the high efficacy at low doses, place SPMs such as RvD1 as important candidates for translational studies and clinical research towards the development of rheumatic disease therapy based on RvD1.

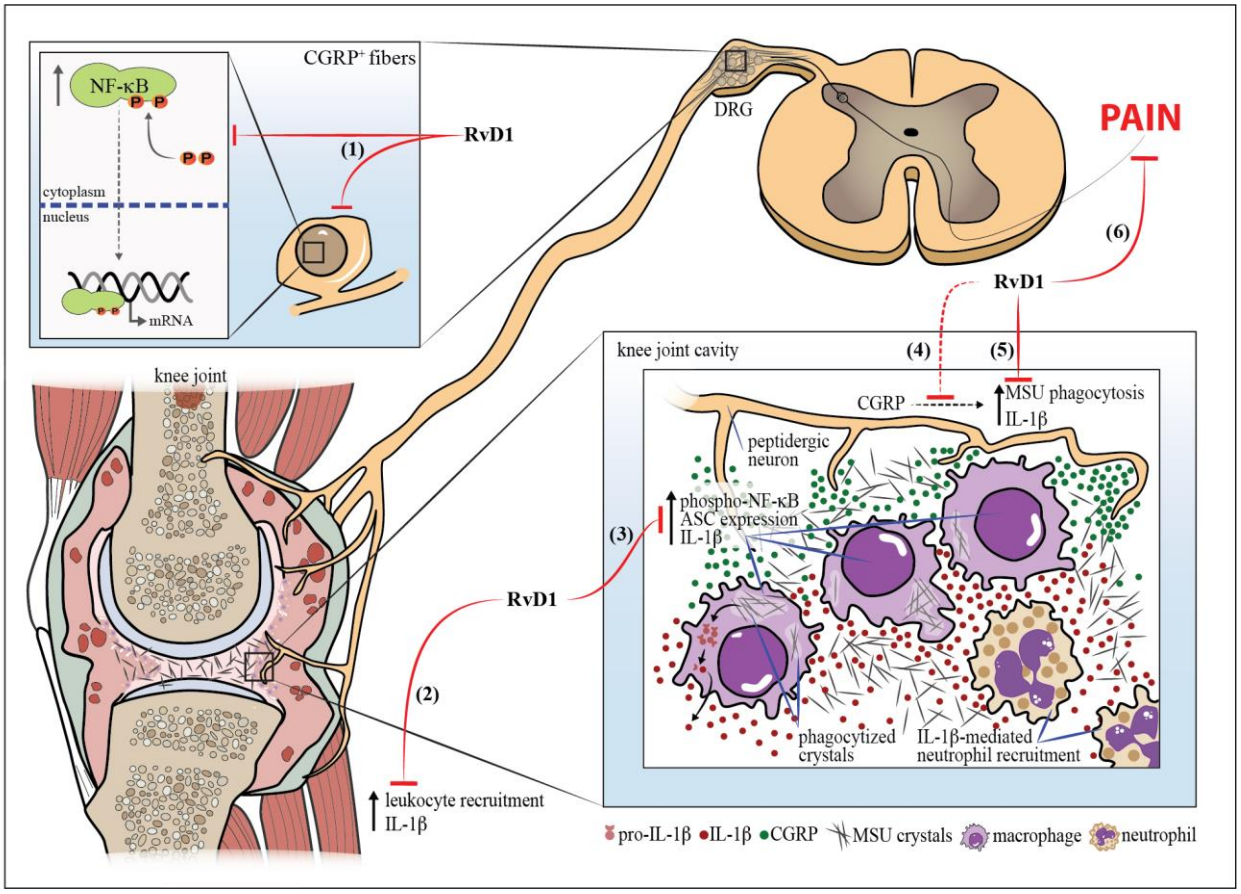

Figure 6. RvD1 action mechanisms in gouty arthritis. (1) Intrathecal RvD1 reduces neuronal activation by decreasing NF-κB activation in peptidergic fibres (CGRP⁺), and *in vitro* CGRP release. (2) Intrathecal or intraperitoneal RvD1 reduces leucocyte recruitment to the knee joint and IL-1β production. (3) In BMDMs, RvD1 reduces macrophage activation by decreasing LPS/MSU-induced NF-kB phosphorylation, ASC expression, and IL-1β maturation and release. (4) RvD1 (i.t.) diminishes CGRP release in the knee joint periarticular tissue, which might be related to RvD1 effects on DRG neurons (1). We also demonstrated that CGRP increases MSU crystal phagocytosis and IL-1β maturation *in vitro*. (5) RvD1 reduces MSU phagocytosis, IL-1β maturation, and CGRP-mediated crystals internalization. Lastly, via all mechanisms herein described, RvD1 (6) abrogates articular pain in this pre-clinical mouse model of gouty arthritis.

Acknowledgments and Funding

The Authors are thankful for the PRONEX grant supported by SETI/Araucária Foundation and MCTI/CNPq; and Paraná State Government (agreement 014/2017, protocol 46.843); Funding Authority for Studies and Projects and State Secretariat of Science, Technology and Higher Education (MCTI/FINEP/CT-INFRA-PROINFRA, Brazil (grant agreements 01.12.0294.00 and

01.13.0049.00); Grants from The J. Willard and Alice S. Marriott Foundation and Marriott Daughters Foundation. T.H.Z., T.S.-S., S.B.-G., M.M.B., F.R.O., N.A.A., and M.F.M. F.A.P.-R. acknowledge PhD scholarship from Coordination for the Improvement of Higher Education Personnel (CAPES, Brazil, finance code 001), K.C.A. acknowledge master's degree scholarship from CAPES. C.R.F. received CNPq Post-Doc fellowship. S.M.B. thanks the fellowship from FUNADESP. F.A.A., M.M.T., R.C. and W.A.V.J. acknowledge the CNPq Researcher fellowship. We also thank the support of CMLP-UEL for the access to equipment free of charge, and Prof. Estefânia Gastaldello Moreira for statistical advice.

Author contribution

Conceptualization: T.H. Zaninelli, V. Fattori, and W.A. Verri; **investigation and data curation:** T.H. Zaninelli, V. Fattori, T. Santos-Saraiva, S. Badaro-Garcia, L. Staurengo-Ferrari, K.C. Andrade, N. A. Artero, C.R. Ferraz, M.M. Bertozzi, F. Rasquel-Oliveira, M.F. Manchope, F.A. Amaral, M.M. Teixeira, S.M. Borghi, M.S. Rogers, R. Casagrande, W.A. Verri Jr; **funding acquisition:** M.S. Rogers, R. Casagrande, and W.A. Verri; **methodology:** T.H. Zaninelli, V. Fattori, and W.A. Verri; **resources:** F.A. Amaral, M.M. Teixeira, M.S. Rogers, R. Casagrande, and W.A. Verri; **project administration:** T.H. Zaninelli; **supervision:** V. Fattori, M.S. Rogers, and W.A. Verri; **visualization:** T.H. Zaninelli, V. Fattori, and W.A. Verri; **writing–original draft:** T.H. Zaninelli, V. Fattori, and W.A. Verri; **writing – editing and reviewing:** all authors. All authors have read and approved the final version of the manuscript.

Declaration of interests

The authors declare no conflicts of interest.

6. References

Allen, B.L., Montague-Cardoso, K., Simeoli, R., Colas, R.A., Oggero, S., Vilar, B., et al. (2020). Imbalance of proresolving lipid mediators in persistent allodynia dissociated from signs of clinical arthritis. Pain *161*: 2155–2166.

Amaral, F.A., Bastos, L.F., Oliveira, T.H., Dias, A.C., Oliveira, V.L., Tavares, L.D., et al. (2016). Transmembrane TNF-alpha is sufficient for articular inflammation and hypernociception in a mouse model of gout. Eur J Immunol *46*: 204–211.

Amaral, F.A., Costa, V. V, Tavares, L.D., Sachs, D., Coelho, F.M., Fagundes, C.T., et al. (2012). NLRP3 inflammasome-mediated neutrophil recruitment and hypernociception depend on leukotriene B(4) in a murine model of gout. Arthritis Rheum *64*: 474–484.

Bang, S., Yoo, S., Yang, T.J., Cho, H., Kim, Y.G., and Hwang, S.W. (2010). Resolvin D1 attenuates activation of sensory transient receptor potential channels leading to multiple anti-nociception. Br J Pharmacol *161*: 707–720.

Bannenberg, G., and Serhan, C.N. (2010). Specialized pro-resolving lipid mediators in the inflammatory response: An update. Biochim Biophys Acta *1801*: 1260–1273.

Bannenberg, G.L., Chiang, N., Ariel, A., Arita, M., Tjonahen, E., Gotlinger, K.H., et al. (2005). Molecular circuits of resolution: formation and actions of resolvins and protectins. J Immunol *174*: 4345–4355.

Bathina, S., and Das, U.N. (2021). Resolvin D1 Decreases Severity of Streptozotocin-Induced Type 1 Diabetes Mellitus by Enhancing BDNF Levels, Reducing Oxidative Stress, and Suppressing Inflammation. Int. J. Mol. Sci. *22*: 1–15.

Benabdoun, H.A., Kulbay, M., Rondon, E.P., Vallières, F., Shi, Q., Fernandes, J., et al. (2019). In vitro and in vivo assessment of the proresolutive and antiresorptive actions of resolvin D1:

Relevance to arthritis. Arthritis Res. Ther. *21*:.

Binshtok, A.M., Wang, H., Zimmermann, K., Amaya, F., Vardeh, D., Shi, L., et al. (2008). Nociceptors are interleukin-1beta sensors. J Neurosci *28*: 14062–14073.

Cai, R., Pan, C., Ghasemigharagoz, A., Todorov, M.I., Förstera, B., Zhao, S., et al. (2019). Panoptic imaging of transparent mice reveals whole-body neuronal projections and skull–meninges connections. Nat. Neurosci. *22*: 317–327.

Dalbeth, N., and Haskard, D.O. (2005). Mechanisms of inflammation in gout. Rheumatol. *44*: 1090–1096.

Dinarello, C.A. (2009). Immunological and inflammatory functions of the interleukin-1 family. Annu. Rev. Immunol. *27*: 519–550.

Erdfelder, E., FAul, F., Buchner, A., and Lang, A.G. (2009). Statistical power analyses using G*Power 3.1: tests for correlation and regression analyses. Behav. Res. Methods *41*: 1149–1160.

Evans, P.L., Prior, J.A., Belcher, J., Hay, C.A., Mallen, C.D., and Roddy, E. (2019). Gender-specific risk factors for gout: a systematic review of cohort studies. Adv. Rheumatol. (London, England) *59*: 24.

Faires, J.S., and Mccarty, D.J. (1962). Acute arthritis in man and dog after intrasynovial injection of sodium urate crystals. Lancet *280*: 682–685.

Fattori, V., Pinho-Ribeiro, F.A., Staurengo-Ferrari, L., Borghi, S.M., Rossaneis, A.C., Casagrande, R., et al. (2019). The specialised pro-resolving lipid mediator maresin 1 reduces inflammatory pain with a long-lasting analgesic effect. Br J Pharmacol *176*: 1728–1744.

Faust, N., Varas, F., Kelly, L.M., Heck, S., and Graf, T. (2000). Insertion of enhanced green fluorescent protein into the lysozyme gene creates mice with green fluorescent granulocytes and macrophages. Blood *96*: 719–726.

Hernanz, A., Miguel, E. De, Romera, N., Perez-ayala, C., Gijon, J., and Arnalich, F. (1993). Calcitonin gene-related peptide II, substance p and vasoactive intestinal peptide in plasma and synovial fluid from patients with inflammatory joint disease. Rheumatology *32*: 31–35.

Hoffmann, O., Keilwerth, N., Bille, M.B., Reuter, U., Angstwurm, K., Schumann, R.R., et al. (2002). Triptans reduce the inflammatory response in bacterial meningitis. J. Cereb. Blood Flow Metab. *22*: 988–996.

Hoffmeister, C., Silva, M.A., Rossato, M.F., Trevisan, G., Oliveira, S.M., Guerra, G.P., et al. (2014). Participation of the TRPV1 receptor in the development of acute gout attacks. Rheumatol. (United Kingdom) *53*: 240–249.

Huang, L., Wang, C.F., Serhan, C.N., and Strichartz, G. (2011). Enduring prevention and transient reduction of postoperative pain by intrathecal resolvin D1. Pain *152*: 557–565.

Ichinose, M., and Sawada, M. (1996). Enhancement of phagocytosis by calcitonin gene-related peptide (CGRP) in cultured mouse peritoneal macrophages. Peptides *17*: 1405–1414.

Ji, R.R., Xu, Z.Z., and Gao, Y.J. (2014). Emerging targets in neuroinflammation-driven chronic pain. Nat. Rev. Drug Discov. *13*: 533–548.

Ji, R.R., Xu, Z.Z., Strichartz, G., and Serhan, C.N. (2011). Emerging roles of resolvins in the resolution of inflammation and pain. Trends Neurosci. *34*: 599–609.

Krishnamoorthy, S., Recchiuti, A., Chiang, N., Yacoubian, S., Lee, C.H., Yang, R., et al. (2010). Resolvin D1 binds human phagocytes with evidence for proresolving receptors. Proc. Natl. Acad. Sci. U. S. A. *107*: 1660–1665.

Kuo, C.F., Grainge, M.J., Zhang, W., and Doherty, M. (2015). Global epidemiology of gout: Prevalence, incidence and risk factors. Nat. Rev. Rheumatol. *11*: 649–662.

Laboureyras, E., Chateauraynaud, J., Richebé, P., and Simonnet, G. (2009). Long-term pain

vulnerability after surgery in rats: Prevention by nefopam, an analgesic with antihyperalgesic properties. Anesth. Analg. *109*: 623–631.

Li, G., Chen, Z., Bhat, O.M., Zhang, Q., Abais-Battad, J.M., Conley, S.M., et al. (2017). NLRP3 inflammasome as a novel target for docosahexaenoic acid metabolites to abrogate glomerular injury. J. Lipid Res. *58*: 1080–1090.

Liao, Z., Dong, J., Wu, W., Yang, T., Wang, T., Guo, L., et al. (2012). Resolvin D1 attenuates inflammation in lipopolysaccharide-induced acute lung injury through a process involving the PPARγ/NF-κB pathway. Respir. Res. *13*: 110.

Lilley, E., Stanford, S.C., Kendall, D.E., Alexander, S.P.H., Cirino, G., Docherty, J.R., et al. (2020). ARRIVE 2.0 and the British Journal of Pharmacology: Updated guidance for 2020. Br. J. Pharmacol. *177*: 3611–3616.

Marcotti, A., Miralles, A., Dominguez, E., Pascual, E., Gomis, A., Belmonte, C., et al. (2018). Joint nociceptor nerve activity and pain in an animal model of acute gout and its modulation by intra-articular hyaluronan. Pain *159*: 739–748.

Martinon, F., Pétrilli, V., Mayor, A., Tardivel, A., and Tschopp, J. (2006). Gout-associated uric acid crystals activate the NALP3 inflammasome. Nature *440*: 237–241.

Mogil, J.S., and Bailey, A.L. (2010). Sex and gender differences in pain and analgesia. Prog. Brain Res. *186*: 140–157.

Nishimura, A., Akahoshi, T., Takahashi, M., Takagishi, K., Itoman, M., Kondo, H., et al. (1997). Attenuation of monosodium urate crystal-induced arthritis in rabbits by a neutralizing antibody against interleukin-8. J. Leukoc. Biol. *62*: 444–449.

Park, C.K., Xu, Z.Z., Liu, T., Lu, N., Serhan, C.N., and Ji, R.R. (2011). Resolvin D2 is a potent endogenous inhibitor for transient receptor potential subtype V1/A1, inflammatory pain, and

spinal cord synaptic plasticity in mice: distinct roles of resolvin D1, D2, and E1. J Neurosci *31*: 18433–18438.

Payrits, M., Horváth, Á., Biró-Sütő, T., Erostyák, J., Makkai, G., Sághy, É., et al. (2020). Resolvin D1 and D2 inhibit transient receptor potential vanilloid 1 and ankyrin 1 ion channel activation on sensory neurons via lipid raft modification. Int. J. Mol. Sci. *21*: 1–17.

Perna, E., Aguilera-Lizarraga, J., Florens, M. V., Jain, P., Theofanous, S.A., Hanning, N., et al. (2020). Effect of resolvins on sensitisation of TRPV1 and visceral hypersensitivity in IBS. Gut.

Pinho-Ribeiro, F.A., Verri, W.A., and Chiu, I.M. (2017). Nociceptor Sensory Neuron–Immune Interactions in Pain and Inflammation. Trends Immunol.

Qiu, J., Xu, X., Zhang, S., Li, G., and Zhang, G. (2021). Modulations of Nav1.8 and Nav1.9 Channels in Monosodium Urate–Induced Gouty Arthritis in Mice. Inflammation.

Recchiuti, A., and Serhan, C.N. (2012). Pro-resolving lipid mediators (SPMs) and their actions in regulating miRNA in novel resolution circuits in inflammation. Front. Immunol. *3*:.

Rees, F., Hui, M., and Doherty, M. (2014). Optimizing current treatment of gout. Nat Rev Rheumatol *10*: 271–283.

Rossaneis, A.C., Longhi-Balbinot, D.T., Bertozzi, M.M., Fattori, V., Segato-Vendrameto, C.Z., Badaro-Garcia, S., et al. (2019). [Ru (bpy) 2 (NO) SO3](PF6), a nitric oxide donating ruthenium complex, reduces gout arthritis in mice. Front Pharmacol *10*: 229.

Ruiz-Miyazawa, K.W., Staurengo-Ferrari, L., Pinho-Ribeiro, F.A., Fattori, V., Zaninelli, T.H., Badaro-Garcia, S., et al. (2018). 15d-PGJ2-loaded nanocapsules ameliorate experimental gout arthritis by reducing pain and inflammation in a PPAR-gamma-sensitive manner in mice. Sci Rep *8*: 13979.

Schlesinger, N., and Thiele, R.G. (2010). The pathogenesis of bone erosions in gouty arthritis.

Ann. Rheum. Dis. *69*: 1907–1912.

So, A.K., and Martinon, F. (2017). Inflammation in gout: mechanisms and therapeutic targets. Nat Rev Rheumatol *13*: 639–647.

Sorge, R.E., Mapplebeck, J.C.S., Rosen, S., Beggs, S., Taves, S., Alexander, J.K., et al. (2015). Different immune cells mediate mechanical pain hypersensitivity in male and female mice. Nat. Neurosci. *18*: 1081.

Staurengo-Ferrari, L., Ruiz-Miyazawa, K.W., Pinho-Ribeiro, F.A., Fattori, V., Zaninelli, T.H., Badaro-Garcia, S., et al. (2018). Trans-chalcone attenuates pain and inflammation in experimental acute gout arthritis in mice. Front. Pharmacol. *9*:.

Sun, W., Ma, J., Zhao, H., Xiao, C., Zhong, H., Ling, H., et al. (2020). Resolvin D1 suppresses pannus formation via decreasing connective tissue growth factor caused by upregulation of miRNA-146a-5p in rheumatoid arthritis. Arthritis Res. Ther. *22*:.

SY, C., SC, L., YT, H., and WH, P. (2011). Trends in hyperuricemia and gout prevalence: Nutrition and Health Survey in Taiwan from 1993-1996 to 2005-2008. Asia Pac. J. Clin. Nutr. *20*: 301–308.

Wu, B., Mottola, G., Chatterjee, A., Lance, K.D., Chen, M., Siguenza, I.O., et al. (2017). Perivascular delivery of resolvin D1 inhibits neointimal hyperplasia in a rat model of arterial injury. In Journal of Vascular Surgery, (Mosby Inc.), pp 207-217.e3.

Xu, Z.Z., Zhang, L., Liu, T., Park, J.Y., Berta, T., Yang, R., et al. (2010). Resolvins RvE1 and RvD1 attenuate inflammatory pain via central and peripheral actions. Nat Med *16*: 592–7, 1p following 597.

Yellepeddi, V.K., Parashar, K., Dean, S.M., Watt, K.M., Constance, J.E., and Baker, O.J. (2021). Predicting Resolvin D1 Pharmacokinetics in Humans with Physiologically-Based

Pharmacokinetic Modeling. Clin. Transl. Sci. *14*: 683–691.

Yin, Y., Chen, F., Wang, W., Wang, H., and Zhang, X. (2017). Resolvin D1 inhibits inflammatory response in STZ-induced diabetic retinopathy rats: Possible involvement of NLRP3 inflammasome and NF-κB signaling pathway. Mol. Vis. *23*: 242–250.

Appendices

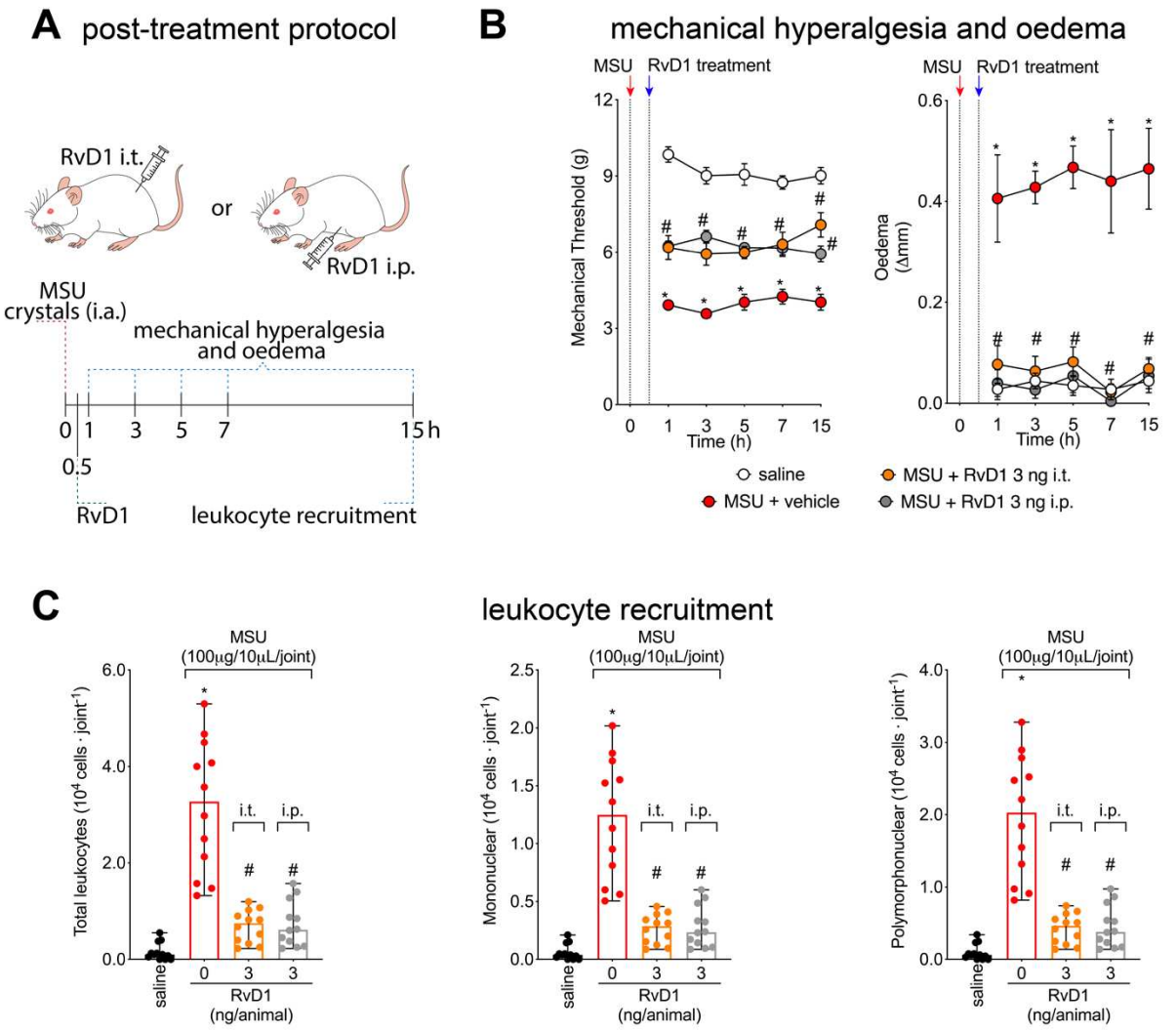

Supplementary Figure S1. RvD1 post-treatment reduces mechanical hyperalgesia, oedema, and leukocyte recruitment. (A) post-treatment protocol scheme. Mechanical hyperalgesia (B left) and oedema (B right) were evaluated 1, 3, 5, 7, and 15h after MSU stimulus (100 μg per knee joint). Results from mechanical hyperalgesia are presented as paw withdrawal threshold (in g) and for oedema as Δ of knee joint size (in mm). Results are presented as mean ± SEM of measurements, n = 6 mice per group (*P < 0.05 vs. saline, # P < 0.05 vs. vehicle-treated group). (C) Leukocyte recruitment to the knee joint was evaluated 15hrs after MSU injection. Results are expressed as number of cells per knee joint cavity, and are presented as median and range, n = 12 mice per group (*P < 0.05 vs. saline, # P < 0.05 vs. vehicle-treated group). All statistical information and analysis are presented in Table S6 in the supplementary material.

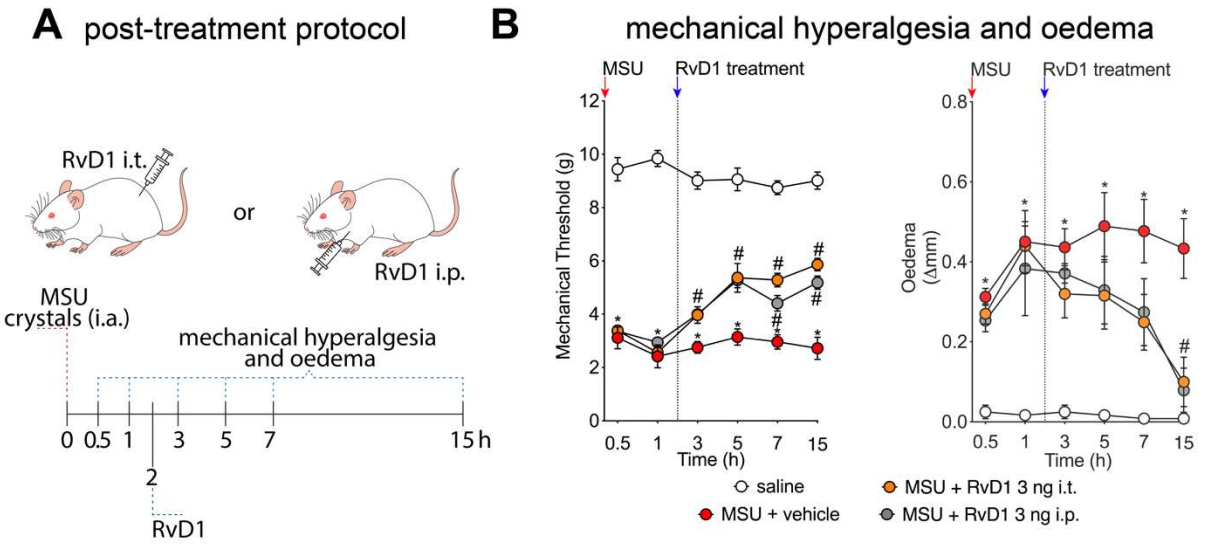

Supplementary Figure S2. RvD1 administrated 2h after MSU injection reduces mechanical hyperalgesia and oedema. (A) post-treatment protocol scheme. Mechanical hyperalgesia (B left) and oedema (B right) were evaluated 0.5, 1, 3, 5, 7, and 15h after MSU stimulus (100 μg per knee joint). Results from mechanical hyperalgesia are presented as paw withdrawal threshold (in g) and for oedema as Δ of knee joint size (in mm). Results are presented as mean ± SEM of measurements, n = 6 mice per group (*P < 0.05 vs. saline, # P < 0.05 vs. vehicle-treated group). All statistical information and analysis are presented in Table S7 in the supplementary material.

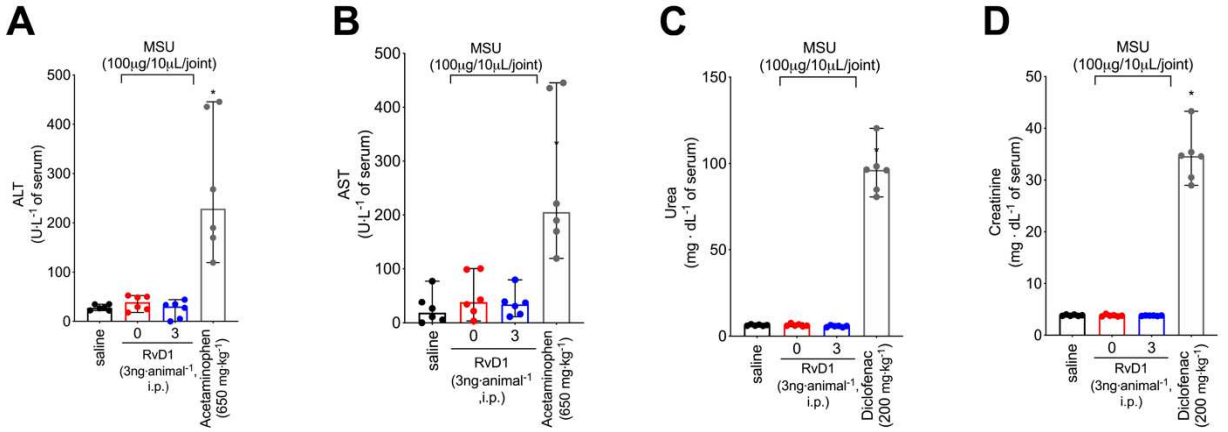

Supplementary Figure S3. Systemic treatment with RvD1 does not induce liver, kidney, or stomach toxicity. Blood was collected 87 h (72h pre-treatment + 15 h of MSU stimulus) after RvD1 (3 ng/animal, i.p.) or vehicle (3.2% ethanol in saline) to assess (A) alanine transaminase (ALT), (B) aspartate aminotransferase (AST) levels in plasma samples. Acetaminophen (650 mg·kg^{-1}, p.o.) was used as a control drug for liver injury and samples were

collected 10h after the stimulus. Plasma samples were also used to determine (C) urea and (D) creatinine levels. Diclofenac (200 $mg \cdot kg^{-1}$, p.o) was used as a control drug for kidney injury and samples were collected 24h after stimulus. Results are expressed as units per litre of serum for AST and ALT, and milligrams per decilitre of serum for urea and creatinine. Results are presented as median and range, n = 6 mice per group. (*$p < 0.05$ vs. all groups). All statistical information and analysis are presented in Table S8 in the supplementary material.

1

Summary of statistical analysis

Table S1. Statistical information from results shown in Figure 1.

Result	Shapiro-Wilk test				Brown-Forsythe		Statistical test	Post-test	F value	P value
	Group	n	W value	P value	F value	P value				
Figure 1B (left)	saline	6	0.8025	0.0849	F (4,20) = 0.2617	0.8990	Two-way ANOVA	Tukey	Time x Dose: F (16, 100) = 3.158	P=0.0002
	Vehicle + MSU	6	0.9192	0.5245					Time: F (3.239, 80.97) = 2.536	P=0.0581
	RvD1 0.3 + MSU	6	0.9975	0.9982					Dose: F (4, 25) = 120.9	P<0.0001
	RvD1 3 + MSU	6	0.8704	0.2680					Subject: F (25, 100) = 2.427	P=0.0010
	RvD1 30 + MSU	6	0.9108	0.4725						
Figure 1B (right)	saline	6	0.8810	0.3140	F (4,20) = 0.6311	0.6460	Two-way ANOVA	Tukey	Time x Dose: F (16, 100) = 1.110	P=0.3566
	Vehicle + MSU	6	0.7857	0.0616					Time: F (3.536, 88.39) = 3.344	P=0.0171
	RvD1 0.3 + MSU	6	0.9193	0.5252					Dose: F (4, 25) = 16.63	P<0.0001
	RvD1 3 + MSU	6	0.8781	0.1129					Subject: F (25, 100) = 9.035	P<0.0001
	RvD1 30 + MSU	6	0.8110	0.2139						
Figure 1C (left)	saline	6	0.8446	0.1779	F (4,20) = 0.4891	0.7437	Two-way ANOVA	Tukey	Time x Dose: F (16, 100) = 4.612	P<0.0001
	Vehicle + MSU	6	0.9083	0.4576					Time: F (2.986, 74.65) = 4.512	P=0.0059
	RvD1 0.3 + MSU	6	0.8676	0.2567					Dose: F (4, 25) = 368.4	P<0.0001
	RvD1 3 + MSU	6	0.9343	0.6258					Subject: F (25, 100) = 2.656	P=0.0003
	RvD1 30 + MSU	6	0.9407	0.6707						

Figure 1C (right)	saline	6	0.8810	0.3140	F (4,20) = 1.121	0.3745	Two-way ANOVA	Tukey	Time x Dose: F (16, 100) = 3.220	P=0.0002
	Vehicle + MSU	6	0.7857	0.0616					Time: F (2.380, 59.51) = 3.144	P=0.0420
	RvD1 0.3 + MSU	6	0.8188	0.1143					Dose: F (4, 25) = 17.65	P<0.0001
	RvD1 3 + MSU	6	0.8770	0.2959					Subject: F (25, 100) = 16.97	P<0.0001
	RvD1 30 + MSU	6	0.8810	0.3140						
Figure 1E (left)	saline	6	0.8582	0.2217	F (5, 24) = 0.5674	0.7241	Two-way ANOVA	Tukey	Time x Dose: F (20, 120) = 2.712	P=0.0004
	Vehicle + MSU	6	0.8803	0.3106					Time: F (2.131, 63.93) = 3.846	P=0.0242
	RvD1 3 (30') + MSU	6	0.9669	0.8552					Dose: F (5, 30) = 135.7	P<0.0001
	RvD1 3 (24h) + MSU	6	0.8435	0.1747						
	RvD1 3 (48h) + MSU	6	0.9876	0.9708						
	RvD1 3 (78h) + MSU	6	0.8881	0.3476					Subject: F (30, 120) = 4.427	P<0.0001
Figure 1E (right)	saline	6	0.8406	0.1665	F (5, 24) = 0.9776	0.4514	Two-way ANOVA	Tukey	Time x Dose: F (20, 120) = 5.535	P<0.0001
	Vehicle + MSU	6	0.7857	0.0616					Time: F (4, 120) = 8.571	P<0.0001
	RvD1 3 (30') + MSU	6	0.8034	0.0863					Dose: F (5, 30) = 14.21	P<0.0001
	RvD1 3 (24h) + MSU	6	0.9396	0.6631						
	RvD1 3 (48h) + MSU	6	0.8659	0.2501						
	RvD1 3 (78h) + MSU	6	0.8608	0.2310					Subject: F (30, 120) = 11.18	P<0.0001
Figure 1F (left)	saline	6	08582	0.2217	F (5, 24) = 1.884	0.1347	Two-way ANOVA	Tukey	Time x Dose: F (20, 120) = 3.218	P<0.0001

	Vehicle + MSU	6	0.9083	0.4576					Time: F (2.927, 87.80) = 1.912	P<0.1350
	RvD1 3 (30') + MSU	6	0.9227	0.5478						
	RvD1 3 (24h) + MSU	6	0.8362	0.1546						
	RvD1 3 (48h) + MSU	6	0.7861	0.0621					Dose: F (5, 30) = 295.6	P<0.0001
	RvD1 3 (78h) + MSU	6	0.9231	0.5502					Subject: F (30, 120) = 6.470	P<0.0001
Figure 1F (right)	saline	6	0.8810	0.3140	F (5, 24) = 0.6116	0.6919	Two-way ANOVA	Tukey	Time x Dose: F (20, 120) = 2.025	P=0.0104
	Vehicle + MSU	6	0.7857	0.0616					Time: F (3.275, 98.24) = 0.8287	P=0.4900
	RvD1 3 (30') + MSU	6	0.9572	0.7887						
	RvD1 3 (24h) + MSU	6	0.9462	0.7103						
	RvD1 3 (48h) + MSU	6	0.9193	0.5251					Dose: F (5, 30) = 16.19	P<0.0001
	RvD1 3 (78h) + MSU	6	0.9204	0.5325					Subject: F (30, 120) = 6.159	P<0.0001
Figure 1G	Saline	5	0.8950	0.3699	F (3,8) = 2.418	0.1415	Two-way ANOVA	Tukey	Time x Dose: F (6, 32) = 3.299	P=0.0122
	Vehicle + MSU	5	0.9994	0.9552					Time: F (2, 32) = 6.248	P=0.0051
	RvD1 i.t. + MSU	5	0.9998	0.9710					Dose: F (3, 16) = 12.50	P=0.0002
	RvD1 i.p. +MSU	5	0.9710	0.7285					Subject: F (16, 32) = 1.177	P=0.3355

Table S2. Statistical information from results shown in Figure 2.

Result		Shapiro-Wilk test			Brown-Forsythe		Statistical test	Post-test	F value	P value
	Group	**n**	**W value**	**P value**	**F value**	**P value**				
Figure 2B (left)	Saline	12	0.5949	<0.0001	F (2, 33) = 7.371	0.0023	Kruskal-Wallis	Dunn	22.60	<0.0001
	Vehicle + MSU	12	0.9415	0.5171						
	RvD1 + MSU	12	0.8317	0.0220						
Figure 2B (middle)	Saline	12	0.6094	<0.0001	F (2, 33) = 7.922	0.0015	Kruskal-Wallis	Dunn	21.59	<0.0001
	Vehicle + MSU	12	0.8772	0.0808						
	RvD1 + MSU	12	0.8637	0.0544						
Figure 2B (right)	Saline	12	0.6026	<0.0001	F (2, 33) = 6.566	0.0040	Kruskal-Wallis	Dunn	22.43	<0.0001
	Vehicle + MSU	12	0.9539	0.6950						
	RvD1 + MSU	12	0.8379	0.0261						
Figure 2C (left)	Saline	12	0.5950	<0.0001	F (2, 33) = 10.38	0.0003	Kruskal-Wallis	Dunn	22.82	<0.0001
	Vehicle + MSU	12	0.9415	0.5171						
	RvD1 + MSU	12	0.9390	0.4850						
Figure 2C (middle)	Saline	12	0.6094	<0.0001	F (2, 33) = 9.355	0.0006	Kruskal-Wallis	Dunn	22.97	<0.0001
	Vehicle + MSU	12	0.8969	0.1446						
	RvD1 + MSU	12	0.8566	0.0443						
Figure 2C (right)	Saline	12	0.6026	<0.0001	F (2, 33) = 8.669	0.0009	Kruskal-Wallis	Dunn	22.52	<0.0001
	Vehicle + MSU	12	0.9539	0.6950						
	RvD1 + MSU	12	0.9176	0.2665						

Figure 2D (left)	Saline	10	0.9254	0.4040	F (2, 27) = 3.726	0.0372	Kruskal-Wallis	Dunn	21.65	<0.0001
	Vehicle + MSU	10	0.9273	0.4220						
	RvD1 + MSU	10	0.9083	0.2697						
Figure 2D (right)	Saline	10	0.9254	0.4040	F (2, 27) = 3.450	0.0463	Kruskal-Wallis	Dunn	21.57	<0.0001
	Vehicle + MSU	10	0.9273	0.4220						
	RvD1 + MSU	10	0.8986	0.2116						

Table S3. Statistical information from results shown in Figure 3.

Result		Shapiro-Wilk test		Brown-Forsythe		Statistical test	Post-test	F value	P value
	Group	**n**	**W value**	**P value**	**F value**	**P value**				
Figure 3B (right)	No stimuli	6	Not included*	Not included*	F (3, 20) = 0.3715	0.7744	One-way ANOVA	Tukey	F (3, 20) = 44.60	<0.0001
	LPS + MSU + vehicle	6	0.9070	0.4169						
	LPS + MSU + RvD1 1 ng	6	0.8913	0.3250						
	LPS + MSU + RvD1 10 ng	6	0.9264	0.5528						
	LPS + MSU + RvD1 100 ng	6	0.9134	0.4589						
Figure 3B (left)	No stimuli	6	0.9244	0.5373	F (5, 30) = 1.606	0.1887	One-way ANOVA	Tukey	F (5, 30) = 1362	<0.0001
	LPS + MSU + vehicle	6	0.8715	0.2321						
	LPS + MSU + RvD1 1 ng	6	0.8512	0.1609						
	LPS + MSU + RvD1 10 ng	6	0.8978	0.3613						
	LPS + MSU + RvD1 100 ng	6	0.8349	0.1181						
	Triton x-100	6	0.8081	0.0694						
Figure 3C (left)	Saline	6	0.8727	0.2370	F (2, 15) = 1.820	0.1960	One-way ANOVA	Tukey	F (2, 15) = 24.41	<0.0001
	Vehicle + MSU	6	0.8594	0.1871						
	RvD1 + MSU	6	0.9202	0.5068						
Figure 3C (right)	Saline	6	0.9740	0.9183	F (2, 15) = 4.746	0.0253	Kruskal-Wallis	Dunn	11.94	0.0002
	Vehicle + MSU	6	0.8384	0.1265						
	RvD1 + MSU	6	0.9598	0.8181						
Figure 3D	Saline	6	0.8875	0.3054	F (2, 15) = 2.293	0.1353	One-way ANOVA	Tukey	F (2, 15) = 30.84	<0.0001
	Vehicle + MSU	6	0.9211	0.5131						
	RvD1 + MSU	6	0.9049	0.4036						

* Non-detected values.

Table S4. Statistical information from results shown in Figure 4.

Result	Shapiro-Wilk test				Brown-Forsythe		Statistical test	Post-test	F value	P value
	Group	n	W value	P value	F value	P value				
Figure 4B (*Trpv1*)	Saline	6	0.9670	0.8720	F (2,15) = 0.7677	0.4815	One-way ANOVA	Tukey	F (2, 15) = 26.64	<0.0001
	Vehicle + MSU	6	0.9136	0.4608						
	RvD1 + MSU	6	0.8892	0.3138						
Figure 4B (*Nav1.8*)	Saline	6	0.9270	0.5572	F (2, 25) = 06011	0.5609	One-way ANOVA	Tukey	F (2, 15) = 23.41	<0.0001
	Vehicle + MSU	6	0.8844	0.2900						
	RvD1 + MSU	6	0.9831	0.9658						
Figure 4B (*Sub P*)	Saline	6	0.9372	0.6364	F (2, 15) = 1.331	0.2936	One-way ANOVA	Tukey	F (2, 15) = 20.34	<0.0001
	Vehicle + MSU	6	0.8724	0.2360						
	RvD1 + MSU	6	0.8730	0.2383						
Figure 4B (*Calca*)	Saline	6	0.9265	0.5537	F (2, 15) = 3.645	0.0513	One-way ANOVA	Tukey	F (2, 15) = 8.752	0.0030
	Vehicle + MSU	6	0.8878	0.3070						
	RvD1 + MSU	6	0.9179	0.4903						
Figure 4C (left)	Saline	6	0.8426	0.1369	F (2, 15) = 1.279	0.3071	One-way ANOVA	Tukey	F (2, 15) = 14.31	0.0003
	Vehicle + MSU	6	0.9068	0.4157						
	RvD1 + MSU	6	0.9796	0.9498						
Figure 4C (right)	Saline	6	0.9489	0.7310	F (2, 15) = 2.849	0.0894	One-way ANOVA	Tukey	F (2, 15) = 25.43	0.0030
	Vehicle + MSU	6	0.9201	0.5060						
	RvD1 + MSU	6	0.9463	0.7102						
Figure 4D	No stimulus	5	0.8516	0.1996	F (4,20) = 0.4872	0.7450	One-way ANOVA	Tukey	F (4, 20) = 5.371	0.0042
	Vehicle +Caps	5	0.8444	0.1775						
	RvD1 1 ng + Caps	5	0.9013	0.4168						
	RvD1 10 ng + Caps	5	0.9368	0.6436						
	RvD1 100 ng + Caps	5	0.9126	0.4834						
Figure 4E (left)	Saline	6	0.8188	0.0861	F (2,15) = 3.621	0.0521	One-way ANOVA	Tukey	F (2, 15) = 31.92	<0.0001
	Vehicle + MSU	6	0.9499	0.7398						
	RvD1 + MSU	6	0.8946	0.3432						

Figure 4E (right)	Saline	6	0.9430	0.6832	F (2,15) = 0.1099	0.8966	Kruskal-Wallis	Dunn	9.556	0.0036
	Vehicle + MSU	6	0.9081	0.4242						
	RvD1 + MSU	6	0.7797	0.0383						

Table S5. Statistical information from results shown in Figure 5.

Result			Shapiro-Wilk test		Brown-Forsythe		Statistical test	Post test	F value	P value
	Group	n	W value	P value	F value	P value				
Figure 5A	No stimuli	8	Not included*	Not included*	F (3, 28) = 1.175	0.3370	One-way ANOVA	Tukey	F (3, 28) = 61.90	<0.0001
	LPS+ vehicle + MSU	8	0.9761	0.9411						
	LPS+CGRP 10 nM +MSU	8	0.9508	0.7197						
	LPS+CGRP 30 nM +MSU	8	0.9477	0.6882						
	LPS+CGRP 100 nM +MSU	8	0.9807	0.9661						
Figure 5C	P1	8	Not included*	Not included*	F (5, 42) = 2.226	0.0693	One-way ANOVA	Tukey	F (5, 42) = 33.32	<0.0001
	P2	8	0.9120	0.3681						
	P3	8	0.8485	0.0919						
	P4	8	0.9614	0.8236						
	P5	8	0.9638	0.8456						
	P6	8	0.9164	0.4012						
	P7	8	0.9528	0.7391						
Figure 5D	P1	8	Not included*	Not included*	F (3, 28) = 2.752	0.0613	One-way ANOVA	Tukey	F (3, 28) = 60.85	<0.0001
	P2	8	Not included*	Not included*						
	P3	8	0.9245	0.4678						
	P4	8	0.9155	0.3941						
	P5	8	0.9249	0.4709						
	P6	8	0.9249	0.4706						
	P7	8	Not included*	Not included*						

* Non-detected values.

Table S6. Statistical information from results shown in Supplementary Figure S1.

Result		Shapiro-Wilk test			Brown-Forsythe		Statistical test	Post-test	F value	P value
	Group	n	W value	P value	F value	P value				
Figure S1B (left)	Saline	6	0.7979	0.0778	F (3,16) = 0.2926	0.8302	Two-way ANOVA	Tukey	Time x Dose: F (12, 80) = 1.998	=0.0350
	Vehicle + MSU	6	0.9255	0.5662					Time: F (3.379, 67.58) = 0.7484	=0.5417
	RvD1 i.t. + MSU	6	0.8263	0.1305					Dose: F (3, 20) = 95.83	<0.0001
	RvD1 i.p. +MSU	6	0.9102	0.4688					Subject: F (20, 80) = 3.106	=0.0002
Figure S1B (right)	Saline	6	0.8192	0.1151	F (3, 16) = 0.7903	0.5168	Two-way ANOVA	Tukey	Time x Dose: F (12, 80) = 0.2813	=0.9907
	Vehicle + MSU	6	0.9297	0.5945					Time: F (2.016, 40.32) = 0.8449	=0.4378
	RvD1 i.t. + MSU	6	0.8274	0.1329					Dose: F (3, 20) = 40.43	<0.0001
	RvD1 i.p. +MSU	6	0.8948	0.3820					Subject: F (20, 80) = 4.843	<0.0001
Figure S1C (left)	Saline	12	0.8021	0.0099	F (3,44) = 21.05	<0.0001	Kruskal-Wallis	Dunn	34.99	<0.0001
	Vehicle + MSU	12	0.9350	0.4360						
	RvD1 i.t. + MSU	12	0.9359	0.4463						
	RvD1 i.p. +MSU	12	0.8968	0.1441						
Figure S1C (middle)	Saline	12	0.8021	0.0099	F (3, 44) = 21.05	<0.0001	Kruskal-Wallis	Dunn	34.99	<0.0001
	Vehicle + MSU	12	0.9350	0.4360						
	RvD1 i.t. + MSU	12	0.9359	0.4463						
	RvD1 i.p. +MSU	12	0.8968	0.1441						
	Saline	12	0.8021	0.0099		<0.0001		Dunn	34.99	<0.0001

Figure S1C (right)	Vehicle + MSU	12	0.9350	0.4360	F (3,44) = 21.05	Kruskal-Wallis
	RvD1 i.t. + MSU	12	0.9359	0.4463		
	RvD1 i.p. +MSU	12	0.8968	0.1441		

Table S7. Statistical information from results shown in Supplementary Figure S2.

Result		Shapiro-Wilk test			Brown-Forsythe		Statistical test	Post test	F value	P value
	Group	**n**	**W value**	**P value**	**F value**	**P value**				
Figure S2B (left)	Saline	6	0.8992	0.3692	F (3,20) = 0.6037	0.620	Two-way ANOVA	Tukey	Time x Dose: F (15, 100) = 7.303	<0.0001
	Vehicle + MSU	6	0.9303	0.5821					Time: F (5, 100) = 12.88	<0.0001
	RvD1 i.t. + MSU	6	0.9248	0.5406					Dose: F (3, 20) = 241.4	<0.0001
	RvD1 i.p. +MSU	6	0.9337	0.6093					Subject: F (20, 100) = 2.359	=0.0028
Figure S2B (right)	Saline	6	0.8532	0.1670	F (3,20) = 2.202	0.1194	Two-way ANOVA	Tukey	Time x Dose: F (15, 100) = 1.608	=0.0848
	Vehicle + MSU	6	0.8107	0.0732					Time: F (5, 100) = 4.939	=0.0004
	RvD1 i.t. + MSU	6	0.9508	0.7470					Dose: F (3, 20) = 29.73	<0.0001
	RvD1 i.p. +MSU	6	0.8727	0.2373					Subject: F (20, 100) = 2.044	=0.0110

Table S8. Statistical information from results shown in Supplementary Figure S3.

Result			Shapiro-Wilk test		Brown-Forsythe		Statistical test	Post test		P value
	Group		W value	P value	F value	P value				
Figure S2A	Saline	6	0.8850	0.2927	F (3, 20) = 9.083	0.0005	Kruskal-Wallis	Dunn	13.81	0.0032
	Vehicle + MSU	6	0.8771	0.2561						
	RvD1 + MSU	6	0.8827	0.2815						
	Acetaminophen + vehicle	6	0.8282	0.1038						
Figure S2B	Saline	6	0.8772	0.2565	F (3, 20) = 3.279	0.0423	Kruskal-Wallis	Dunn	14.05	0.0028
	Vehicle + MSU	6	0.8609	0.1923						
	RvD1 + MSU	6	0.8912	0.3247						
	Acetaminophen + vehicle	6	0.8712	0.2311						
Figure S2C	Saline	6	0.8835	0.2853	F (3, 20) = 4.534	0.0140	Kruskal-Wallis	Dunn	16.10	0.0011
	Vehicle + MSU	6	0.8590	0.1857						
	RvD1 + MSU	6	0.9428	0.6817						
	Diclofenac + vehicle	6	0.8996	0.3717						
Figure S2D	Saline	6	0.8304	0.1083	F (3, 20) = 4.711	0.0120	Kruskal-Wallis	Dunn	13.38	0.0039
	Vehicle + MSU	6	0.8656	0.2093						
	RvD1 + MSU	6	0.8558	0.1751						
	Diclofenac + vehicle	6	0.8996	0.3717						

Table S9. Summary list of experiments

Experiment	n (animals or biological samples) per experimental group	Method description topic	Figure	Statistical details
Mechanical hyperalgesia (electronic Von Frey)	6	2.4 Evaluation of knee joint mechanical hyperalgesia and oedema	Fig. 1B, C, E, and F (left) Fig. S1 B (left) Fig. S2 B (left)	Table S1 Table S6 Table S7
Knee joint oedema measurement (calliper)	6	2.4 Evaluation of knee joint mechanical hyperalgesia and oedema	Fig. 1B, C, E, and F (right) Fig. S1 B (right) Fig. S2 B (right)	Table S1 Table S6 Table S7
Static weight bearing (SWB)	5	2.5. Static weight bearing (SWB)	Fig. 1G	Table S1
Leukocyte recruitment (knee joint wash)	12	2.6. Leukocyte migration	Fig. 2 B, C Fig. S1 C	Table S2 Table S6
Knee joint IL-1β levels (ELISA)	10	2.12. Cytokine measurement	Fig. 2 D	Table S2
In vitro IL-1β maturation assay	6	2.10. Bone marrow-derived macrophages (BMDM) preparation and IL-1β maturation assay	Fig. 3 B (left)	Table S3
Cell viability (LDH leakage)	6		Fig. 3B (right)	
In vitro pNF-κB and ASC immunofluorescence and colocalization analysis	6	2.7. Immunofluorescence staining	Fig. 3 C, D	
mRNA expression levels (RT-qPCR)	6	2.8. RT-qPCR	Fig. 4 B	Table S4
CGRP and pNF-κB immunofluorescence in the dorsal root ganglia (DRG)	6	2.7. Immunofluorescence staining	Fig. 4 C	
In vitro capsaicin-induced CGRP release	5	2.9. CGRP release	Fig. 4 D	
LysM-eGFP mice knee joint and CGRP immunostaining	6	2.7. Immunofluorescence staining	Fig. 4 E, F	

CGRP effects in IL-1β maturation (ELISA)	8	2.10. Bone marrow-derived macrophages (BMDM) preparation and IL-1β maturation assay	Fig. 5 A	Table S5
Phagocytosis index	8	2.11. Phagocytosis assay	Fig. 5 B, C, E	
RvD1 and CGRP effects in IL-1β maturation (ELISA)	8	2.10. Bone marrow-derived macrophages (BMDM) preparation and IL-1β maturation assay	Fig. 5 B, D	
In vivo RvD1 toxicity (biochemical tests)	6	AST, ALT, Urea, and creatinine levels	Fig. S3	Table S8

Research article – in preparation

3.4 Inhibition of soluble epoxide hydrolase with TPPU ameliorates MSU-induced pain in a mouse model of gouty arthritis

Tiago H. Zaninelli[1], Victor Fattori[1], Telma Saraiva-Santos[1], Mariana M. Bertozzi[1], Marilia F. Manchope[1], Camila R. Ferraz[1], Nayara A. Artero[1], Juliana T. Clemente-Napimoga[2], Rubia Casagrande[3], Marcelo Napimoga[2], Waldiceu A. Verri Jr[1]*

[1]Laboratory of Pain, Inflammation, Neuropathy, and Cancer, Department of Pathology, Center of Biological Sciences, Londrina State University, Londrina, Paraná, Brazil.

[2]Faculdade São Leopoldo Mandic, Instituto de Pesquisas São Leopoldo Mandic, Laboratoy of Neuroimmune Interface of Pain Research, Campinas, São Paulo, Brazil.

[3]Laboratory of Antioxidants and Inflammation, Department of Pharmaceutical Sciences, Center of Health Sciences, Londrina State University, Londrina, Paraná, Brazil.

* Corresponding author.

Present address: Departamento de Ciências Patológicas, Universidade Estadual de Londrina, Rodovia Celso Garcia Cid Km480 PR445, 86057-970, Post-office box 10.011, Londrina, Paraná, Brazil. E-mail address: waverri@uel.br

Abstract

The contemporary understanding of the resolution of inflammation process places lipid mediators as important players in tissue regeneration. During inflammation, the metabolism of aracdonic acid, in a specific enzyme-dependent manner, yield lipoxins, prostaglandins, leukotrienes, and epoxyeicosatrienoic acids (EETs). EETs and specialized pro-resolving mediators (SPMs) are endogenous molecules that exerts anti-inflammatory and analgesic effects. The biological action of EETs, however, is limited due to their rapid metabolism by soluble epoxide hydrolase (sEH). Gouty arthritis is an intermittent inflammatory disease that affects approximately 10% of word population. Gout is characterized by acute flares accompanied joint inflammation and unbearable pain spaced by asymptomatic phases. Available therapies present limited efficacy, undesired side effects, and high costs. Thus, the development of novel therapies is necessary. Therefore, the aim of this study was to investigate the effects of systemic treatment with N-[1-(1-oxopropyl)-4-piperidinyl]-N'-[4-(trifluoromethoxy)phenyl)-urea (TPPU), in a mouse model of MSU-induced gouty arthritis. For that, mice were treated with TPPU per oral gavage (p.o.) 0.5h before and 8h after MSU intra-articular injection in the right knee joint. Knee joint mechanical (electronic version of the von Frey filament) and thermal hyperalgesia (Hargreaves), and edema (caliper) were determined 1, 3, 5, 7, and 15h after stimulus. Changes in rear member weight distribution were assessed by the static weight bearing at 1, 5, and 15 h after MSU injection. IL-1β levels in the knee joint was determined 15 h after gout induction by ELISA. We observed that TPPU treatments at 1 mg/kg (p.o.) 0.5h before and 8h after gout induction reduced mechanical and thermal hyperalgesia, decreased MSU-induced edema, and restored rear limbs weight distribution. Treatments also decreased the levels of IL-1β in the knee joint, a key cytokine in gouty arthritis physiopathology. We provide evidence that systemic TPPU administration produces analgesic effects in a MSU-induced gout model, and therefore it might be an important therapeutic tool towards developing treatments for gouty arthritis pain.

Keywords: epoxyeicosatrienoic acids, soluble epoxide hydrolase, hyperalgesia.

1. Introduction

Gouty arthritis is the most common case of inflammatory arthritis and is considered one of the most painful acute conditions (Ragab et al., 2017). Epidemiologically, the incidence and prevalence of gout have increased numbers in both developed and developing countries affecting approximately 10% of the word population (Kuo et al., 2015; So and Martinon, 2017). Gout is caused by increased levels of uric acid (hyperuricaemia) resulting in the formation and deposition of monosodium urate (MSU) crystal on articular and periarticular tissues (Dalbeth and Haskard, 2005). The recognition of MSU crystals by macrophages evokes neutrophil recruitment (Dinarello, 2009), intense production of pro-inflammatory mediators (McGonagle and McDermott, 2006), and excruciating pain (Faires and Mccarty, 1962). This prototypical inflammatory disease physiopathology lay on NLRP3 inflammasome engagement, activation, and its IL-1β-mediated maturation (Martinon et al., 2006; Amaral et al., 2012). The pro-inflammatory cytokine IL-1β is a key molecule in gout physiopathology (Martinon et al., 2006).

Despite, gouty arthritis is self-limited in human (up to 10 days), if left untreated, the continued MSU deposition can induce joint damage, movement limitation, and increases the probability of acute flares (Schlesinger and Thiele, 2010; So and Martinon, 2017). The management of gout consists in urate-lowering therapies and control of acute flares. Currently, steroidal and non-steroidal anti-inflammatories, colchicine, and biological agents are used in the control of gout flares (So and Martinon, 2017). However, these drugs lack safety for a significant fraction of patients, offer undesirable side effects, present high costs, and offer non-satisfactory analgesic effects for some patients (Rees et al., 2014). Therefore, novel analgesic drugs are still needed to the treatment of gout.

Epoxyeicosatrienoic acids (EETs) are eicosanoids derived from the metabolism of arachidonic acid via enzymes of cytochrome P450, specifically by CYP450-2C and CYP2J (Shi et al., 2022). The metabolism yields four biologically active EET, the 5,6-EET, 8,9-EET, 11,12-EET, and 14,15-EET (Shi et al., 2022) that are rapidly converted in less active dihydroxy-eicosatrienoic acids (DHETs) by soluble epoxide hydrolase (sEH). Therefore, sEH activity is considered one of the main determinants of bioavailable EETs. Compelling evidence has demonstrated that EETs have protective properties, including anti-inflammatory, analgesic, and anti-fibrotic effects (Bystrom et al., 2011; Imig, 2012; Inceoglu et al., 2012; Chen et al., 2015). However, due the rapid metabolism of EETs by sEH, pharmacological approaches with isolated EETs are challenging. Therefore, targeting the inhibition of sEH might be an improved alternative to overcome the endogenous activity of EETs (Wagner et al., 2017). The present study aimed to evaluate the effects of N-[1-(1-oxopropyl)-4-piperidinyl]-N'-[4-(trifluoromethoxy)phenyl)-urea (TPPU), an sEH inhibitor, in MSU-induced acute gouty arthritis in mice.

2. Material and Methods

2.1. Experimental Procedures

Mice were treated with TPPU (0.3, 1, or 3 mg/kg, p.o.) or vehicle (2% DMSO, 20% Tween 80 in saline) 0.5 h before intra-articular injection of MSU (100 μg/10 μL, i.a.). Mechanical hyperalgesia and edema were evaluated 1, 3, 5, 7, and 15 h after MSU stimulus. Based on these results, mice were treated with TPPU (1 mg/kg, p.o. gavage) or vehicle 0.5 h before and 8h after gouty arthritis induction. Mechanical hyperalgesia and edema were evaluated 1, 3, 5, 7, and 15 h after intra-articular stimulus. Based on these results, 1 mg/kg (p.o. gavage) and two treatments (0.5 h before and 8 h after MSU stimulus) were chosen to conduce the following experiments. Heat thermal hyperalgesia was assessed by hot plate and Hargreaves apparatus at 1, 3, 5, 7, and 15 h after MSU intra-articular injection. Rear limb weight distribution was evaluated using Static Weight Bearing at 1, 5, and 15 hours after stimulus.

2.2. Animals

Male Swiss (8 weeks old, 25-30 g) mice from Londrina State University (Londrina, Paraná, Brazil), were used in this study. All mice were housed in standard clear cages with free access to food and water, light/dark cycle of 12/12h and temperature of 21°±1°C. All behavioral testing was performed between 9 a.m. and 5 p.m. in a temperature-controlled room. Animal care and handling procedures were approved by Londrina State University Ethics Committee (process number 2518.2018.40) and were in accordance with the International Association for Study of Pain (IASP) guidelines. All efforts were made to minimize the number of animals used and their suffering.

2.3. Chemicals and Drugs

Materials were obtained from the following sources: Uric acid (Sigma, Saint Louis, Missouri, USA), N-[1-(1-oxopropyl)-4-piperidinyl]-N'-[4-(trifluoromethoxy)phenyl)-urea (TPPU) (Cayman Chemicals, Ann Arbor, Michigan, USA).

2.4. MSU Crystal preparation and Induction of MSU-induced knee inflammation

MSU crystals were prepared as previously described (Nishimura et al., 1997). Briefly, 672 mg of uric acid (cat. sc-213135A, Santa Cruz Biotechnology, Dallas, TX, USA), was dissolved in 200 mL of boiling single distilled water containing 800 mg of NaOH (cat. # 01H1028.01.AH, Labsynth, Diadema, SP, Brazil). The pH was adjusted to 7.2 and the solution was gradually cooled by stirring at room temperature. The crystals were collected by centrifugation (3000g, 2 min at 4ºC). The crystals were evaporated and sterilized by heating at 180 ºC for 2h and stored in a sterile environment until use. The joint inflammation was induced by the intra-articular (i.a.) administration of MSU (100 μg/10 μL) into the right knee joint of mice under isoflurane anesthesia as previously described (Zaninelli et al., 2022). Control animals received an i.a. injection of sterile saline (10μL).

2.5. Evaluation of knee joint hyperalgesia and edema

The mechanical hyperalgesia of femur-tibial joint was evaluated by an electronic von Frey apparatus. Mice were placed in acrylic cages with a wire grid floor, and the stimulations were performed only when the animals were quiet and with the four paws on the grid floor. This method consists of an electronic pressure-meter, with force transducer fitted with polypropylene tip (Insight instruments, Ribeirao Preto, SP, Brazil). To evaluate knee joint pain, it was used a large tip (4.15 mm^2), to exclude subcutaneous effect (Guerrero et al., 2006). An increase perpendicular

force was applied to the central area of the plantar surface of the hind paw to induce flexion of femur-tibial joint followed by hind paw withdrawal. A digital analgesimeter recorded the intensity of the force applied (in grams) when the paw was withdrawal. The test was performed at 1, 3, 5, 7, and 15 h (Zaninelli et al., 2022). The investigators were blinded to the treatment and groups. The results are expressed as withdrawal mechanical threshold in grams.

Keen joint edema was assessed with a dial thickness gauge caliper (Mitutoyo) before (zero time), and after MSU intra-articular injections at 1, 3, 5, 7, and 15 h. The edema was determined for each mouse knee joint by the difference between the times indicated and zero time. The results are expressed as Δmm/joint.

2.6. Static weight bearing (SWB)

Unilateral peripheral inflammation produces changes in weight distribution toward the non-injured paw (Laboureyras et al., 2009). Changes in rear member weight distribution were evaluated using the SWB apparatus (model BIO-SWB-TOUCH-M, Bioseb, France). Mice were habituated for at least four consecutive days prior to the behavioural testing. During the experiment, animals were comfortably maintained in acrylic chamber while the hind paws rest on two individual weight sensor plates (left and right). The animal stands and makes a natural adjustment to the degree of pain by adapting weight distribution on the non-injured rear limb. The measurements were performed before (baseline values), 7 and 15 h after the MSU stimulus. The results are expressed as left/right limb ratio, which was calculated by using the mean of three measurements at 0 (baseline value), 1, 5, and 15 h after MSU injection (Zaninelli et al., 2022).

2.7. Thermal hyperalgesia (hot plate)

Heat thermal hyperalgesia was performed using a hot plate at 52 °C ± 1ºC as previously described (Fattori et al., 2019). The endpoint was characterized by the removal of the paw followed by clear hind paw flinching or licking movements. The reaction time was registered when the following responses were observed jumping, clear paw flinching or paw licking. The results are expressed by withdrawal latency (in seconds) of measurements at 1, 3, 5,7, and 15 h after intra-articular MSU injection. A cut-off of 20 seconds was set to avoid tissue damage. The investigators were blinded to the treatment and experimental groups.

2.8. Thermal hyperalgesia (Hargreaves apparatus)

Mice were allowed to habituate to the apparatus for at least 2h during three consecutive days before the measurements. After habituation, a baseline measurement was obtained. To measure pain sensitivity to a heat stimulus (heat hyperalgesia), mice were placed on a glass plate of a Hargreaves apparatus (Model 390G, IITC Life Science, Woodland Hills, CA, USA). A radiant heat source was used to stimulate the paw by gradually increasing the temperature of the plantar surface. The results are expressed by withdrawal latency (in seconds) of measurements at 1, 3, 5,7, and 15 h after intra-articular MSU injection. In this experiment, the device was set to 30% of radiant heat source intensity and a cut-off time of 15s of exposure to prevent tissue damage. The investigators were blinded to the treatment and experimental groups.

2.9. Cytokine measurement

Knee joint samples were homogenized in 500 μL of buffer containing protease inhibitors. Samples were centrifuged (3000 rpm × 15 min × 4°C). IL-1β levels were determined from the supernatant by enzyme-linked immunosorbent assay (ELISA), using eBioscience kits (Thermo Fisher Scientific, Vienna, Austria). The results are expressed as pictograms (pg) of cytokine per mg of protein.

2.10. Data analysis

Data were analyzed using GraphPad Prism statistical software (GraphPad Software, Inc., USA-500.288, version 8.0). Results are presented as means ±SEM of measurements made on 6 mice/samples per group per experiment and are representative of two independent experiments. Two-way repeated measures ANOVA was used to compare groups and doses at different time points. The analyzed factors were treatments, time, and time versus treatment interaction. Data collected in a single time point, with normal Gaussian distribution and variance homogeneity was analyzed by one-way ANOVA followed by Tukey's test. $P<0.05$ was considered significant.

3. Results

3.1. TPPU decreases MSU-induced mechanical hyperalgesia and edema

We first addressed whether TPPU could reduce MSU-induced mechanical hyperalgesia and edema. MSU injection induced mechanical hyperalgesia (Fig. 1B left) and edema (Fig. 1B right) at all evaluated time points. Treatment with TPPU at 0.3, 1 or 3 mg/kg (p.o.) reduced mechanical hiperalgesia up to 7 and 3 hours after MSU injection, respectively. The dose of 1 mg/kg/p.o. reduced MSU-induced edema at time points of 5, 7 and 15 h after the stimulus (Fig. 1B right). The vehicle (2% DMSO, 20% Tween 80 in saline) showed no effect.

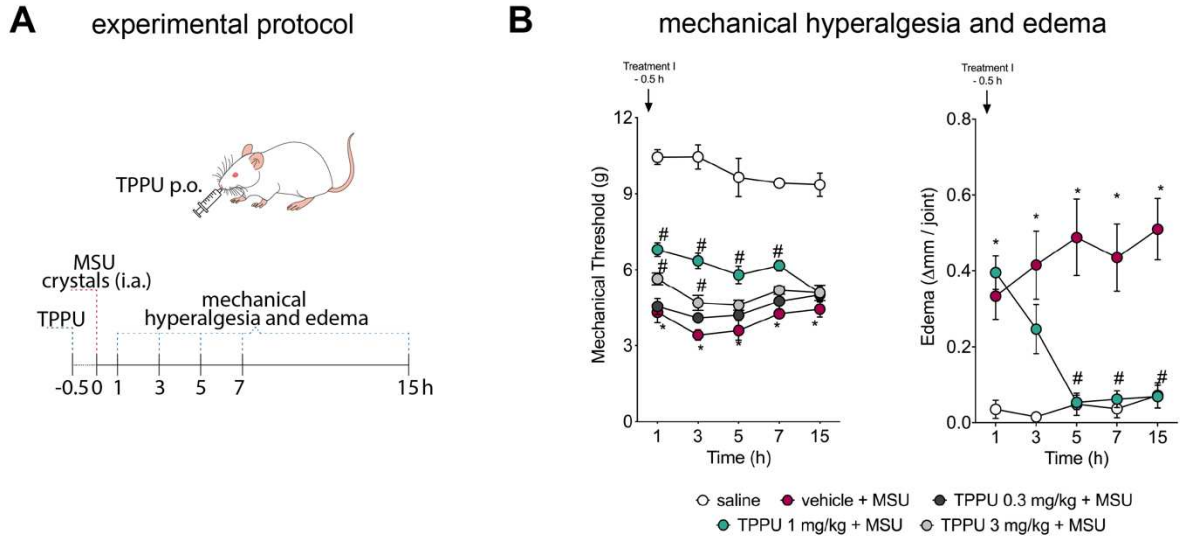

Figure 1. TPPU reduces MSU-induced hyperalgesia and edema. A. scheme of experimental protocol for mechanical hyperalgesia and edema measurements as well as treatment schedule. Mechanical hyperalgesia (B left) and edema (B right) were evaluated 1, 3, 5, 7, and 15h after MSU stimulus (100 μg per knee joint). Results from mechanical hyperalgesia are presented as paw withdrawal threshold (in grams) and for edema as Δ of knee joint size (in mm). Results are

presented as mean ± SEM of measurements, n = 6 mice per group (*P < 0.05 vs. saline, # P < 0.05 vs. vehicle-treated group).

3.2. A second treatment with TPPU prolongs its analgesic effects

Next, we addressed whether a second treatment with TPPU 8 h after the stimulus would prolong or offer additional analgesic effects (Fig. 2A). Thus, mice were treated with TPPU (0.3, 1, or 3 mg/kg/p.o.) 0.5 h before and 8 h after MSU injection. TPPU at 1 mg/kg/p.o. reduced mechanical hiperalgesia (Fig. 2B left) and edema (Fig. 2B right) in all evaluated time points. Therefore 1 mg/kg/p.o. administered 0.5 h before and 8 h after MSU injection was chosen for the following experiments.

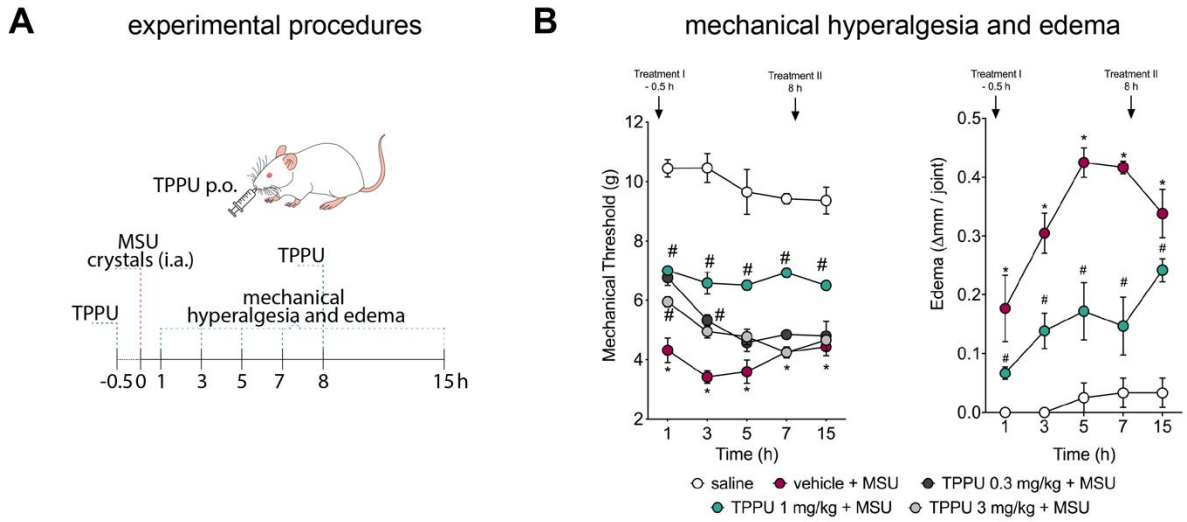

Figure 2. A second treatment with TPPU prolongs its analgesic effects. A. scheme of experimental protocol for mechanical hyperalgesia and edema measurement as well as with the two treatments with TPPU, 0.5h before and 8 h after MSU stimulus. Mechanical hyperalgesia (B left) and edema (B right) were evaluated 1, 3, 5, 7, and 15h after MSU stimulus (100 μg per knee

joint). Results from mechanical hyperalgesia are presented as paw withdrawal threshold (in grams) and for edema as Δ of knee joint size (in mm). Results are presented as mean ± SEM of measurements, n = 6 mice per group (*P < 0.05 vs. saline, # P < 0.05 vs. vehicle-treated group).

3.3. TPPU reduces MSU-induced heat thermal hyperalgesia and restores changes in rear limbs weight distribution

Intra-articular MSU injection induces thermal hyperalgesia (Hoffmeister et al., 2014). Therefore, we next evaluate the effect of TPPU treatments in heat thermal hyperalgesia by hot plate test and Hargreaves apparatus. TPPU reduced heat thermal hyperalgesia in at 3, 5, and 7 h after MSU injection as per hot plate test (Fig. 3B). On the other hand, as observed per Hargreaves apparatus test (Fig. 3C), TPPU treatments reverted MSU-induced thermal hyperalgesia at the time points of 1, 3, 5, and 15 h after the stimulus. In another set of experiments, we determined the effects of TPPU in changes in rear members weight distribution. Vehicle-treated mice dislocated weight distribution towards the no-injured paw, weight on the left paw is higher than in the right paw (Fig. 3D). TPPU treatments restored MSU-induced changes in weight distribution, equalizing the weight equally to both paw (Fig. 3D).

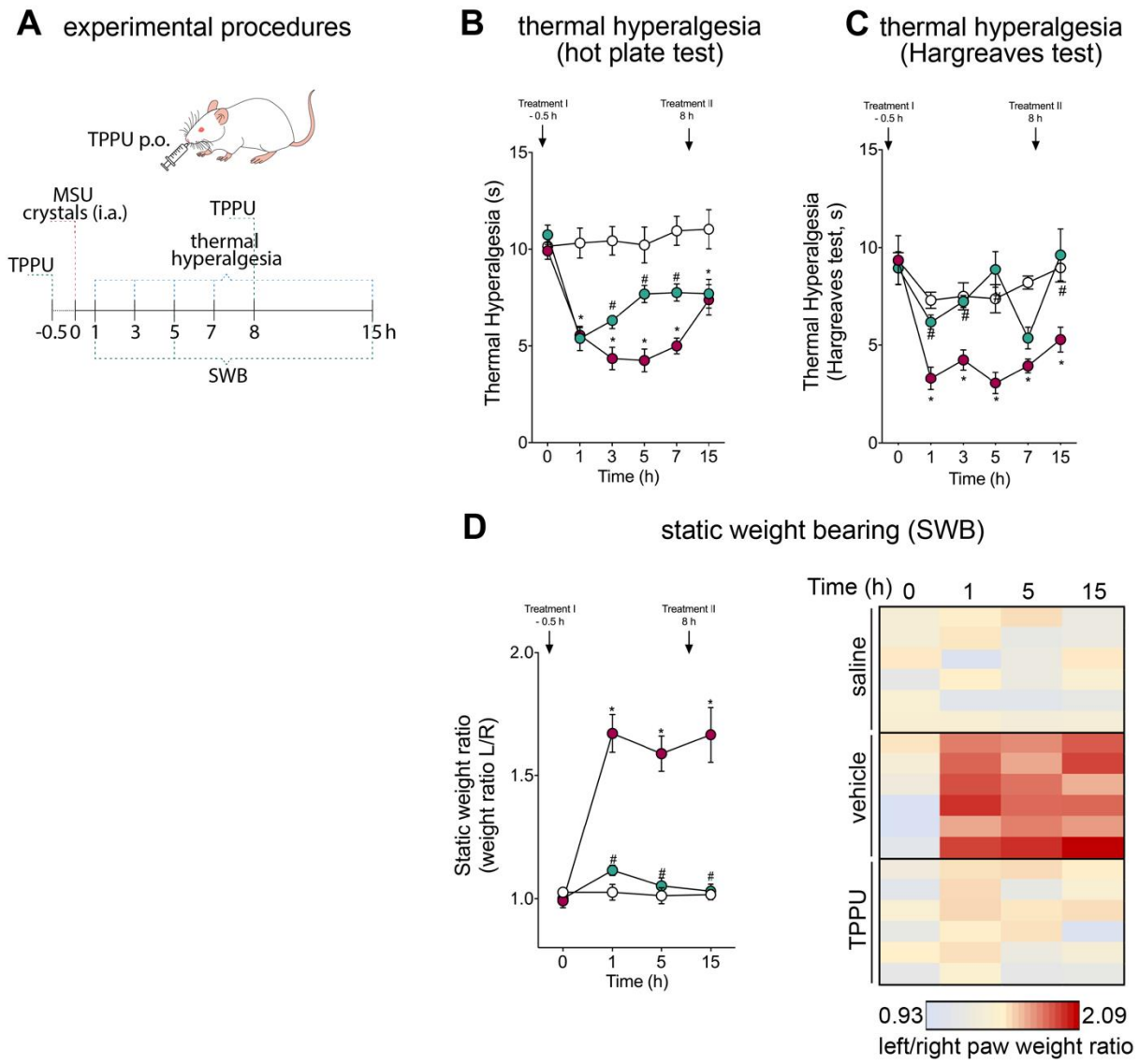

64

65 **Figure 3.** ***TPPU reduces MSU-induced heat thermal hyperalgesia and restores changes in rear***
66 ***limbs weight distribution.*** A. scheme of experimental protocol scheme for thermal hyperalgesia
67 and the static weight bearing as well as treatment schedule. Thermal hyperalgesia by hot plate test
68 (B) and as per Hargreaves test (C) were evaluated 1, 3, 5, 7, and 15h after MSU stimulus (100 µg
69 per knee joint). (D) SWB (Static Weight Bearing) was used as a nonreflexive method of pain
70 measurement and was assessed 1, 5, and 15h after MSU stimulus. Results from thermal
71 hyperalgesia are presented latency in seconds and for SWB as left per right paw weight ratio.

Results are presented as mean ± SEM of measurements, n = 6 mice per group (*P < 0.05 vs. saline, # P < 0.05 vs. vehicle-treated group).

3.4. TPPU reduces knee joint levels of IL-1β

IL-1β is a pivotal cytokine in gouty arthritis pathophysiology (Martinon et al., 2006). In fact, TPPU has been shown to reduce inflammasome assembly and thereby IL-1β production by mouse peritoneal cavity macrophages (Luo et al., 2020). Thus, we next evaluate the effects of TPPU treatments in the levels of IL-1β in the knee joint by ELISA. We observed that TPPU reduced MSU-induced levels of IL-1β (Fig. 4B).

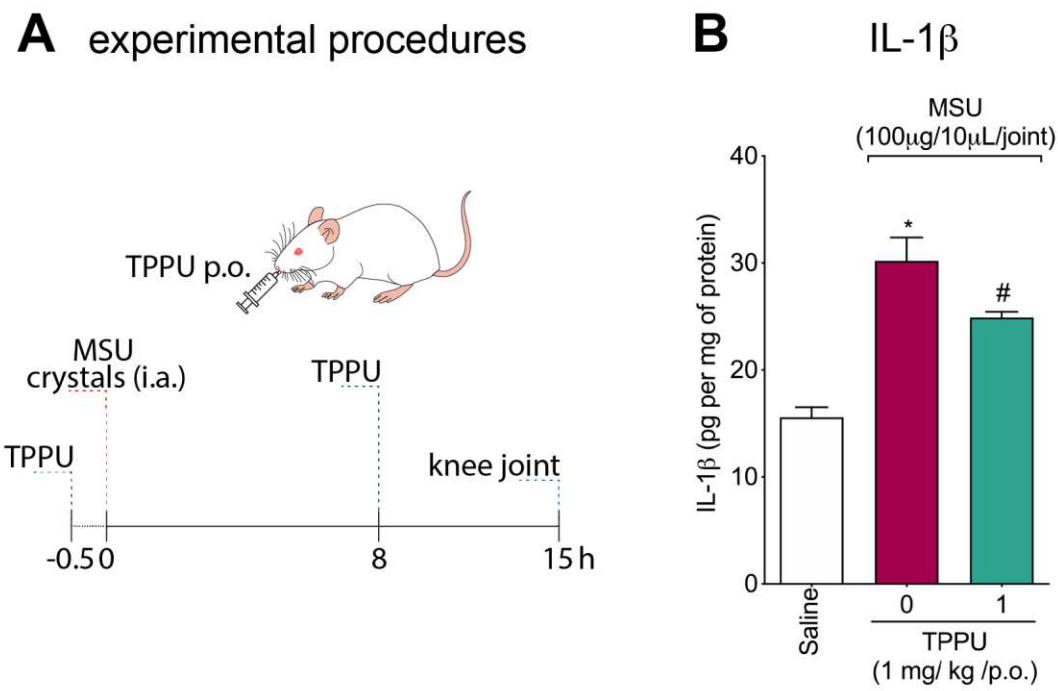

Figure 4. TPPU reduces knee joint levels of IL-1β. A. scheme of experimental protocol for knee joint sampling and IL-1β level determination. (B) Fifteen hours after the stimulus the knee joint tissue was processed and the concentration of IL-1β was determined by ELISA. Results are expressed as picograms per milligram of protein, and are presented as median and range of measurements, n = 8 mice per group per experiment (*P < 0.05 vs. saline, # P < 0.05 vs. vehicle-treated group).

4. Discussion

In this study, we demonstrated that systemic inhibition of soluble epoxide hydrolase (sEH) reduced MSU-induced pain. TPPU treatment reduced mechanical and thermal hyperalgesia, decreased edema, and restored changes in rear member weight distribution. Moreover, TPPU decreases the levels of IL-1β in the knee joint, a pivotal cytokine in this condition.

Currently, the management of gout acute flares consists in the use of NSAIDs, colchicine, glucocorticoids and biological agents (So and Martinon, 2017). However, these drugs must be used with caution in patients with comorbidities (NSAIDs), often causes severe side effects (NSAIDs, colchicine, and corticoids), present high cost (biological agents), or possess non-satisfactory analgesic effects in some patients (Rees et al., 2014). The contemporary understanding of the inflammation resolution shed light in the imperative role of pro-resolutive lipid mediators in the process (Fattori et al., 2020). In fact, endogenous levels of pro-resolutive mediators might be correlated to rheumatic diseases status and symptoms (Zaninelli et al., 2021). Therefore, targeting lipid metabolism in the resolution of inflammation might be an assertive therapeutic approach.

Although aracdonic acid metabolites are remembered for their pro-inflammatory profile, the cytochrome P450 catalyzes the reactions to form EETs, lipid mediators with well described protective effect (Shi et al., 2022) that are also precursors for SPMs synthesis (Schmelzer et al., 2005). However, due to EETs rapid conversion by sHE in less bioactive compounds, the literature on its pharmacological activity is very scarce, at least in the field of rhematic conditions. For instance, although 14,15-EET was demonstrated to inhibit bone resorption and osteoclastogenesis in ovariectomized rat (Guan et al., 2015), however is imperative to consider the activity of sEH and its implication in this scenario. Therefore, the use of sEH inhibitors (sEHi) is a widely explored

approach for arthritis treatment. Herein, we demonstrate that TPPU, an sEHi, diminish MSU-induced mechanical and thermal pain in a mouse model of gout, which corroborate other studies evaluating TPPU pharmacological proprieties in rhematic conditions (Teixeira et al., 2020; Trindade-da-Silva et al., 2020).

In gouty arthritis, the ion channel transient receptor potential cation channel subfamily V member 1 (TRPV1) is upregulated in nociceptor neurons (Xu et al., 2022) and have been described to participate in MSU-induced hyperalgesia and edema (Hoffmeister et al., 2011, 2014). Since thermal hyperalgesia is also a significant complain among patients, we next sought determined whether TPPU would reduce heat thermal hyperalgesia. We observed that treatment with TPPU significatively reduced MSU-induced thermal hyperalgesia. TRPV1 is activated by heat, therefore, while our data suggest that TPPU might modulate TRPV1 expression or activation, it remains to be determined whether this is a direct effect or secondary to the inhibition of inflammation.

The pro-inflammatory cytokine Il-1β is a pivotal molecule in gout pathophysiology (Martinon et al., 2006) and pain signaling (Binshtok et al., 2008). In fact, mice lacking NLPR3 show reduced pain and edema during gout (Amaral et al., 2012). Importantly, both treatment schedules with TPPU reduce MSU-induced IL-1β levels in the knee joint, which contribute to TPPU-induced analgesic effects. Our data corroborates previous research showing that TPPU inhibits IL-1β maturation by blocking NLRP3 inflammasome assembly *in vivo* in a mouse model of LPS-induced lung injury and *in vitro* in mouse peritoneal macrophages (Luo et al., 2020). It is also noteworthy mentioning that TPPU restores MSU-induced changes in rear limbs weight distribution, corroborating the analgesic results obtained by evoked-pain measurements (mechanical and thermal hyperalgesia). Altogether, our findings suggest that TPPU may serve as an important

136 therapeutic tool towards developing novel treatment for gouty arthritis pain and might increase the
137 life quality of affected individuals.
138

Conflict of interest

Authors declare no conflict of interest.

Acknowledgements

This work was supported by Programa para o Sistema Único de Saúde (PPSUS) grant supported by Departamento de Ciência e Tecnologia da Secretaria de Ciência, Tecnologia e Insumos Estratégicos, Ministério da Saúde (Decit/SCTIE/MS, Brazil) intermediated by Conselho Nacional de Desenvolvimento Científico e Tecnológico (CNPq, Brazil) with support of Fundação Araucária and Secretaria Estadual de Saúde, Paraná (SESA-PR, Brazil); São Paulo Research Foundation (FAPESP, Brazil) (#2017-22334-9);Coordenadoria de Aperfeiçoamento de Pessoal de Nível Superior (CAPES, Brazil); and Financiadora de Estudos e Projetos and Secretaria de Estado da Ciência, Tecnologia e Ensino Superior do Paraná under grant agreements 01.12.0294.00 (0476/11) (FINEP/SETI-PR, Brazil).

References

Amaral, F. A., Costa, V. V, Tavares, L. D., Sachs, D., Coelho, F. M., Fagundes, C. T., et al. (2012). NLRP3 inflammasome-mediated neutrophil recruitment and hypernociception depend on leukotriene B(4) in a murine model of gout. *Arthritis Rheum* 64, 474–484. doi:10.1002/art.33355.

Binshtok, A. M., Wang, H., Zimmermann, K., Amaya, F., Vardeh, D., Shi, L., et al. (2008). Nociceptors are interleukin-1beta sensors. *J Neurosci* 28, 14062–14073. doi:10.1523/JNEUROSCI.3795-08.2008.

Bystrom, J., Wray, J. A., Sugden, M. C., Holness, M. J., Swales, K. E., Warner, T. D., et al. (2011). Endogenous epoxygenases are modulators of monocyte/macrophage activity. *PLoS One* 6. doi:10.1371/JOURNAL.PONE.0026591.

Chen, W., Yang, S., Ping, W., Fu, X., Xu, Q., and Wang, J. (2015). CYP2J2 and EETs protect against lung ischemia/reperfusion injury via anti-inflammatory effects in vivo and in vitro. *Cell. Physiol. Biochem.* 35, 2043–2054. doi:10.1159/000374011.

Dalbeth, N., and Haskard, D. O. (2005). Mechanisms of inflammation in gout. *Rheumatol.* 44, 1090–1096. doi:10.1093/rheumatology/keh640.

Dinarello, C. A. (2009). Immunological and inflammatory functions of the interleukin-1 family. *Annu. Rev. Immunol.* 27, 519–550. doi:10.1146/annurev.immunol.021908.132612.

Faires, J. S., and Mccarty, D. J. (1962). ACUTE ARTHRITIS IN MAN AND DOG AFTER INTRASYNOVIAL INJECTION OF SODIUM URATE CRYSTALS. *Lancet* 280, 682–685. doi:10.1016/S0140-6736(62)90501-9.

Fattori, V., Pinho-Ribeiro, F. A., Staurengo-Ferrari, L., Borghi, S. M., Rossaneis, A. C., Casagrande, R., et al. (2019). The specialised pro-resolving lipid mediator maresin 1 reduces inflammatory pain with a long-lasting analgesic effect. *Br J Pharmacol* 176,

1728–1744. doi:10.1111/bph.14647.

Fattori, V., Zaninelli, T. H., Rasquel-Oliveira, F. S., Casagrande, R., and Verri, W. A. (2020). Specialized pro-resolving lipid mediators: A new class of non-immunosuppressive and non-opioid analgesic drugs. *Pharmacol. Res.* 151. doi:10.1016/j.phrs.2019.104549.

Guan, H., Zhao, L., Cao, H., Chen, A., and Xiao, J. (2015). Epoxyeicosanoids suppress osteoclastogenesis and prevent ovariectomy-induced bone loss. *FASEB J.* 29, 1092–1101. doi:10.1096/FJ.14-262055.

Guerrero, A. T., Verri Jr., W. A., Cunha, T. M., Silva, T. A., Rocha, F. A., Ferreira, S. H., et al. (2006). Hypernociception elicited by tibio-tarsal joint flexion in mice: a novel experimental arthritis model for pharmacological screening. *Pharmacol Biochem Behav* 84, 244–251. doi:10.1016/j.pbb.2006.05.008.

Hoffmeister, C., Silva, M. A., Rossato, M. F., Trevisan, G., Oliveira, S. M., Guerra, G. P., et al. (2014). Participation of the TRPV1 receptor in the development of acute gout attacks. *Rheumatol. (United Kingdom)* 53, 240–249. doi:10.1093/rheumatology/ket352.

Hoffmeister, C., Trevisan, G., Rossato, M. F., De Oliveira, S. M., Gomez, M. V., and Ferreira, J. (2011). Role of TRPV1 in nociception and edema induced by monosodium urate crystals in rats. *Pain* 152, 1777–1788. doi:10.1016/j.pain.2011.03.025.

Imig, J. D. (2012). Epoxides and soluble epoxide hydrolase in cardiovascular physiology. *Physiol. Rev.* 92, 101–130. doi:10.1152/PHYSREV.00021.2011.

Inceoglu, B., Wagner, K. M., Yang, J., Bettaieb, A., Schebb, N. H., Hwang, S. H., et al. (2012). Acute augmentation of epoxygenated fatty acid levels rapidly reduces pain-related behavior in a rat model of type I diabetes. *Proc. Natl. Acad. Sci. U. S. A.* 109, 11390–11395. doi:10.1073/PNAS.1208708109/-/DCSUPPLEMENTAL/PNAS.201208708SI.PDF.

Kuo, C. F., Grainge, M. J., Zhang, W., and Doherty, M. (2015). Global epidemiology of gout:

Prevalence, incidence and risk factors. *Nat. Rev. Rheumatol.* 11, 649–662. doi:10.1038/nrrheum.2015.91.

Laboureyras, E., Chateauraynaud, J., Richebé, P., and Simonnet, G. (2009). Long-term pain vulnerability after surgery in rats: Prevention by nefopam, an analgesic with antihyperalgesic properties. *Anesth. Analg.* 109, 623–631. doi:10.1213/ANE.0B013E3181AA956B.

Luo, X. Q., Duan, J. X., Yang, H. H., Zhang, C. Y., Sun, C. C., Guan, X. X., et al. (2020). Epoxyeicosatrienoic acids inhibit the activation of NLRP3 inflammasome in murine macrophages. *J. Cell. Physiol.* 235, 9910–9921. doi:10.1002/JCP.29806.

Martinon, F., Pétrilli, V., Mayor, A., Tardivel, A., and Tschopp, J. (2006). Gout-associated uric acid crystals activate the NALP3 inflammasome. *Nature* 440, 237–241. doi:10.1038/nature04516.

McGonagle, D., and McDermott, M. F. (2006). A proposed classification of the immunological diseases. *PLoS Med.* 3, 1242–1248. doi:10.1371/JOURNAL.PMED.0030297.

Nishimura, A., Akahoshi, T., Takahashi, M., Takagishi, K., Itoman, M., Kondo, H., et al. (1997). Attenuation of monosodium urate crystal-induced arthritis in rabbits by a neutralizing antibody against interleukin-8. *J. Leukoc. Biol.* 62, 444–449. doi:10.1002/jlb.62.4.444.

Ragab, G., Elshahaly, M., and Bardin, T. (2017). Gout: An old disease in new perspective - A review. *J Adv Res* 8, 495–511. doi:10.1016/j.jare.2017.04.008.

Rees, F., Hui, M., and Doherty, M. (2014). Optimizing current treatment of gout. *Nat Rev Rheumatol* 10, 271–283. doi:10.1038/nrrheum.2014.32.

Schlesinger, N., and Thiele, R. G. (2010). The pathogenesis of bone erosions in gouty arthritis. *Ann. Rheum. Dis.* 69, 1907–1912. doi:10.1136/ARD.2010.128454.

Schmelzer, K. R., Kubala, L., Newman, J. W., Kim, I. H., Eiserich, J. P., and Hammock, B. D. (2005). Soluble epoxide hydrolase is a therapeutic target for acute inflammation. *Proc. Natl. Acad. Sci. U. S. A.* 102, 9772–9777. doi:10.1073/PNAS.0503279102.

Shi, Z., He, Z., and Wang, D. W. (2022). CYP450 Epoxygenase Metabolites, Epoxyeicosatrienoic Acids, as Novel Anti-Inflammatory Mediators. *Molecules* 27, 3873. doi:10.3390/MOLECULES27123873.

So, A. K., and Martinon, F. (2017). Inflammation in gout: mechanisms and therapeutic targets. *Nat Rev Rheumatol* 13, 639–647. doi:10.1038/nrrheum.2017.155.

Teixeira, J. M., Abdalla, H. B., Basting, R. T., Hammock, B. D., Napimoga, M. H., and Clemente-Napimoga, J. T. (2020). Peripheral soluble epoxide hydrolase inhibition reduces hypernociception and inflammation in albumin-induced arthritis in temporomandibular joint of rats. *Int. Immunopharmacol.* 87. doi:10.1016/J.INTIMP.2020.106841.

Trindade-da-Silva, C. A., Clemente-Napimoga, J. T., Abdalla, H. B., Rosa, S. M., Ueira-Vieira, C., Morisseau, C., et al. (2020). Soluble epoxide hydrolase inhibitor, TPPU, increases regulatory T cells pathway in an arthritis model. *FASEB J.* 34, 9074–9086. doi:10.1096/FJ.202000415R.

Wagner, K. M., McReynolds, C. B., Schmidt, W. K., and Hammock, B. D. (2017). Soluble epoxide hydrolase as a therapeutic target for pain, inflammatory and neurodegenerative diseases. *Pharmacol. Ther.* 180, 62–76. doi:10.1016/J.PHARMTHERA.2017.06.006.

Xu, X., Yuan, Z., Zhang, S., Li, G., and Zhang, G. (2022). Regulation of TRPV1 channel in monosodium urate-induced gouty arthritis in mice. *Inflamm. Res.* 71, 485–495. doi:10.1007/S00011-022-01561-7.

Zaninelli, T. H., Fattori, V., Saraiva-Santos, T., Badaro-Garcia, S., Staurengo-Ferrari, L., Andrade, K. C., et al. (2022). RvD1 disrupts nociceptor neuron and macrophage

activation and neuroimmune communication, reducing pain and inflammation in gouty arthritis in mice. *Br. J. Pharmacol.* doi:10.1111/BPH.15897.

Zaninelli, T. H., Fattori, V., and Verri, W. A. J. (2021). Harnessing Inflammation Resolution in Arthritis: Current Understanding of Specialized Pro-resolving Lipid Mediators' Contribution to Arthritis Physiopathology and Future Perspectives. *Front. Physiol.* 0, 1444. doi:10.3389/FPHYS.2021.729134.

4 CONSIDERAÇÕES FINAIS

No presente trabalho foi demonstrado que o processo de resolução da inflamação está intimamente ligado aos sinais e sintomas de doenças reumáticas. Além disso, explorar esse sistema pode ser uma alternativa terapêutica para doenças de caráter inflamatório. Neste sentido, foi demonstrado que o SPM RvD1, e o sEHi TPPU apresentam efeitos analgésicos em um modelo de artrite gotosa induzido por cristais de MSU em camundongo. Especificamente referente ao item 3.2 desta tese, RvD1 reduz os sinais clínicos da AG, através da redução da hiperalgesia mecânica, edema, e recrutamento de leucócitos totais para a articulação do joelho. RvD1 também reduz a liberação de IL-1β, uma citocina chave na fisiopatologia da doença. Importantemente, esses efeitos foram observados através do tratamento sistêmico (intraperitoneal) ou via intratecal (i.t.). Portando, sugerindo um possível efeito da RvD1 em neurônios nociceptores e a existência de um eixo neuroimune na AG. De fato, o presente trabalho demonstrou que a RvD1 inibe a ativação de neurônios nociceptores e reduz a liberação de CGRP *in vitro* e *in vitro*. Além disso, foi estabelecido pela primeira vez que o CGRP aumenta a fagocitose de cristais de MSU e a liberação de IL-1β em cultura de macrófagos, fenômenos que são reduzidos com o tratamento com a RvD1. Portanto nesse artigo concluímos não apenas os efeitos analgésico e anti-inflamatórios da RvD1, mas também estabelecemos um novo alvo terapêutico sobre a participação do CGRP na fisiopatologia da AG. No segundo artigo de pesquisa (item 3.3), foi demonstrado que o sEHi TPPU também apresenta efeitos analgésicos e anti-inflamatórios, reduzindo a hiperalgesia mecânica, térmica e o edema, além de reduzir a produção de IL-1β no tecido articular. Em conclusão, neste trabalho demonstramos o papel analgésico de duas moléculas explorando a terapêutica da resolução do processo inflamatório. Além disso, também desvendamos um eixo de comunicação neuroimune na artrite gotosa, contribuindo para a compreensão de novos mecanismos fisiopatológicos da doença e estabelecendo novos alvos terapêuticos.

REFERÊNCIAS DA REVISÃO DA LITERATURA

AMARAL, F. A. et al. NLRP3 Inflammasome-Mediated Neutrophil Recruitment and Hypernociception Depend on Leukotriene B(4) in a Murine Model of Gout. **Arthritis Rheum**, v. 64, n. 2, p. 474–484, 2012. Disponível em: <http://www.ncbi.nlm.nih.gov/pubmed/21952942>.

AN, G. et al. Target-Mediated Drug Disposition-A Class Effect of Soluble Epoxide Hydrolase Inhibitors. **Journal of clinical pharmacology**, v. 61, n. 4, p. 531–537, 1 Apr. 2021. Disponível em: <https://pubmed.ncbi.nlm.nih.gov/33078430/>. Acesso em: 1 nov. 2022.

AN, L. L. et al. Complement C5a Potentiates Uric Acid Crystal-Induced IL-1β Production. **European journal of immunology**, v. 44, n. 12, p. 3669–3679, 1 Dec. 2014. Disponível em: <https://pubmed.ncbi.nlm.nih.gov/25229885/>. Acesso em: 30 oct. 2022.

AURSNES, M. et al. Synthesis of the 16S,17S-Epoxyprotectin Intermediate in the Biosynthesis of Protectins by Human Macrophages. **Journal of natural products**, v. 78, n. 12, p. 2924–2931, 24 Dec. 2015. Disponível em: <https://pubmed.ncbi.nlm.nih.gov/26580578/>. Acesso em: 31 oct. 2022.

BANG, S. et al. Resolvin D1 Attenuates Activation of Sensory Transient Receptor Potential Channels Leading to Multiple Anti-Nociception. **Br J Pharmacol**, v. 161, n. 3, p. 707–720, 2010. Disponível em: <http://www.ncbi.nlm.nih.gov/pubmed/20880407>.

BASBAUM, A. I. et al. Cellular and Molecular Mechanisms of Pain. **Cell**, v. 139, n. 2, p. 267–284, 2009. Disponível em: <http://www.ncbi.nlm.nih.gov/pubmed/19837031>.

BERSELLINI FARINOTTI, A. et al. Cartilage-Binding Antibodies Induce Pain through Immune Complex-Mediated Activation of Neurons. **J Exp Med**, v. 216, n. 8, p. 1904–

1924, 2019. Disponível em: <http://www.ncbi.nlm.nih.gov/pubmed/31196979>.

BLAKE, K. J. et al. Staphylococcus Aureus Produces Pain through Pore-Forming Toxins and Neuronal TRPV1 That Is Silenced by QX-314. **Nat Commun**, v. 9, n. 1, p. 37, 2018. Disponível em: <http://www.ncbi.nlm.nih.gov/pubmed/29295977>.

BRANDOLINI, L. et al. Paclitaxel Binds and Activates C5aR1: A New Potential Therapeutic Target for the Prevention of Chemotherapy-Induced Peripheral Neuropathy and Hypersensitivity Reactions. **Cell death & disease**, v. 13, n. 5, 1 May 2022. Disponível em: <https://pubmed.ncbi.nlm.nih.gov/35614037/>. Acesso em: 28 oct. 2022.

BRAZ, J. et al. Transmitting Pain and Itch Messages: A Contemporary View of the Spinal Cord Circuits That Generate Gate Control. **Neuron**, v. 82, n. 3, p. 522–536, 7 May 2014. Disponível em: <https://pubmed.ncbi.nlm.nih.gov/24811377/>. Acesso em: 27 oct. 2022.

BUCKLEY, C. D.; GILROY, D. W.; SERHAN, C. N. **Proresolving lipid mediators and mechanisms in the resolution of acute inflammationImmunity**, 2014. .

BUSHNELL, M. C.; ČEKO, M.; LOW, L. A. Cognitive and Emotional Control of Pain and Its Disruption in Chronic Pain. **Nature reviews. Neuroscience**, v. 14, n. 7, p. 502–511, Jul. 2013. Disponível em: <https://pubmed.ncbi.nlm.nih.gov/23719569/>. Acesso em: 27 oct. 2022.

CALATI, R. et al. The Impact of Physical Pain on Suicidal Thoughts and Behaviors: Meta-Analyses. **J Psychiatr Res**, v. 71, p. 16–32, 1 Dec. 2015. Disponível em: <http://www.ncbi.nlm.nih.gov/pubmed/26522868>. Acesso em: 23 mar. 2021.

CAMPBELL, J. J.; FOXMAN, E. F.; BUTCHER, E. C. Chemoattractant Receptor Cross Talk as a Regulatory Mechanism in Leukocyte Adhesion and Migration. **Eur J Immunol**, v. 27, n. 10, p. 2571–2578, 1997. Disponível em:

1 <http://www.ncbi.nlm.nih.gov/pubmed/9368612>.
2 CHIAMVIMONVAT, N. et al. The Soluble Epoxide Hydrolase as a Pharmaceutical
3 Target for Hypertension. **Journal of cardiovascular pharmacology**, v. 50, n. 3, p.
4 225–237, Sep. 2007. Disponível em: <https://pubmed.ncbi.nlm.nih.gov/17878749/>.
5 Acesso em: 1 nov. 2022.
6 CHIANG, N. et al. Resolvin T-Series Reduce Neutrophil Extracellular Traps. **Blood**,
7 v. 139, n. 8, p. 1222–1233, 24 Feb. 2022. Disponível em:
8 <https://pubmed.ncbi.nlm.nih.gov/34814186/>. Acesso em: 30 oct. 2022.
9 CHIANG, N.; SERHA, C. N. Specialized Pro-Resolving Mediator Network: An Update
10 on Production and Actions. **Essays in biochemistry**, v. 64, n. 3, p. 443–462, 2020.
11 Disponível em: <https://pubmed.ncbi.nlm.nih.gov/32885825/>. Acesso em: 31 jan.
12 2022.
13 CHIU, I. M. et al. Bacteria Activate Sensory Neurons That Modulate Pain and
14 Inflammation. **Nature**, v. 501, n. 7465, p. 52–57, 2013.
15 COHEN, J. A. et al. Cutaneous TRPV1(+) Neurons Trigger Protective Innate Type 17
16 Anticipatory Immunity. **Cell**, v. 178, n. 4, p. 919- 932 e14, 2019. Disponível em:
17 <http://www.ncbi.nlm.nih.gov/pubmed/31353219>.
18 CUNHA, F. Q.; FERREIRA, S. H. The Release of a Neutrophil Chemotactic Factor
19 from Peritoneal Macrophages by Endotoxin: Inhibition by Glucocorticoids. **Eur J**
20 **Pharmacol**, v. 129, n. 1–2, p. 65–76, 1986. Disponível em:
21 <http://www.ncbi.nlm.nih.gov/pubmed/2429849>.
22 CUNHA, T. M. et al. A Cascade of Cytokines Mediates Mechanical Inflammatory
23 Hypernociception in Mice. **Proc Natl Acad Sci U S A**, v. 102, n. 5, p. 1755–1760,
24 2005. Disponível em: <http://www.ncbi.nlm.nih.gov/pubmed/15665080>.
25 CUNHA, T. M. et al. Crucial Role of Neutrophils in the Development of Mechanical

Inflammatory Hypernociception. **J Leukoc Biol**, v. 83, n. 4, p. 824–832, 2008. Disponível em: <http://www.ncbi.nlm.nih.gov/pubmed/18203872>.

DALBETH, N.; HASKARD, D. O. Mechanisms of Inflammation in Gout. **Rheumatology (Oxford)**, v. 44, n. 9, p. 1090–1096, 2005. Disponível em: <https://www.ncbi.nlm.nih.gov/pubmed/15956094>.

DINARELLO, C. A. **Immunological and inflammatory functions of the interleukin-1 familyAnnual Review of Immunology**Annu Rev Immunol, , 2009. . Disponível em: <https://pubmed.ncbi.nlm.nih.gov/19302047/>. Acesso em: 16 apr. 2021.

DUEWELL, P. et al. NLRP3 Inflammasomes Are Required for Atherogenesis and Activated by Cholesterol Crystals. **Nature**, v. 464, n. 7293, p. 1357–1361, 29 Apr. 2010. Disponível em: <https://pubmed.ncbi.nlm.nih.gov/20428172/>. Acesso em: 30 oct. 2022.

DUFFIELD, J. S. et al. Resolvin D Series and Protectin D1 Mitigate Acute Kidney Injury. **J Immunol**, v. 177, n. 9, p. 5902–5911, 2006. Disponível em: <http://www.ncbi.nlm.nih.gov/pubmed/17056514>.

FAIRES, J. S.; MCCARTY, D. J. ACUTE ARTHRITIS IN MAN AND DOG AFTER INTRASYNOVIAL INJECTION OF SODIUM URATE CRYSTALS. **The Lancet**, v. 280, n. 7258, p. 682–685, 6 Oct. 1962. Disponível em: <http://www.thelancet.com/article/S0140673662905019/fulltext>. Acesso em: 16 apr. 2021.

FATTORI, V. et al. The Specialized Pro-Resolving Lipid Mediator Maresin-1 Reduces Inflammatory Pain with a Long-Lasting Analgesic Effect. **British journal of pharmacology**, 2018.

FATTORI, V. et al. The Specialised Pro-Resolving Lipid Mediator Maresin 1 Reduces

Inflammatory Pain with a Long-Lasting Analgesic Effect. **Br J Pharmacol**, v. 176, n. 11, p. 1728–1744, Jun. 2019. Disponível em: <https://pubmed.ncbi.nlm.nih.gov/30830967/>.

FATTORI, V. et al. Specialized pro-resolving lipid mediators: A new class of non-immunosuppressive and non-opioid analgesic drugs. . 1 Jan. 2020.

FATTORI, V. et al. Resolving Neuroinflammation and Pain with Maresin 1, a Specialized pro-Resolving Lipid Mediator. **Treatments, Mechanisms, and Adverse Reactions of Anesthetics and Analgesics**, p. 431–441, 1 Jan. 2022.

FATTORI, V.; AMARAL, F. A.; VERRI JR., W. A. Neutrophils and Arthritis: Role in Disease and Pharmacological Perspectives. **Pharmacol Res**, v. 112, p. 84–98, 2016. Disponível em: <http://www.ncbi.nlm.nih.gov/pubmed/26826283>.

FERREIRA, S. H.; ROMITELLI, M.; DE NUCCI, G. Endothelin-1 Participation in Overt and Inflammatory Pain. **Journal of cardiovascular pharmacology**, v. 13 Suppl 5, p. S220–S222, 1989. Disponível em: <https://pubmed.ncbi.nlm.nih.gov/2473319/>. Acesso em: 27 oct. 2022.

FOXMAN, E. F.; CAMPBELL, J. J.; BUTCHER, E. C. Multistep Navigation and the Combinatorial Control of Leukocyte Chemotaxis. **The Journal of cell biology**, v. 139, n. 5, p. 1349–1360, 1 Dec. 1997. Disponível em: <https://pubmed.ncbi.nlm.nih.gov/9382879/>. Acesso em: 27 oct. 2022.

GILBERT, K. et al. Resolvin D1 Reduces Infarct Size Through a Phosphoinositide 3-Kinase/Protein Kinase B Mechanism. **Journal of Cardiovascular Pharmacology**, v. 66, n. 1, p. 72–79, 23 Jul. 2015. Disponível em: <https://pubmed.ncbi.nlm.nih.gov/25806690/>. Acesso em: 16 apr. 2021.

GUAN, H. et al. Epoxyeicosanoids Suppress Osteoclastogenesis and Prevent Ovariectomy-Induced Bone Loss. **FASEB journal : official publication of the**

Federation of American Societies for Experimental Biology, v. 29, n. 3, p. 1092–1101, 1 Mar. 2015. Disponível em: <https://pubmed.ncbi.nlm.nih.gov/25466887/>. Acesso em: 29 aug. 2022.

GUERRERO, A. T. G. et al. Involvement of LTB4 in Zymosan-Induced Joint Nociception in Mice: Participation of Neutrophils and PGE2. **Journal of leukocyte biology**, v. 83, n. 1, p. 122–130, Jan. 2008. Disponível em: <https://pubmed.ncbi.nlm.nih.gov/17913976/>. Acesso em: 23 nov. 2021.

HAEGGSTRÖM, J. Z. et al. Advances in Eicosanoid Research, Novel Therapeutic Implications. **Biochemical and biophysical research communications**, v. 396, n. 1, p. 135–139, 21 May 2010. Disponível em: <https://pubmed.ncbi.nlm.nih.gov/20494126/>. Acesso em: 1 nov. 2022.

HE, Y. et al. NEK7 Is an Essential Mediator of NLRP3 Activation Downstream of Potassium Efflux. **Nature**, v. 530, n. 7590, p. 354–357, 18 Feb. 2016. Disponível em: <https://pubmed.ncbi.nlm.nih.gov/26814970/>. Acesso em: 30 oct. 2022.

HERNANZ, A. et al. Calcitonin Gene-Related Peptide II, Substance p and Vasoactive Intestinal Peptide in Plasma and Synovial Fluid from Patients with Inflammatory Joint Disease. **Rheumatology**, v. 32, n. 1, p. 31–35, Jan. 1993. Disponível em: <https://pubmed.ncbi.nlm.nih.gov/7678534/>. Acesso em: 16 apr. 2021.

HOLZINGER, D. et al. Myeloid-Related Proteins 8 and 14 Contribute to Monosodium Urate Monohydrate Crystal-Induced Inflammation in Gout. **Arthritis & rheumatology (Hoboken, N.J.)**, v. 66, n. 5, p. 1327–1339, 2014. Disponível em: <https://pubmed.ncbi.nlm.nih.gov/24470119/>. Acesso em: 30 oct. 2022.

HONG, S. et al. Novel Docosatrienes and 17S-Resolvins Generated from Docosahexaenoic Acid in Murine Brain, Human Blood, and Glial Cells: Autacoids in Anti-Inflammation. **Journal of Biological Chemistry**, v. 278, n. 17, p. 14677–14687,

2003.

HUANG, L. et al. Enduring Prevention and Transient Reduction of Postoperative Pain by Intrathecal Resolvin D1. **Pain**, v. 152, n. 3, p. 557–565, 2011. Disponível em: <http://www.ncbi.nlm.nih.gov/pubmed/21255928>.

HUNTER, J. A Treatise on the Blood, Inflammation, and Gun-Shot Wounds. 1794. **Clinical orthopaedics and related research**, v. 458, p. 27–34, May 2007.

IMIG, J. D. Epoxides and Soluble Epoxide Hydrolase in Cardiovascular Physiology. **Physiological reviews**, v. 92, n. 1, p. 101–130, Jan. 2012. Disponível em: <https://pubmed.ncbi.nlm.nih.gov/22298653/>. Acesso em: 29 aug. 2022.

INCEOGLU, B. et al. Endoplasmic Reticulum Stress in the Peripheral Nervous System Is a Significant Driver of Neuropathic Pain. **Proceedings of the National Academy of Sciences of the United States of America**, v. 112, n. 29, p. 9082–9087, 21 Jul. 2015. Disponível em: <https://pubmed.ncbi.nlm.nih.gov/26150506/>. Acesso em: 1 nov. 2022.

IWASAKI, A.; MEDZHITOV, R. Regulation of Adaptive Immunity by the Innate Immune System. **Science**, v. 327, n. 5963, p. 291–295, 2010. Disponível em: <http://www.ncbi.nlm.nih.gov/pubmed/20075244>.

JONSSON, H.; ALLEN, P.; PENG, S. L. Inflammatory Arthritis Requires Foxo3a to Prevent Fas Ligand-Induced Neutrophil Apoptosis. **Nat Med**, v. 11, n. 6, p. 666–671, 2005. Disponível em: <http://www.ncbi.nlm.nih.gov/pubmed/15895074>.

JOOSTEN, L. A. B. et al. Engagement of Fatty Acids with Toll-like Receptor 2 Drives Interleukin-1β Production via the ASC/Caspase 1 Pathway in Monosodium Urate Monohydrate Crystal-Induced Gouty Arthritis. **Arthritis and rheumatism**, v. 62, n. 11, p. 3237–3248, Nov. 2010. Disponível em: <https://pubmed.ncbi.nlm.nih.gov/20662061/>. Acesso em: 30 oct. 2022.

KHAMENEH, H. J. et al. C5a Regulates IL-1β Production and Leukocyte Recruitment in a Murine Model of Monosodium Urate Crystal-Induced Peritonitis. **Frontiers in pharmacology**, v. 8, n. JAN, 23 Jan. 2017. Disponível em: <https://pubmed.ncbi.nlm.nih.gov/28167912/>. Acesso em: 30 oct. 2022.

KUO, C. F. et al. **Global epidemiology of gout: Prevalence, incidence and risk factorsNature Reviews Rheumatology**Nature Publishing Group, , 1 Nov. 2015. . Disponível em: <https://pubmed.ncbi.nlm.nih.gov/26150127/>. Acesso em: 10 apr. 2021.

LAI, N. Y. et al. Gut-Innervating Nociceptor Neurons Regulate Peyer's Patch Microfold Cells and SFB Levels to Mediate Salmonella Host Defense. **Cell**, 2019. Disponível em: <http://www.ncbi.nlm.nih.gov/pubmed/31813624>.

LAI, N. Y. et al. Gut-Innervating Nociceptor Neurons Regulate Peyer's Patch Microfold Cells and SFB Levels to Mediate Salmonella Host Defense. **Cell**, v. 180, n. 1, p. 33-- 49.e22, Jan. 2020. Disponível em: <https://linkinghub.elsevier.com/retrieve/pii/S009286741931270X>.

LAWRENCE, T.; WILLOUGHBY, D. A.; GILROY, D. W. Anti-Inflammatory Lipid Mediators and Insights into the Resolution of Inflammation. **Nat Rev Immunol**, v. 2, n. 10, p. 787–795, 2002. Disponível em: <http://www.ncbi.nlm.nih.gov/pubmed/12360216>.

LEE, C. H. Resolvins as New Fascinating Drug Candidates for Inflammatory Diseases. **Arch Pharm Res**, v. 35, n. 1, p. 3–7, Jan. 2012. Disponível em: <https://pubmed.ncbi.nlm.nih.gov/22297737/>. Acesso em: 23 mar. 2021.

LEVY, B. D. et al. Lipid Mediator Class Switching during Acute Inflammation: Signals in Resolution. **Nat Immunol**, v. 2, n. 7, p. 612–619, 2001. Disponível em: <http://www.ncbi.nlm.nih.gov/pubmed/11429545>.

LIAO, Z. et al. Resolvin D1 Attenuates Inflammation in Lipopolysaccharide-Induced Acute Lung Injury through a Process Involving the PPARγ/NF-KB Pathway. **Respiratory research**, v. 13, n. 1, p. 110, 2 Dec. 2012. Disponível em: <https://pubmed.ncbi.nlm.nih.gov/23199346/>. Acesso em: 16 apr. 2021.

LIU-BRYAN, R. et al. Innate Immunity Conferred by Toll-like Receptors 2 and 4 and Myeloid Differentiation Factor 88 Expression Is Pivotal to Monosodium Urate Monohydrate Crystal-Induced Inflammation. **Arthritis and rheumatism**, v. 52, n. 9, p. 2936–2946, 2005. Disponível em: <https://pubmed.ncbi.nlm.nih.gov/16142712/>. Acesso em: 30 oct. 2022.

LIU, T. et al. Toll-like Receptor 7 Mediates Pruritus. **Nat Neurosci**, v. 13, n. 12, p. 1460–1462, 2010. Disponível em: <http://www.ncbi.nlm.nih.gov/pubmed/21037581>.

LUO, X. Q. et al. Epoxyeicosatrienoic Acids Inhibit the Activation of NLRP3 Inflammasome in Murine Macrophages. **Journal of cellular physiology**, v. 235, n. 12, p. 9910–9921, 1 Dec. 2020. Disponível em: <https://pubmed.ncbi.nlm.nih.gov/32452554/>. Acesso em: 30 aug. 2022.

MADERNA, P.; GODSON, C. Lipoxins: Resolutionary Road. **Br J Pharmacol**, v. 158, n. 4, p. 947–959, 2009. Disponível em: <http://www.ncbi.nlm.nih.gov/pubmed/19785661>.

MARNETT, L. J. The COXIB Experience: A Look in the Rearview Mirror. **Annual review of pharmacology and toxicology**, v. 49, p. 265–290, 2009. Disponível em: <https://pubmed.ncbi.nlm.nih.gov/18851701/>. Acesso em: 1 nov. 2022.

MARTINON, F. et al. Gout-Associated Uric Acid Crystals Activate the NALP3 Inflammasome. **Nature**, v. 440, n. 7081, p. 237–241, 9 Mar. 2006. Disponível em: <https://pubmed.ncbi.nlm.nih.gov/16407889/>. Acesso em: 1 apr. 2021.

MARUYAMA, K. et al. Nociceptors Boost the Resolution of Fungal

Osteoinflammation via the TRP Channel-CGRP-Jdp2 Axis. **Cell Rep**, v. 19, n. 13, p. 2730–2742, 2017. Disponível em: <http://www.ncbi.nlm.nih.gov/pubmed/28658621>.

MCDONALD, B. et al. Intravascular Neutrophil Extracellular Traps Capture Bacteria from the Bloodstream during Sepsis. **Cell Host Microbe**, v. 12, n. 3, p. 324–333, 2012. Disponível em: <http://www.ncbi.nlm.nih.gov/pubmed/22980329>.

MCQUALTER, J. L. et al. Evidence of an Epithelial Stem/Progenitor Cell Hierarchy in the Adult Mouse Lung. **Proceedings of the National Academy of Sciences of the United States of America**, v. 107, n. 4, p. 1414–1419, 26 Jan. 2010. Disponível em: <https://pubmed.ncbi.nlm.nih.gov/20080639/>. Acesso em: 1 nov. 2022.

MEDZHITOV, R. Origin and Physiological Roles of Inflammation. **Nature**, v. 454, n. 7203, p. 428–435, 24 Jul. 2008. Disponível em: <https://pubmed.ncbi.nlm.nih.gov/18650913/>. Acesso em: 27 oct. 2022.

MITROULIS, I. et al. Neutrophil Extracellular Trap Formation Is Associated with IL-1beta and Autophagy-Related Signaling in Gout. **PLoS One**, v. 6, n. 12, p. e29318–e29318, 2011. Disponível em: <http://www.ncbi.nlm.nih.gov/pubmed/22195044>.

MITROULIS, I.; KAMBAS, K.; RITIS, K. Neutrophils, IL-1beta, and Gout: Is There a Link? **Semin Immunopathol**, v. 35, n. 4, p. 501–512, 2013. Disponível em: <http://www.ncbi.nlm.nih.gov/pubmed/23344781>.

MOAYEDI, M.; DAVIS, K. D. Theories of Pain: From Specificity to Gate Control. **J Neurophysiol**, v. 109, n. 1, p. 5–12, 2013. Disponível em: <http://www.ncbi.nlm.nih.gov/pubmed/23034364>.

MOGIL, J. S.; YU, L.; BASBAUM, A. I. Pain Genes?: Natural Variation and Transgenic Mutants. **Annu Rev Neurosci**, v. 23, p. 777–811, 2000. Disponível em: <http://www.ncbi.nlm.nih.gov/pubmed/10845081>.

NODE, K. et al. Anti-Inflammatory Properties of Cytochrome P450 Epoxygenase-

Derived Eicosanoids. **Science (New York, N.Y.)**, v. 285, n. 5431, p. 1276–1279, 20 Aug. 1999. Disponível em: <https://pubmed.ncbi.nlm.nih.gov/10455056/>. Acesso em: 1 nov. 2022.

NORLING, L. V.; PERRETTI, M. The Role of Omega-3 Derived Resolvins in Arthritis. **Curr Opin Pharmacol**, v. 13, n. 3, p. 476–481, Jun. 2013. Disponível em: <http://www.ncbi.nlm.nih.gov/pubmed/23434193>. Acesso em: 23 mar. 2021.

NUKI, G.; SIMKIN, P. A. A Concise History of Gout and Hyperuricemia and Their Treatment. **Arthritis Research & Therapy**, v. 8, n. Suppl 1, p. S1, Apr. 2006. Disponível em: </pmc/articles/PMC3226106/>. Acesso em: 30 oct. 2022.

PARK, C. K. et al. Resolving TRPV1- and TNF-α-Mediated Spinal Cord Synaptic Plasticity and Inflammatory Pain with Neuroprotectin D1. **Journal of Neuroscience**, v. 31, n. 42, p. 15072–15085, 19 Oct. 2011. Disponível em: <https://pubmed.ncbi.nlm.nih.gov/22016541/>. Acesso em: 23 mar. 2021.

PERRETTI, M.; D'ACQUISTO, F. Annexin A1 and Glucocorticoids as Effectors of the Resolution of Inflammation. **Nature reviews. Immunology**, v. 9, n. 1, p. 62–70, Jan. 2009. Disponível em: <https://pubmed.ncbi.nlm.nih.gov/19104500/>. Acesso em: 30 oct. 2022.

PÉTRILLI, V. et al. Activation of the NALP3 Inflammasome Is Triggered by Low Intracellular Potassium Concentration. **Cell death and differentiation**, v. 14, n. 9, p. 1583–1589, Sep. 2007. Disponível em: <https://pubmed.ncbi.nlm.nih.gov/17599094/>. Acesso em: 30 oct. 2022.

PINHO-RIBEIRO, F. A. et al. Blocking Neuronal Signaling to Immune Cells Treats Streptococcal Invasive Infection. **Cell**, v. 173, n. 5, p. 1083- 1097 e22, 17 May 2018. Disponível em: <http://www.ncbi.nlm.nih.gov/pubmed/29754819>. Acesso em: 23 mar. 2021.

PINHO-RIBEIRO, F. A.; VERRI, W. A.; CHIU, I. M. **Nociceptor Sensory Neuron–Immune Interactions in Pain and InflammationTrends in Immunology**, 2017. .

POPA-NITA, O. et al. Crystal-Induced Neutrophil Activation. IX. Syk-Dependent Activation of Class Ia Phosphatidylinositol 3-Kinase. **J Leukoc Biol**, v. 82, n. 3, p. 763–773, 2007. Disponível em: <http://www.ncbi.nlm.nih.gov/pubmed/17535983>.

QI, J. et al. Painful Pathways Induced by TLR Stimulation of Dorsal Root Ganglion Neurons. **J Immunol**, v. 186, n. 11, p. 6417–6426, 2011. Disponível em: <http://www.ncbi.nlm.nih.gov/pubmed/21515789>.

RAGAB, G.; ELSHAHALY, M.; BARDIN, T. Gout: An Old Disease in New Perspective - A Review. **J Adv Res**, v. 8, n. 5, p. 495–511, 2017. Disponível em: <https://www.ncbi.nlm.nih.gov/pubmed/28748116>.

RECCHIUTI, A. et al. MicroRNAs in Resolution of Acute Inflammation: Identification of Novel Resolvin D1-MiRNA Circuits. **The FASEB journal : official publication of the Federation of American Societies for Experimental Biology**, v. 25, n. 2, p. 544–560, 2011. Disponível em: <http://www.pubmedcentral.nih.gov/articlerender.fcgi?artid=3023392&tool=pmcentrez&rendertype=abstract>.

RECCHIUTI, A.; SERHAN, C. N. **Pro-resolving lipid mediators (SPMs) and their actions in regulating miRNA in novel resolution circuits in inflammationFrontiers in Immunology**Front Immunol, , 2012. . Disponível em: <https://pubmed.ncbi.nlm.nih.gov/23093949/>. Acesso em: 12 apr. 2021.

REES, F.; HUI, M.; DOHERTY, M. Optimizing Current Treatment of Gout. **Nat Rev Rheumatol**, v. 10, n. 5, p. 271–283, 2014. Disponível em: <http://www.ncbi.nlm.nih.gov/pubmed/24614592>.

REICHLING, D. B.; LEVINE, J. D. Critical Role of Nociceptor Plasticity in Chronic

Pain. **Trends in neurosciences**, v. 32, n. 12, p. 611–618, Dec. 2009. Disponível em: <https://pubmed.ncbi.nlm.nih.gov/19781793/>. Acesso em: 1 feb. 2022.

RIBEIRO, R. A. et al. Role of Resident Mast Cells and Macrophages in the Neutrophil Migration Induced by LTB4, FMLP and C5a Des Arg. **International archives of allergy and immunology**, v. 112, n. 1, p. 27–35, 1 Jan. 1997. Disponível em: <https://pubmed.ncbi.nlm.nih.gov/8980461/>. Acesso em: 27 oct. 2022.

ROCHA E SILVA, M. A Brief Survey of the History of Inflammation. 1978. **Agents and actions**, v. 43, n. 3–4, p. 86–90, 1994. Disponível em: <http://www.ncbi.nlm.nih.gov/pubmed/7725981>.

ROSE, T. E. et al. 1-Aryl-3-(1-Acylpiperidin-4-Yl)Urea Inhibitors of Human and Murine Soluble Epoxide Hydrolase: Structure-Activity Relationships, Pharmacokinetics, and Reduction of Inflammatory Pain. **Journal of medicinal chemistry**, v. 53, n. 19, p. 7067–7075, 14 Oct. 2010. Disponível em: <https://pubmed.ncbi.nlm.nih.gov/20812725/>. Acesso em: 1 nov. 2022.

SASSO, O. et al. Peripheral FAAH and Soluble Epoxide Hydrolase Inhibitors Are Synergistically Antinociceptive. **Pharmacological research**, v. 97, p. 7–15, 1 Jul. 2015. Disponível em: <https://pubmed.ncbi.nlm.nih.gov/25882247/>. Acesso em: 1 nov. 2022.

SCHAUER, C. et al. Aggregated Neutrophil Extracellular Traps Limit Inflammation by Degrading Cytokines and Chemokines. **Nat Med**, v. 20, n. 5, p. 511–517, 2014. Disponível em: <http://www.ncbi.nlm.nih.gov/pubmed/24784231>.

SCHLESINGER, N.; THIELE, R. G. The pathogenesis of bone erosions in gouty arthritis. . Nov. 2010, p. 1907–1912.

SCHMID-BURGK, J. L. et al. A Genome-Wide CRISPR (Clustered Regularly

Interspaced Short Palindromic Repeats) Screen Identifies NEK7 as an Essential Component of NLRP3 Inflammasome Activation. **The Journal of biological chemistry**, v. 291, n. 1, p. 103–109, 1 Jan. 2016. Disponível em: <https://pubmed.ncbi.nlm.nih.gov/26553871/>. Acesso em: 30 oct. 2022.

SCHMIDT, A.; WEBER, O. F. In Memoriam of Rudolf Virchow: A Historical Retrospective Including Aspects of Inflammation, Infection and Neoplasia. **Contributions to microbiology**, v. 13, p. 1–15, 2006.

SCHOLZ, J.; WOOLF, C. J. Can We Conquer Pain? **Nature neuroscience**, v. 5 Suppl, n. 11s, p. 1062–1067, 2002. Disponível em: <https://pubmed.ncbi.nlm.nih.gov/12403987/>. Acesso em: 1 feb. 2022.

SERHAN, C. N. et al. Novel Functional Sets of Lipid-Derived Mediators with Antiinflammatory Actions Generated from Omega-3 Fatty Acids via Cyclooxygenase 2-Nonsteroidal Antiinflammatory Drugs and Transcellular Processing. **J Exp Med**, v. 192, n. 8, p. 1197–1204, 2000. Disponível em: <http://www.ncbi.nlm.nih.gov/pubmed/11034610>.

SERHAN, C. N. et al. Resolvins. **The Journal of Experimental Medicine**, v. 196, n. 8, p. 1025–1037, 2002a. Disponível em: <http://www.jem.org/lookup/doi/10.1084/jem.20020760>.

SERHAN, C. N. et al. Resolvins: A Family of Bioactive Products of Omega-3 Fatty Acid Transformation Circuits Initiated by Aspirin Treatment That Counter Proinflammation Signals. **The Journal of Experimental Medicine**, v. 196, n. 8, p. 1025–1037, 2002b. Disponível em: <http://jem.rupress.org/content/196/8/1025.abstract>.

SERHAN, C. N. A Search for Endogenous Mechanisms of Anti-Inflammation Uncovers Novel Chemical Mediators: Missing Links to Resolution. **Histochemistry**

and cell biology, v. 122, n. 4, p. 305–321, Oct. 2004. Disponível em: <https://pubmed.ncbi.nlm.nih.gov/15322859/>. Acesso em: 30 oct. 2022.

SERHAN, C. N. Novel Pro-Resolving Lipid Mediators in Inflammation Are Leads for Resolution Physiology. **Nature**, v. 510, n. 7503, p. 92–101, 2014.

SERHAN, C. N.; CHIANG, N.; DALLI, J. The Resolution Code of Acute Inflammation: Novel pro-Resolving Lipid Mediators in Resolution. **Seminars in Immunology**, v. 27, n. 3, p. 200–215, 2015. Disponível em: <http://www.ncbi.nlm.nih.gov/pubmed/25857211%5Cnhttp://www.pubmedcentral.nih.gov/articlerender.fcgi?artid=PMC4515371%5Cnhttp://dx.doi.org/10.1016/j.smim.2015.03.004>.

SERHAN, C. N.; PETASIS, N. A. Resolvins and Protectins in Inflammation Resolution. **Chemical Reviews**, v. 111, n. 10, p. 5922–5943, 2011. Disponível em: <https://pubs.acs.org/doi/10.1021/cr100396c>.

SHI, H. et al. NLRP3 Activation and Mitosis Are Mutually Exclusive Events Coordinated by NEK7, a New Inflammasome Component. **Nature immunology**, v. 17, n. 3, p. 250–258, 1 Feb. 2016. Disponível em: <https://pubmed.ncbi.nlm.nih.gov/26642356/>. Acesso em: 30 oct. 2022.

SO, A. K.; MARTINON, F. Inflammation in Gout: Mechanisms and Therapeutic Targets. **Nat Rev Rheumatol**, v. 13, n. 11, p. 639–647, 2017. Disponível em: <https://www.ncbi.nlm.nih.gov/pubmed/28959043>.

SPECTOR, A. A.; KIM, H. Y. Cytochrome P450 Epoxygenase Pathway of Polyunsaturated Fatty Acid Metabolism. **Biochimica et biophysica acta**, v. 1851, n. 4, p. 356, 2015. Disponível em: </pmc/articles/PMC4314516/>. Acesso em: 1 nov. 2022.

SREERAMKUMAR, V. et al. Neutrophils Scan for Activated Platelets to Initiate

Inflammation. **Science**, v. 346, n. 6214, p. 1234–1238, 2014. Disponível em: <http://www.ncbi.nlm.nih.gov/pubmed/25477463>.

TAKEUCHI, O.; AKIRA, S. Pattern Recognition Receptors and Inflammation. **Cell**, v. 140, n. 6, p. 805–820, 2010. Disponível em: <http://www.ncbi.nlm.nih.gov/pubmed/20303872>.

TEIXEIRA, J. M. et al. Peripheral Soluble Epoxide Hydrolase Inhibition Reduces Hypernociception and Inflammation in Albumin-Induced Arthritis in Temporomandibular Joint of Rats. **International immunopharmacology**, v. 87, 1 Oct. 2020. Disponível em: <https://pubmed.ncbi.nlm.nih.gov/32736189/>. Acesso em: 29 aug. 2022.

TING, E. et al. Role of Complement C5a in Mechanical Inflammatory Hypernociception: Potential Use of C5a Receptor Antagonists to Control Inflammatory Pain. **British journal of pharmacology**, v. 153, n. 5, p. 1043–1053, 2008. Disponível em: <https://pubmed.ncbi.nlm.nih.gov/18084313/>. Acesso em: 28 oct. 2022.

TRINDADE-DA-SILVA, C. A. et al. Soluble Epoxide Hydrolase Pharmacological Inhibition Decreases Alveolar Bone Loss by Modulating Host Inflammatory Response, RANK-Related Signaling, Endoplasmic Reticulum Stress, and Apoptosis. **Journal of Pharmacology and Experimental Therapeutics**, v. 361, n. 3, p. 408–416, 1 Jun. 2017. Disponível em: <https://jpet.aspetjournals.org/content/361/3/408>. Acesso em: 1 nov. 2022.

TRINDADE-DA-SILVA, C. A. et al. Soluble Epoxide Hydrolase Inhibitor, TPPU, Increases Regulatory T Cells Pathway in an Arthritis Model. **FASEB journal : official publication of the Federation of American Societies for Experimental Biology**, v. 34, n. 7, p. 9074–9086, 1 Jul. 2020. Disponível em:

1 <https://pubmed.ncbi.nlm.nih.gov/32400048/>. Acesso em: 29 aug. 2022.
2 TSAI, H. J. et al. Pharmacokinetic Screening of Soluble Epoxide Hydrolase Inhibitors
3 in Dogs. **European journal of pharmaceutical sciences : official journal of the**
4 **European Federation for Pharmaceutical Sciences**, v. 40, n. 3, p. 222–238, Jun.
5 2010. Disponível em: <https://pubmed.ncbi.nlm.nih.gov/20359531/>. Acesso em: 1
6 nov. 2022.
7 ULU, A. et al. Pharmacokinetics and in Vivo Potency of Soluble Epoxide Hydrolase
8 Inhibitors in Cynomolgus Monkeys. **British journal of pharmacology**, v. 165, n. 5, p.
9 1401–1412, Mar. 2012. Disponível em:
10 <https://pubmed.ncbi.nlm.nih.gov/21880036/>. Acesso em: 1 nov. 2022.
11 VERRI, W. A. et al. IL-15 Mediates Immune Inflammatory Hypernociception by
12 Triggering a Sequential Release of IFN-Gamma, Endothelin, and Prostaglandin.
13 **Proceedings of the National Academy of Sciences of the United States of**
14 **America**, v. 103, n. 25, p. 9721–9725, 2006. Disponível em:
15 <http://www.pubmedcentral.nih.gov/articlerender.fcgi?artid=1480473&tool=pmcentre
16 z&rendertype=abstract>.
17 WANG, C. S. et al. ALX/FPR2 Modulates Anti-Inflammatory Responses in Mouse
18 Submandibular Gland. **Scientific Reports**, v. 6, n. April, p. 1–10, 2016.
19 WANG, D.; DUBOIS, R. N. Epoxyeicosatrienoic Acids: A Double-Edged Sword in
20 Cardiovascular Diseases and Cancer. **The Journal of clinical investigation**, v. 122,
21 n. 1, p. 19–22, 3 Jan. 2012. Disponível em:
22 <https://pubmed.ncbi.nlm.nih.gov/22182836/>. Acesso em: 1 nov. 2022.
23 WIECH, K. et al. Influence of Prior Information on Pain Involves Biased Perceptual
24 Decision-Making. **Current biology : CB**, v. 24, n. 15, 4 Aug. 2014. Disponível em:
25 <https://pubmed.ncbi.nlm.nih.gov/25093555/>. Acesso em: 27 oct. 2022.

WILLIAMS, J. M. et al. 20-Hydroxyeicosatetraeonic Acid: A New Target for the Treatment of Hypertension. **Journal of cardiovascular pharmacology**, v. 56, n. 4, p. 336–344, Oct. 2010. Disponível em: <https://pubmed.ncbi.nlm.nih.gov/20930591/>. Acesso em: 1 nov. 2022.

WOOLF, C. J.; SALTER, M. W. Neuronal Plasticity: Increasing the Gain in Pain. **Science (New York, N.Y.)**, v. 288, n. 5472, p. 1765–1768, 9 Jun. 2000. Disponível em: <https://pubmed.ncbi.nlm.nih.gov/10846153/>. Acesso em: 27 oct. 2022.

WRIGHT, H. L. et al. Neutrophil Function in Inflammation and Inflammatory Diseases. **Rheumatology (Oxford)**, v. 49, n. 9, p. 1618–1631, 2010. Disponível em: <http://www.ncbi.nlm.nih.gov/pubmed/20338884>.

XU, Z. Z. et al. Resolvins RvE1 and RvD1 Attenuate Inflammatory Pain via Central and Peripheral Actions. **Nat Med**, v. 16, n. 5, p. 592–7, 1p following 597, 2010. Disponível em: <http://www.ncbi.nlm.nih.gov/pubmed/20383154>.

XU, Z. Z.; JI, R. R. Resolvins Are Potent Analgesics for Arthritic Pain. **British journal of pharmacology**, v. 164, n. 2, p. 274–277, Sep. 2011. Disponível em: <https://pubmed.ncbi.nlm.nih.gov/21418190/>. Acesso em: 1 nov. 2022.

YARON, J. R. et al. K(+) Regulates Ca(2+) to Drive Inflammasome Signaling: Dynamic Visualization of Ion Flux in Live Cells. **Cell death & disease**, v. 6, n. 10, 1 Oct. 2015. Disponível em: <https://pubmed.ncbi.nlm.nih.gov/26512962/>. Acesso em: 30 oct. 2022.

YELLEPEDDI, V. K. et al. Predicting Resolvin D1 Pharmacokinetics in Humans with Physiologically-Based Pharmacokinetic Modeling. **Clinical and Translational Science**, v. 14, n. 2, p. 683–691, 1 Mar. 2021. Disponível em: <www.cts-journal.com>. Acesso em: 6 may. 2021.

ZANINELLI, T. H. et al. RvD1 Disrupts Nociceptor Neuron and Macrophage

Activation, and Neuroimmune Communication Reducing Pain and Inflammation in Gouty Arthritis in Mice. **British Journal of Pharmacology**, 7 Jul. 2022. Disponível em: <https://pubmed.ncbi.nlm.nih.gov/35716378/>. Acesso em: 1 aug. 2022.

ZANINELLI, T. H.; FATTORI, V.; VERRI, W. A. J. Harnessing Inflammation Resolution in Arthritis: Current Understanding of Specialized Pro-Resolving Lipid Mediators' Contribution to Arthritis Physiopathology and Future Perspectives. **Frontiers in Physiology**, v. 0, p. 1444, 1 Sep. 2021. Disponível em: <https://pubmed.ncbi.nlm.nih.gov/34539449/>. Acesso em: 17 oct. 2021.

ZARPELON, A. C. et al. The Nitroxyl Donor, Angeli's Salt, Inhibits Inflammatory Hyperalgesia in Rats. **Neuropharmacology**, v. 71, p. 1–9, Aug. 2013. Disponível em: <https://pubmed.ncbi.nlm.nih.gov/23541720/>. Acesso em: 25 nov. 2021.

APÊNDICE A

APÊNDICE A – Publicações de artigos científicos durante o período de doutorado (2018-2022)

Bertozzi, Mariana M., Telma Saraiva-Santos, **Tiago H. Zaninelli**, Felipe A. Pinho-Ribeiro, Victor Fattori, Larissa Staurengo-Ferrari, Camila R. Ferraz, et al. **2022**. “Ehrlich Tumor Induces TRPV1-Dependent Evoked and Non-Evoked Pain-like Behavior in Mice.” Brain Sciences 12 (9): 1247. https://doi.org/10.3390/BRAINSCI12091247.

Borghi, Sergio M., Sylvia K.D. Bussulo, Felipe A. Pinho-Ribeiro, Victor Fattori, Thacyana T. Carvalho, Fernanda S. Rasquel-Oliveira, **Tiago H. Zaninelli**, et al. **2022**. “Intense Acute Swimming Induces Delayed-Onset Muscle Soreness Dependent on Spinal Cord Neuroinflammation.” Frontiers in Pharmacology 12 (January). https://doi.org/10.3389/FPHAR.2021.734091.

Borghi, Sergio M., Victor Fattori, Thacyana T. Carvalho, Vera L.H. Tatakihara, **Tiago H. Zaninelli**, Felipe A. Pinho-Ribeiro, Camila R. Ferraz, et al. **2021**. “Experimental Trypanosoma Cruzi Infection Induces Pain in Mice Dependent on Early Spinal Cord Glial Cells and NFκB Activation and Cytokine Production.” Frontiers in Immunology 11 (January). https://doi.org/10.3389/FIMMU.2020.539086.

Borghi, Sergio M., Victor Fattori, Felipe A. Pinho-Ribeiro, Talita P. Domiciano, Milena M. Miranda-Sapla, **Tiago H. Zaninelli**, Rubia Casagrande, et al. **2019**. “Contribution of Spinal Cord Glial Cells to L. Amazonensis Experimental Infection-Induced Pain in BALB/c Mice.” Journal of Neuroinflammation 16 (1). https://doi.org/10.1186/S12974-019-1496-2.

Bussmann, Allan J. C., **Tiago H. Zaninelli**, Telma Saraiva-Santos, Victor Fattori, Carla F. S. Guazelli, Mariana M. Bertozzi, Ketlem C. Andrade, et al. **2022.** “The Flavonoid Hesperidin Methyl Chalcone Targets Cytokines and Oxidative Stress to Reduce Diclofenac-Induced Acute Renal Injury: Contribution of the Nrf2 Redox-Sensitive Pathway.” Antioxidants (Basel, Switzerland) 11 (7): 1261. https://doi.org/10.3390/ANTIOX11071261.

Bussmann, Allan J.C., Sergio M. Borghi, **Tiago H. Zaninelli**, Telma S. dos Santos, Carla F.S. Guazelli, Victor Fattori, Talita P. Domiciano, et al. **2019.** “The Citrus Flavanone Naringenin Attenuates Zymosan-Induced Mouse Joint Inflammation: Induction of Nrf2 Expression in Recruited CD45 + Hematopoietic Cells.” Inflammopharmacology 27 (6): 1229–42. https://doi.org/10.1007/S10787-018-00561-6.

Bussmann, Allan J.C., Camila R. Ferraz, Aline V.A. Lima, João G.S. Castro, Patrícia D. Ritter, **Tiago H. Zaninelli**, Telma Saraiva-Santos, Waldiceu A. Verri, and Sergio M. Borghi. **2022.** “Association between IL-10 Systemic Low Level and Highest Pain Score in Patients during Symptomatic SARS-CoV-2 Infection.” Pain Practice : The Official Journal of World Institute of Pain 22 (4): 453–62. https://doi.org/10.1111/PAPR.13101.

Colombo, Bárbara B., Victor Fattori, Carla F.S. Guazelli, **Tiago H. Zaninelli**, Thacyana T. Carvalho, Camila R. Ferraz, Allan J.C. Bussmann, et al. **2018**. "Vinpocetine Ameliorates Acetic Acid-Induced Colitis by Inhibiting NF-KB Activation in Mice." Inflammation 41 (4): 1276–89. https://doi.org/10.1007/S10753-018-0776-9.

Fattori, Victor, Larissa Staurengo-Ferrari, **Tiago H. Zaninelli**, Rubia Casagrande, Rene D. Oliveira, Paulo Louzada-Junior, Thiago M. Cunha, et al. **2020**. "IL-33 Enhances Macrophage Release of IL-1β and Promotes Pain and Inflammation in Gouty Arthritis." Inflammation Research : Official Journal of the European Histamine Research Society ... [et Al.] 69 (12): 1271–82. https://doi.org/10.1007/S00011-020-01399-X.

Fattori, Victor, **Tiago H. Zaninelli**, Camila R. Ferraz, Luisa Brasil-Silva, Sergio M. Borghi, Joice M. Cunha, Juliana G. Chichorro, Rubia Casagrande, and Waldiceu A. Verri. **2022**. "Maresin 2 Is an Analgesic Specialized Pro-Resolution Lipid Mediator in Mice by Inhibiting Neutrophil and Monocyte Recruitment, Nociceptor Neuron TRPV1 and TRPA1 Activation, and CGRP Release." Neuropharmacology 216 (September): 109189. https://doi.org/10.1016/J.NEUROPHARM.2022.109189.

Fattori, Victor, **Tiago H. Zaninelli**, Fernanda S. Rasquel-Oliveira, Rubia Casagrande, and Waldiceu A. Verri. **2020.** "Specialized Pro-Resolving Lipid Mediators: A New Class of Non-Immunosuppressive and Non-Opioid Analgesic Drugs." Pharmacological Research 151 (January). https://doi.org/10.1016/J.PHRS.2019.104549.

Fattori, Victor, Ana C. Zarpelon, Larissa Staurengo-Ferrari, Sergio M. Borghi, **Tiago H. Zaninelli**, Fernando B. Da Costa, Jose C. Alves-Filho, et al. **2018**. "Budlein A, a Sesquiterpene Lactone From Viguiera Robusta, Alleviates Pain and Inflammation in a Model of Acute Gout Arthritis in Mice." Frontiers in Pharmacology 9 (SEP). https://doi.org/10.3389/FPHAR.2018.01076.

Ferraz, Camila R., Thacyana T. Carvalho, Victor Fattori, Telma Saraiva-Santos, Felipe A. Pinho-Ribeiro, Sergio M. Borghi, Marília F. Manchope, **Tiago H. Zaninelli**, et al. 2021. "Jararhagin, a Snake Venom Metalloproteinase, Induces Mechanical Hyperalgesia in Mice with the Neuroinflammatory Contribution of Spinal Cord Microglia and Astrocytes." International Journal of Biological Macromolecules 179 (May): 610–19. https://doi.org/10.1016/J.IJBIOMAC.2021.02.178.

Ferraz, Camila R., Marília F. Manchope, Ketlem C. Andrade, Telma Saraiva-Santos, Anelise Franciosi, **Tiago H. Zaninelli,** Julia Bagatim-Souza, et al. **2021**. "Peripheral Mechanisms Involved in Tityus Bahiensis Venom-Induced Pain." Toxicon : Official Journal of the International Society on Toxinology 200 (September): 3–12. https://doi.org/10.1016/J.TOXICON.2021.06.013.

Lourenco-Gonzalez, Yuri, Victor Fattori, Talita P. Domiciano, Ana C. Rossaneis, Sergio M. Borghi, **Tiago H. Zaninelli**, Catia C.F. Bernardy, et al. **2019**. "Repurposing of the Nootropic Drug Vinpocetine as an Analgesic and Anti-

Inflammatory Agent: Evidence in a Mouse Model of Superoxide Anion-Triggered Inflammation." Mediators of Inflammation 2019. https://doi.org/10.1155/2019/6481812.

Rasquel-Oliveira, Fernanda S., Marilia F. Manchope, Larissa Staurengo-Ferrari, Camila R. Ferraz, Telma Saraiva-Santos, **Tiago H. Zaninelli**, Victor Fattori, et al. **2020**. "Hesperidin Methyl Chalcone Interacts with NFκB Ser276 and Inhibits Zymosan-Induced Joint Pain and Inflammation, and RAW 264.7 Macrophage Activation." Inflammopharmacology 28 (4): 979–92. https://doi.org/10.1007/S10787-020-00686-7.

Rossaneis, Ana C., Daniela T. Longhi-Balbinot, Mariana M. Bertozzi, Victor Fattori, Carina Z. Segato-Vendrameto, Stephanie Badaro-Garcia, **Tiago H. Zaninelli**, et al. **2019**. "[Ru(Bpy) 2(NO)SO 3](PF 6), a Nitric Oxide Donating Ruthenium Complex, Reduces Gout Arthritis in Mice." Frontiers in Pharmacology 10 (March). https://doi.org/10.3389/FPHAR.2019.00229.

Ruiz-Miyazawa, Kenji W., Larissa Staurengo-Ferrari, Felipe A. Pinho-Ribeiro, Victor Fattori, **Tiago H. Zaninelli**, Stephanie Badaro-Garcia, Sergio M. Borghi, et al. **2018**. "15d-PGJ 2-Loaded Nanocapsules Ameliorate Experimental Gout Arthritis by Reducing Pain and Inflammation in a PPAR-Gamma-Sensitive Manner in Mice." Scientific Reports 8 (1). https://doi.org/10.1038/S41598-018-32334-0.

Souza, Cássia Milena de, Hugo Felix Perini, Waldiceu Aparecido Verri, **Tiago Henrique Zaninelli**, Luciana Furlaneto-Maia, and Marcia Cristina Furlaneto. **2021**. "Changes in Adhesion of Candida Tropicalis Clinical Isolates Exhibiting Switch Phenotypes to Polystyrene and HeLa Cells." Mycopathologia 186 (1): 81–91. https://doi.org/10.1007/S11046-020-00504-2.

Staurengo-Ferrari, Larissa, Stephanie Badaro-Garcia, Miriam S.N. Hohmann, Marília F. Manchope, **Tiago H. Zaninelli**, Rubia Casagrande, and Waldiceu A. Verri. **2019**. "Contribution of Nrf2 Modulation to the Mechanism of Action of Analgesic and Anti-Inflammatory Drugs in Pre-Clinical and Clinical Stages." Frontiers in Pharmacology 9 (JAN). https://doi.org/10.3389/FPHAR.2018.01536.

Staurengo-Ferrari, Larissa, Kenji W. Ruiz-Miyazawa, Felipe A. Pinho-Ribeiro, Victor Fattori, **Tiago H. Zaninelli**, Stephanie Badaro-Garcia, Sergio M. Borghi, et al. **2018**. "Trans-Chalcone Attenuates Pain and Inflammation in Experimental Acute Gout Arthritis in Mice." Frontiers in Pharmacology 9 (OCT). https://doi.org/10.3389/FPHAR.2018.01123.

Zaninelli, Tiago H., Victor Fattori, Telma Saraiva-Santos, Stephanie Badaro-Garcia, Larissa Staurengo-Ferrari, Ketlem C. Andrade, Nayara A. Artero, et al. **2022**. "RvD1 Disrupts Nociceptor Neuron and Macrophage Activation and Neuroimmune Communication, Reducing Pain and Inflammation in Gouty Arthritis in Mice." British Journal of Pharmacology, July. https://doi.org/10.1111/BPH.15897.

Zaninelli, Tiago H., Victor Fattori, and Waldiceu A. Verri. **2021**. “Harnessing Inflammation Resolution in Arthritis: Current Understanding of Specialized Pro-Resolving Lipid Mediators’ Contribution to Arthritis Physiopathology and Future Perspectives.” Frontiers in Physiology 12 (September). https://doi.org/10.3389/FPHYS.2021.729134.

APÊNDICE B

APÊNDICE B – TRABALHO DESENVOLVIDO NO PERÍODO DE DOUTORAMENTO SANDUÍCHE – PROGRAMA DE DOUTORADO-SANDUÍCHE NO EXTERIOR (PDSE) (2019-2020)

Targeting NGF but not VEGF or BDNF signaling reduce endometriosis-associated pain in mice

Tiago H. Zaninelli[1,2], Victor Fattori[1], Olivia K. Heintz[1], Kristeena R. Wright[1], Philip R. Bennallack[1], Danielle Sim[1], Hussain Bukhari[1], Avacir C. Andrello[3], Raymond M. Anchan[4], Stephen K. Godin[5], Dara Bree[5], Waldiceu A. Verri Jr[2], Michael S. Rogers[1]*

[1]Vascular Biology Program, Department of Surgery, Boston Children's Hospital, Harvard Medical School, Boston, MA, United States.

[2]Laboratory of Pain, Inflammation, Neuropathy, and Cancer, Department of Pathology, Center of Biological Sciences, Londrina State University, Londrina, PR, Brazil.

[3]Department of Physics, Center of Exact Sciences, Londrina State University, Londrina, PR, Brazil.

[4] Division of Reproductive Endocrinology and Infertility, Department of Obstetrics, Gynecology and Reproductive Biology, Brigham and Women's Hospital, Harvard Medical School, Boston, MA, USA.

[5] Cygnal Therapeutics, Cambridge, MA, USA.

*** Corresponding author**

Address: Vascular Biology Program, Boston Children's Hospital, Department of Surgery, Harvard Medical School, 11.211 Karp Family Research Bldg, 300 Longwood Ave, Boston, MA 02115, United States. E-mail address: Michael.Rogers@childrens.harvard.edu (M.S. Rogers).

Abstract

Endometriosis is a painful estrogen-dependent inflammatory disease that affects ~15% of the female population. Current therapies present limited to no efficacy for a significant fraction of patients. While linked to endometriosis, a direct demonstration of the contribution of vascular endothelial growth factor receptor-1 (VEGFR1), nerve growth factor (NGF), or brain-derived nerve factor (BDNF) have yet to be investigated. We found that the VEGFR1 agonists VEGFA, VEGFB, PlGF, and sVEGFR1 were abundant in peritoneal fluid of endometriosis patients. Despite receptor occupancy revealing that VEGFR1 agonist levels might be sufficient to elicit pain, blocking VEGF signaling with anti-VEGF or in tamoxifen-induced VEGFR1 knockout did not reduce pain or lesion size in mice. Similar effects were observed by targeting BDNF-TrkB with an anti-BDNF. On the other hand, entrectinib (pan-Trk inhibitor) or anti-NGF treatments reduced evoked pain, spontaneous pain, and thermal discomfort. This suggests NGF-TrkA signaling, but not BDNF-TrkB or VEGF-VEGFR1, mediates endometriosis-associated pain.

Keywords: neurotrophins, VEGFR1, visceral pain

1. Introduction

Endometriosis is an estrogen-dependent inflammatory disease characterized by the presence of endometrial-like tissue in the abdominal cavity or pelvic space (Bulun, 2009). The disease affects 10% - 15% of the worldwide female population in reproductive age (Parasar et al., 2017). The most accepted theory to endometriosis genesis is the retrograde menstruation (Laux-Biehlmann et al., 2015; McKinnon et al., 2015). During this process, danger-associated molecular patterns (DAMPs) activate resident immune cells and trigger inflammation (Izumi et al., 2018). The inflammatory process is orchestrated by pro-inflammatory mediators and growth factors secreted by activated immune cells (Wu et al., 2017; Izumi et al., 2018). The inflammatory milieu enriched in growth factors favors processes of angiogenesis and neurogenesis, resulting in vascularized and innervated endometriotic lesions teemed of activated immune cells (Abramiuk et al., 2022). This inflammation is key to pain, which is the main clinical feature of endometriosis (Laux-Biehlmann et al., 2015; McKinnon et al., 2015).

Endometriosis-associated pain appears as chronic pelvic pain, dysmenorrhea, dyspareunia, and dyschezia, affecting the social and professional life quality and mental health of patients with endometriosis (Facchin et al., 2015). For instance, patients with endometriosis lose approximately 10.8 h of work weekly, because of reduced effectiveness during work due to pain (Nnoaham et al., 2011). Currently, endometriosis-associated pain treatment lies on non-steroidal anti-inflammatory drugs (NSAIDS), analgesics, hormonal therapy, and the surgical removal of the lesions (Anaf et al., 2002). Nevertheless, current treatments show limited efficacy in reducing pain and often present unwanted side effects (Anaf et al., 2002). Importantly, up to 30% of patients with endometriosis do not respond to the current therapies. Therefore, there is an unmet need to develop or repurpose effective and safe drugs for the treatment of endometriosis-associated pain.

In the endometriotic milieu, nerve growth factor (NGF) and vascular endothelial growth factor (VEGF) are important mediators in the process of neurogenesis and angiogenesis, respectively. In addition to their growth-related role, those mediators are also described to be involved in pain (Bonnington and McNaughton, 2003; Selvaraj et al., 2015). Strong evidence suggest that lesion growth and inflammatory milieu maintenance is dependent of VEGFR1 (Sekiguchi et al., 2019). VEGF, moreover, is among a 28 panel of biomarker candidates for non-invasive endometriosis diagnose confirmation (Vodolazkaia et al., 2012). In addition, VEGF levels correlate with C-reactive protein in endometriosis patents, suggesting excessive systemic angiogenic activity in endometriosis patients (Xavier et al., 2006). In cancer, tumor-

derived VEGF-A/B, and PlGF-2 are involved in increased pain sensitivity through selective activation of VEGFR1 (Selvaraj et al., 2015). Similarly, compelling evidence demonstrate that NGF might be involved in endometriosis pain (Kajitani et al., 2013). High expression of NGF in deep adenomyotic nodules is correlated to hyperalgesia (Anaf et al., 2002) and both NGF and TrkA expression in human lesions correlate with deep dyspareunia (Peng et al., 2018). Supporting this, a recent GWAS study highlights that NGF is associated with migraine and dysmenorrhea during endometriosis (Nilufer et al., 2018). This might indicate that genetic variations on NGF could be predictive for endometriosis pain. Therefore, targeting this signaling might be an alternative to endometriosis-associated pain treatment.

Although they have an imperative role as growth factors in endometriosis progression and possible participation in endometriosis-associated pain, VEGFR1 or TrkA signaling has yet to be explored as therapeutic targets. Therefore, we aimed at determining the role of the angiogenic factor VEGF as well as the neurotrophins NGF and BDNF during in endometriosis-associated pain using our validated mouse model of endometriosis. This model mimics neuronal and behavioral changes consistent with the disease phenotype in women (Fattori et al., 2020). Moreover, resulting lesions exhibit features that resemble human lesions such as the presence of nerve fibers, glands, and immune cells. The model responds to clinically active drugs such as letrozole and danazol, and therefore, might be useful for finding novel or repurposed analgesic therapies (Fattori et al., 2020).

2. Materials and Methods

2.1. Patient samples

Samples of peritoneal fluid (PF) were collected from patients undergoing exploratory laparoscopy surgery for endometriosis at Brigham and Women Hospital (Boston, MA, USA). The samples were collected by the surgeon Raymond M. Anchan and kept frozen until the determination of VEGFR1 agonist levels. The procedures were approved by the Ethics Committee, and PF sampling was performed only after patients' signed consent.

2.2. Animals

Healthy and immunological competent C57BL/6 (8 weeks old, 20-25g, female, strain # 664 [RRID:IMSR_JAX:000664]), B6.Cg-Flt1$^{tm1.1Fong}$/J (8 weeks old, 20-25g, male and female, Vegfr-1^{flox}, strain # 28098 [RRID:IMSR_JAX:028098]), and B6;129-Gt(ROSA)26Sor$^{tm1(cre/ERT)Nat}$/J (8 weeks old, 20-25g, male and female, R26CreER, strain # 4847 [RRID:IMSR_JAX:004847]) mice were purchased from The Jackson Laboratory (Bar Harbor, Maine, USA). Vegfr-1^{flox} and R26CreER were bred to generate tamoxifen-inducible Vegfr-1 knockout mice (Vegfr-1$^{flox/flox}$R26CreER$^{+/-}$, Vegfr-1$^{flox/flox}$R26CreER$^{+/+}$), and littermate controls (Vegfr-1$^{flox/flox}$R26CreER$^{-/-}$). All mice were housed in standard clear cages with free access to food and water. Light/dark cycle of 12/12h and controlled temperature (21°±1°C). The investigators were blind to groups and treatments in all experiments, including data acquisition, sample processing, and data analyses. The animals were under isoflurane anesthesia (3% v/v in O_2) for endometriosis induction, and tail snip sampling for genotyping. Carbon oxide (CO_2) inhalation was used for euthanasia. Animal care and handling procedures were approved by Boston Children's Hospital Institutional Animal Care and Use Committee (IACUC, protocol number 19-12-4054R) and were in accordance with the International Association for Study of Pain (IASP) and ARRIVE 2.0 guidelines. All efforts were made to minimize the number of animals and their suffering.

2.3. Drugs and antibodies

Tamoxifen (Sigma-Aldrich, cat# T5648), Entrectinib (InvivoChem, Libertyville, IL, USA, CAS 1108743-60-7, cat# V0609); rat anti-mouse VEGFR IgG1antibody (Company, Cat# LSN3078374). anti-NGF (provided by Cygnal Therapeutics), anti-BDNF (provided by Cygnal Therapeutics), IgG control (provided by Cygnal Therapeutics).

2.4. Generation of VEGFR1 knockout mice

VEGFR1 knockout was induced by tamoxifen treatment in Vegfr-1$^{flox/flox}$R26CreER$^{+/-}$ and Vegfr-1$^{flox/flox}$R26CreER$^{+/+}$ mice. Littermate controls (Vegfr-1$^{flox/flox}$R26CreER) also received the treatment. Mice were treated via oral gavage with Tamoxifen (6 mg/mice/150 μL of corn oil) every other day for 10 consecutive days. Endometriosis was induced 7 days after the last tamoxifen administration. VEGFR1 KO was confirmed by genotyping and dorsal root ganglia (DRG) immunohistochemistry.

2.5. Induction of endometriosis

A non-surgical model of endometriosis-associated pain was induced as previously described (Fattori et al., 2020). Briefly, the mice were acclimatized at least one week before the experiment begin. Donor mice received a subcutaneous (s.c.) injection of 3 μg/mouse estradiol benzoate in sesame oil to stimulate the growth of the endometrium. Seven days later, the uteri of the donor mice were dissected and placed into a Petri dish containing Hank's Balanced Salt Solution (HBSS, Thermo Fisher Scientific, Waltham, MA, USA). The uteri horns were split longitudinally with a pair of scissors and the horns from each donor mouse were minced with scissors and scalpel one at the time, ensuring that the maximal diameter of each fragment was consistently smaller than 1 millimeter (mm). Each dissociated uterine horn was then injected intraperitoneally into a recipient mouse in 500 μL of HBSS. One donor mouse was used for every two endometriosis mice. Sham mice received an intraperitoneal injection of 500 μL of HBSS.

2.6. Experimental design

2.6.1. VEGFR1 signaling blockage

We used two approaches for VEGFR1 signaling blockage in endometriosis: i) immunotherapy using anti-VEGFR monoclonal antibody and ii) VEGFR1 knockout (KO). Mice bearing endometriosis were treated with a monoclonal antibody anti-VEGFR or IgG isotope (MF1, 45 mg/kg) subcutaneously (s.c.), twice a week starting 29 days post induction (29-56 d.p.i.). Mechanical hyperalgesia was assessed weekly. In the last week of treatments (42 – 56 d.p.i.) spontaneous abdominal behavior and thermal discomfort were quantified. On the 56th day mice were euthanatized, and lesion size was determined. In another set of experiments,

VEGFR1 conditional knockout was performed in CreER$^+$ mice by tamoxifen administration (6 mg/animal) p.o. gavage every other day for 10 days. To account for the effects of VEGFR1 in the tissue of donor and recipient mice, endometriosis was induced in KO and littermate controls using uteri horn from KO or littermate control donor mice, totaling 4 experimental groups. After endometriosis induction, mechanical hyperalgesia was determined weekly using von Frey filaments. On the 56th d.p.i., lesions and DRG were harvested for VEGFR1 KO confirmation by immunohistochemistry.

2.6.2. NGF and BDNF signaling blockage

To target neurotrophin signaling two strategies were used: i) immunotherapy using neutralizing antibodies anti-NGF and anti-BDNF, and ii) pharmacological treatment with entrectinib a pan-selective inhibitor of tropomyosin receptor kinase (Trk) A, B, and C. Mice with endometriosis were treated with antibodies anti-NGF, anti-BDNF, or IgG isotope (10 mg/kg) subcutaneously (s.c.), twice a week beginning on day 29 post induction (29-56 d.p.i.). Mechanical hyperalgesia was assessed weekly. In the last week of treatments (42 – 56 d.p.i.) spontaneous abdominal behavior and thermal discomfort were quantified. Similarly, entrectinib was administered per oral gavage in different treatment schedules to total 60 mg/kg/week per group. Therefore, group 1 received entrectinib at 60 mg/kg once a week, group 2 at 20 mg/kg three times a week, and group 3 at 15 mg/kg every other day. On the 56th day mice were euthanatized, and lesion size was determined. In the last week of treatments (42 – 56 d.p.i.) thermal discomfort was assessed for all groups, while spontaneous abdominal behavior was quantified in group 1, which received a single weekly treatment with 60 mg/kg. On the 56th day, lesions, blood, and femur were harvested for lesion size determination, liver and kidney toxicity, and bone health assessment, respectively.

2.7. Determination of VEGFR1 ligand levels

The levels of VEGFA, VEGFB, PlGF, and soluble VEGFR1 (sFL-1) were determined by Ella Automated Immunoassay System according to manufacturer's instructions (ProteinSimple, Bio-Techne, Minneapolis, MN, USA). VEGFR1 occupancy was calculated according to ligand-receptor affinity, as previously described (Kdr et al., 1994; Mac Gabhann and Popel, 2004; Fischer et al., 2008; Wu et al., 2009; Papadopoulos et al., 2012; Anisimov et al., 2013; Clegg and Mac Gabhann, 2017). The measurement of VEGF from mouse endometriosis lesions was

performed according to manufacturer's instructions using mouse VEGF quantikine ELISA Kit (Cat# MMV00, R&D systems, Minneapolis, MN, USA).

2.8. Immunostaining

For VEGFR1 immunohistochemistry, the mouse dorsal root ganglia (DRG) were dissected 56 days after endometriosis induction and post-fixed in 4% paraformaldehyde in phosphate buffered saline (PBS) (m/v) for 24h at room temperature (RT). Samples were dehydrated, paraffin imbibed, and sectioned in a microtome (Harvard Medical School Histology Core). The sections with 7 μm of thickness were deparaffinized and hydrated before antigen retrieval in citrate buffer. Slides were heated in a microwave until they reached 90ºC and let cooldown at RT. Peroxidase blockage was performed with 3% hydrogen peroxide in methanol (v/v) for 15 min at RT. Sections were blocked in 3% bovine serum albumin (BSA) in PBS 0.5% triton-X 100 (m/v/v) for 1h at RT. Samples were incubated with primary antibody rabbit anti-mouse VEGFR1 (Abcam, Cambridge, UK, cat# 32152, 1:200 dilution in PBS-T [RRID:AB_778798]) overnight at 4ºC. Slides were washed and incubated with gout anti-rabbit-HRP secondary antibody for 30 min at RT (Vector Laboratories, Newark, CA, USA, cat# MP-7451 [RRID:AB_2631198]). Color was developed using HRP substrate kit (Vector Laboratories, cat# SK-4105 [RRID:AB_2336520]) for 1 min and 45 seconds at RT. Slides were washed and counterstained with gills III Formulation hematoxylin for 6 seconds, washed and dehydrated before slide mounting with Permount™ mounting medium (Fisher Scientific, Waltham, MA, USA, cat# SP15-100).

For immunofluorescence analysis, mice DRG and endometriotic lesions were dissected and post-fixed in 4% paraformaldehyde in phosphate buffered saline (PBS) (m/v) for 24h at 4ºC. Samples were then dehydrated with 30% sucrose in PBS (m/v) for 48h at 4ºC, following by 30% sucrose in PBS and optimum temperature cutting reagent (OCT) (1:1, v/v) for 24h at 4ºC. DRG and lesions were frozen in OCT, sectioned in a cryostat (16 μm of thickness), and placed in salinized slides. Sections were hydrated with PBS, blocked in 5% BSA in PBS 0.5% triton-X 100 (m/v/v) for 1h at RT, following overnight incubation at 4ºC with primary antibodies. Mouse anti-mouse phosphorylated-NF-κB (pNF-κB, Santa Cruz Biotechnology, Dallas, TX, USA, cat# sc-136548, 1:200 [RRID:AB_10610391]), rabbit anti-mouse TrkA (Invitrogen, Waltham MA, USA, cat. # MA5-32123, 1:100 [RRID:AB_2809414]), rabbit anti-mouse NGF (Abcam, Boston, MA, USA, cat. # AB52918, 1:300 [RRID:AB_881254]), and β-III tubulin

(Novus Biologicals, Centennial, CO, USA, cat. # NB120-11314, 1:200 [RRID:AB_792496]). Slices were than incubated with specific secondary antibody as follows: goat anti-mouse Alexa Fluor 594 secondary antibody (1:500, cat. # A21125, Thermo Fisher Scientific [RRID:AB_141593]), goat anti-rabbit Alexa Fluor 647 secondary (1:500, cat. # A-21235, Thermo Fisher Scientific [RRID:AB_2535804]), and goat anti-rabbit Alexa Fluor 488 (1:500, cat. # A-11008, Thermo Fisher Scientific [RRID:AB_143165]). DAPI was used to stain nuclei (Cayman Chemicals, Ann Arbor, MI, USA, cat. # 14285). Images were aquired and processed on a confocal microscope using 20x objective (Zeiss LSM 880 laser scanning microscope with Airyscan, Carl Zeiss Microscopy, Thornwood, NY, USA).

2.9. Animal behavior

2.9.1. Evoked abdominal mechanical hyperalgesia

Mechanical hyperalgesia was assessed as previorly described (Fattori et al., 2020). Briefly, mice were allowed to habituate to the apparatus for at least 2 hduring three consecutive days before the beginning of measurements. Pain intensity to a mechanical stimulus (mechanical hyperalgesia) was measured using von Frey filaments. The experimenter was trained, and care was taken to not stimulate the same point consecutively and the area of external genitalia was avoided. Jump or paw flinches were considered as a withdrawal response (Laird et al., 2001; Gonzalez-Cano et al., 2013). The mechanical threshold was determined by the up and down method starting with 0.4g filament and calculated using a modified version of the open source software Up-Down Reader (Gonzalez-Cano et al., 2018).

2.9.2. Thermal gradient

The thermal gradient assay was perforemed as previorly described (Fattori et al., 2020). Mice were placed in a metalic base catwalk with a continuous temperature gradient (7–50 °C). Animals walked freely while being video-recorded from above (Bioseb, France). Each run lasted 1.5 h, and two mice were simultaneously recorded in separate corridors. After an exploration period (30 minutes), the mouse showed a distinct preference, indicating the most comfortable temperature range. Data was presented by the time spent (in seconds) on each zone set at specific temperatures during 60 minutes.

2.9.3. Spontaneous pain behaviors

For spontaneous abdominal pain measurements, it was quantified by licking of the abdomen, stretching the abdomen (abdominal contortions), and squashing of the lower abdomen against the floor as previously described (Fattori et al., 2020). Briefly, direct abdominal licking was quantified during 10 minutes using bottom-up video recording as the number of times the mouse directly groomed the abdominal region without going for any other region before or after the behavior. For the abdominal contortion, mice were placed in individual chambers and the number of abdominal contortions was quantified for 10 minutes. Positive responses consist of a contraction of the abdominal muscle together with stretching of hind limbs. For abdominal squashing, it was quantified the number of times the mice pressed the lower abdominal region against the floor for 5 min. In all testing, the investigators were blinded to the groups and treatments.

2.10. Liver and kidney toxicity determination

On the 56th d.p.i., mice were euthanatized, and the blood was collected into heparinized collection tubes through cardiac punction. Plasma was separated by centrifugation (3200 rpm, 10 min, 4^{o}C). Kidney or liver toxicity was determined by the levels of urea, alanine aminotransferase (ALT), and aspartate aminotransferase (AST) in the plasma. The levels were determined by commercial kinetics kits according to manufacturer's instructions.

2.11. Micro-computerized tomography analysis (μCT)

The right femur was collected 56 days after endometriosis induction from entrectinib or vehicle treated mice. Samples were fixed in paraformaldehyde 4% in PBS (m/v) for 24 h and maintained in 70% ethanol (v/v) until μCT analysis. The samples were scanned on a Bruker SkyScan 1173 microtomograph (Bruker BioSpin Corporation, Kontich, Belgium). The NRecon, DataViewer, CTVox, and CTAn softwares were used for reconstruction and treatment of the images. The parameters analyzed after image acquisition were bone surface, volume, density, total porosity, and open-pore volume.

2.12. Statistical analysis

Results are presented as mean ± SEM. The data was analyzed using the software GraphPad Prism version 8 (GraphPad Software, San Diego, CA, USA). Mechanical hyperalgesia was analyzed by Two-way repeated measure analysis of variance (ANOVA), followed by Tukey's *post hoc*. One-way ANOVA followed by Tukey's *post hoc* was used to analyze data from experiments of single time point. Comparison between two groups was conducted using Student's t-test. For all analysis, statistical differences were considered significant when $p < 0.05$.

3. Results

3.1. Levels of VEGFR1 ligands are increased in the peritoneal fluid of endometriosis patients and in mouse lesions

VEGF has been long recognized as one of the most important proangiogenic factors in endometriosis (McLaren et al., 1996; Xavier et al., 2006; Kajdos et al., 2022). Therefore, we first addressed the levels of VEGFR1 agonists in the peritoneal fluid of patients undergoing endometriosis surgery **(Fig. 1 A-B)**. We found that the levels of VEGFA, VEGFB, PlGF, and sVEGFR1 were abundant in most evaluated samples **(Fig. 1B)**. Based on the VGFR1 calculated occupancy, the levels of VEGFR1 agonists are believed to be sufficient to elicit pain **(Fig. 1C)**. To determine whether VEGF would be also present in our model, we next measured VEGFA levels in the mouse lesions. We demonstrated that VEGFA levels are increased in endometriotic lesions **(Fig. 1F)** and that its receptor VEGFR1 is consistently expressed in DRG neurons in naïve and endometriosis-bearing mice **(Fig. 1G)**. Therefore, based in previous published work (Selvaraj et al., 2015) and the present evidence, we hypothesized that VEGF – VEGFR1 signaling might be important in endometriosis-associated pain.

3.2. VEGF neutralization or VEGFR1 ablation do not reduce endometriosis-associated pain or thermal discomfort in mice

To determine the extent to which VEGF signaling is important for endometriosis-associated pain, we next targeted this signaling using two different strategies. First, we want to determine whether VEGFR1 neutralization with an anti-VEGFR1 monoclonal antibody (MF-1) would reduce endometriosis-associated pain in mice. We found that treatment with anti-VEGFR1 did not alter endometriosis-induced mechanical hyperalgesia **(Fig. 2B left)** or lesion size **(Fig. 2B right)**. Since spontaneous pain is the main complaint of patients with endometriosis, we next determined whether treatment with MF-1 would reduce endometriosis-associated spontaneous pain. We found that none of the spontaneous abdominal-related behaviors (licking, squashing, or contortions) were reduced by the treatment **(Fig. 2C)**. Next, we assessed the mice's own determination of discomfort using the thermal gradient assay. We confirmed that sham mice prefer temperatures 27 to 36 $^{\circ}$C with a stronger preference for 34 $^{\circ}$C while mice with endometriosis exhibited a more dispersed pattern ranging from 22 to 36 $^{\circ}$C with no single preferred temperature (Fattori et al., 2020). In corroboration with our previous results, blocking VEGF-VEGFR1 signaling did restore the changes in thermal selection, as observed the disperse pattern in MF-1-treated mice **(Fig. 2D).** Since we observed that treatment with anti-VEGFR1 did not reduce pain, we next wanted to establish whether the presence of VEGFR1 in donor

tissue could be the reason why lesions are able to establish in the peritoneal cavity. Therefore, we first developed a conditional tamoxifen-induced cre-dependent knockout mouse line **(Fig. 2E and F)**. VEGR1 floxed mice and littermate controls (LM) were treated with tamoxifen to induce VEGFR1 cre-dependent ablation **(Fig. 2F)**. Ablation of VEGFR1 was confirmed by immunohistochemistry in the dorsal root ganglia (DGR) **(Fig. 2G)**. We performed a four-group experiment using VEGFR1-floxed and LM control mice as donors or recipients to determine extent to which the lack of VEGFR1 in donor tissue (mimicking retrograde menstruation) or in a combination of donor and recipient play a role in endometriosis lesion formation and pain **(Fig. 2H left)**. In none of the investigated scenarios of VEGFR1 depletion did they demonstrate to have analgesic effects **(Fig. 2H right)**. Therefore, while levels of VEGFR1 ligands are increased (both in humans and mice), our data indicate that neither VEGFR1 from donor nor from recipient mice contribute to endometriosis-associated pain.

3.3. NGF-TrkA signaling is activated during endometriosis

Patients with endometriosis have higher levels of NGF in lesion as well as genetic variations that correlates NGF to pain (Woolf et al., 1994; Guerios et al., 2006; Kajitani et al., 2013; Nilufer et al., 2018). This indicates that NGF might play an important role in endometriosis. Thus, we next investigated whether NGF could play a role in endometriosis using our validated mouse model **(Fig. 3A)**. By immunofluorescence we showed that NGF is present in mouse lesions, and interestingly, nociceptors seem to be closely located to this NGF gradient, as observed by colocalization between NGF and β-tubulin III (TUJ3), a pan-neuronal marker **(Fig. 3B)**. In the DRG, lesion bearing mice displayed higher percentage of TrkA-expressing neurons as well as increased percentage of $TrkA^{+}pNF\text{-}\kappa B^{+}$ in comparison to sham **(Fig. 3C bottom, D)**. Altogether, this data suggests that NGF-TrkA signaling is activated during endometriosis and might contribute to pain in this model.

3.4. NGF neutralization, but not BDNF, reduces endometriosis-associated pain and thermal discomfort in mice

We next sought to determine the contribution of the neurotrophins NGF and BDNF in our validated mouse model of endometriosis-associated pain. For that, we disrupted neurotrophin receptor signaling using neutralizing antibodies and determined mechanical hyperalgesia, lesion size, spontaneous behaviors, and thermal discomfort **(Fig. 4A)**. We observed that anti-NGF immunotherapy, but not anti-BDNF, considerably reduced mechanical hyperalgesia from

the 42nd to 56th days after endometriosis induction **(Fig. 4B left)**. Although analgesic effects were maintained up to 56 d.p.i. in mice treated with anti-NGF, no differences were observed in lesion size **(Fig. 4B right)**. Based on these results, we next analyzed non-evoked pain-associated behaviors and thermal discomfort only using anti-NGF therapy **(Fig. 4C-D)**. We found that the treatment with anti-NGF reduced endometriosis-induced abdominal licking **(Fig. 4C left)** and squashing **(Fig. 4C middle)**. A decrease in abdominal contortions was also observed, however it was not statistically different from IgG-treated mice **(Fig. 4C right)**. Lastly, we investigated the effects of anti-NGF therapy in thermal discomfort using the thermogradient assay **(Fig. 4D)**. Anti-NGF reduced thermal discomfort, restoring the amplitude of time spent in specific thermal zones, when compared to isotope-treated mice **(fig. 4D)**. Therefore, our results show that NGF-TrkA signaling, but not BDNF-TrkB, contributes to endometriosis-associate pain.

3.5. Entrectinib, a pan-Trk inhibitor, reduces endometriosis-associated pain and thermal discomfort in mice

Given that we found NGF-TrkA signaling be activated during endometriosis, we next sought to investigate whether entrectinib (a pan Trk inhibitor), an FDA-approved drug for cancer (Drilon et al., 2017; Desai et al., 2022; Mercier et al., 2022; Osman and Tuncbilek, 2022), could show efficacy in our model. Since entrectinib has been linked to increased risk of bone fractures (clinicaltrials.gov, NCT02650401)(Desai et al., 2022), we wanted to first determine a treatment schedule that could reduce pain and would not induce bone loss. We chose a weekly dose of 60 mg/kg in three different treatment schedules **(Fig. 5A, T1, T2, and T3)**. Entrectinib reduced mechanical hyperalgesia in all selected treatment schedules from day 42 to 56 post endometriosis induction **(Fig. 5B left)**. Although entrectinib treatment did not change lesion size **(Fig. 5B right)**, the weekly delivery of 60 mg/kg was more effective in restore thermal comfort when compared to vehicle treated mice **(Fig. 5C)**. The effects of T1 and T2 showed a milder reduction to thermal discomfort, and therefore, the weekly dose of 60 mg/kg was chosen for the next experiments **(Fig. 5C)**. Next, we determined the effect of weekly treatment with entrectinib in spontaneous pain and found that it reduced all endometriosis-associated spontaneous behaviors **(Fig. 5D)**. Therefore, our data suggest that disruption in neurotrophins-Trk signaling is effective in reducing endometriosis-associated pain.

3.6. Weekly treatment with entrectinib does not induce weight change, liver or kidney toxicity, or bone loss in mice

As mentioned, clinical trials with entrectinib in children and young adults demonstrated a high incidence of bone fractures (clinicaltrials.gov, NCT02650401)(Desai et al., 2022). Even though the weekly dose proposed here is much lower than the ones used in clinical trials, even after human equivalent dose determination, we sought to determine kidney and liver function, and bone loss in mice **(Fig. 6A)**. Weekly treatment with entrectinib did not induce weight changes **(Fig. 6B)**, nor kidney or liver function alteration as per levels of urea **(Fig. 6C)**, alanine aminotransferase (ALT) **(Fig. 6D Left)**, or aspartate transaminase (AST) **(Fig. 6D right)** in the plasma, respectively. Moreover, weekly treatment did not alter bone parameters in the femur, as determined per micro-computerized tomography analysis **(Fig. 6E)**. No significant changes were observed in femur surface, volume, density, or porosity in the evaluated dose and schedules of treatment. We found, however, that increased dosing, such as every other day **(Fig 6, T1)** or three times a week **(Fig 6, T2),** reduced bone porosity **(Fig. 6E)**. This indicates that increased treatment schedules, rather than dose, might be a limiting factor for entrectinib use.

4. Discussion

In this study we demonstrated that NGF, but not VEGFR1 signaling, is associated to endometriosis-related spontaneous and evoked pain responses. Neither the neutralization of VEGFR1 with antibodies nor the VEGFR1 conditional knockout mice relieved endometriosis-associated pain. On the other hand, we showed that blocking NGF signaling with entrectinib a pan-Trk inhibitor, reduced abdominal mechanical pain as well as spontaneous pain. Specifically, we demonstrated that pain during endometriosis is mediated via NGF-TrkA signaling, since blocking NGF (but not BDNF) reduced pain.

While it is widely recognized that VEGFR1 and its ligands (*e.g.,* VEGF, PlGF, or soluble VEGFR1) are present in the fluids of endometriosis patients, there is very limited evidence of the therapeutic benefit of targeting VEGF. To the best of our knowledge, there is no evidence of targeting this angiogenic growth factor for endometriosis-related pain (Liu et al., 2016). Importantly, VEGF receptors are pivotal in embryo implantation and development, which explain how some pregnancies in tyrosine kinase inhibitor-treated cancer patients have been linked to miscarriage and birth defects (Pye et al., 2008; Vandenbroucke et al., 2017). This was later confirmed in animal models (Abe et al., 2013), which might be a limiting factor to the use of VEGFR-targeting therapies and explain the lack of data exploring this axis. In corroboration with the literature, we observed that VEGFA/B, PlGF, and sVEGFR1 were elevated in the peritoneal fluid of patients undergoing endometriosis surgery. Moreover, through occupancy mathematical determination, the levels of those mediators are abundant to induce VEGFR1 activation and potential signaling. In addition, using our validated mouse model, we found high levels of VEGF in the lesions as well as the presence of its receptor in primary nociceptor neurons, suggesting a possible signaling axis to pain sensitivity. Nonetheless, blocking VEGF signaling with anti-VEGF or cKO did not reduce pain or lesion size. This indicates that while present in the lesion and peritoneal fluid, VEGF-VEGFR1 signaling does not mediate pain in our model.

Neurotrophic factors, such as NGF, have been described to participate in inflammatory pain (Woolf et al., 1994) and neuropathic pain (Reis et al., 2022). NGF contributes indirectly and directly to nociceptor neuron sensitization and pain. NGF signaling via tropomyosin receptor kinase A (TrkA) in immune cells (e.g., mast cells, basophils, macrophages) (Bischoff and Dahinden, 1992; Horigome et al., 1993; Susaki et al., 1996; Tal and Liberman, 1997) result in the release of NGF and other pro-nociceptive molecules, such as interleukin (IL)-1β (Lindholm et al., 1987). Directly, NGF induced nociceptor neurons sensitization and activation (Bonnington and McNaughton, 2003). For instance, in a rat model of complete Freund's

adjuvant (CFA)-induced inflammatory pain, treatment with anti-NGF reduced thermal and mechanical hyperalgesia (Woolf et al., 1997). Specifically for endometriosis, a recent GWAS study highlights that variance among genes, such as NGF is associated with pain during the disease (Nilufer et al., 2018). Therefore, we hypothesized that neurotrophins (*e.g.,* NGF and BDNF) participate in endometriosis-associated pain. Our data shows that NGF is co-localized with TUJ3 in endometriosis and that $TrkA^+$ DRG neurons are activated during endometriosis. This corroborates human findings that show both NGF and TrkA are highly expressed in endometriosis lesions, and this is correlated with nerve fiber density and deep dyspareunia (Peng et al., 2018). In corroboration, we found that anti-NGF immunotherapy reduced endometriosis-associated evoked and spontaneous pain behaviors in mice. Anti-NGF treatment reduced mechanical hyperalgesia, abdominal licking, squashing, and contortions, and decreased thermal discomfort. Similarly, in a model of cyclophosphamide-induced cystitis, treatment with anti-NGF reduces peripheral hypersensitivity in mice (Guerios et al., 2006). Pain inhibition was also observed in the same model of cystitis in rats, when animals were treated with the NGF sequestering protein REN1820 (Hu et al., 2005). Humanized anti-NGF monoclonal antibodies have been clinically tested in osteoarthritis (Lane et al., 2010; Brown et al., 2012a, 2013; Spierings et al., 2013; Balanescu et al., 2014), low back pain (Katz et al., 2011), diabetes-associated neuropathy (Bramson et al., 2013), and interstitial cystitis (Evans et al., 2011), corroborating the observed phenomena. On the other hand, we found that anti-BDNF immunotherapy did not reduce any of the evaluated parameters. Altogether, this indicates that NGF-TrkA signaling, but not BDNF-TrkB, mediates pain during endometriosis in our model.

To further test our hypothesis, we treated mice with entrectinib, a small molecule approved by the FDA to treat solid tumors (Osman and Tuncbilek, 2022). Herein, we demonstrated weekly treatments with low doses of entrectinib (60 mg/kg) reduced evoked and non-evoked pain behaviors in mice. This suggests that punctual disturbance in NGF-TrkA signaling, by weekly treatments with entrectinib, is sufficient to decrease endometriosis-associated pain. This effect is likely to be via NGF-TrkA signaling since pain (evoked and spontaneous) in our model was reduced after treatment with anti-NGF, but not anti-BDNF. It is important to mention that spontaneous pain is the most common feature of endometriosis. In our model, spontaneous pain behaviors such as abdominal licking, contortions, and squashing are observed throughout the duration of the model. These behaviors are partially reduced by hormonal drugs such as letrozole and danazol, indicating this model accurately reflects endometriosis pain pathophysiology (Fattori et al., 2020). Herein, we observed that both entrectinib and anti-NGF treatments were able to restore not only evoked pain, but also the changes in the spontaneous

behaviors and in thermal selection. Since lack of drug efficacy at reducing ongoing pain drives most endometriosis therapy failure, our data indicates that targeting NGF-TrkA signaling might be effective at reducing endometriosis pain.

It is also noteworthy to mention that NGF targeting therapies are often linked to undesired side effects. For instance, peripheral edema, paresthesia, arthralgia, and headache are listed as the most common side effects with anti-NGF therapy (Bannwarth and Kostine, 2014; Yang et al., 2020). Moreover, while all studies show that anti-NGF decrease pain, in a portion of patients with osteoarthritis, anti-NGF therapy was correlated to joint destruction and the need of total joint replacement (Brown et al., 2012b; Hochberg, 2015). Similarly, treatments with entrectinib in children and young adults increased the incidence of bone fractures (clinicaltrials.gov, NCT02650401) (Desai et al., 2022). Based on the clinical relevance of NGF-targeting treatment for endometriosis pain management, we addressed the safety of entrectinib in the dose and schedule of treatment tested in this study. Herein, we demonstrated that weekly treatment with entrectinib at 60 mg/kg did not induce changes in weight gain, liver, or kidney toxicity, nor bone morphology. Therefore, at the pre-clinical level, we found that low doses of entrectinib reduces endometriosis-associated pain while not showing significant side effects.

5. Conclusion

In this study we demonstrated that while VEGFR1 agonists are upregulated in the peritoneal fluid of endometriosis patients, blocking this signaling does not reduce pain. On the other hand, we found that the neurotrophin NGF (but not BDNF) is key for endometriosis-associated pain. Blocking this signaling with anti-NGF or entrectinib is effective at reducing abdominal mechanical pain, spontaneous pain, and thermal discomfort in our model. Moreover, weekly treatments with entrectinib did not show significant side effects in mice. Lack of drug efficacy at reducing ongoing pain drives most endometriosis therapy failure. Therefore, our study pinpoints NGF as key in endometriosis-associated pain and establishes NGF-TrkA signaling as a potential target for the development of novel therapies for endometriosis.

Funding

This work was supported by grants from The J. Willard and Alice S. Marriott Foundation and Marriott Daughters Foundation.

Acknowledgments

T.H.Z. acknowledges international split PhD scholarship (*Programa de Doutorado Sanduíche no Exterior* – PDSE) from Coordination for the Improvement of Higher Education Personnel (CAPES, Brazil, finance code 001). We also thank the support of Multiuser Center for Research Laboratories of Londrina State University for the access to μCT equipment free of charge. We are also thankful for the collaboration of Rachel Arredondo for English editing this manuscript.

Author contribution

Conceptualization: T.H. Zaninelli, V. Fattori, and M.S. Rogers; **investigation and data curation:** T.H. Zaninelli, V. Fattori, O.K. Heintz, K.R. Wright; A.C. Andrello, W.A. Verri Jr, M.S. Rogers; **funding acquisition:** M.S. Rogers; **methodology:** T.H. Zaninelli, V. Fattori, and M.S. Rogers; **human sample collection:** R.M. Anchan; **animal breading and VEGFR1 ablation:** D. Sim and H. Bukhari; **resources:** A.C. Andrello; D. Bree, T. Zheng, J. Wagner, W.A. Verri Jr, and M.S. Rogers; **project administration:** T.H. Zaninelli; **supervision:** V. Fattori, W.A. Verri Jr, and M.S. Rogers; **visualization:** T.H. Zaninelli, V. Fattori, W.A. Verri Jr, and M.S. Rogers; **writing–original draft:** T.H. Zaninelli; **writing – editing and reviewing:** all authors. All authors have read and approved the final version of the manuscript.

Declaration of interests

The authors declare no conflicts of interest.

References

Abe, N., Nakahara, T., Morita, A., Wada, Y., Mori, A., Sakamoto, K., et al. (2013). KRN633, an inhibitor of vascular endothelial growth factor receptor tyrosine kinase, induces intrauterine growth restriction in mice. *Birth Defects Res. B. Dev. Reprod. Toxicol.* 98, 297–303. doi:10.1002/BDRB.21064.

Abramiuk, M., Grywalska, E., Małkowska, P., Sierawska, O., Hrynkiewicz, R., and Niedźwiedzka-Rystwej, P. (2022). The Role of the Immune System in the Development of Endometriosis. *Cells* 11. doi:10.3390/CELLS11132028.

Anaf, V., Simon, P., El Nakadi, I., Fayt, I., Simonart, T., Buxant, F., et al. (2002). Hyperalgesia, nerve infiltration and nerve growth factor expression in deep adenomyotic nodules, peritoneal and ovarian endometriosis. *Hum. Reprod.* 17, 1895–1900. doi:10.1093/HUMREP/17.7.1895.

Anisimov, A., Leppänen, V. M., Tvorogov, D., Zarkada, G., Jeltsch, M., Holopainen, T., et al. (2013). The basis for the distinct biological activities of vascular endothelial growth factor receptor-1 ligands. *Sci. Signal.* 6. doi:10.1126/SCISIGNAL.2003905/SUPPL_FILE/6_RA52_SM.PDF.

Balanescu, A. R., Feist, E., Wolfram, G., Davignon, I., Smith, M. D., Brown, M. T., et al. (2014). Efficacy and safety of tanezumab added on to diclofenac sustained release in patients with knee or hip osteoarthritis: a double-blind, placebo-controlled, parallel-group, multicentre phase III randomised clinical trial. *Ann. Rheum. Dis.* 73, 1665–1672. doi:10.1136/ANNRHEUMDIS-2012-203164.

Bannwarth, B., and Kostine, M. (2014). Targeting nerve growth factor (NGF) for pain management: what does the future hold for NGF antagonists? *Drugs* 74, 619–626. doi:10.1007/S40265-014-0208-6.

Bischoff, S., and Dahinden, C. (1992). Effect of Nerve Growth Factor on the Release of Inflammatory Mediators by Mature Human Basophils. *Blood* 79, 2662–2669. doi:10.1182/BLOOD.V79.10.2662.2662.

Bonnington, J. K., and McNaughton, P. A. (2003). Signalling pathways involved in the sensitisation of mouse nociceptive neurones by nerve growth factor. *J. Physiol.* 551, 433. doi:10.1113/JPHYSIOL.2003.039990.

Bramson, C., Herrmann, D., Biton, V., Carey, W., Keller, D., Brown, M., et al. (2013). Efficacy and safety of subcutaneous tanezumab in patients with pain related to diabetic peripheral neuropathy (NCT01087203). *J. Pain* 14, S68. doi:10.1016/j.jpain.2013.01.610.

Brown, M. T., Murphy, F. T., Radin, D. M., Davignon, I., Smith, M. D., and West, C. R. (2012a). Tanezumab reduces osteoarthritic knee pain: results of a randomized, double-blind, placebo-controlled phase III trial. *J. pain* 13, 790–798. doi:10.1016/J.JPAIN.2012.05.006.

Brown, M. T., Murphy, F. T., Radin, D. M., Davignon, I., Smith, M. D., and West, C. R. (2012b). Tanezumab Reduces Osteoarthritic Knee Pain: Results of a Randomized, Double-Blind, Placebo-Controlled Phase III Trial. *J. Pain* 13, 790–798. doi:10.1016/J.JPAIN.2012.05.006.

Brown, M. T., Murphy, F. T., Radin, D. M., Davignon, I., Smith, M. D., and West, C. R. (2013). Tanezumab reduces osteoarthritic hip pain: results of a randomized, double-blind, placebo-controlled phase III trial. *Arthritis Rheum.* 65, 1795–1803. doi:10.1002/ART.37950.

Bulun, S. E. (2009). Endometriosis. *N Engl J Med* 360, 268–279. doi:10.1056/NEJMra0804690.

Clegg, L. E., and Mac Gabhann, F. (2017). A computational analysis of in vivo VEGFR activation by multiple co-expressed ligands. *PLoS Comput. Biol.* 13. doi:10.1371/JOURNAL.PCBI.1005445.

Desai, A. V, Robinson, G. W., Gauvain, K., Basu, E. M., Macy, M. E., Maese, L., et al. (2022). Entrectinib in children and young adults with solid or primary CNS tumors harboring NTRK, ROS1, or ALK aberrations (STARTRK-NG). *Neuro. Oncol.* 24. doi:10.1093/NEUONC/NOAC087.

Drilon, A., Siena, S., Ou, S. H. I., Patel, M., Ahn, M. J., Lee, J., et al. (2017). Safety and Antitumor Activity of the Multitargeted Pan-TRK, ROS1, and ALK Inhibitor Entrectinib: Combined Results from Two Phase I Trials (ALKA-372-001 and STARTRK-1). *Cancer Discov.* 7, 400–409. doi:10.1158/2159-8290.CD-16-1237.

Evans, R. J., Moldwin, R. M., Cossons, N., Darekar, A., Mills, I. W., and Scholfield, D. (2011). Proof of concept trial of tanezumab for the treatment of symptoms associated with interstitial cystitis. *J. Urol.* 185, 1716–1721. doi:10.1016/J.JURO.2010.12.088.

Facchin, F., Barbara, G., Saita, E., Mosconi, P., Roberto, A., Fedele, L., et al. (2015). Impact of endometriosis on quality of life and mental health: pelvic pain makes the difference. *J Psychosom Obs. Gynaecol* 36, 135–141. doi:10.3109/0167482X.2015.1074173.

Fattori, V., Franklin, N. S., Gonzalez-Cano, R., Peterse, D., Ghalali, A., Madrian, E., et al. (2020). Nonsurgical mouse model of endometriosis-associated pain that responds to clinically active drugs. *Pain* 161, 1321–1331. doi:10.1097/J.PAIN.0000000000001832.

Fischer, C., Mazzone, M., Jonckx, B., and Carmeliet, P. (2008). FLT1 and its ligands VEGFB and PlGF: drug targets for anti-angiogenic therapy? *Nat. Rev. Cancer 2008 812* 8, 942–956. doi:10.1038/nrc2524.

Gonzalez-Cano, R., Boivin, B., Bullock, D., Cornelissen, L., Andrews, N., and Costigan, M. (2018). Up-Down reader: An open source program for efficiently processing 50% von frey thresholds. *Front. Pharmacol.* 9. doi:10.3389/fphar.2018.00433.

Gonzalez-Cano, R., Merlos, M., Baeyens, J. M., and Cendan, C. M. (2013). sigma1 receptors are involved in the visceral pain induced by intracolonic administration of capsaicin in mice. *Anesthesiology* 118, 691–700. doi:10.1097/ALN.0b013e318280a60a.

Guerios, S. D., Wang, Z. Y., and Bjorling, D. E. (2006). Nerve growth factor mediates peripheral mechanical hypersensitivity that accompanies experimental cystitis in mice. *Neurosci. Lett.* 392, 193–197. doi:10.1016/J.NEULET.2005.09.026.

Hochberg, M. C. (2015). Serious joint-related adverse events in randomized controlled trials of anti-nerve growth factor monoclonal antibodies. *Osteoarthr. Cartil.* 23, S18–S21. doi:10.1016/J.JOCA.2014.10.005.

Horigome, K., Pryor, J. C., Bullock, E. D., and Johnson, E. M. (1993). Mediator release from mast cells by nerve growth factor. Neurotrophin specificity and receptor mediation. *J. Biol. Chem.* 268, 14881–14887. doi:10.1016/S0021-9258(18)82415-2.

Hu, V. Y., Zvara, P., Dattilio, A., Redman, T. L., Allen, S. J., Dawbarn, D., et al. (2005). Decrease in bladder overactivity with REN1820 in rats with cyclophosphamide induced cystitis. *J. Urol.* 173, 1016–1021. doi:10.1097/01.JU.0000155170.15023.E5.

Izumi, G., Koga, K., Takamura, M., Makabe, T., Satake, E., Takeuchi, A., et al. (2018). Involvement of immune cells in the pathogenesis of endometriosis. *J. Obstet. Gynaecol. Res.* 44, 191–198. doi:10.1111/jog.13559.

Kajdos, M., Szymanski, J., Jerczynska, H., Stetkiewicz, T., and Wilczynski, J. R. (2022). Microvesicles released from ectopic endometrial foci as a potential biomarker of endometriosis. *Ginekol. Pol.* doi:10.5603/GP.A2022.0096.

Kajitani, T., Maruyama, T., Asada, H., Uchida, H., Oda, H., Uchida, S., et al. (2013). Possible involvement of nerve growth factor in dysmenorrhea and dyspareunia associated with endometriosis. *Endocr. J.* 60, 1155–1164. doi:10.1507/ENDOCRJ.EJ13-0027.

Katz, N., Borenstein, D. G., Birbara, C., Bramson, C., Nemeth, M. A., Smith, M. D., et al. (2011). Efficacy and safety of tanezumab in the treatment of chronic low back pain. *Pain* 152, 2248–2258. doi:10.1016/J.PAIN.2011.05.003.

Kdr, F.-L. /, Park, J. E., Chen, H. H., Winer, J., Houcks, K. A., and Ferrarao, N. (1994).

Placenta growth factor. Potentiation of vascular endothelial growth factor bioactivity, in vitro and in vivo, and high affinity binding to Flt-1 but not to Flk-1/KDR. 269, 2564625654. doi:10.1016/S0021-9258(18)47298-5.

Laird, J. M., Martinez-Caro, L., Garcia-Nicas, E., and Cervero, F. (2001). A new model of visceral pain and referred hyperalgesia in the mouse. *Pain* 92, 335–342. Available at: http://www.ncbi.nlm.nih.gov/pubmed/11376906.

Lane, N. E., Schnitzer, T. J., Birbara, C. A., Mokhtarani, M., Shelton, D. L., Smith, M. D., et al. (2010). Tanezumab for the treatment of pain from osteoarthritis of the knee. *N. Engl. J. Med.* 363, 1521–1531. doi:10.1056/NEJMOA0901510.

Laux-Biehlmann, A., d'Hooghe, T., and Zollner, T. M. (2015). Menstruation pulls the trigger for inflammation and pain in endometriosis. *Trends Pharmacol Sci* 36, 270–276. doi:10.1016/j.tips.2015.03.004.

Lindholm, D., Heumann, R., Meyer, M., and Thoenen, H. (1987). Interleukin-1 regulates synthesis of nerve growth factor in non-neuronal cells of rat sciatic nerve. *Nature* 330, 658–659. doi:10.1038/330658A0.

Liu, S., Xin, X., Hua, T., Shi, R., Chi, S., Jin, Z., et al. (2016). Efficacy of Anti-VEGF/VEGFR Agents on Animal Models of Endometriosis: A Systematic Review and Meta-Analysis. *PLoS One* 11. doi:10.1371/JOURNAL.PONE.0166658.

Mac Gabhann, F., and Popel, A. S. (2004). Model of competitive binding of vascular endothelial growth factor and placental growth factor to VEGF receptors on endothelial cells. *Am. J. Physiol. Heart Circ. Physiol.* 286. doi:10.1152/AJPHEART.00254.2003.

McKinnon, B. D., Bertschi, D., Bersinger, N. A., and Mueller, M. D. (2015). Inflammation and nerve fiber interaction in endometriotic pain. *Trends Endocrinol Metab* 26, 1–10. doi:10.1016/j.tem.2014.10.003.

McLaren, J., Prentice, A., Charnock-Jones, D. S., and Smith, S. K. (1996). Vascular endothelial growth factor (VEGF) concentrations are elevated in peritoneal fluid of women with endometriosis. *Hum. Reprod.* 11, 220–223. doi:10.1093/oxfordjournals.humrep.a019023.

Mercier, F., Djebli, N., González-Sales, M., Jaminion, F., and Meneses-Lorente, G. (2022). Efficacy and safety exposure-response analyses of entrectinib in patients with advanced or metastatic solid tumors. *Cancer Chemother. Pharmacol.* 89, 363–372. doi:10.1007/S00280-022-04402-W.

Nilufer, R., Karina, B., Paraskevi, C., Rebecca, D., Genevieve, G., Ayush, G., et al. (2018). Large-scale genome-wide association meta-analysis of endometriosis reveals 13 novel

loci and genetically-associated comorbidity with other pain conditions. *bioRxiv*, 406967. doi:10.1101/406967.

Nnoaham, K. E., Hummelshoj, L., Webster, P., D'Hooghe, T., De Cicco Nardone, F., De Cicco Nardone, C., et al. (2011). Impact of endometriosis on quality of life and work productivity: A multicenter study across ten countries. *Fertil. Steril.* 96. doi:10.1016/j.fertnstert.2011.05.090.

Osman, H. M., and Tuncbilek, M. (2022). Entrectinib: A New Selective Tyrosine Kinase Inhibitor Approved for the Treatment of Pediatric and Adult Patients with NTRK Fusionpositive, Recurrent or Advanced Solid Tumors. *Curr. Med. Chem.* 29, 2602–2616. doi:10.2174/0929867328666210914121324.

Papadopoulos, N., Martin, J., Ruan, Q., Rafique, A., Rosconi, M. P., Shi, E., et al. (2012). Binding and neutralization of vascular endothelial growth factor (VEGF) and related ligands by VEGF Trap, ranibizumab and bevacizumab. *Angiogenesis* 15, 171. doi:10.1007/S10456-011-9249-6.

Parasar, P., Ozcan, P., and Terry, K. L. (2017). Endometriosis: Epidemiology, Diagnosis and Clinical Management. *Curr. Obstet. Gynecol. Rep.* 6, 34–41. doi:10.1007/S13669-017-0187-1/TABLES/2.

Peng, B., Zhan, H., Alotaibi, F., Alkusayer, G. M., Bedaiwy, M. A., and Yong, P. J. (2018). Nerve Growth Factor Is Associated With Sexual Pain in Women With Endometriosis. *Reprod. Sci.* 25, 540–549. doi:10.1177/1933719117716778.

Pye, S. M., Cortes, J., Ault, P., Hatfield, A., Kantarjian, H., Pilot, R., et al. (2008). The effects of imatinib on pregnancy outcome. *Blood* 111, 5505–5508. doi:10.1182/BLOOD-2007-10-114900.

Reis, C., Chambel, S., Ferreira, A., and Cruz, C. D. (2022). Involvement of nerve growth factor (NGF) in chronic neuropathic pain - a systematic review. *Rev. Neurosci.* 0. doi:10.1515/REVNEURO-2022-0037.

Sekiguchi, K., Ito, Y., Hattori, K., Inoue, T., Hosono, K., Honda, M., et al. (2019). VEGF Receptor 1-Expressing Macrophages Recruited from Bone Marrow Enhances Angiogenesis in Endometrial Tissues. *Sci. Rep.* 9. doi:10.1038/S41598-019-43185-8.

Selvaraj, D., Gangadharan, V., Michalski, C. W., Kurejova, M., Stosser, S., Srivastava, K., et al. (2015). A Functional Role for VEGFR1 Expressed in Peripheral Sensory Neurons in Cancer Pain. *Cancer Cell* 27, 780–796. doi:10.1016/j.ccell.2015.04.017.

Spierings, E. L. H., Fidelholtz, J., Wolfram, G., Smith, M. D., Brown, M. T., and West, C. R. (2013). A phase III placebo- and oxycodone-controlled study of tanezumab in adults

with osteoarthritis pain of the hip or knee. *Pain* 154, 1603–1612. doi:10.1016/J.PAIN.2013.04.035.

Susaki, Y., Shimizu, S., Katakura, K., Watanabe, N., Kawamoto, K., Matsumoto, M., et al. (1996). Functional Properties of Murine Macrophages Promoted by Nerve Growth Factor. *Blood* 88, 4630–4637. doi:10.1182/BLOOD.V88.12.4630.BLOODJOURNAL88124630.

Tal, M., and Liberman, R. (1997). Local injection of nerve growth factor (NGF) triggers degranulation of mast cells in rat paw. *Neurosci. Lett.* 221, 129–132. doi:10.1016/S0304-3940(96)13318-8.

Vandenbroucke, T., Verheecke, M., Fumagalli, M., Lok, C., and Amant, F. (2017). Effects of cancer treatment during pregnancy on fetal and child development. *Lancet. Child Adolesc. Heal.* 1, 302–310. doi:10.1016/S2352-4642(17)30091-3.

Vodolazkaia, A., El-Aalamat, Y., Popovic, D., Mihalyi, A., Bossuyt, X., Kyama, C. M., et al. (2012). Evaluation of a panel of 28 biomarkers for the non-invasive diagnosis of endometriosis. *Hum. Reprod.* 27, 2698–2711. doi:10.1093/HUMREP/DES234.

Woolf, C. J., Allchorne, A., Safieh-Garabedian, B., and Poole, S. (1997). Cytokines, nerve growth factor and inflammatory hyperalgesia: the contribution of tumour necrosis factor alpha. *Br J Pharmacol* 121, 417–424. doi:10.1038/sj.bjp.0701148.

Woolf, C. J., Safieh-Garabedian, B., Ma, Q. P., Crilly, P., and Winter, J. (1994). Nerve growth factor contributes to the generation of inflammatory sensory hypersensitivity. *Neuroscience* 62, 327–331. doi:10.1016/0306-4522(94)90366-2.

Wu, F. T. H., Stefanini, M. O., Mac Gabhann, F., and Popel, A. S. (2009). A Compartment Model of VEGF Distribution in Humans in the Presence of Soluble VEGF Receptor-1 Acting as a Ligand Trap. *PLoS One* 4, e5108. doi:10.1371/JOURNAL.PONE.0005108.

Wu, J., Xie, H., Yao, S., and Liang, Y. (2017). Macrophage and nerve interaction in endometriosis. *J Neuroinflammation* 14, 53. doi:10.1186/s12974-017-0828-3.

Xavier, P., Belo, L., Beires, J., Rebelo, I., Martinez-de-Oliveira, J., Lunet, N., et al. (2006). Serum levels of VEGF and TNF-alpha and their association with C-reactive protein in patients with endometriosis. *Arch. Gynecol. Obstet.* 273, 227–231. doi:10.1007/S00404-005-0080-4.

Yang, S., Huang, Y., Ye, Z., Li, L., and Zhang, Y. (2020). The efficacy of nerve growth factor antibody for the treatment of osteoarthritis pain and chronic low-back pain: A meta-analysis. *Front. Pharmacol.* 11, 817. doi:10.3389/FPHAR.2020.00817/BIBTEX.

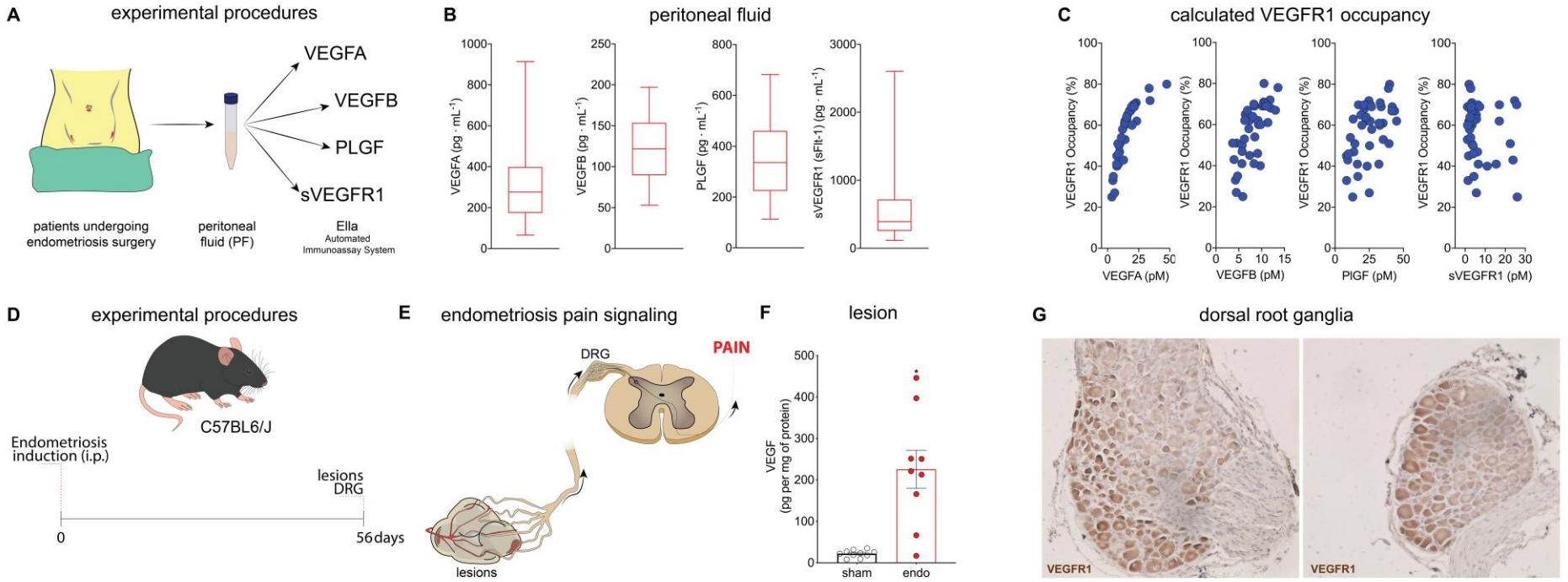

Figure 1. Levels of VEGFR1 ligands are increased in the peritoneal fluid of endometriosis patients and in mouse lesions. (A) experimental procedures for peritoneal fluid collection of endometriosis patients (B) levels of VEGFA, VEGFB, PlGF, and sVEGFR1 in peritoneal fluid samples determined by Ella®. Data is present in box and whisker charts representing the levels of each mediator in pg . mL^{-1}. (C) VEGFR1 mathematical calculated occupancy (D) Experimental procedures and timepoints for tissue collection in our mouse model. (E) scheme of pain signalling in endometriosis: endometriotic lesions are highly innervated by nociceptor sensory neurons, which have their cell bodies in the dorsal root ganglia (DRG). Upon activation, those pseudo-unipolar neurons synapse in the spinal cord with second orders neurons that transfer the message to the brain to be interpreted as pain. (F) 56 days after endometriosis induction, lesions were collected for determination of VEGF levels by ELISA.

Results are presented as mean ± SEM of VEGF levels, n = 10 (sham – uteri horn tissue), and n = 9 (endo) mice per group (*P < 0.05 vs. sham). (G) expression profile of VEGFR1 expression in DRG nociceptors determined by immunohistochemistry 56 days after endometriosis induction.

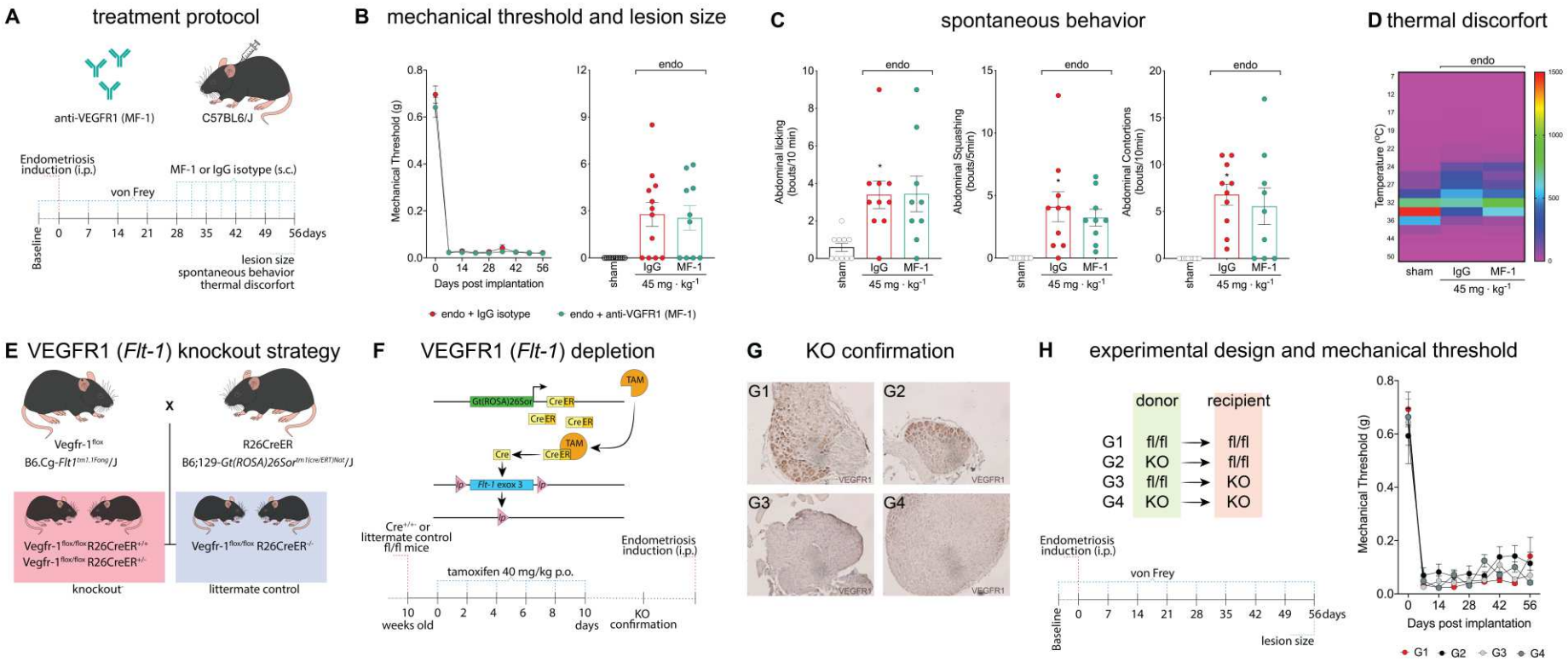

Figure 2. VEGF neutralization or VEGFR1 ablation do not reduce endometriosis-associated pain or thermal discomfort in mice. (A) scheme of the treatment protocol with anti-VEGFR1 (MF-1) antibody and IgG control. (B) mechanical response before (zero) and after (7, 14, 21,

28, 35, 42, and 56 days) endometriosis induction was determined using von Frey filaments. Results are presented as mean ± SEM of mechanical threshold, n = 10 mice per group. (C) spontaneous behaviours measurements. Results are expressed as mean ± SEM of abdominal licking, squashing, and contortions bouts per minute, n = 10. (*P < 0.05 vs. sham). (D) thermal discomfort heatmap. Heatmap shows mean time spent in each temperature zone for IgG control- or MF-1-treated mice. Data is present as mean ± SEM of the amplitude of permanence in seconds in each thermal zone during 60 min. (E) breading scheming for generation of VEGFR1 tamoxifen-induced cre-dependent knockout strategy. (F) scheme of tamoxifen-induced cre-dependent VEGFR1 knockout and tamoxifen treatment protocol. (G) DRG neuron representative images for VEGFR1 knockout confirmation determined per IHC analysis. G1-G2 from littermate controls and G3-G4 from knockout mice n = 10. (H) Endometriosis induction protocol scheme with receptor and donor combinations. Mechanical response before (zero) and after (7, 14, 21, 28, 35, 42, and 56 days) endometriosis induction using von Frey filaments. Results are presented as mean ± SEM of mechanical threshold, n = 10 mice per group.

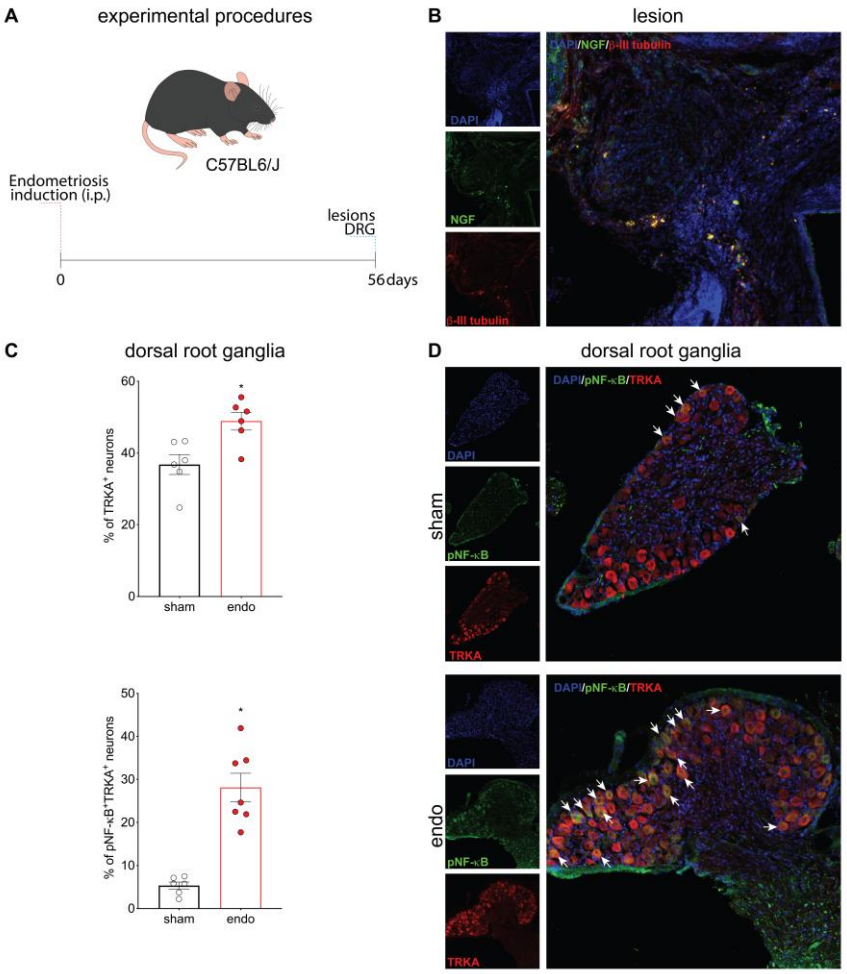

Figure 3. NGF-TrkA signaling is activated during endometriosis. (A) scheme of experimental procedures. (B) representative image from endometriotic lesions stained for NGF and beta-III tubulin. (C) quantification of $TrkA^+$ and $pNF\text{-}\kappa B^+TrkA^+$ neurons in dorsal root ganglia (DRG) of sham and endometriosis lesion-bearing mice. Results are presented as mean ± SEM of the percentage of positive neurons. n = 6 or 7 mice per group. (*$P < 0.05$ vs. sham). (D) Representative images of DRG neurons stained for TrkA (red) and p-NF-kB (green) by confocal microscopy.

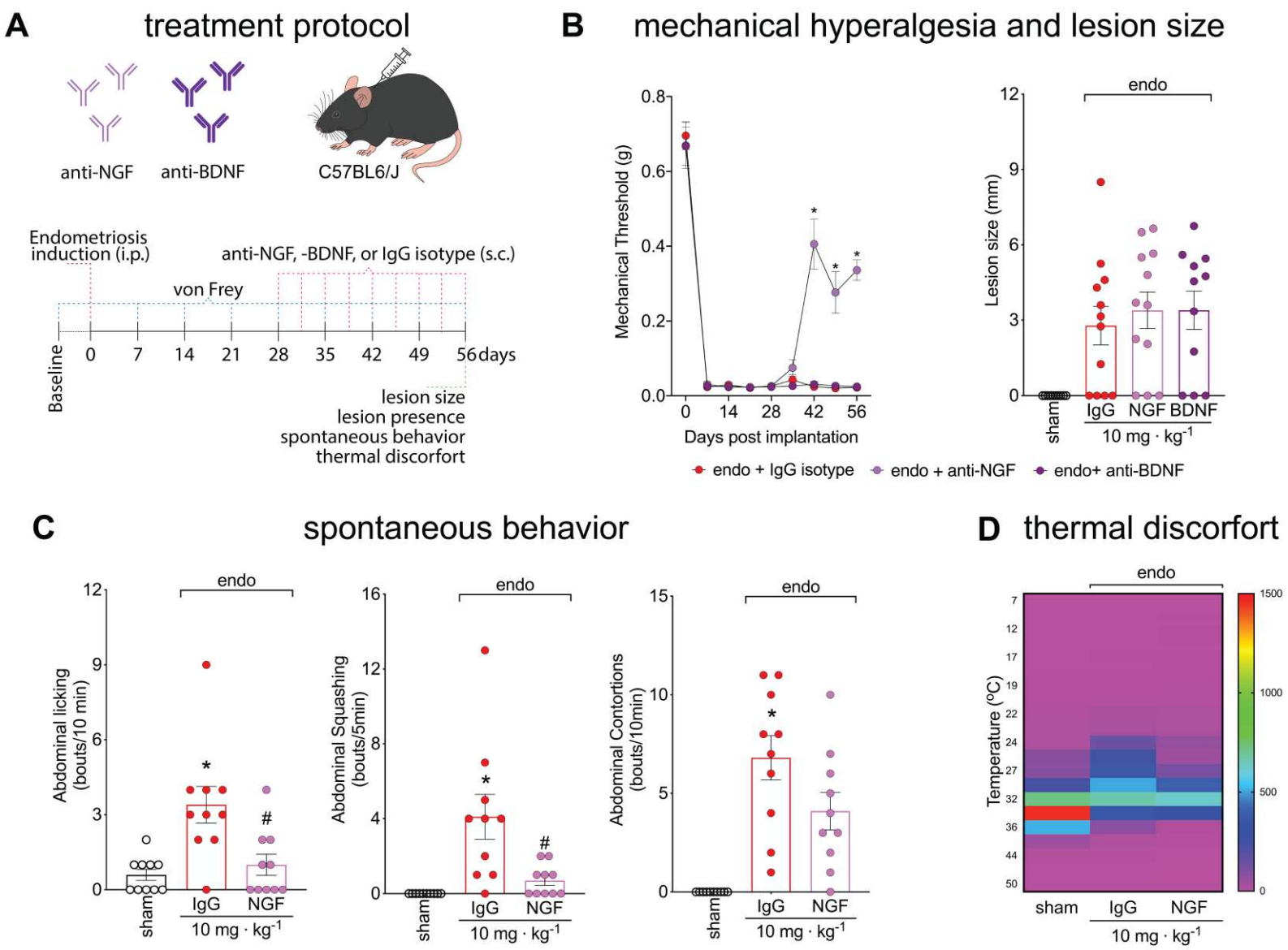
A
treatment protocol
anti-NGF
anti-BDNF
C57BL6/J
Endometriosis induction (i.p.)
anti-NGF, -BDNF, or IgG isotype (s.c.)
von Frey
Baseline
0 7 14 21 28 35 42 49 56 days
lesion size
lesion presence
spontaneous behavior
thermal discorfort
B
mechanical hyperalgesia and lesion size
Mechanical Threshold (g)
Days post implantation
Lesion size (mm)
endo
sham
IgG
NGF
BDNF
10 mg · kg-1
endo + IgG isotype
endo + anti-NGF
endo+ anti-BDNF
C
spontaneous behavior
Abdominal licking (bouts/10 min)
Abdominal Squashing (bouts/5min)
Abdominal Contortions (bouts/10min)
D
thermal discorfort
Temperature (°C)

Figure 4. NGF neutralization, but not BDNF, reduces endometriosis-associated pain and thermal discomfort in mice. (A) scheme of the treatment protocol with IgG control, anti-NGF, or anti-BDNF antibodies. (B) mechanical response before (zero) and after (7, 14, 21, 28, 35, 42, and 56 days) endometriosis induction using von Frey filaments. Results are presented as mean ± SEM of mechanical threshold, n = 10-12 mice per group (*P < 0.05 vs. IgG treated group). (C) spontaneous behaviours measurements. For abdominal licking, the total number of times that mice directly groomed the abdominal region (without going for any other body region before or after the behavior) was quantified for 10 minutes. For abdominal squashing, the number of times the mice pressed the lower abdominal region against the floor was quantified for 5minutes. Sham mice do not display abdominal squashing. Abdominal contortions were quantified for 10 minutes by counting the number of contractions of the abdominal muscle together with stretching of hind limbs. Sham mice did not display abdominal contortions. Results are expressed as mean ± SEM of abdominal licking, squashing, and contortions bouts per minute, n = 10. (*P < 0.05 vs. sham, # P < 0.05 vs. IgG control). (D) thermal discomfort heatmap. Heatmap shows mean time spent in each temperature zone for IgG control-, anti-NGF-, or anti-BDNF-treated mice. Data is present as mean ± SEM of the amplitude of permanence in seconds in each thermal zone during 60 min.

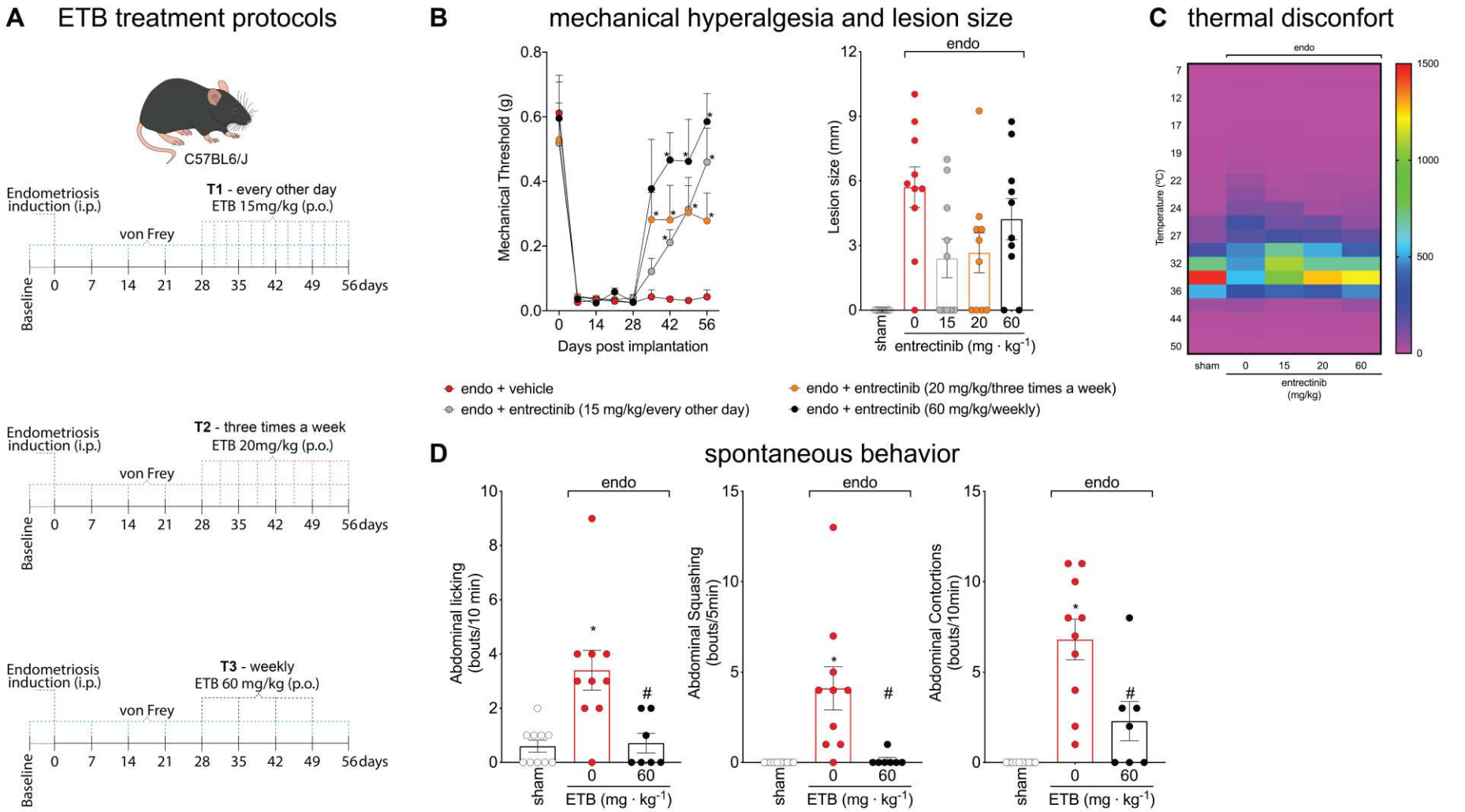

Figure 5. Entrectinib, a pan-Trk inhibitor, reduces endometriosis-associated pain and thermal discomfort. (A) scheme of the treatment protocol with entrectinib. T1 – 15 mg/kg every other day; T2 – 20 mg/kg three times a week; and T3 – 60 mg/kg weekly. In all schedules of

treatment, the weekly dose is 60 mg/kg. (B left) mechanical response before (zero) and after (7, 14, 21, 28, 35, 42, and 56 days) endometriosis induction using von Frey filaments. Results are presented as mean ± SEM of mechanical threshold, n = 10 mice per group (*P < 0.05 vs. vehicle-treated group). (B right) lesion size. Results are presented as mean ± SEM of lesion size in mm, n = 10 mice per group. (C) spontaneous behaviours measurements. For abdominal licking, the total number of times that mice directly groomed the abdominal region (without going for any other body region before or after the behaviour) was quantified for 10 minutes. For abdominal squashing, the number of times the mice pressed the lower abdominal region against the floor was quantified for 5 minutes. Sham mice do not display abdominal squashing. Abdominal contortions were quantified for 10 minutes by counting the number of contractions of the abdominal muscle together with stretching of hind limbs. Sham mice did not display abdominal contortions. Results are expressed as mean ± SEM of abdominal licking, squashing, and contortions bouts per minute, n = 10. (*P < 0.05 vs. sham, # P < 0.05 vs. vehicle-treated group). (D) thermal discomfort heatmap. Data is present as mean ± SEM of the amplitude of permanence in seconds in each thermal zone during 60 min.

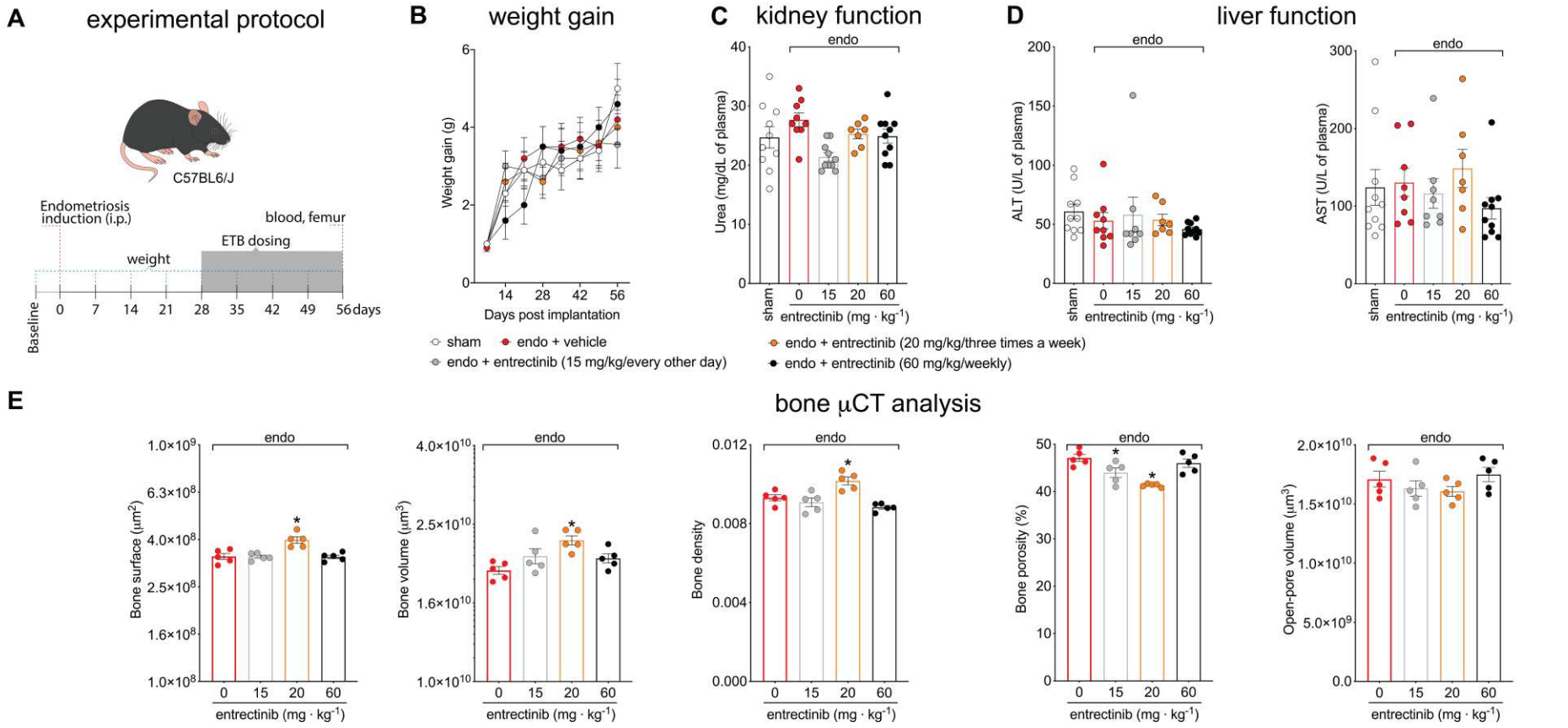

Figure 6. Weekly treatment with entrectinib does not induce weight change, liver or kidney toxicity, or bone loss in mice. (A) scheme of experimental protocol for determination of entrectinib safety using the different treatment schedules. (B) mouse weight was determined weekly. Results are presented as mean ± SEM in grams, n = 7-10 mice per group. (C) kidney function was determined by measuring urea plasma levels. Results are presented as mean ± SEM of urea levels, n = 7-10 mice per group. (D) liver function was determined by measuring ALT and AST

plasma levels. Results are presented as mean ± SEM of AST and ALT levels, n = 7-10 mice per group. (E) Microcomputed tomography of bone (femur) was used to determine bone loss. Results are presented as mean ± SEM, n = 5 mice per group.

ANEXO I

ANEXO I – Comprovante de publicação do artigo de revisão no periódico *Frontiers in Physiology*

frontiers in Physiology

REVIEW
published: 01 September 2021
doi: 10.3389/fphys.2021.729134

OPEN ACCESS

Edited by:
Jue Wang,
The University of Texas Health Science Center at Tyler, United States

Reviewed by:
Javier Conde,
Health Research Institute of Santiago de Compostela (IDIS), Spain
Paul "Li-Hao" Huang,
Fudan University, China

Harnessing Inflammation Resolution in Arthritis: Current Understanding of Specialized Pro-resolving Lipid Mediators' Contribution to Arthritis Physiopathology and Future Perspectives

Tiago H. Zaninelli[1†], Victor Fattori[2†] and Waldiceu A. Verri Jr.[1*†]*

[1] Laboratory of Pain, Inflammation, Neuropathy, and Cancer, Department of Pathology, Londrina State University, Londrina, Brazil, [2] Vascular Biology Program, Boston Children's Hospital, Department of Surgery, Harvard Medical School, Boston, MA, United States

ANEXO II

ANEXO II – Comprovante de submissão do artigo científico no periódico *Expert Opinion on Therapeutic Targets*

Please download and read the instructions before proceeding to the peer review

New drug targets for the treatment of gout: What's new?

Journal:	*Expert Opinion On Therapeutic Targets*
Manuscript ID	EOTT-2023-ST-0074
Manuscript Type:	Review
Keywords:	natural products, specialized pro-resolving lipid mediators, drug repurposing, multitargeting drug, gout arthritis, pain, inflammation, interleukin-1beta, inflammasome

SCHOLARONE™
Manuscripts

ANEXO III

ANEXO III – Comprovante de publicação do artigo científico no periódico *British Journal of Pharmacology*

Received: 12 July 2021 | Revised: 27 April 2022 | Accepted: 25 May 2022

DOI: 10.1111/bph.15897

RESEARCH ARTICLE

RvD1 disrupts nociceptor neuron and macrophage activation and neuroimmune communication, reducing pain and inflammation in gouty arthritis in mice

Tiago H. Zaninelli[1] | Victor Fattori[1,2] | Telma Saraiva-Santos[1] | Stephanie Badaro-Garcia[1] | Larissa Staurengo-Ferrari[1] | Ketlem C. Andrade[1] | Nayara A. Artero[1] | Camila R. Ferraz[1] | Mariana M. Bertozzi[1] | Fernanda Rasquel-Oliveira[1] | Marilia F. Manchope[1] | Flávio A. Amaral[3] | Mauro M. Teixeira[3] | Sergio M. Borghi[1] | Michael S. Rogers[2] | Rubia Casagrande[4] | Waldiceu A. Verri Jr[1]